Synthesis and characterisation of some main-group compounds with bulky electron-withdrawring substituents

Cornet, Stephanie M. M.

University of Durham

Department of Chemistry

Synthesis and Characterisation of Some Main-Group Compounds with Bulky Electron-withdrawing Substituents

Stéphanie M. M. Cornet

Graduate Society

A thesis submitted in part fulfillment of the requirements for the degree of Doctor of Philosophy at the University of Durham.

October 2002

Table of Contents

Table of Contents ... ii
Table of Figures ... ix
Table of Equations and Schemes ... xi
Table of Tables ... xiii
Abstract ... xvi
Acknowledgements ... xix
Abbreviations ... xxii

Chapter 1 ... 1

Introduction ... 1

1.1 Bulky and electron-withdrawing substituents ... 2
1.1.1 Introduction ... 2
1.1.2 1,3,5-tris(trifluoromethyl)benzene (FluoromesitylH, ArH) ... 2
1.1.2.1 Introduction ... 2
1.1.2.2 Advantages of ArH ... 4
1.1.2.3 Reaction with heavier main group elements or transition metals ... 4
1.1.3 1,3-bis(trifluoromethyl)benzene (FluoroxylH, Ar'H) ... 23
1.1.3.1 Properties ... 23
1.1.3.2 Comparison between ArH and Ar'H ... 23
1.1.3.3 Reaction with heavier main group elements or transition metals ... 25
1.2 Diphosphenes ... 28
1.2.1 Fluoromes ... 29
1.2.1.1 Synthetic route ... 29
1.2.1.2 Coordination chemistry ... 31
1.2.2 Fluoroxyl ... 32
References ... 33

Chapter 2 ... 38

Group 13 Derivatives ... 38

2.1 Introduction ... 39
2.2 Reaction with 2,4,6-tris(trifluoromethyl)phenyl lithium (ArLi) ... 41
2.3 Reaction with a 2,6-bis(trifluoromethyl)phenyl lithium / 2,4-bis(trifluoromethyl)phenyl lithium mixture (Ar'Li/Ar"Li)) ... 46
2.4 Boronic Acids ... 54
2.5 Discussion ... 57
2.5.1 Comparison of the chemical shifts ... 57
2.5.2 Comparison of the molecular structures ... 59

2.5.3 Short contact distances 61
2.5.4 Optimised geometry 61
2.6 Attempted reactions with Aluminium *62*
2.6.1 Reaction with 2,6-bis(trifluoromethyl)phenyl lithium (Ar'Li) / 2,4-bis(trifluoromethyl)phenyl lithium (Ar"Li) 62
2.6.2 Reaction with 2,4,6-tris(trifluoromethyl)phenyl lithium (Ar'Li) 62
2.7 Experimental *64*
2.7.1 Introduction 64
2.7.2 Synthesis of ArH 65
2.7.3 Preparation of ArLi 67
2.7.4 Preparation of Ar'Li/Ar"Li 67
2.7.5 Synthesis of $ArBCl_2$ 68
2.7.6 Synthesis of Ar_2BF 68
2.7.7 Synthesis of $Ar'BCl_2$ 69
2.7.8 Synthesis of $Ar"_2BF$ 60
2.7.9 Synthesis of $Ar"_3B$ 60
References 72

Chapter 3 74

Group 14 Derivatives 74

3.1 Introduction *75*
3.1.1 Organosilicons 75
3.1.2 Organogermanium derivatives 76
3.1.3 Organotin compounds[4,5] 76
3.2 Silicon derivatives *78*
3.2.1 Reaction of $SiCl_4$ with 2,4,6-tris(trifluoromethyl)phenyl lithium 78
3.2.2 Reaction of $SiCl_4$ with a 2,6-bis(trifluoromethyl)phenyl lithium / 2,4-bis(trifluoromethyl)phenyl lithium mixture (Ar'Li/Ar"Li) 79
3.3 Germanium derivatives *86*
3.3.1 Reaction of $GeCl_4$ with 2,4,6-tris(trifluoromethyl)phenyl lithium (ArLi) 86
3.3.2 Reaction of $GeCl_4$ with a 2,6-bis(trifluoromethyl)phenyl lithium / 2,4-bis(trifluoromethyl)phenyl lithium mixture (Ar'Li/Ar"Li) 91
3.4 Tin derivatives *92*
3.4.1 Reaction of $SnCl_4$ with 2,4,6-tris(trifluoromethyl)phenyl lithium (ArLi) 92
3.4.2 Reaction of $SnCl_4$ with a 2,6-bis(trifluoromethyl)phenyl lithium / 2,4-bis(trifluoromethyl)phenyl lithium mixture (Ar'Li/Ar"Li) 93
3.5 Discussion *96*
3.5.1 Solution-state NMR Spectroscopy 96
3.5.2 X-ray Crystallography 98
3.6 Experimental *101*
3.6.1 Introduction 101
3.6.2 Synthesis of Ar_2SiF_2 101
3.6.3 Synthesis of $Ar"_2SiCl_2$ 102

3.6.4 Synthesis of Ar'_2SiF_2 103
3.6.5 Synthesis of $ArGeCl_3$ 103
3.6.6 Synthesis of Ar_2GeCl_2 104
3.6.7 Synthesis of $Ar"_2GeCl_2$ 105
3.6.8 Synthesis of $ArSnCl_3/Ar_2SnCl_2$ 105
3.6.9 Synthesis of $Ar'_2SnCl_2/Ar"_2SnCl_2$ 106
References 108

Chapter 4 110

Group 15 Derivatives 110

4.1 Introduction *111*
4.2 Phosphorus Derivatives *112*
4.2.1 Reaction with 2,4,6-tris(trifluoromethyl)phenyl lithium (ArLi) 112
4.2.1.1 $ArPCl_2$ 112
4.2.1.2 Ar_2PCl 113
4.2.1.3 $ArPBr_2$ 117
4.2.1.4 Ar_2PBr 121
4.2.2 Reaction with 2,6-bis(trifluoromethyl)phenyl lithium (Ar'Li) / 2,4-bis(trifluoromethyl)phenyl lithium (Ar"Li) 121
4.2.2.1 $Ar'PCl_2$ 122
4.2.2.2 $Ar"PCl_2$ 122
4.2.2.3 $Ar"_2PCl$ 123
4.2.2.4 Ar'Ar"PCl 127
4.2.2.5 $Ar'PBr_2$ 131
4.2.2.6 $Ar"PBr_2$ 131
4.2.2.7 $Ar"_2PBr$ 132
4.2.2.8 Ar'Ar"PBr 134
4.2.2.9 $Ar"_2PH$ 134
4.2.2.10 Ar'Ar"PH 136
4.2.2.11 Attempted synthesis of Ar'Ar"PF 137
4.2.2.12 Attempted synthesis of $Ar"_2PF$ 137
4.2.2.13 ArAr'PCl/ArAr"PCl 138
4.3 Arsenic Derivatives *139*
4.3.1 Reaction with 2,4,6-tris(trifluoromethyl)phenyl lithium (ArLi) 140
4.3.1.1 $ArAsCl_2$ 140
4.3.1.2 Ar_2AsCl 140
4.3.1.3 $ArAsBr_2$ 141
4.3.1.4 Ar_2AsBr 141
4.3.1.5 $ArAsH_2$ 142
4.3.1.6 Ar_2AsH 142
4.3.2 Reaction with 2,6-bis(trifluoromethyl)phenyl lithium (Ar'Li) / 2,4-bis(trifluoromethyl)phenyl lithium (Ar"Li) 143

4.3.2.1 Ar'$AsCl_2$/Ar"$AsCl_2$ 143
4.3.2.2 Ar'Ar"AsCl 144
4.3.2.3 Ar'$AsBr_2$/Ar"$AsBr_2$ 148
4.3.2.4 Ar'Ar"AsBr 148
4.3.2.5 Ar"$_2$AsBr 150
4.3.2.6 Ar'Ar"AsH 151
4.4 Antimony and bismuth derivatives 154
4.4.1 Antimony derivatives 154
4.4.1.1 Ar'$SbCl_2$/Ar"$SbCl_2$ 154
4.4.1.2 Ar'$_2$SbCl/Ar"$_2$SbCl 155
4.4.1.3 Ar'Ar"$_2$Sb 156
4.4.2 Bismuth derivatives 160
4.5 Discussion 160
4.5.1 Solution-state NMR spectroscopy 160
4.5.2 X-ray Crystallography 162
4.6 Experimental 168
4.6.1 Introduction 168
4.6.2 Synthesis of $ArPCl_2$ 169
4.6.3 Synthesis of Ar_2PCl 170
4.6.4 Synthesis of $ArPBr_2$ 170
4.6.5 Synthesis of Ar'PCl_2/Ar"PCl_2 171
4.6.6 Synthesis of Ar"$_2$PCl 172
4.6.7 Synthesis of Ar'PBr_2/Ar"PBr_2 , and Ar"$_2$PBr/Ar'Ar"PBr 172
4.6.8 Synthesis of Ar"$_2$PH 173
4.6.9 Synthesis of Ar'Ar"PH 174
4.6.10 Attempted synthesis of Ar"$_2$PF 175
4.6.11 Attempted synthesis of Ar'Ar"PF 175
4.6.12 Synthesis of ArAr'PCl/ArAr"PCl 176
4.6.13 Synthesis of $ArAsCl_2$/Ar_2AsCl 176
4.6.14 Synthesis of $ArAsH_2$ 177
4.6.15 Synthesis of $ArAsBr_2$/Ar_2AsBr 177
4.6.16 Synthesis of Ar_2AsH 178
4.6.17 Synthesis of Ar'$AsCl_2$/Ar"$AsCl_2$/Ar'Ar"AsCl 178
4.6.18 Synthesis of Ar'$AsBr_2$/Ar"$AsBr_2$, Ar"$_2$Br and Ar'Ar"AsBr 179
4.6.19 Synthesis of Ar'Ar"AsH 181
4.6.20 Synthesis of Ar'$SbCl_2$/Ar"$SbCl_2$/Ar'$_2$SbCl/Ar"$_2$SbCl/Ar'Ar"$_2$Sb 181
4.6.26 Attempted reaction between Ar'Li/Ar"Li and $BiCl_3$ 182
References 183

Chapter 5 187

^{19}F Variable Temperature NMR Studies 187

5.1 Introduction *188*
5.2 Phosphorus compounds *190*
5.2.1 Ar'Ar"PCl 190
5.2.2 Ar'Ar"PH 195
5.2.3 ArAr"PCl/ArAr'PCl 197
5.3 Arsenic compounds *202*
5.3.1 Ar'Ar"AsCl 202
5.3.2 Ar'Ar"AsBr 204
5.3.3 Ar'Ar"AsH 206
5.4 Discussions. *210*
5.5 Experimental *212*
5.5.1 Syntheses 212
5.5.2 NMR spectroscopy 212
5.5.3 Lineshape analysis 212
References 213

Chapter 6 214

Synthesis of Platinum Complexes 214

6.1 Introduction *215*
6.2 Platinum complexes *215*
6.2.1 Platinum complexes as chemotherapeutic agents 217
6.2.2 NMR spectroscopy 217
6.3 The "platinum dimer" *218*
6.3.1 Reactions with low coordinate phosphorus species 219
6.4 Synthesis of some Platinum-Phosphane Compounds *222*
6.4.1 Synthesis of the Pt dimer 222
6.4.2 Reaction between Ar'Ar"PCl and Pt dimer 224
6.4.3 Reaction between Ar"$_2$PCl and $[PtCl_2(PEt_3)]_2$ 225
6.4.4 Reaction between Ar"$_2$PH and $[PtCl_2(PEt_3)]_2$ 226
6.4.5 Reaction between $ArPBr_2$ and $[PtCl_2(PEt_3)]_2$ 227
6.4.6 Reaction between Ar'PBr_2/Ar"PBr_2 and $[PtCl_2(PEt_3)]_2$ 228
6.4.7 Reaction between Ar"$_2$PBr and $[PtCl_2(PEt_3)]_2$ 230
6.4.8 Synthesis of $[PtBr_2(PEt_3)]_2$ 232
6.4.9 Reaction between $ArPBr_2$ and $[PtBr_2(PEt_3)]_2$ 233
6.4.10 Reaction between Ar"$_2$PBr and $[PtBr_2(PEt_3)]_2$ 234
6.4.11 Reaction between Ar'PBr_2/Ar"PBr_2 and $[PtBr_2(PEt_3)]_2$ 234
6.5 Attempted synthesis of Platinum-Arsane Compounds *236*
6.6 Discussion *236*
6.6.1 Change in the chemical shifts 236
6.6.2 Comparison of the coupling constants 238

6.7 Experimental *240*
6.7.1 Introduction 240
6.7.2 Synthesis of *cis*-[$PtCl_2(PhCN)_2$] 241
6.7.3 Synthesis of *cis*-[$PtCl_2(PEt_3)_2$] 241
6.7.4 Synthesis of *trans*-[$PtCl_2(PEt_3)]_2$ 242
6.7.5 Synthesis of *trans*-[$PtCl_2(PEt_3)_2$(Ar'Ar"PCl)] 242
6.7.6 Synthesis of *trans*-[$PtCl_2(PEt_3)$(Ar"$_2$PCl)] 242
6.7.7 Synthesis of *trans*-[$PtCl_2(PEt_3)$(Ar"$_2$PH)] 243
6.7.8 Synthesis of *cis*-[$PtCl_2(PEt_3)(ArPBr_2)$] 243
6.7.9 Synthesis of *cis*-[$PtCl_2(PEt_3)$(Ar"PBr_2)]and *cis*-[$PtCl_2(PEt_3)$(Ar'PBr_2)] 244
6.7.10 Synthesis of *trans*-[$PtCl_2(PEt_3)$(Ar"$_2$PBr)] 244
6.7.11 Synthesis of *cis*-[$PtBr_2(PhCN)_2$] 245
6.7.12 Synthesis of *cis*-[$PtBr_2(PEt_3)_2$] 245
6.7.13 Synthesis of *trans*-[$PtBr_2(PEt_3)]_2$ 245
6.7.14 Synthesis of *cis*-[$PtBr_2(PEt_3)(ArPBr_2)$] 246
6.7.15 Synthesis of *trans*-[$PtBr_2(PEt_3)$(Ar"$_2$PBr)] 246
6.7.16 Synthesis of *cis*-[$PtBr_2(PEt_3)$(Ar'PBr_2)], *trans*-[$PtBr_2(PEt_3)$(Ar"PBr_2)] and cis-[$PtBr_2(PEt_3)$(Ar"PBr_2)] 247
6.7.17 Attempted synthesis of [$PtCl_2(PEt_3)(ArAsCl_2)$] 247
6.7.18 Attempted synthesis of [$PtCl_2(PEt_3)(Ar_2AsCl)$] 248
6.7.19 Attempted synthesis of [$PtCl_2(PEt_3)$(Ar'Ar"AsCl)] 248
References 249

Chapter 7 251

Synthesis of multiple bonded phosphorus compounds 251

7.1 Double bonded compounds between heavier group14 and 15 elements *252*
7.1.1 Diphosphenes 252
7.1.2 Other multiple-bonded main group derivatives 253
7.1.3 Synthetic routes 253
7.1.4 Synthetic routes and Chemical shifts of RP=ER' systems 258
7.2 Disphosphenes and related species *261*
7.2.1 Reaction of $ArPCl_2$ with $W(PMe_3)_6$ 261
7.2.2 Reaction of Ar'PCl_2/Ar"PCl_2 with $W(PMe_3)_6$ 262
7.2.3 Reaction between $ArPCl_2$, $ArAsCl_2$ and $W(PMe_3)_6$ 262
7.2.4 Reaction between $ArPCl_2$, Ar_2GeCl_2 and $W(PMe_3)_6$ 263
7.2.5 Reaction between $ArPCl_2$, Ar_2SnCl_2 and $W(PMe_3)_6$ 263
7.2.6 Conclusion 264
7.3 Phosphaalkenes and Phosphaalkynes *264*
7.3.1 Phosphaalkenes 264
7.3.2 Phosphaalkynes 265
7.3.3 Preparation of Phosphaalkenes 267
7.3.3.1 Synthesis of $ArP(Cl)CHCl_2$ 267
7.3.3.2 Synthesis of $ArP{=}CCl_2$ 268

7.3.3.3 Synthesis of $Ar'P(Cl)CHCl_2$ 269
7.3.3.4 Synthesis of $Ar'P=CCl_2$ 270
7.4 Attempted preparation of phosphaalkynes *271*
7.4.1 Reaction between $ArP=CCl_2$ and $Pt(PPh_3)_4$ 271
7.4.2 Reaction between $Ar'P=CCl_2$ and $Pt(PPh_3)_4$ 275
7.5 Experimental *277*
7.5.1 Introduction 277
7.5.2 Synthesis of ArP=PAr 278
7.5.3 Synthesis of Ar'P=PAr' 279
7.5.4 Attempted synthesis of ArP=AsAr 279
7.5.5 Attempted synthesis of $ArP=GeAr_2$ 279
7.5.6 Attempted synthesis of $ArP=SnAr_2$ 279
7.5.7 Synthesis of $Pt(PPh_3)_4$ 280
7.5.8 Synthesis of $ArP(Cl)CHCl_2$ 280
7.5.9 Synthesis of $ArP=CCl_2$ 281
7.5.10 Synthesis of $Ar'P(Cl)CHCl_2$ 281
7.5.11 Synthesis of $Ar'P=CCl_2$ 282
7.5.12 Synthesis of $[PtCl(ClC=PAr)(PPh_3)_2]$ 282
7.5.13 Synthesis of $[PtCl(CCl=PAr')(PPh_3)_2]$ 283
References 284

Conclusions and Future Work 287

Table of Figures

Figure 1.1	Molecule of Ar_2BN_3	5
Figure 1.2	Intramolecular Sn---F interactions	8
Figure 1.3	Formation of heterocycles from Ar_2Sn	9
Figure 1.4	Interactions between the metal and the fluorines atoms	20
Figure 1.5	1,3-bis(trisfluoromethyl)benzene	24
Figure 1.6	Substitution sites in Fluoromes and Fluoroxyl	24
Figure 1.7	Probable lithiation sites for |Fluoroxyl	24
Figure 1.8	Different products of the reaction of Ar'Li/Ar"Li with MX_3	25
Figure 1.9	Different products of the reaction between Ar'Li/Ar"Li with PCl_3	27
Figure 1.10	Coordination chemistry of diphosphenes	31
Figure 2.1	Molecular Structure of Ar_2BF	44
Figure 2.2	Variable temperature ^{19}F NMR spectra of $Ar"_3B$	48
Figure 2.3	Different conformations for $Ar"_3B$	49
Figure 2.4	Lettering Scheme for Carbon Assignments in $Ar"_3B$	49
Figure 2.5	Lettering Scheme for Hydrogen Assignments in $Ar"_3B$	50
Figure 2.6	Molecular Structure of $Ar"_3B$	51
Figure 2.7	Molecular Structure of $Ar_2B(OH)$	55
Figure 2.8	Molecular Structure of $Ar'B(OH)_2$	56
Figure 2.9	Electron Donation from Fluorine to Boron	58
Figure 2.10	Steel Vacuum Line for SF_4 Transfer	65
Figure 2.11	Autoclave for SF_4 Fluorination Reactions	66
Figure 3.1	^{19}F NMR Spectrum of the Reaction between Ar'Li/Ar"Li and $SiCl_4$	80
Figure 3.2	^{19}F NMR Region for the Si-F_2 Signals in Ar'_2SiF_2 and $Ar"_2SiF_2$	81
Figure 3.3	Molecular Structure of $Ar"_2SiCl_2$	82
Figure 3.4	Molecular Structure of Ar'_2SiF_2	82
Figure 3.5	Si---F Short Contacts	85
Figure 3.6	Coordination Environment around Silicon	85
Figure 3.7	Molecular Structure of $ArGeCl_3$	87
Figure 3.8	Molecular Structure of Ar_2GeCl_2	88
Figure 3.9	^{19}F NMR Spectrum of the Reaction between Ar'Li/Ar"Li and $GeCl_4$	91
Figure 3.10	Molecular Structure of Ar_2SnCl_2	93
Figure 3.11	^{19}F NMR Spectrum of $Ar'_2SnCl_2/Ar"_2SnCl_2$	94
Figure 3.12	Molecular Structure of Ar'_2SnCl_2	95
Figure 4.1	^{31}P NMR Spectrum of $ArPCl_2$	113
Figure 4.2	Molecular Structure of Ar_2PCl	114
Figure 4.3	Molecular Structure of $ArPBr_2$	117
Figure 4.4	^{31}P NMR Spectrum of the mixture $Ar'PCl_2/Ar"PCl_2$	123
Figure 4.5	Lettering Scheme for Carbon atoms in $Ar"_2PCl$	124
Figure 4.6	Molecular Structure of $Ar"_2PCl$	126
Figure 4.7	The Ar'Ar"PCl Molecule	127
Figure 4.8	^{31}P NMR Spectrum of the mixture Ar'Ar"PCl	127
Figure 4.9	^{19}F NMR Spectrum of the mixture Ar'Ar"PCl	128
Figure 4.10	Lettering Scheme for Carbon atoms in Ar'Ar"PCl	128
Figure 4.11	Molecular Structure of Ar'Ar"PCl	130

Figure 4.12	Molecular Structure of Ar"$_2$PBr	132
Figure 4.13	Lettering Scheme for Ar"$_2$PH	135
Figure 4.14	^{19}F NMR Spectrum of Ar'Ar"AsCl	145
Figure 4.15	Lettering Scheme for Ar'Ar"AsCl	145
Figure 4.16	Molecular Structure of Ar'Ar"AsCl	146
Figure 4.17	Molecular Structure of Ar'Ar"AsBr	149
Figure 4.18	Lettering Scheme for Ar'Ar"AsH	151
Figure 4.19	Molecular Structure of Ar'Ar"AsH	152
Figure 4.20	Lettering Scheme for Ar'Ar"$_2$Sb	157
Figure 4.21	Molecular Structure of Ar'Ar"$_2$Sb	158
Figure 5.1	Room Temperature ^{19}F NMR Spectrum of Ar'Ar"AsCl	188
Figure 5.2	Variable Temperature ^{19}F NMR Spectrum of Ar'Ar"PCl	191
Figure 5.3	Inequivalent CF_3 groups in the ^{19}F NMR at Low Temperature	192
Figure 5.4	^{19}F NMR Spectrum at -90°C	192
Figure 5.5	Equivalent CF_3 groups in the ^{19}F NMR spectrum at high temperature	193
Figure 5.6	Simulated and Experimental ^{19}F NMR Spectra at -20°C	194
Figure 5.7	Eyring Plot for Ar'Ar"PCl	195
Figure 5.8	Section of the Variable Temperature ^{19}F NMR Spectra of Ar'Ar"PH	196
Figure 5.9	Eyring Plot for Ar'Ar"PH	197
Figure 5.10	^{19}F NMR Spectrum of the *o*-CF_3 groups of ArAr'PCl at Room Temperature	198
Figure 5.11	Low Temperature Spectra of ArAr"PCl/ArAr'PCl	198
Figure 5.12	Section of the ^{19}F NMR Spectra of ArAr'PCl	199
Figure 5.13	Eyring Plot of ArAr"PCl	200
Figure 5.14	Section of Variable Temperature NMR Spectra of Ar'Ar"AsCl	202
Figure 5.15	Eyring Plot for Ar'Ar"AsCl	203
Figure 5.16	^{19}F NMR Spectrum of Ar'Ar"AsBr at -50°C	204
Figure 5.17	^{19}F NMR Spectrum of Ar'Ar"AsBr at 100°C	204
Figure 5.18	Eyring Plot for Ar'Ar"AsBr	205
Figure 5.19	^{19}F NMR Spectrum of Ar'Ar"AsH at -87°C	206
Figure 5.20	Eyring Plot of Ar'Ar"AsH	207
Figure 5.21	Simulated and Experimental ^{19}F NMR Spectra of Ar'Ar"AsH	209
Figure 6.1	Electron-pairing in a Square Planar Complex	216
Figure 6.2	Formation of the two Possible Isomers	220
Figure 6.3	Rearrangement of the Initial *trans* product to give the thermodynamically more stable *cis*-product	221
Figure 6.4	^{31}P NMR Spectrum of $[PtCl_2(PEt_3)]_2$	223
Figure 6.5	Molecular Structure of $[PtCl_2(PEt_3)]_2$	223
Figure 6.6	^{31}P NMR Spectrum of $[PtCl_2(PEt_3)(Ar"_2PCl)]$	225
Figure 6.7	^{31}P NMR Spectrum of $[PtCl_2(PEt_3)(Ar"_2PBr)]$ (Phosphane region)	231
Figure 6.8	^{31}P NMR Spectrum of $[PtCl_2(PEt_3)(Ar"_2PBr)]$ (PEt_3 region)	231
Figure 6.9	Molecular Structure of $[PtBr_2(PEt_3)]_2$	232
Figure 6.10	Back Donation of Electrons from the Metal to Phosphorus Atom	237
Figure 7.1	^{31}P NMR Spectrum of $R^1P{=}PR^2$	256
Figure 7.2	Metathesis Mechanism	257
Figure 7.3	^{31}P NMR Spectrum of $ArP{=}CCl_2$	268

Figure 7.4 ^{19}F NMR Spectrum of $ArP{=}CCl_2$ 269
Figure 7.5 *Trans* and *cis*-$[PtCl(PEt_3)_2(ArP{=}CCl)]$ 272
Figure 7.6 Molecular Structure of *Trans*-$[PtCl(CCl{=}PAr)(PPh_3)_2]$ 274
Figure 7.7 *Trans* and *cis*-$[PtCl(PEt_3)(Ar'P{=}CCl)]$ 276
Figure 7.8 Possible Intermediate in the Reaction 277

Table of Equations and Scheme

Equation 1.1 Synthesis of ArH 3
Equation 1.2 Synthesis of ArLi 3
Equation 1.3 Synthesis of ArCOOH 7
Equation 1.4 Possible Mechanism for the formation of the difluoride derivative 7
Equation 1.5 Synthesis of Ar_2SnCl_2 10
Equation 1.6 Synthesis of Ar_2Pb 10
Equation 1.7 Formation of dimer 11
Equation 1.8 Synthesis of $ArPCl_2/Ar_2PCl$ 12
Equation 1.9 Synthesis of $ArAsCl_2/Ar_2AsCl$ 14
Equation 1.10 Synthesis of ArOH 15
Equation 1.11 Synthesis of $(ArOTl)_2$ and $(ArOIn)_2$ 16
Equation 1.12 Attempted Synthesis of $(ArO)_3Bi$ 16
Equation 1.13 Synthesis of $ArSe(Cp^*_2Sm(THF))$ 19
Equation 1.14 Synthesis of Ar_2M 21
Equation 1.15 Synthesis of $M(\eta^6\text{-ArH})$ 22
Equation 1.16 Synthesis of $Ar"_2MCl_2$ 26
Equation 1.17 Synthesis of Ar*P=PAr* 28
Equation 1.18 Synthesis of ArP=PAr 29
Equation 1.19 Synthesis of Ar*P=PAr* with $W(PMe_3)_6$ 30
Equation 2.1 Proposed Mechanism for the F/Cl exchange 43
Equation 2.2 Synthesis of $Ar'BCl_2$ 46
Equation 2.3 Synthesis of $Ar"_2BF$ 46
Equation 2.4 Synthesis of $Ar"_3B$ 47
Equation 3.1 Synthesis of Ar_2SiF_2 78
Scheme 3.1 Possible Mechanism of the formation of Ar_2SiF_2 79
Scheme 3.2 Different Products of the Reaction between Ar'Li/Ar"Li and $SiCl_4$ 80
Equation 3.2 Synthesis of $ArGeCl_3$ 86
Equation 3.3 Synthesis of Ar_2GeCl_2 87
Equation 3.4 Synthesis of $ArSnCl_3$ 92
Equation 3.5 Synthesis of Ar_2SnCl_2 92
Equation 3.6 Synthesis of Ar'_2SnCl_2 92
Equation 3.7 Synthesis of $Ar"_2SnCl_2$ 95
Equation 4.1 Synthesis of $ArPCl_2$ 112
Equation 4.2 Synthesis of Ar_2PCl 113

Equation 4.3	Synthesis of $ArPBr_2$	117
Scheme 4.1	Different products of the reaction between Ar'Li/Ar"Li and PCl_3	121
Equation 4.4	Synthesis of $Ar'PCl_2$	122
Equation 4.5	Synthesis of $Ar"PCl_2$	122
Equation 4.6	Synthesis of $Ar"_2PCl$	123
Equation 4.7	Synthesis of $Ar'PBr_2$	131
Equation 4.8	Synthesis of $Ar"PBr_2$	131
Equation 4.9	Synthesis of $Ar"_2PBr$	132
Equation 4.10	Synthesis of Ar'Ar"PBr	134
Equation 4.11	Synthesis of $Ar"_2PH$	134
Equation 4.12	Synthesis of Ar'Ar"PH	136
Equation 4.13	Attempted Synthesis of Ar'Ar"PF	137
Equation 4.14	Attempted Synthesis of $Ar"_2PF$	137
Equation 4.15	Synthesis of ArAr'PCl/ArAr"PCl	138
Equation 4.16	Synthesis of $ArAsCl_2$	140
Equation 4.17	Synthesis of Ar_2AsCl	140
Equation 4.18	Synthesis of $ArAsBr_2$	141
Equation 4.19	Synthesis of Ar_2AsBr	141
Equation 4.20	Synthesis of $ArAsH_2$	142
Equation 4.21	Synthesis of Ar_2AsH	142
Equation 4.22	Synthesis of $Ar'AsCl_2$/$Ar"AsCl_2$	143
Equation 4.23	Synthesis of Ar'Ar"AsCl	144
Equation 4.24	Synthesis of $Ar'AsBr_2$/$Ar"AsBr_2$	148
Equation 4.25	Synthesis of Ar'Ar"AsBr	148
Equation 4.26	Synthesis of $Ar"_2AsBr$	150
Equation 4.27	Synthesis of Ar'Ar"AsH	151
Equation 4.28	Synthesis of $Ar'SbCl_2$/$Ar"SbCl_2$	154
Equation 4.29:	Synthesis of Ar'_2SbCl/$Ar"_2SbCl$	155
Equation 4.30:	Synthesis of $Ar'Ar"_2Sb$	156
Equation 6.1	Synthesis of Pt Dimer	219
Equation 6.2	Synthesis of trans-$[PtCl_2(PEt_3)]_2$	222
Equation 6.3	Synthesis of trans-$[PtCl_2(PEt_3)(Ar'Ar"PCl)]$	224
Equation 6.4	Synthesis of trans-$[PtCl_2(PEt_3)(Ar"_2PCl)]$	225
Equation 6.5	Synthesis of $[PtCl_2(PEt_3)_2(Ar"_2PH)]$	226
Equation 6.6	Synthesis of $[PtCl_2(PEt_3)(ArPBr_2)]$	227
Equation 6.7	Synthesis of $[PtCl_2(PEt_3)(Ar"_2PBr)]$	230
Equation 6.8	Synthesis of $[PtBr_2(PEt_3)(Ar"_2PBr)]$	234
Equation 6.9	Synthesis of $[PtBr_2(PEt_3)(Ar'PBr_2)]$ and $[PtBr_2(PEt_3)(Ar'"PBr_2)]$	234
Equation 7.1	Mechanism of the formation of diphosphenes with $W(PMe_3)_6$	255
Equation 7.2	Synthetic routes to phosphasilenes	258
Equation 7.3	Synthetic routes to germaphosphenes	259
Equation 7.4	Synthetic routes to stannaphosphenes	259
Equation 7.5	Synthesis of ArP=PAr	261
Equation 7.6	Synthesis of Ar'P=PAr'	262
Equation 7.7	Synthesis of ArP=AsAr	262
Equation 7.8	Synthesis of ArP=GeAr	263

Equation 7.9	Synthesis of ArP=SnAr	263
Equation 7.10	Proposed mechanism for the synthesis of a phosphaalkyne using PdL_4 and $RP=CCl_2$	265
Equation 7.11	Mechanism demonstrated by Angelici et al	266
Equation 7.12	Synthesis of $ArP(Cl)CHCl_2$	267
Equation 7.13	Synthesis of $ArP=CCl_2$	268
Equation 7.14	Synthesis of $Ar'P(Cl)CHCl_2$	269
Equation 7.15	Synthesis of $Ar'P(Cl)CHCl_2$	270

Table of Tables

Table 2.1	^{19}F and ^{11}B NMR data for the products of the reaction between ArLi and BCl_3	42
Table 2.2	NMR Data for $BF_nCl_{3-n}.Et_2O$ adducts ($3 \leq n \leq 0$)	42
Table 2.3	Selected Bond Distances and Angles for Ar_2BF	45
Table 2.4	δ ^{13}C (ppm) for $Ar"_3B$	50
Table 2.5	δ ^{1}H (ppm) for $Ar"_3B$	51
Table 2.6	Selected Bond Distances (Å) and Angles (°) for Ph_3B, Mes_3B, $Ar"_3B$ and $(2\text{-}CF_3C_6H_4)_3B$	53
Table 2.7	Short B---F contacts in $Ar*_3B$ and $Ar"_3B$	54
Table 2.8	^{11}B NMR chemical shifts for RBX_2 or R_2BX compounds	57
Table 2.9	Comparison between δ ^{11}B calculated and experimental	59
Table 2.10	Selected Bond Lengths (Å) and Angles (°) for Ar_2BX compounds	60
Table 2.11	Selected Bond Distances (Å) and Angles (°) for $Ar'B(OH)_2$ and $Ar"_3B$	60
Table 2.12	Short B---F Contacts (Å)	61
Table 2.13	Comparison between optimised and experimental structural data*	63
Table 3.1	δ ^{19}F for the different products of the reaction between Ar'Li/Ar"Li and $SiCl_4$	81
Table 3.2	Selected Bond Distances (Å) and Angles (°) for Ar_2SiHF, Ar_2SiF_2 and Ar'_2SiF_2	84
Table 3.3	Selected Bond distances (Å) and Angles (°) for $ArGeCl_3$	89
Table 3.4	Selected Bond Distances (Å) and Angles (°) in Ar_2GeCl_2 and $Ar"2GeCl_2$	90
Table 3.5	^{19}F NMR data for Silicon (IV) Compounds	96
Table 3.6	^{19}F NMR and ^{119}Sn NMR data for Germanium (IV) and Tin (IV) Compounds	97
Table 3.7	Selected Bond Distances(Å) and Angles (°) for Ar_2GeCl_2 and Ar_2SnCl_2	99
Table 3.8	Short E---F contacts	100
Table 4.1	Selected Bond lengths (Å) and Angles (°) for Ar_2PCl	115
Table 4.2	Comparison of Key Bond Distances (Å) and Angles (°) for Ar_2ECl (E=P, As, Sb or Bi)	116

Table 4.3	Selected Bond distances (Å) and Angles (°) for $ArPBr_2$.....	118
Table 4.4	Selected Bond distances and Angles for $RPBr_2$ compounds.....	120
Table 4.5	Signal assignments for ^{13}C spectrum of $Ar"_2PCl$.....	125
Table 4.6	Selected Bond distances (Å) and Angles (°) for $Ar"_2PCl$.....	126
Table 4.7	δ ^{13}C Assignments.....	129
Table 4.8	Selected Bond Distances (Å) and Angles(°) for $Ar"_2PBr$.....	133
Table 4.9	δ ^{1}H assignments for $Ar"_2PH$.....	135
Table 4.10	δ ^{1}H Assignments.....	146
Table 4.11	Selected Bond Distances (Å) and Angles (°) in Ar'Ar"AsCl and Ar_2AsCl.....	147
Table 4.12	δ ^{1}H assignments for Ar'Ar"AsCl.....	152
Table 4.13	Selected Bond distances (Å) and Angles (°) for Ar'Ar"AsH.....	153
Table 4.14	δ ^{13}C for $Ar'Ar"_2Sb$.....	157
Table 4.15	Selected Bond distances (Å) and Angles (°) for $Ar'Ar"_2Sb$, Ar_2SbCl and $SbAr_2OSO_2CF_3$.....	159
Table 4.16	δ ^{19}F and ^{31}P(ppm) for phosphorus compounds with Ar, Ar" and/or Ar" substituents.....	161
Table 4.17	δ ^{19}F chemicals shifts of arsenic compounds.....	162
Table 4.18	Selected Bond Distances (Å) and Angles (°) for Phosphorus Compounds.....	164
Table 4.19	Selected Bond Distances (Å) and Angles (°) for Arsenic Compounds.....	165
Table 4.20	Short E-F Contacts (E=P, As or Sb).....	167
Table 5.1	Comparison of fluorine chemical shift data at different temperatures.....	193
Table 5.2	Rates Determined by Lineshape Analysis.....	194
Table 5.3	Comparison of fluorine chemical shift data at different temperatures.....	196
Table 5.4	Comparison of fluorine chemical shift data at different temperatures.....	200
Table 5.5	$^{4}J_{P-F}$ coupling constants at different temperatures.....	201
Table 5.6	Comparison of fluorine chemical shifts at different temperatures for Ar'Ar"AsCl.....	203
Table 5.7	^{19}F chemical shifts at different temperatures for Ar'Ar"AsBr.....	205
Table 5.8	Comparison of the fluorine chemical shifts at different temperatures for Ar'Ar"AsH.....	206
Table 5.9	Thermodynamic parameters for Ar'Ar"EX and ArAr"PCl.....	210
Table 5.10	Bond distances (Å) in Ar'Ar"EX compounds.....	211
Table 5.11	Bond Angles (°) in Ar'Ar"EX compounds.....	211
Table 6.1	Different oxidation states of platinum.....	215
Table 6.2	Comparison of selected bond distances (Å) and angles (°) of $[PtCl_2(PEt_3)]_2$ at different temperatures.....	224
Table 6.3	δ ^{31}P and ^{19}F NMR data for $[PtCl_2(PEt_3)(Ar"_2PH)]_2$.....	227
Table 6.4	Initial δ ^{31}P NMR data for $[PtCl_2(PEt_3)(Ar'PBr_2)]$ and $[PtCl_2(PEt_3)(Ar"PBr_2)]$.....	229

Table 6.5 δ ^{19}F NMR data for $[PtCl_2(PEt_3)(Ar'PBr_2)]$ and $[PtCl_2(PEt_3)(Ar"PBr_2)]$..... 229

Table 6.6 ^{31}P chemical shifts and coupling constants of different products of the reaction between $Ar'PBr_2/Ar"PBr_2$ and $[PtCl_2(PEt_3)]_2$..... 230

Table 6.7 Comparison of crystal data between $[PtCl_2(PEt_3)]_2$ and $[PtBr_2(PEt_3)]_2$..... 233

Table 6.8 δ ^{31}P and ^{19}F NMR data for $[PtBr_2(PEt_3)(ArPBr_2)]$..... 233

Table 6.9 δ ^{31}P and ^{19}F NMR data for $[PtBr_2(PEt_3)(Ar"_2PBr)]$..... 234

Table 6.10 δ ^{31}P NMR data for $[PtBr_2(PEt_3)(Ar"PBr_2)]$and $[PtBr_2(PEt_3)(Ar'PBr_2)]$..... 235

Table 6.11 δ ^{19}F data for $[PBrl_2(PEt_3)(Ar"PBr_2)]$and $[PBrl_2(PEt_3)(Ar'PBr_2)]$.... 235

Table 6.12 Comparison of the chemical shifts upon bonding to the chloro-dimer..... 236

Table 6.13 Comparison of the chemical shifts upon bonding to bromo-dimer.... 237

Table 6.14 Coupling constant data for some Pt(II) complexes of phosphanes with Ar, Ar' or Ar" substituents..... 239

Table 7.1 δ ^{31}P, ^{29}Si and ^{119}Sn for metallaphosphenes..... 260

Table 7.2 Comparison of δ ^{31}P and ^{19}F between phosphanes and phosphaalkenes..... 271

Table 7.3 Assignments for *cis* and *trans* isomers..... 273

Table 7.4 Selected bond angles (°) and distances (Å)..... 274

Table 7.5 Assignments for *cis* and *trans* isomers..... 276

Abstract

Synthesis and Characterisation of Some Main-Group Compounds with Bulky Electron-withdrawing Substituents

Several new group 13, 14 and 15 derivatives with the ligands 2,4,6-$(CF_3)_3C_6H_2$ (Ar), 2,6-$(CF_3)_2C_6H_3$ (Ar') and / or 2,4-$(CF_3)_2C_6H_3$ (Ar") have been prepared. They have been characterised by multinuclear NMR spectroscopy and, for all isolated compounds, by elemental analysis and, where possible, single crystal X-ray diffraction.

Reaction of ArLi or the mixture Ar'Li/Ar"Li with BCl_3 has led to the characterisation of several mono- and disubstituted compounds, but attempted substitution in $AlCl_3$ was unsuccessful. Reaction of ECl_4 (E = Si, Ge, Sn) with the Ar'Li/Ar"Li mixture yielded predominantly the less sterically hindered disubstituted product $Ar"_2ECl_2$ for E = Si and Ge but to Ar'_2ECl_2 for E = Sn. In the case of B or Si, chlorine exchange is observed and Ar_2BF, Ar_2SiF_2 and Ar'_2SiF_2 have been synthesised. Ar_2SiF_2 is the only product identified in the reaction of ArLi with $SiCl_4$.

Reaction of ArLi or the Ar'Li/Ar"Li mixture, in an appropriate ratio, with group 15 derivatives gave rise to several mono-or disubstituted compounds of the type $ArEX_2$, Ar_2EX, $Ar'EX_2$, $Ar"EX_2$, $Ar"_2EX$ and Ar'Ar"EX (E = P or As; X = H, Cl or Br). ^{19}F NMR spectra of Ar'Ar"EX show that, for the two *ortho*-CF_3 groups of the Ar' moiety, there is free rotation of the aryl group around the central atom. A series of variable temperature studies has been carried out, and allowed the determination of the rotational energy barrier of the molecule.

For the first time, the molecular structures of derivatives containing three fluoroxyl ligands have been determined ($Ar"_3B$ and $Ar'Ar"_2Sb$).

The synthesis of some new platinum complexes has been facilitated by reaction of phosphanes with the platinum dimer $[(PtCl_2(PEt_3)]_2$ or $[(PtBr_2(PEt_3)]_2$. Reactions of the platinum dimer with arsane derivatives have not been successful. Halogen exchange was observed between bromophosphane ligands and Cl groups on the platinum.

Attempts have been made to synthesise new P=E derivatives containing the electron-withdrawing substituents Ar or Ar' via reaction with the chlorine abstractor $W(PMe_3)_6$. ArP=PAr and Ar'P=PAr' have been prepared. Synthesis of the first phosphaalkyne containing Ar or Ar' has been attempted by reacting a phosphaalkene with a Pt(0) species.

Stéphanie Cornet

Copyright

Declaration

This work was conducted in the Department of Chemistry at the University of Durham between October 1999 and October 2002. The work has not been submitted for a degree in this, or any other university. It is my own work, unless otherwise indicated.

"And now here is my secret, a very simple secret: It is only with the heart that one can see rightly; what is essential is invisible to the eye"

" Et maintenant voici mon secret, c'est très simple: On ne voit bien qu'avec le Coeur, l'essentiel est invisible pour les yeux"

Le Petit Prince.
Antoine de St Exupery

Acknowledgements

First and foremost, I would like to thank my supervisor, Dr. Keith Dillon, for his constant support and encouragement throughout my time in Durham. Thank you for making me enjoy research so much.

I am very grateful to all the technical staff: glassblowers, technicians, cleaners and everyone else who kept the department running and have helped to make my time here, at Durham, all the more pleasant. Thanks Val for keeping our lab as clean and tidy as possible and Dave Hunter for his help with the high-pressure experiments and his company in the "roof lab".
Special thanks go to Alan, Catherine and Ian in the NMR service for their kindness and good mood. They somehow managed to keep smiling even when I asked for loads of variable temperature experiments!

My gratitude goes to Dr Paul Hazendonk and Dr Mark Fox for their help with the calculations.
Many thanks extend to Dr Andrés Goeta and Dr Andrei Batsanov for determining some of my crystal structures, and a big hug to Amber Thompson for struggling with most of my crystals but after hours of hard work, succeeding in solving the structures.

Thank to all my colleagues and friends in the department: John, Aileen, Mark, Steven, Mark and David, Bob who had to share the lab 108 with a "frenchy" and for teaching me some nice English and Geordie expressions; Ben, I will miss our tea break and after work discussions; Lorna, Alison for our mad discussions and gym sessions; the "French connection" for their precious friendship, Elodie and Anne, for your friendship, your patience and teaching me how to cook; Jordan for your energy, your good mood and your support; Amel for your support and your kindness, Samia, Christophe and Romain for entertaining our lunchbreaks.
I met so great people since I arrived in Durham: Agathi, Michelle, Barbara, Shaheen, Bahma, etc, a part of me is now spread all over the world. May our friendship last forever despite the distances.
Sonia, without you, I would not have reached the end. I thank you for everything: your presence, your support, and our long conversations, for being my friend.

And everyone back to France, I wish to thank :

- the "chemistry gang". You all know who you are and if I try to name you all I'd sure miss someone out. Instead, I'll just thank you all for the laughs, and particularly, Sophe, my

half for practical classes and also your friendship. Soph, who were there for the good and bad time.

- the "scout family", Laurent, Julie, Fabien, Sandra, Cecile. Special hugs go to Mapie and Jeannot for their support when needed and letting me stay at their place so many times.
- the long term friends: Fred, Marina just for being there.
- and everyone I could have forgotten.

At last, I would like to thank my family, my parents who always believed in me, Cyril, Frédérique and Thierry, my grandmothers for their support and encouragements. Thanks are given for your letters, which kept me going throughout those three years. Thanks also go to my dad, my granddad and my uncle who, unfortunately, will not have the chance to read this thesis. Without all of you, this would have not been possible.

Remerciements

En premier lieu, je souhaite remercier mon superviseur, Dr Keith Dillon, pour son soutien et ses encouragements au cours de ces trois années a Durham. Merci pour m'avoir fait aimer la Recherche.

J'exprime toute ma gratitude à tout le personnel technique du département: les verriers, les techniciens, les femmes de ménages et tous ceux qui, de près ou de loin, aident à l'organisation du département. Merci à Val pour le ménage de notre labo et à Dave Hunter pour son aide avec les experiences à haute pression ainsi que pour m'avoir tenu compagnie dans le "roof lab". Un merci tout particulier au personnel de RMN, Alan, Catherine et Ian pour leur gentillesse et leur bonne humeur.

Ma gratitude va aussi à Dr Paul Hazendonk et Dr Mark Fox pour leur aide avec les calculs inclus dans ce travail.
Merci à Dr Andrés Goeta, Dr Andrei Batsanov pour la détermination de certaines structures crystallines. La plupart des structures ont été déterminées par Amber Thompson, que je remercie de sa patience et sa détermination.

Merci à tous mes collegues et amis du Département:

- John, Aileen, Mark, Steven, David et Bob qui ont partagé le lab 108 avec une "frenchy", et avoir aidé à l'amélioration de mon vocabulaire anglais et Geordie;
- Ben, nos pauses cafés, nos parties de solitaires, et nos discussions vont me manquer;

- Lorna et Alison pour nos folles conversations, votre amitié et nos sessions sportives.
- La "French connection" pour votre précieuse amitié: Elodie et Anne pour votre soutien, votre patience et vos leçons de cuisine; Jordan pour ta joie de vivre et ton soutien; Amel pour ta gentillesse et ton amitié. Samia, Christophe et Romain pour avoir animé nos pauses dêjeuner.

J'ai rencontré à Durham, des personnes formidables: Agathi, Michelle, Barbara, Shaheen, Bahma,... une part de moi est dispersée au quatre coins du monde. J'espère que notre amitié durera malgré la distance.

Sonia, sans toi, je n'y serai pas arrivé. Merci pour tout: ta présence, ton soutien, nos longues conversations téléphoniques. Merci d'être mon amie.

Un grand merci à tous ceux qui sont resté en France:

- "le gang de chimie": s'il vous arrive de lire ces lignes, vous vous reconnaitrez car si j'essaie de nommer tout le monde, je vais certainement en oublier. Merci pour tous les bons moments passés ensemble. Un merci particulier à Sophe, ma binome, et Soph, copines des bons et mauvais moments.
- le "famille scoute": Laurent, Julie, Fabien, Sandra, Cécile. Un merci particulier à Mapie et Jeannot pour votre soutien et pour votre hospitalité.
- les amies de longues... très longue date: Fred, Marina.
- et tous ceux que j'aurai pu oublier.

Enfin, je souhaite remercier ma famille: mes parents pour avoir toujours cru en moi, Cyril, Frédérique et Thierry, mes grand-mères pour m'avoir encouragé et soutenu. Merci à Papa, Papy et Jacques qui, malheureusement, n'auront pas la chance de lire cette thèse. Sans vous tous, ceci n'aurait jamais abouti.

ABBREVIATIONS

Ar, Fluoromes	2,4,6-tris(trifluoromethyl)phenyl
Ar', Fluoroxyl	2.6-bis(trifluoromethyl)phenyl
Ar"	2,4-bis(trifluoromethyl)phenyl
DBU	1,8-diazabicyclo[5,4,0]undec-2-ene
Ar*, Mes*, Supermes	2,4,6-tris(tertiarybutyl)phenyl
Mes	2,4,6-tris(trimethyl)phenyl
THF	Tetrahydrofuran
NMR	Nuclear Magnetic Resonance
s	singlet
d	doublet
m	multiplet
J	coupling constant
ppm	parts per million
Hz	Hertz
Me	methyl
Ph	phenyl
tBu	*tert*-butyl
HOMO	highest occupied molecular orbital
LUMO	lowest unoccupied molecular orbital
tht	tetrahydrothiophene
CCD	Charge Couple Device
tht	tetrahydrothiophene

Chapter 1
Introduction

1.1 Bulky and electron-withdrawing substituents

1.1.1 Introduction

The synthesis of multiple bonds between main group elements is generally achieved using kinetic stabilisation methods by the use of sterically demanding substituents.[1] The employment of a substantial number of bulky ligands appeared to be successful: t-butyl, mesityl, 2,4,6-tri(i-propyl)phenyl, 2,4,6-tri-(t-butyl)phenyl (supermesityl), tris(trimethylsilyl)methyl, etc. Bulky amido ligands such as $-N(SiMe_3)_2$, $-N(SiMe_2Ph)_2$ or $-Nmes(Bmes_2)$[2] have also shown great ability for the stabilisation of transition metal complexes with low coordination numbers. In addition, the use of bulky substituents to prepare multiple bond compounds such as Si=N,[3] Si=P,[4] and As=As[5] has been described. Thus, the ligands 2,4,6-tris(trifluoromethyl)phenyl (fluoromes) and 2,6-bis(trifluoromethyl)phenyl (fluoroxyl) should also be regarded as capable of stabilising the same kinds of compounds.

1.1.2 1,3,5-tris(trifluoromethyl)benzene (FluoromesitylH, ArH)

1.1.2.1 Introduction

1,3,5-Tris(trifluoromethyl)benzene was first prepared by McBee and Leech in 1947.[6] Later, Chambers *et al*[7] reported a new synthesis of this compound. This method involves the fluorination of benzene-1,3,5-tricarboxylic acid with SF_4 at high temperatures, to obtain the compound in 33% yield after work-up. Subsequently, Edelmann and co-workers[8] managed to increase this yield to 95%.

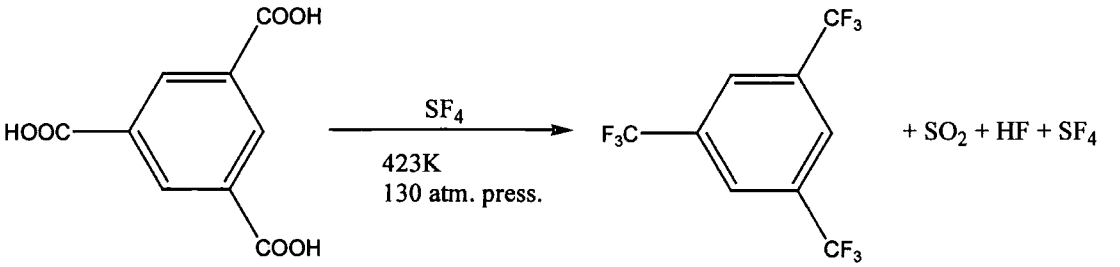

***Equation 1.1**: Synthesis of ArH*

Fluoromes is a very interesting ligand because of the ability of ArH to react with n-BuLi to give the lithiated product ArLi.

The first report concerning ArLi dates back to 1950 by McBee and Sanford.[9] In 1987, Chambers *et al*[7] described an improved synthesis via direct metallation of ArH with n-BuLi.

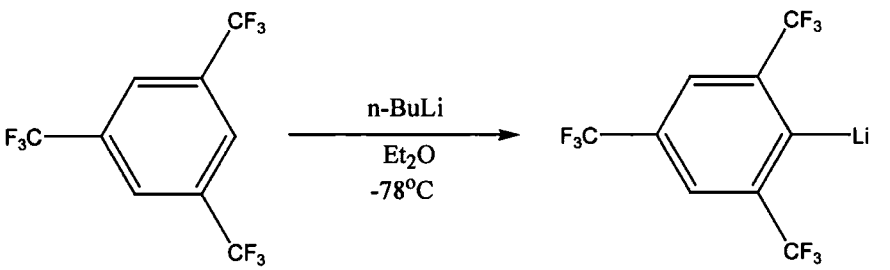

***Equation 1.2**: Synthesis of ArLi*

It has been found very convenient to prepare ArLi *in situ* and use the resulting solutions in diethyl ether/hexanes without further purification for subsequent reactions. $[ArLi.Et_2O]_2$ can be isolated by complete removal of the solvent and recrystallisation of the residue from hexanes.[10]

ArLi can be used to prepare numerous organometallic compounds. It can also be included in compounds of main group elements such as P, Ge, Sn, As, etc, usually by reaction with a suitable halogeno-derivative of the element.

1.1.2.2 Advantages of ArH

- Properties

Pure $1,3,5(CF_3)_3C_6H_3$ is a stable colourless liquid which boils at 118°C under atmospheric pressure. It has a faint, characteristic odour.

- Comparison with aryl or alkyl groups

By comparison with other aryl and alkyl groups, Ar is more oxygen- and moisture-stable when bonded to a main group element. Sterically, Ar is more bulky than 2,4,6-trimethylphenyl (mesityl), and less than 2,4,6-tri-^{t}butylphenyl (supermesityl).

When fluoromes is bonded to another element, the positions of the CF_3 groups play an important role:

- *ortho* and *para* CF_3 groups cause a withdrawal of electrons from the atom to which they are bonded. This element becomes then less electron-rich and less susceptible to electrophilic attack;
- as CF_3 groups are bulky electron-withdrawing groups, they are sterically hindering when they are in the *ortho*-position. Thus, any attack on the element to which the fluoromes ligand is attached is restricted. The CF_3 groups can also interact with this atom.

1.1.2.3 Reaction with heavier main group elements or transition metals

During the last 15 years, the Ar ligand has been demonstrated to be a highly versatile building block in main group chemistry. Due to its ideal combination of sterically and electronically stabilising effects, it has been successfully employed in the stabilisation of low coordination numbers around various main groups elements (groups 13, 14, 15, 16) and transition metals.

The easiest way to attach an element to the ligand is to react the lithiated compound ArLi with a metal halide, as described by Chambers and co-workers:[7]

$$x\ ArLi + MX_n \longrightarrow Ar_xMX_{n-x} + x\ LiX$$

- Group 13 derivatives

Very little use of the fluoromes ligand has been made in the context of the group 13 elements.

Goodwin[11,12] first reported the reaction of ArLi with boron trichloride to prepare $ArBCl_2$, Ar_2BCl, and Ar_3B. Interestingly, the formation of Ar_2BF via a chlorine/fluorine exchange was also mentioned.

$$ArLi + BCl_3 \longrightarrow ArBCl_2$$

$$2\ ArLi + BCl_3 \longrightarrow Ar_2BCl$$

$$3\ ArLi + BCl_3 \longrightarrow Ar_3B$$

$$Ar_2BCl \xrightarrow{F/Cl\ exch.} Ar_2BF$$

More recently, Gibson *et al*[13] reported the synthesis of a new boronic acid $Ar_2B(OH)$ and the preparation of transition metal complexes containing $-OBAr_2$. In a study of fluorophenylboron azides, Fraenk and co-workers[14] described the preparation and molecular structure of Ar_2BN_3 and Ar_2BOH.

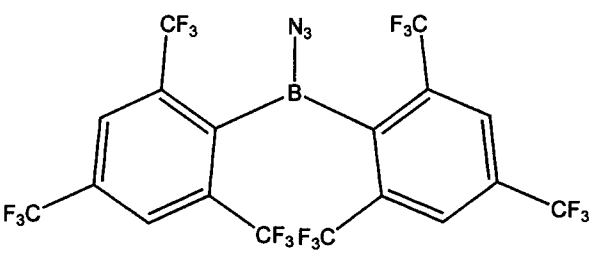

Figure 1.1: *Molecule of Ar_2BN_3*

No attempts have been reported with aluminium or thallium so far.

In 1993, Schluter *et al*[15] synthesised the first Ar derivatives of indium and gallium, and proved the capability of the fluoromes ligand to stabilise either Ga(III) or In(III) derivatives with M-M bonds:

$$MCl_x + ArLi \xrightarrow[-78^oC]{Et_2O} Ar_2M\text{-}MAr_2 \qquad (M= In, Ga)$$

The Ar ligand has also permitted the isolation of triaryl compounds Ar_3In or Ar_3Ga.[16] Interestingly, the reaction of ArLi with $GaCl_3$ gives a diethyl ether adduct, which when heated to 75°C leads to a dimeric product $[ArGa(\mu\text{-}Cl)Cl]_2$

$$ArLi + GaCl_3.Et_2O \xrightarrow{75^oC} [ArGa(\mu\text{–}Cl)Cl]_2$$

The *trans* isomer is formed preferentially because this conformation minimises the repulsions between the Ar moeties.

The chemistry of the 2,4,6-tris(trifluoromethyl)phenyl ligand with group 13 elements leads to the formation of mono, di- and tri-substituted compounds. M-M bonds and dimeric products have also been prepared. However, this group of elements remains an open field for the study of the Ar ligand, since just a few examples have been published.

- Group 14 derivatives

Contrary to group 13, there has been a wide use of the Ar ligand with group 14 elements. This includes a variety of purely organic compounds. A number of carbon-carbon reactions have been studied by Chambers and Filler.[7,17] Among the products is the carboxylic acid ArCOOH, the synthesis of which is simple and straightforward. Due to its strong steric hindrance, ArCOOH failed to undergo reactions such as esterification with ethanol.[17] Aldehydes and alcohols have also been prepared.

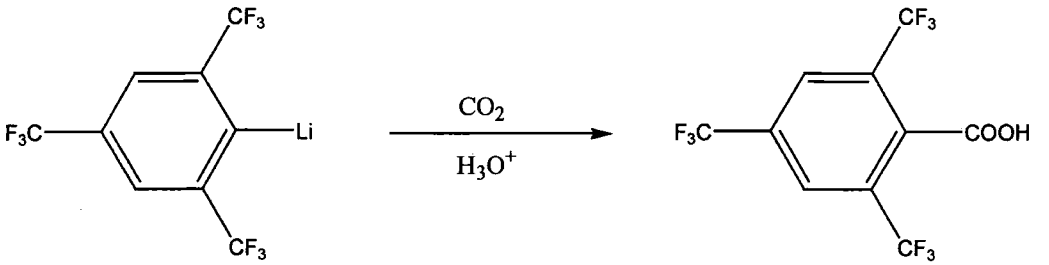

Equation 1.3: *Synthesis of ArCOOH*

Only four silicon derivatives have been described: $ArSiMe_3$,[7] Ar_2SiF_2,[18] Ar_2SiHF and Ar_2SiH_2.[19] Ar_2SiF_2 is the only isolable product when ArLi is reacted with $SiCl_4$ in a 2:1 ratio. The formation of this difluoride compound is the result of a fluorine exchange reaction involving the CF_3 groups of the fluoromes ligands.

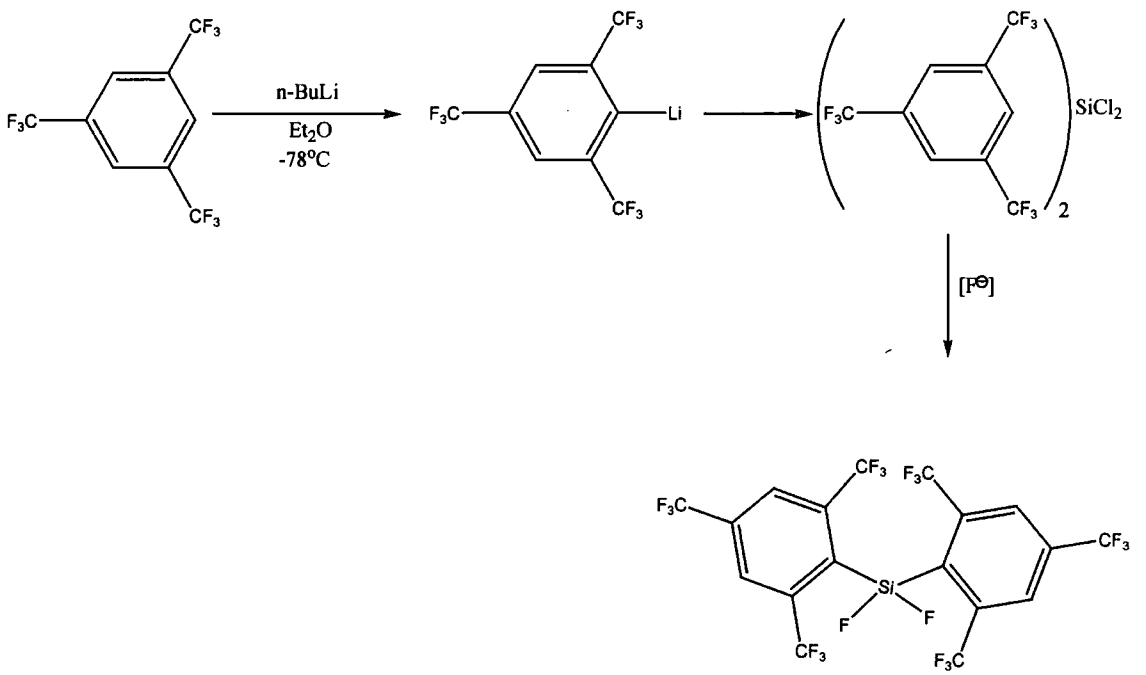

Equation 1.4: *Possible Mechanism for the formation of the difluoride derivative*[18]

This Cl/F halogen exchange also occurred in the reaction of trichlorosilane with ArLi:[19]

$$2\ ArLi + HSiCl_3 \xrightarrow[0^oC]{Et_2O} Ar_2SiHF$$

The first germanium derivative was synthesised by Bender *et al*[20] as a Ge(II) compound: Ar_2Ge formed by the reaction of ArLi with $GeCl_2$.dioxane. To explore the issue of M-Ge π bonding, $[(PPh_3)_2NiGeAr]$[20] has been synthesised. Ar_2GeH_2[21] was also prepared. The reaction of ArLi with $GeCl_4$ leads to Ge(IV) derivatives, $ArGeCl_3$ and Ar_2GeCl_2.[22]

Tin derivatives have been more extensively studied. The reaction of ArLi with $SnCl_2$ led to the formation of the first monomeric diarylstannylene Ar_2Sn.[23] This compound is stabilised by intramolecular fluorine-tin contacts (Figure 1.2). Ar_2Sn represents a useful starting material for the preparation of novel tin(IV) derivatives containing the Ar ligand.[24,25]

The reaction of Ar_2Sn with PhSnSnPh or $Ag(O_2CCF_3)$ gives rise to $Ar_2Sn(SnPh)_2$ and $Ar_2Sn(O_2CCF_3)_2$ respectively.

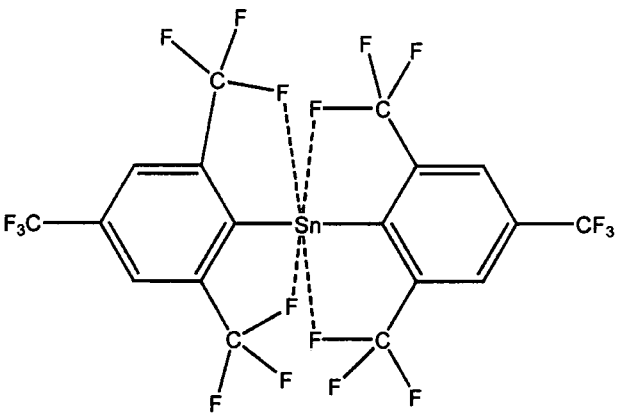

Figure 1.2: *Intramolecular Sn---F interactions*[26]

Some dimeric species have been isolated. Oxidation of Ar_2Sn in the presence of Cl^- led to the formation of the μ_2-oxo bridged dimeric tin(IV) species $Ar_2(Cl)Sn(\mu_2\text{-}O)Sn(Cl)Ar_2$.[27] One crystal modification of Ar_2Sn consists of the dimeric compound $Ar_2Sn\text{-}SnAr_2$ (as found for In and Ga) that shows a very weak tin-tin interaction. Ar_2Sn is a useful precursor for cycloaddition reactions leading to three-, four-, or five- membered tin-

containing rings systems.[28] Figure 1.3 below summarizes a series of heterocycles, which can be formed:

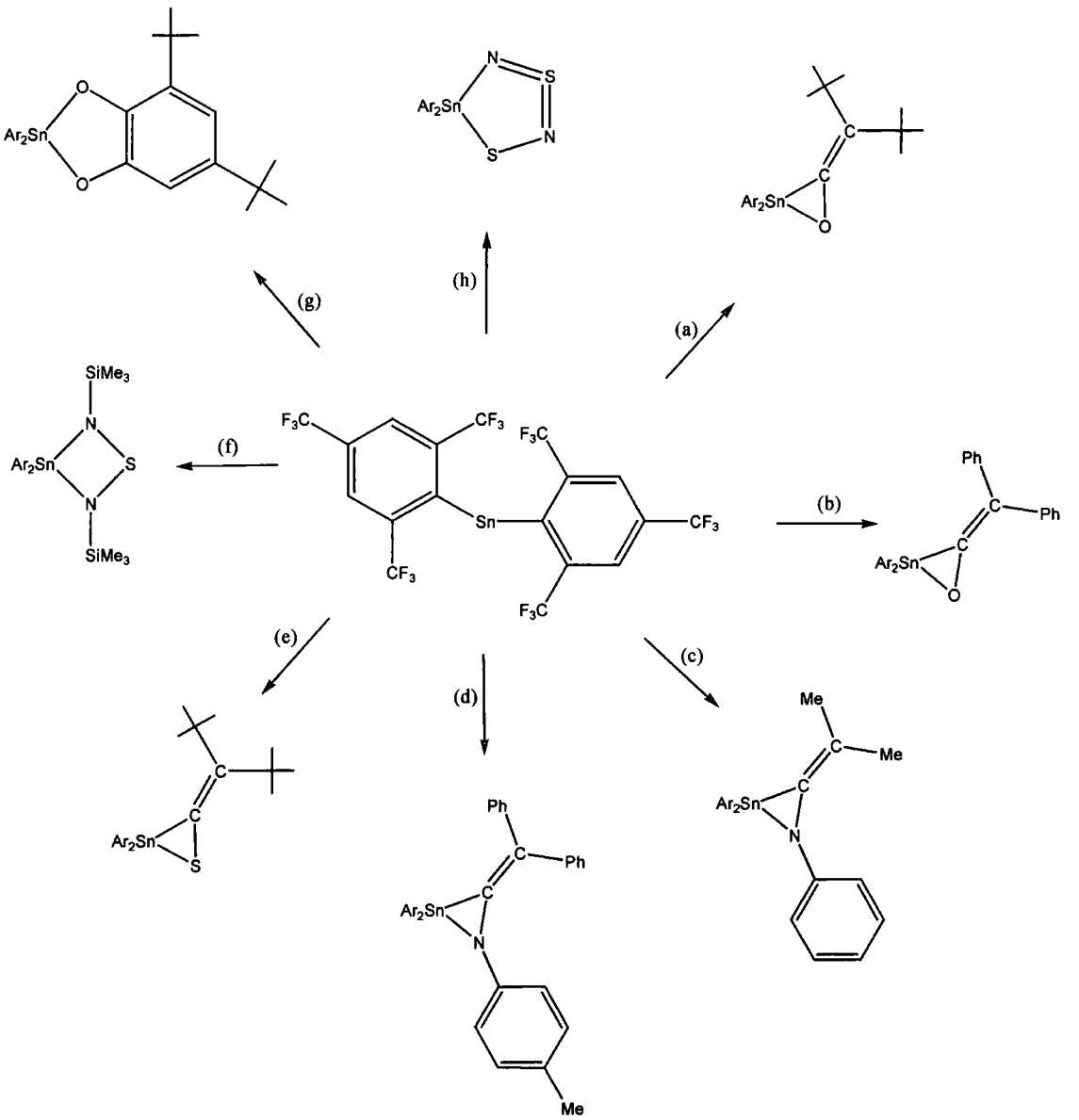

Reagents: (a) t-$Bu_2C{=}C{=}O$, (b) $Ph_2C{=}C{=}O$, (c) $Me_2C{=}C{=}NPh$, (d) $Ph_2C{=}C{=}NC_6H_4Me$-*p*, (e) t-$Bu_2C{=}C{=}S$, (f) $Me_3SiN{=}S{=}NSiMe_3$, (g) 3,5-di-t-butyl-o-benzoquinone, (h) S_4N_4

Figure 1.3: *Formation of heterocycles from* Ar_2Sn

Ar_2Sn readily undergoes oxidation reactions to afford the corresponding Sn(IV) species. For example, treatment of Ar_2Sn with AsF_5 yields Ar_2SnF_2.[25] In addition, fluorination of Ar_2Sn using XeF_2 also provides Ar_2SnF_2. Ar_2SnCl_2 can be prepared by chlorinating Ar_2Sn with elemental chlorine.

$$Ar_2Sn \xrightarrow{AsF_2 \text{ or } XeF_2} Ar_2SnF_2$$

$$Ar_2Sn \xrightarrow{Cl_2} Ar_2SnCl_2$$

Tin(IV) derivatives can also easily be prepared by reacting ArLi directly with $SnCl_4$:[22]

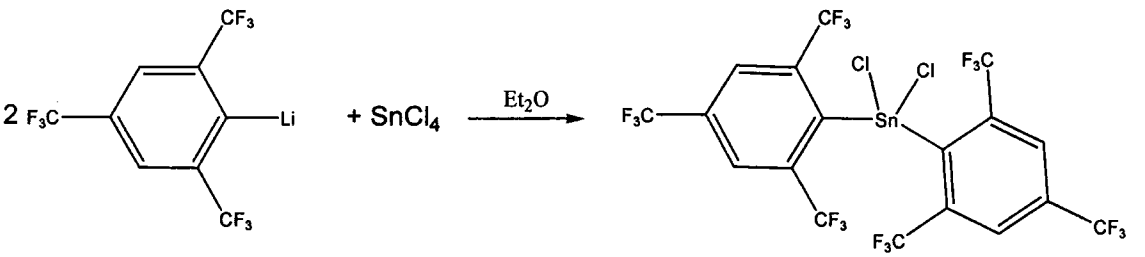

Equation 1.5: *Synthesis of Ar_2SnCl_2*

The steric properties of Ar also allowed the preparation of the first diarylplumbylene by the reaction of ArLi with $PbCl_2$.[29]

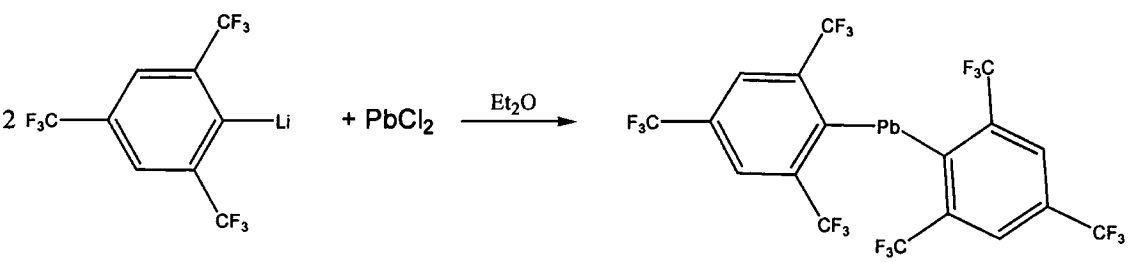

Equation 1.6: *Synthesis of Ar_2Pb*

This compound is far less reactive than its tin homologue Ar_2Sn:[23,30,31] Ar_2Pb does not undergo reaction leading to organolead(IV) compounds. The only other lead derivatives containing the Ar ligand reported are the plumbylene $(SiMe_3)ArPb=PbAr(SiMe_3)$[32] and a thiolate cluster $Pb_5O(SAr)_8.2C_7H_8$.[33]

- Group 15 derivatives

The 2,4,6-tris(trifluoromethyl)phenylamino ligand has shown a great ability to stabilise group 15 compounds as well as transition metal derivatives. 2,4,6-tris(trifluoromethyl)phenylamine reacts with KH to give ArNHK. The latter can react with main group element halides such as PCl_3 or $AsCl_3$, leading to the formation of a dimer.[34]

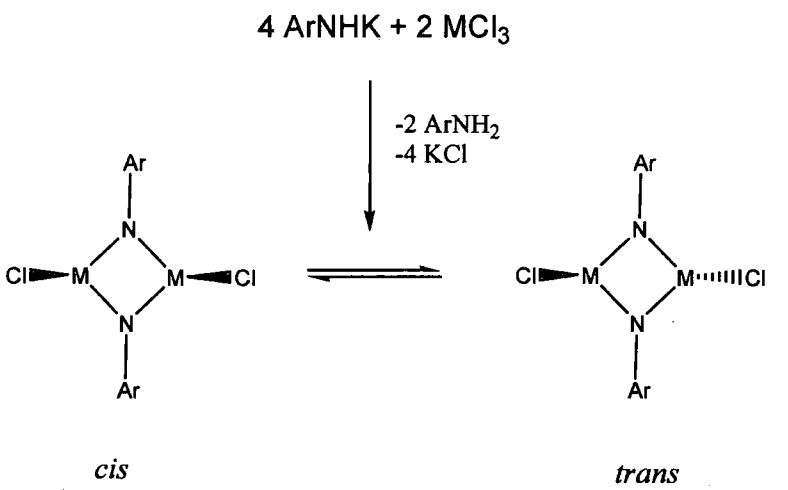

Equation 1.7: *Formation of dimer*

Recently, Roesky *et al* described the preparation of 2,4,6-tris(trifluoromethyl)phenylamine in a four-step synthesis.[35] The phenylamine ligand can then be used in various reactions to form monosilylated and bisilylated amines.

Phosphorus derivatives containing the fluoromes substituent constitute a fairly large and well-investigated class of compounds. Treatment of ArLi with the appropriate amount of

phosphorus trichloride leads to the formation of the mono- or di-substituted compounds, $ArPCl_2$ or Ar_2PCl.[8,11]

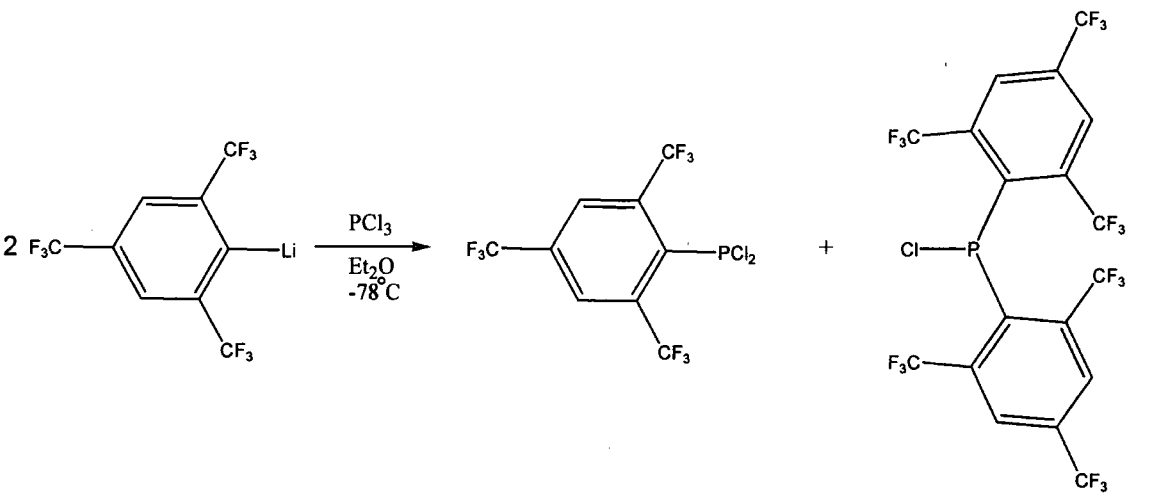

Equation 1.8: *Synthesis of $ArPCl_2/Ar_2PCl$*

The dichlorophosphane $ArPCl_2$ is easily reduced by $LiAlH_4$[8] or Bu_3SnH[12,36] to give the primary phosphane $ArPH_2$. The action of SbF_3 on $ArPCl_2$ leads to the formation of $ArPF_2$. $ArP(CN)_2$ is obtained by cyanide substitution of chloride. Ar_2PH was obtained by reduction of Ar_2PCl. However, the fluorination of the di-substituted product with SbF_3 only led to a very small amount of Ar_2PF (5% conversion).[37] Steric hindrance around the P-Cl bond makes substitution reactions (S_N1 or S_N2) difficult.

$$ArPCl_2 + 2\ Bu_3SnH \longrightarrow ArPH_2 + 2\ Bu_3SnCl$$

$$ArPCl_2 + 1/2\ LiAlH_4 \longrightarrow ArPH_2 + 1/2\ LiAlCl_4$$

$$ArPCl_2 + SbF_3 \longrightarrow ArPF_2 + SbCl_2F$$

$$ArPCl_2 + 2\ AgCN \longrightarrow ArP(CN)_2 + 2\ AgCl$$

Ar_2PH was used as a starting material to synthesise the first phosphonium phosphide $(Ph_3PMe)^+(Ar_2P)^-$:[38]

$$Ph_3P{=}CHR + Ar_2PH \xrightarrow{\text{toluene}} (Ph_3\overset{\oplus}{P}CH_2R\text{----}\overset{\ominus}{P}Ar_2)$$

$ArPCl_2$ appears to be a good precursor to form phosphorus compounds containing the Ar ligand.[39]

$$Li(C_5Me_5) + ArPCl_2 \longrightarrow C_5Me_5P(Cl)Ar + LiCl$$

The fluoromes ligand has also allowed the formation of multiple bonded compounds. The condensation of $ArPCl_2$ with $ArPH_2$ has led to the first diphosphene containing the Ar ligand.[8,11] This compound has shown an unusual stability. The chemistry of diphosphenes will be more extensively described later in this chapter (section 1.2). In addition, Dillon and co-workers[40] first reported the preparation of phosphaalkenes containing the Ar group on phosphorus.

$$CHLiCl_2 + ArPCl_2 \longrightarrow ArP(CHCl_2)Cl \xrightarrow{DBU} ArP{=}CCl_2$$

Much less is known about fluoromes derivatives of the heavier group 15 elements. A 1:1 ratio reaction between ArLi and $AsCl_3$ was attempted and resulted in the formation of the di-substituted product Ar_2AsCl,[41] whose crystal structure was reported very recently by Burford *et al.*[42] The synthesis of the dichloroarsane $ArAsCl_2$ was first described by Roesky and co-workers,[43] and more recently by Xue.[22]

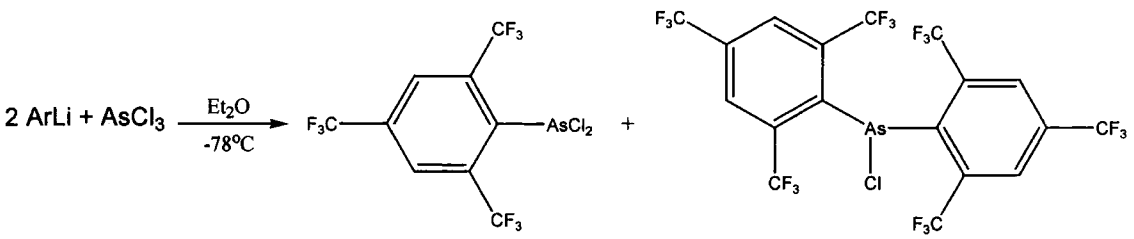

Equation 1.9: *Synthesis of $ArAsCl_2/Ar_2AsCl$*

ArLi readily reacts with AsF_3 to give the disubstituted product Ar_2AsF. $LiAlH_4$ reduction of Ar_2AsF produces the secondary arsine Ar_2AsH.[25] Treatment of $ArAsCl_2$ with potassium 2,4,6-tris(trifluoromethyl)anilide led to the formation of the first iminoarsane.[43]

Antimony trichloride reacts with ArLi in a 1:1 or 1:2 ratio to give $ArSbCl_2$ or Ar_2SbCl respectively.[11,18] The reaction of Ar_2SbCl with $AgOSO_2CF_3$ afforded crystals of $Ar_2Sb(OSO_2CF_3)$.[42]

Only two well-characterised bismuth derivatives are known: Ar_2BiCl and Ar_3Bi.[44] The latter was the first example of a group 15 atom accommodating three bulky Ar ligands.

$$3\ ArLi + 2\ SbCl_3 \xrightarrow[0^oC]{Et_2O} ArSbCl_2 + Ar_2SbCl$$

$$5\ ArLi + 2\ BiCl_3 \xrightarrow{Et_2O} Ar_2BiCl + Ar_3Bi$$

- Group 16 derivatives

The chemistry of fluoromes with this group of elements has been focused on ArOH and ArSH, which have been found to be highly valuable precursors for a number of unusual Ar derivatives.

ArOH is prepared by reacting ArLi with $Me_3SiOOSiMe_3$:[45]

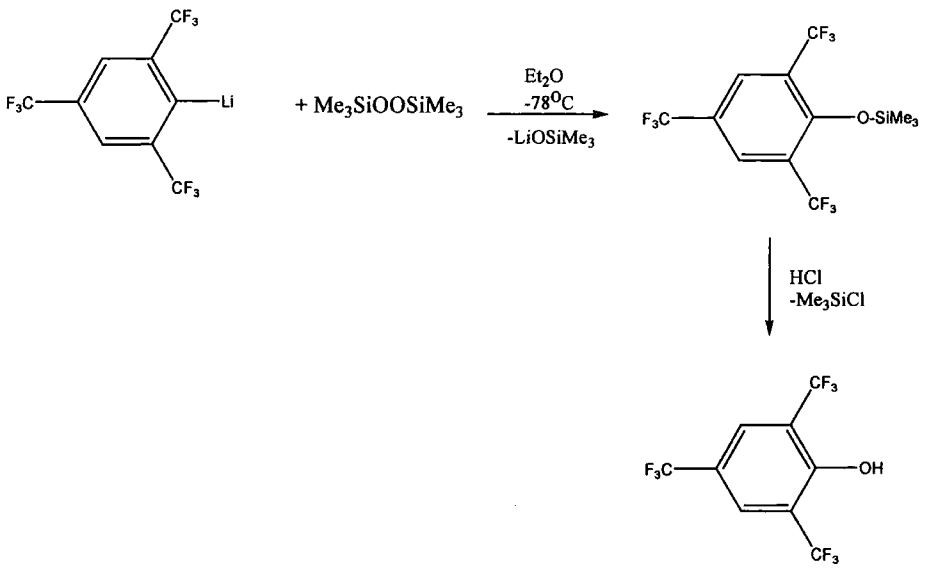

***Equation 1.10**: Synthesis of ArOH*

The phenol served as a starting material for a variety of main group and transition metal phenoxides.

Alkali metal phenoxides can be prepared by direct reaction of ArOH with n-BuLi or NaH to give $LiOAr.Et_2O$ and NaOAr.THF respectively. ArOH can also react with $MN(SiMe_3)_2$ (M=Li, Na, K), leading to the formation of $[MOAr(THF)_x]_2$.[46,47] Bis(phenoxides) have also been isolated as their THF adducts.$(ArO)_2M(THF)x$ (x = 1, M = Ba, Be, Sn; x = 2, M = Cd,; x = 3, M = Mg, Ca, Mn).[46] Edelmann *et al*[45] were first to describe the preparation of the ArO- ligand. Like Ar, the ArO- ligand has been found to stabilise low-coordination numbers around metal atoms: for example Tl(I) and In(I) derivatives.[48]

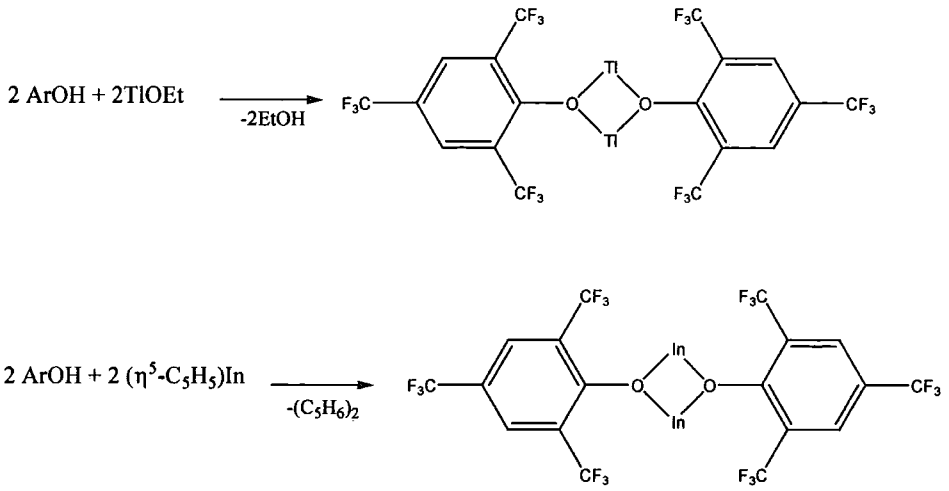

***Equation 1.11**: Synthesis of $(ArOTl)_2$ and $(ArOIn)_2$*

These compounds represent the first structurally characterised examples of two-coordination at thallium and indium.

A C-F bond activation has been noticed in an attempted synthesis of $(ArO)_3Bi$ by reaction of $BiCl_3$ with NaOAr in THF. Instead, this led to the formation of a highly crowded condensation product arising from the coupling of the ArO units with elimination of three *ortho*-fluorine atoms (Equation 1.12).[44]

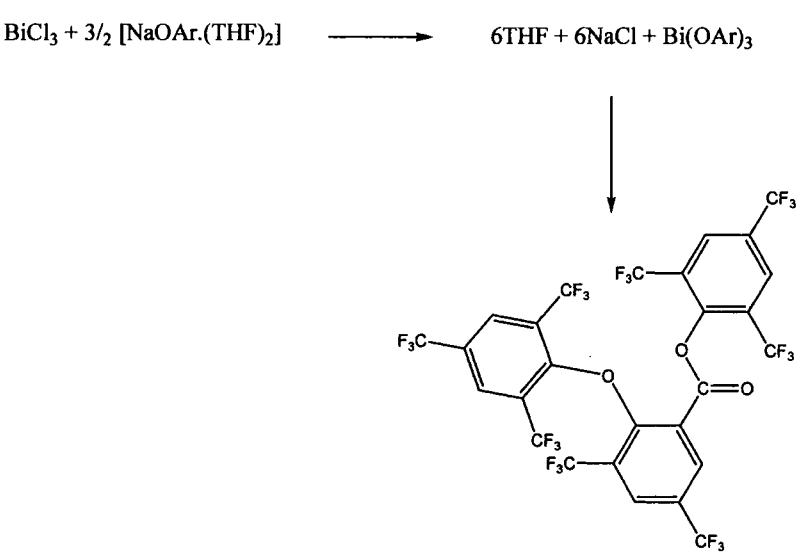

***Equation 1.12:** Attempted synthesis of $(ArO)_3Bi$*

2,4,6-tris(trifluoromethyl)phenol can also react with the lanthanide compounds $(C_5H_5)_3Ln$ (Ln = Nd, Sm, Yb) to give the mononuclear bis(cyclopentadienyl)lanthanide alkoxides $(C_5H_5)_2Ln(THF)(OAr)$.[49]

Another precursor is the thiol ArSH, which was first prepared by Chambers *et al,*[7] by treatment of ArLi with elemental sulfur.

$$ArLi + S_8 \longrightarrow ArSH$$

Like ArOH, ArSH can be used to prepare various main group and transition metal derivatives. Two main routes are used to synthesise these compounds:[50]

- metathesis reactions between NaSAr and metal halides
- protolysis of metal bis(trimethylsilyl)amides with ArSH.

For example:

$$ZnCl_2 + 2\ NaSAr \xrightarrow{Et_2O} Zn(SAr)_2 + 2\ NaCl$$

$$PbAr_2 + 2\ ArSH \xrightarrow{\text{n-hexane}} Pb(SAr)_2 + 2\ ArH$$

$$PbCl_2 + 2\ NaSAr \xrightarrow{Et_2O} Pb(SAr)_2 + 2\ NaCl$$

$$Mn((NSiMe_3)_2)_2.THF + 2\ ArSH \xrightarrow{\text{toluene}} Mn(SAr)_2.THF + 2\ HN(SiMe_3)_2$$

Some thallium and indium derivatives have also been described.[51]

$$TlOEt + ArSH \longrightarrow 1/n\ [TlSAr]_n + EtOH$$

$$Tl_2CO_3 + 2\ ArSNa \longrightarrow 2/n\ [TlSAr]_n + Na_2CO_3$$

Coordination of three fluoromes ligands has been observed in the indium derivative $(ArS)_3In(Et_2O)$.

Like the phenol ligand, ArSH reacts with lanthanide compounds such as $Yb(C_5H_5)_3$ in THF to give $(C_5H_5)_2Yb(thf)(SAr)$.[25]

Selenium also provides a rich field in fluoromes chemistry. Selenium may be inserted into ArLi to give the intermediate ArSeLi, which appears to be highly air-sensitive. Complete air-oxidation of ArSeLi leads to the formation of ArSe-SeAr.[52]

$$ArLi + 1/_8\ Se_8 \longrightarrow ArSeLi$$

$$ArSeLi + 2\ H_3O^+ + 1/_2\ O_2 \longrightarrow [ArSe]_2 + 2\ Li^+ + 3\ H_2O$$

$[ArSe]_2$ is cleaved by Cl_2 or Br_2 to produce ArSeCl or ArSeBr respectively. These halogeno-compounds have served as starting materials to form new selenium-nitrogen bonds:

$$[ArSe]_2 + X_2 \longrightarrow 2\ ArSeX \qquad (X=Cl, Br)$$

$$2\ ArSeX + (Me_3SiN)_2S \longrightarrow [ArSeN]_2 + 2\ XSiMe_3$$

$$ArSeX + Me_3SiNSO \longrightarrow ArSeNSO + XSiMe_3$$

The discovery of the stable selenol ArSeH allowed the formation of various main group and transition metal selenolate derivatives containing the ArSe moiety. The synthetic method involves the reaction of metal bis(trimethylsilyl)amides with appropriate amounts of ArSeH (M=Mn, Zn, Cd, Hg, Ge, Sn, Pb):[50]

$$M[N(SiMe_3)_2]_2 + 2\ ArSeH \longrightarrow M(SeAr)_2 + 2\ HN(SiMe_3)_2$$

Indium, antimony and bismuth ArSe derivatives are prepared by reacting metal halides with the corresponding alkali metal selenophenolates:

$$MCl_3 + 3\ NaSeAr \longrightarrow M(SeAr)_3 + 3\ NaCl$$

Recently, Edelmann and co-workers[39] reported the synthesis of a tin(IV) complex $Sn(SeAr)_4$. The latter was obtained by treatment of the tin(II) complex of bis[bis(trimethylsilyl)amide] with ArSeH

$$2\ Sn[N(SiMe_3)_2]_2 + 4\ ArSeH \longrightarrow Sn(SeAr)_4 + Sn^0 + 4\ HN(SiMe_3)_2$$

Insertion reactions of carbenes and carbene fragments have been studied. ArSe-SeAr reacts with diazomethane to give rise to $ArSe\text{-}CH_2\text{-}SeAr$. Complexes containing Sm-E bonds (E = S, Se, Te) have also been synthesised by reaction of $[ArSe]_2$ with $Cp_2^*Sm(THF)_2$.[53]

$$1/_2\ [ArSe]_2 + Cp_2^*Sm(THF)_2 \xrightarrow[-THF]{toluene}$$

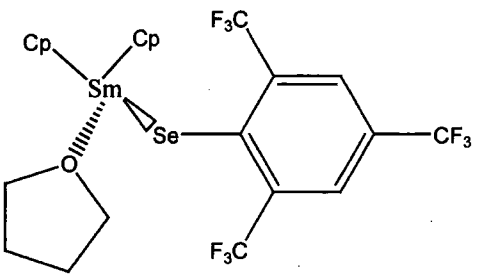

Equation 1.13: *Synthesis of $ArSe(Cp_2^*Sm(THF))$*

The chemistry of tellurium compounds is not well developed.[25] It was found that ArLi does not react directly with elemental tellurium to form the corresponding ArTeLi. However, this intermediate is formed when $Bu^n{}_3PTe$ is used as a soluble tellurium source. ArTeLi is readily oxidised to form $[ArTe]_2$. $[ArTe]_2$ decomposes under the influence of heat or light to form Ar_2Te:[39]

$$ArLi + Bu^n{}_3PTe \longrightarrow ArTeli + Bu^n{}_3P$$

$$2\ ArTeLi + O_2 \longrightarrow Ar_2Te_2 + Li_2O$$

$$Te_2Ar_2 \longrightarrow Ar_2Te + Te$$

- Transition and other metal derivatives

The chemistry of transition metal containing σ-bonded fluoromes ligand remains an open field. Because of the possibility of short M---F interactions involving the *o*-CF_3 groups, the Ar ligand was thought to be an interesting ligand for transition metals. Several points of interest can arise with fluoromes ligand:

- crowding restricts rotation around M-C bonds;
- M---F interactions are frequently found in Ar complexes involving *o*-CF_3;
- fluoromes should give a high degree of axial protection in a square planar configuration.

Initial studies have indicated that Ar is not likely to be a good ligand for early transition metals. Treatment of $NbCl_5$ or WCl_6 with various equivalents of ArLi did not produce any isolable compounds.[25] The preparation of $ArReO_3$ has been reported by reaction of Ar_2Zn with Re_2O_7.[25] More recently, Gibson and co-workers[54] reported the synthesis of vanadium complexes obtained by treatment of ArLi with $[VCl_3(thf)_3]$. Group 6 transition metal (Cr or Mo) complexes containing σ-bonded fluoromes ligand have also been described.[55,56] These compounds contain M---F secondary interactions, which play a significant role in stabilising the structures of Ar complexes of group 6 transition metals. These interactions seem to lengthen the C *ipso*-C *ortho* distances.

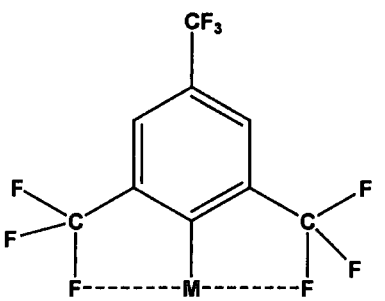

Figure 1.4: *Interactions between the metal and the fluorine atoms*

Some complexes containing group 9 and 10 elements have been reported: Ar_2Co, Ar_2Ni[57]and $Ar_2Ni(MeOCH_2CH_2OMe)$.[58] Variable temperature NMR studies of the latter Ni complex have shown that only two of the fluorines in *o*-CF_3 groups interact with the Ni centre. Some palladium complexes have been prepared by treatment of ArLi with a variety of chloro complexes of palladium(II).[59] The coordination of two bulky Ar groups on Pd(II) led to the formation of very crowded square planar complexes.

Few examples have been given with group 11 elements. A complex containing Cu(I) has been mentioned. Recently, Espinet *et al* reported the first Ar derivatives of Au(I) and Au(III).[60]

$$ArLi + [AuCl(tht)] \longrightarrow [AuAr(tht)]$$

[AuAr(tht)]* is a general precursor for various gold complexes. (tht) can easily be replaced by others ligands such as PPh_3 or P(*o*-tol)$_3$.

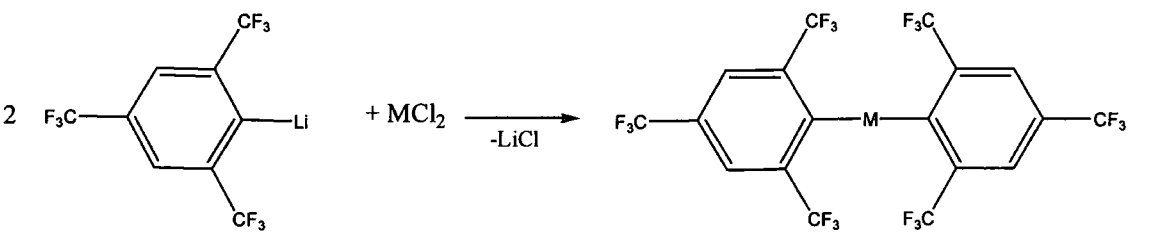

M= Zn, Cd, Hg

Equation 1.14: *Synthesis of Ar_2M (M = Zn, Cd, Hg)*

Significant results have been obtained with Ar derivatives of the group 12 elements. ArLi reacts with anhydrous $ZnCl_2$ to give Ar_2Zn.[61]

The corresponding cadmium and mercury[7] compounds were prepared analogously from cadmium diiodide or mercury dichloride. The two-coordinate monomeric structure of Ar_2Zn represents a new structural type for zinc diaryls.

* tht: tetrahydrothiophene

Using the Metal Vapour Synthesis method (MVS), Sequeira[62] prepared a series of π-complexes containing 1,3,5-tris(trifluoromethyl)benzene as a ligand.: $M(\eta^6\text{-ArH})_2$ with M=Cr, V, Nb, Ru. The ArH ligand has demonstrated the ability to bind to metals in a η^6-arene fashion.

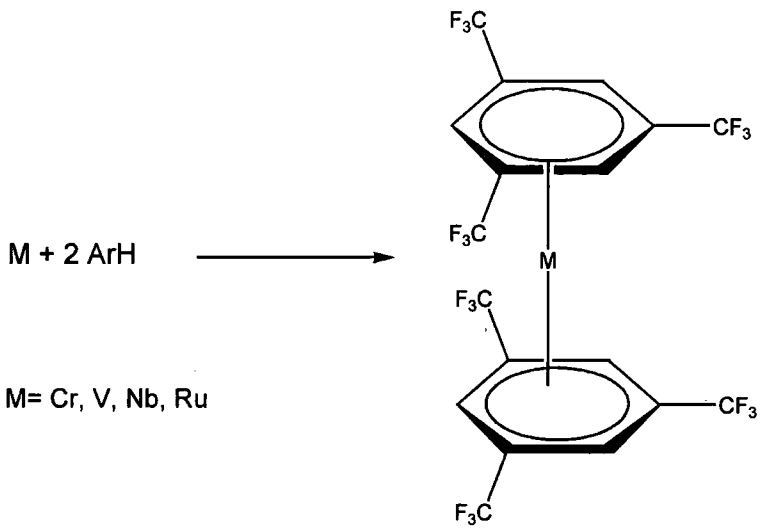

Equation 1.15: *Synthesis of* $M(\eta^6\text{-ArH})_2$

- Conclusion

In most of the Ar main group element compounds, structural analyses have shown that the M-C bond distance is longer than in the mesityl analogues, reflecting the large steric demands of the Ar ligands. However, in some cases, this is also due to electrostatic ligand-ligand repulsions, which lead to a lengthening of the bond rather than a widening of angles.

M---F intramolecular interactions between the central atom and some of the fluorines of the *ortho*-CF_3 groups are also responsible for the stabilisation of complexes containing the fluoromes ligand. The potential of forming weak M---F interactions means that the Ar group is capable of inhibiting oligomerisation, which is shown, for example, by its ability to stabilise a diaryl stannylene.[28]

1.1.3 1,3-bis(trifluoromethyl)benzene (FluoroxylH, Ar'H)

1.1.3.1 Properties

Fluoroxyl groups are quite similar to fluoromes. Instead of containing three CF_3 groups, they only have two. This substituent can easily be bonded to main group elements via a lithiated product. Like fluoromes, fluoroxyl is strongly electron-withdrawing. This is particularly caused by the position of the CF_3 groups, which can be both in the *ortho*, or one in the *ortho* and one in the *para* position. The boiling point of 1,3-bis(trifluoromethyl)benzene is 116°C

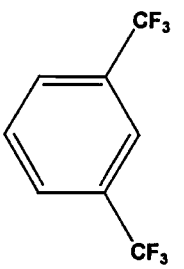

***Figure 1.5**: 1,3-bis(trifluoromethyl)benzene*

1.1.3.2 Comparison between ArH and Ar'H

Fluoromesityl and fluoroxyl are both bulky and strongly electron-withdrawing substituents, due to the presence of CF_3 groups in the *ortho* position. The greatest differences between them are the number of bulky trifluoromethyl groups, and then the number of reaction sites. In fluoromesityl, there is only one reaction site available, resulting in two CF_3 groups in *ortho* positions and one CF_3 group in the *para* position (site A, Figure 1.6). Fluoroxyl has three different reaction sites (Figure 1.6):

- two CF_3 groups in the *ortho* position (site B)
- one CF_3 group in the *ortho* position and one in the *para* (site C)

- two CF_3 groups in the *meta* position (site D)

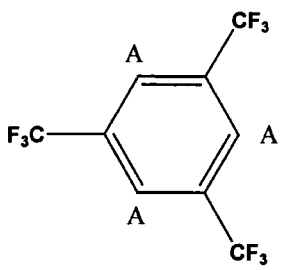

Fluoromes

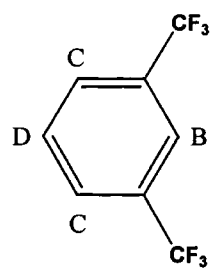

Fluoroxyl

Figure 1.6: *Substitution sites in Fluoromes and Fluoroxyl*

The reaction site D is the least likely site in the reaction with BuLi because of the absence of CF_3 groups in the *ortho* position, which play an important role in the stabilisation of the molecule. D is also disfavoured because the activated sites for Li substitution are the positions *ortho* and *para* to CF_3 groups.

Like ArH, Ar'H reacts easily with BuLi to form a lithiated compound. The lithiation of fluoromes leads to only one product. In fluoroxyl, due to the directional functionality of the CF_3 groups, the *ortho* and *para* positions will become electron-deficient, and then the hydrogen atom will be susceptible to nucleopilic attack by the butyl group.

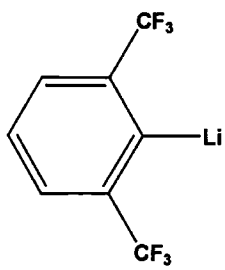

Ar'Li

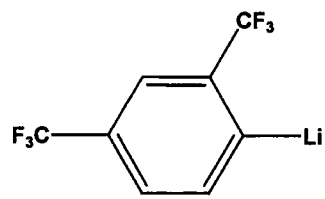

Ar"Li

Figure 1.7: *Probable lithiation sites for Fluoroxyl*

With two *ortho*-CF_3 groups in the Ar'Li compound, the lithiated site is sterically hindered. An interaction between Li and some of the fluorine atoms is therefore probable. In the Ar"Li compound, one CF_3 group only hinders the lithiated site and Li---F interactions may thus be fewer than in Ar'Li. The reaction of a metal chloride MX_3 (for a group 13 or 15 element) with lithiated compounds can lead to mono and di-substituted products. (Figure 1.8)

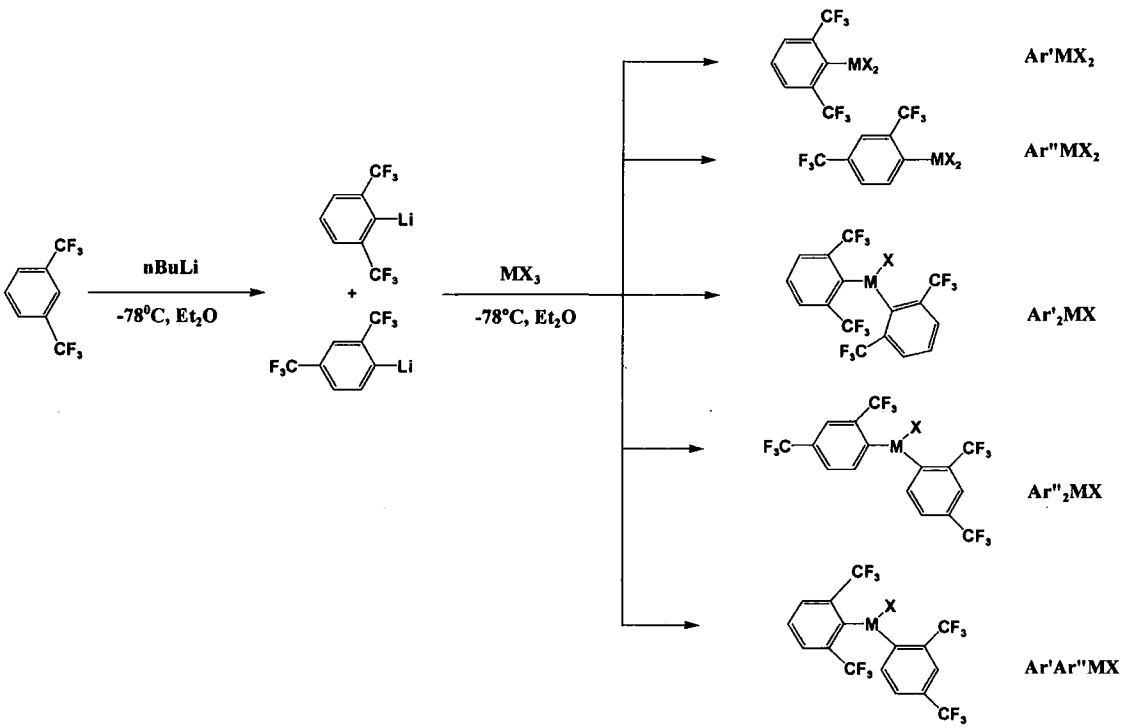

Figure 1.8: *Different products of the reaction of A'Li/Ar"Li with MX_3*

1.1.3.3 Reaction with heavier main group elements or transition metals

To date, little has been published about the 2,6-$(CF_3)_2C_6H_3$ group as a substituent, partly because of the complications in the chemistry of the precursor 1,3-bis(trifluoromethyl)benzene, Ar'H. As explained earlier, this can lithiate in two positions, giving rise to a mixture of 2,6-$(CF_3)_2C_6H_3$ (Ar') and 2,4-$(CF_3)_2C_6H_3$ (Ar'') derivatives.

- Group 14 derivatives

Xue[22] synthesised a series of Si and Ge derivatives, which are symmetrical molecules containing two Ar" moieties; $Ar"_2SiCl_2$ and $Ar"_2GeCl_2$. They were prepared by reaction of the mixture Ar'Li/Ar"Li with $SiCl_4$ or $GeCl_4$ respectively and were characterised by elemental analyses, ^{19}F NMR spectroscopy and single crystal X-Ray diffraction.

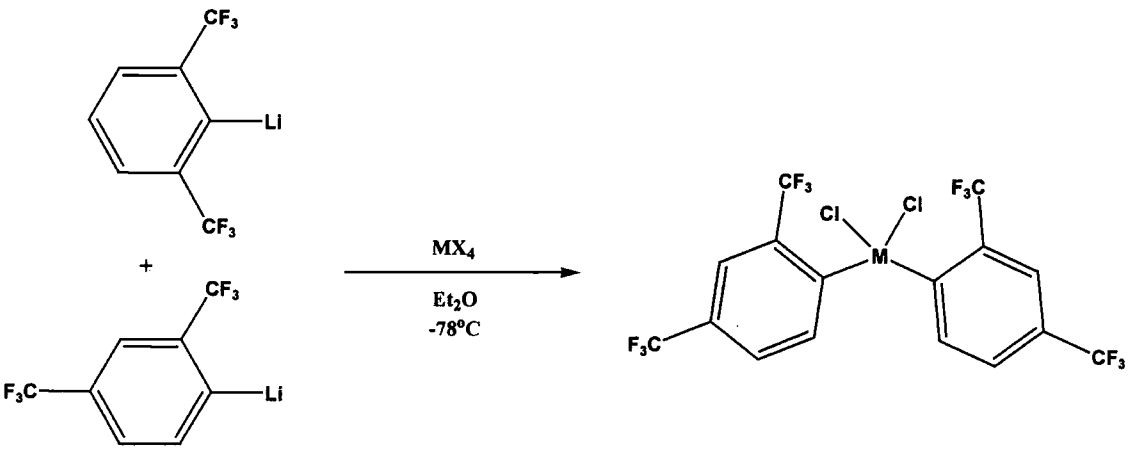

Equation 1.16: *Synthesis of $Ar"_2MCl_2$*

Tin compounds were the first derivatives containing a fluoroxyl ligand reported. $Ar'SnMe_3$ and $Ar"SnMe_3$ were prepared from Ar'Li/Ar"Li with Me_3SnCl. The lithiated mixture reacts with $SnCl_2$ to give a tin(II) derivative Ar'_2Sn.[63]

$$2\ Ar'Li.\ TMED + SnCl_2 \longrightarrow Ar'_2Sn$$

Ar'_2Sn can be a precursor for the preparation of other tin derivatives containing a fluoroxyl ligand.

$$Ar'_2Sn + MeOH \xrightarrow{benzene} Ar'Sn\text{-}OMe + Ar'H$$

Xue[22] synthesised some tin(IV) derivatives. Reaction of Ar'Li/Ar"Li with $SnCl_4$ led to the formation of Ar'_2SnCl_2, which was characterised crystallographically.

- Group 15 derivatives

The first chlorophosphine containing Ar' has been described by Escudié *et al.*[36]

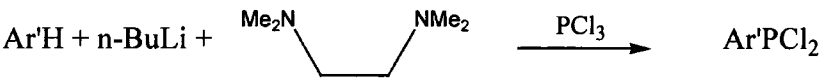

Roden[37] has prepared a series of phosphorus derivatives containing fluoroxyl. Treatment of the mixture Ar'Li/Ar"Li with an appropriate amount of PCl_3 gave rise to a mixture of three different products: $Ar'PCl_2$, $Ar"PCl_2$ and the unsymmetrical disubstituted molecule Ar'Ar"PCl (Figure1.9).[64]

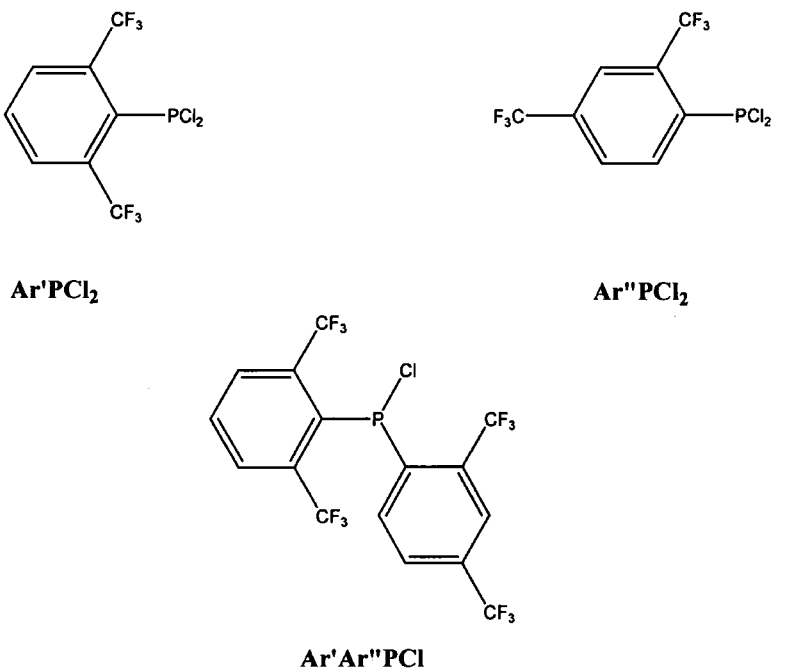

Figure 1.9: *Different products of the reaction between Ar'Li/Ar"Li and PCl_3*

Ar'PBr_2 and Ar"PBr_2 can be prepared from PBr_3. Reduction of the chloride compounds with Bu_3SnH or $LiAlH_4$ leads to the formation of the hydride derivatives. Fluorination with SbF_3 affords the fluoride substituents.

$$Ar'PX_2 \xrightarrow{Bu_3SnH} Ar'PH_2$$

$$Ar'PX_2 \xrightarrow{SbF_3} Ar'PF_2$$

Treatment of the Ar'Li/Ar"Li mixture with PF_2Cl yields Ar"PF_2 and Ar'Ar"PF, the first disubstituted compounds containing fluoroxyl ligands described in the literature.[65]
The ^{19}F NMR spectra of Ar'Ar"PCl or Ar'Ar"PF showed a broad singlet for the two CF_3 groups of the Ar' moiety, reflecting the inequivalence of the trifluoromethyl groups.
Some multiple-bond compounds, such as Ar'P=PAr', have also been described; this compound has had its X-ray structure ascertained.[66]

Some preliminary work on the synthesis of arsenic derivatives has been attempted by Xue.[22]
No examples have been published with antimony or bismuth.

- Transition metal derivatives

The only example of a transition metal complex containing the Ar' ligand is a chromacene. This compound contains the Ar' ligand in a sandwich complex with chromium.[67]

1.2 Diphosphenes

Simple substituted diphosphene derivatives, RP=PR (R=Alkyl, aryl) are usually highly unstable. In 1981, Yoshifuji *et al*[68] reported the synthesis of the first stable diphosphene

(by reaction between Ar^*PCl_2 and Mg metal) containing a bulky electron-withdrawing substituent as a protecting group (2,4,6-tris-^{t}butylphenyl) (supermes or Ar*).

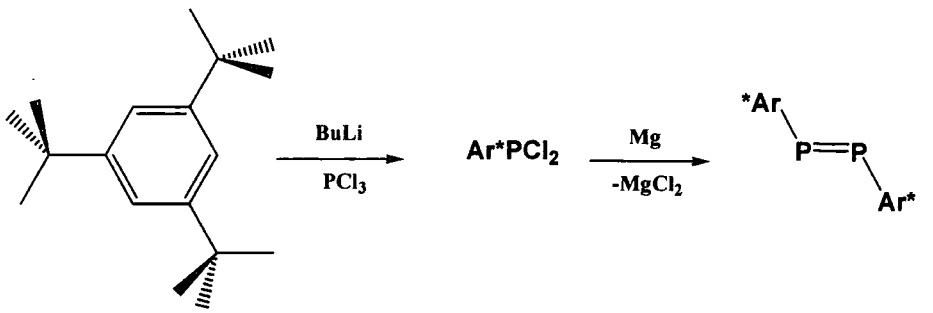

Equation 1.17: *Synthesis of Ar*P=PAr**

Therefore, it has been thought that substituents like 2,4,6-tris(trifluoromethyl)phenyl or 2,6-bis(trifluoromethyl)phenyl could be good ligands to stabilise such species.

1.2.1 Fluoromes

1.2.1.1 Synthetic route

The first diphosphene containing the Ar ligand was obtained by reaction of $ArPCl_2$ with $ArPH_2$ in the presence of a base (DBU):[8,11,69]

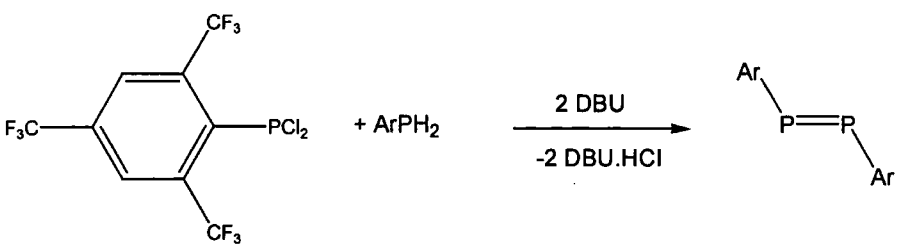

Equation 1.18: *Synthesis of ArP=PAr*

This diphosphene can also be prepared via the Mg route, and via a reaction of dechlorination with a base, 1,3,1',3',-tetraethyl-2,2'-bis(imidazolidine).[8,70]

Another synthetic route to the diphosphenes was discovered by Dillon, Gibson and Sequeira:[71] transition metal-catalysed metathesis of double bonds. They used the highly reducing nature and labile coordination sphere of the zerovalent tungsten complex, $W(PMe_3)_6$, as an efficient chloride ion abstractor. Dichlorophosphines react with $W(PMe_3)_6$ in benzene smoothly over several hours to give the diphosphene RP=PR [R:2,4,6-tris-^{t}butylphenyl, 2,4,6-tris(trifluoromethyl)phenyl, 2,6-tris(trifluoromethyl)phenyl]. The proposed mechanism is shown below (Equation 1.19).

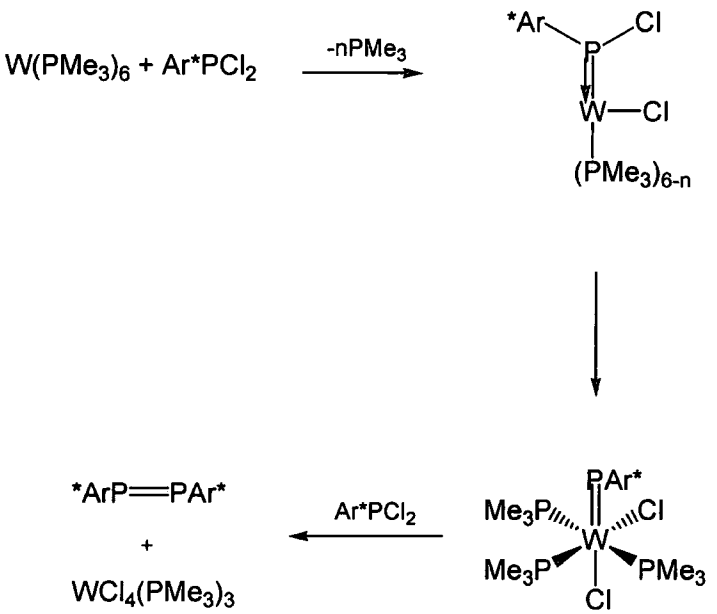

Equation 1.19: *Synthesis of Ar*P=PAr* with $W(PMe_3)_6$*

1.2.1.2 Coordination chemistry

ArP=PAr is surprisingly an air- and moisture stable solid at room temperature and binds less strongly to transition metals than its hydrocarbon analogues.

Several modes of coordination are possible with diphosphenes. They can coordinate to suitable acceptors either in a η^1-fashion, via a lone pair on phosphorus, or in a η^2-mode, via the π system of the double bond, or by combination of these modes.

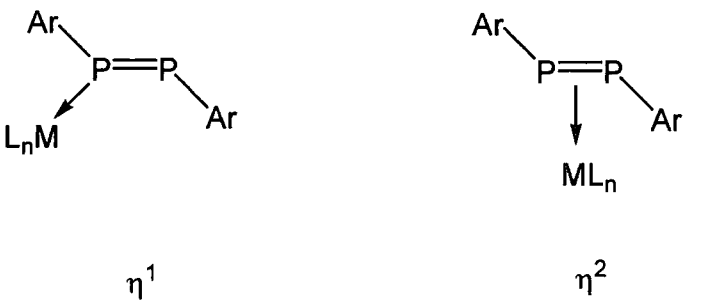

Figure 1.10: *Coordination chemistry of diphosphene*

Although the reactivity of ArP=PAr is apparently low, the synthesis of a few stable carbonyl complexes have been mentioned: $(ArP=PAr)ML_n$ (ML_n= $Fe(CO)_4$, $Cr(CO)_5$, $Mo(CO)_5$).[25] Dillon and Goodwin reported the synthesis of $ArP=PAr.Mo(CO)_5$, $ArP=PAr.W(CO)_5$, and of *cis*-$[Pt(ArP=PAr)(PEt_3)Cl_2]$.[69]

The synthesis of the first complexes containing η^2-bonded ArP=PAr has been described more recently.[72]

$ArPCl_2$ served as the starting material for the synthesis of a number of interesting diphosphenyl metal complexes,[73,74] such as $Cp^*(CO)_2Fe$-P=P=Ar. Apparently, no attempts have been made to synthesise multiple-bonded compounds with heavier group 15 elements containing fluoromes such as ArAs=AsAr.

1.2.2 Fluoroxyl

The first diphosphene containing the Ar' group (Ar'P=PAr') was synthesised by Escudié *et al.*[66] The behaviour of this compound was unexpected, and very different from that previously reported for other diphosphenes: such derivatives react with electrophiles, nucleophiles or transition metals.[75] However, no addition reactions to the P=P double bond of Ar'P=Ar'P have been observed.

References

1 A. H. Cowley, *Acc. Chem. Res.*, **1984**, *17*, 386.

2 L. Weber, K. Reizig, D. Bungart, R. Boese, *Organometallics,* **1987**, *6*, 110.

3 C. N. Smit, F. M. Lock, F. Bickelhaupt, *Tetrahedron Lett.*, **1984**, *25*, 3011.

4 M. Hesse, U. Klingebiel, *Angew. Chem., Int. Ed. Engl.*, **1986**, *25*, 649.

5 C. Couret, J. Escudié, Y. Madule, H. Ranaivonjatovo, J. G. Wolf, *Tetrahedron Lett.*, **1983**, *24*, 2769.

6 E. T. McBee, R. E. Leech, *Ind. Eng. Chem.*, **1947**, *39*, 394.

7 G. E. Carr, R. D. Chambers, T. F. Holmes, D. G. Parker, *J. Organomet. Chem.*, **1987**, *325*, 13.

8 M. Scholz, H. W. Roesky, D. Stalke, K. Keller, F. T. Edelmann, *J. Organomet. Chem.*, **1989**, *366*, 73.

9 E. T. McBee, R. A. Sanford, *J. Am. Chem. Soc.*, **1950**, *72*, 5574.

10 D. Stalke, K.H.Whitemire, *J. Chem. Soc., Chem. Commun.*, **1990**, 833.

11 K. B. Dillon, H. P. Goodwin, T. A. Straw, R. D. Chambers, Euchem Conference, *Phosphorus, Silicon, Boron, and Related Elements in Low Coordination States,* Paris-Palaiseau, **1988**.

12 H. P. Goodwin, *Ph. D. Thesis*, Durham, **1990**.

13 V. C. Gibson, C. Redshaw, W. Clegg, M. R. J. Elsegood, *Polyhedron,* **1997**, *16*, 2637.

14 W. Fraenk, T. M. Klapötke, B. Krumm, P. Mayer, H. Nöth, H. Iotrowski, M. Suter, *J. Fluorine Chem.*, **2001**, *112*, 73.

15 R. D. Schluter, A. H. Cowley, D. A. Atwood, R. A. Jones, M. R. Bond, C. J. Carrano, *J. Am. Chem. Soc.*, **1993**, *115*, 2070.

16 R. D. Schluter, H. S. Isom, A. H. Cowley, D. A. Atwood, R. A. Jones, F. Olbritch, S. Corbelin, R. J. Lagow, *Organometallics,* **1994**, *13*, 4058.

17 R. Filler, W. K. Gnandt, W. Chen, S. Lin, *J. Fluorine Chem.*, **1991**, *52*, 99.

18 J. K. Buijink, M. Noltemeyer, F. T. Edelmann, *J. Fluorine Chem.*, **1993**, *61*, 51.

19 J. Braddock-Wilking, M. Schieser, L. Brammer, J. Huhmann, R. Shaltout, *J. Organomet. Chem.*, **1995**, *499*, 89.

20 J. E. Bender, M. M. Banaszak-Holl, J. W. Kampf, *Organometallics,* **1999**, *18*, 1547.

21 J. E. Bender, M. M. B. Holl, A. Mitchell, N. J. Wells, J. W. Kampf, *Organometallics,* **1998**, *17*, 5166.

22 B. Y. Xue, *M.Sc. Thesis*, Durham, **1999**.

23 H. Grutzmacher, H. Pritzkow, F. T. Edelmann, *Organometallics,* **1991**, *10*, 23.

24 H. Grutzmacher, H. Pritzkow, *Angew. Chem., Int. Ed. Engl.*, **1991**, *30*, 1017.

25 F. T. Edelmann, *Comments Inorg. Chem.*, **1992**, *12*, 259.

26 H. Grutzmacher, H. Pritzkow, *Angew. Chem.*, **1991**, *103*, 976.

27 S. Brooker, F. T. Edelmann, D. Stalke, *Acta Cryst.*, **1991**, *C47*, 2527.

28 F. T. Edelmann, M. Belay, *J. Fluorine Chem.*, **1997**, *84*, 29.

29 S. Brooker, J. Buijink, F. T. Edelmann, *Organometallics,* **1991**, *10*, 25.

30 P. Poremba, H. Pritskow, F. T. Edelmann, *J. Fluorine Chem.*, **1997**, *82*, 43.

31 M. Belay, F. T. Edelmann, *J. Fluorine Chem.*, **1997**, *84*, 29.

32 K. W. Klinkhammer, T. F. Fassler, H. Grutzmacher, *Angew. Chem., Int. Ed. Engl.*, **1998**, *34*.

33 F. T. Edelmann, J. K. F. Buijink, S. A. Brooker, R. Herbst-Irmer, U. Kilimann, F. M. Bohnen, *Inorg. Chem.*, **2000**, *39*, 6134.

34 J. T. Alhemann, H. W. Roesky, R. Murugavel, E. Parisini, M. Noltemeyer, H. G. Schmidt, O. Müller, R. Herbst-Irmer, L. N. Markovskii, Y. G. Shermolovich, *Chem. Ber.*, **1997**, *130*, 1113.

35 J. T. Alhemann, H. W. Roesky, M. Noltemeyer, H. G. Schmidt, L. N. Markovsky, Y. G. Shermolovich, *J. Fluorine Chem.*, **1998**, *87*, 87.

36 J. Escudié, C. Couret, H. Ranaivonjatovo, M. Lazraq, J. Satgé, *Phosphorus and Sulfur,* **1987**, *31*, 27.

37 M. D. Roden, *Ph . D. Thesis*, Durham, **1998**.

38 M. G. Davidson, K. B. Dillon, J. A. K. Howard, S. Lamb, M. D. Roden, *J. Organomet. Chem.*, **1998**, *550*, 481.

39 H. Voelker, D. Labahn, F. M. Bohnen, R. Herbst-Irmer, H. W. Roesky, D. Stalke, F. T. Edelmann, *New J. Chem,* **1999**, *23*, 905.

40 K. B. Dillon, H. P. Goodwin, *J. Organomet. Chem.,* **1994**, *469*, 125.

41 T. A. Straw, *Ph. D. Thesis*, Durham, **1990**.

42 N. Burford, C. L. B. MacDonald, D. J. Leblanc, J. S. Cameron, *Organometallics,* **2000**, *19*, 152.

43 J. T. Alhemann, A. Kunzel, H. W. Roesky, M. Noltemeyer, L. Markovskii, H. G. Schmidt, *Inorg. Chem,* **1996**, *35*, 6644.

44 K. H. Whitemire, H. W. Roesky, S. Brooker, G. M. Sheldrick, *J. Organomet. Chem.,* **1991**, *402*, C4.

45 H. W. Roesky, M. Scholz, M. Noltemeyer, F. T. Edelmann, *Inorg. Chem.,* **1989**, *28*, 3829.

46 H. W. Roesky, M. Scholz, M. Noltemeyer, *Chem. Ber.,* **1990**, *123*, 2303.

47 S. Brooker, F. T. Edelmann, T. Kottke, H. W. Roesky, G. M. Sheldrick, D. Stalke, K. H. Whitemire, *J. Chem. Soc., Chem. Commun.,,* **1991**, *3*, 144.

48 M. Scholz, M. Noltemeyer, H. W. Roesky, *Angew. Chem., Int. Ed. Engl.,* **1989**, *10*, 28.

49 P. Poremba, M. Noltemeyer, H. G. Schmidt, F.T.Edelmann, *J. Organomet. Chem.,* **1995**, *501*, 315.

50 D. Labahn, S. Brooker, G. M. Sheldrick, H. W. Roesky, *Z. Anorg. Allg. Chem,* **1992**, *610*, 163.

51 D. Labahn, E. Pohl, R. Herbst-Irmer, D. Stalke, H. W. Roesky, G. M. Sheldrick, *Chem. Ber.,* **1991**, *124*, 1127.

52 N. Bertel, H. W. Roesky, F. T. Edelmann, M. Noltemeyer, H. G. Schmidt, *Z. Anorg. Allg. Chem.,* **1990**, *586*, 7.

53 A. Recknagel, M. Noltemeyer, D. Stalke, U. Pieper, H. G. Schmidt, F. T. Edelmann, *J. Organomet. Chem.,* **1991**, *411*, 347.

54 V. C. Gibson, C. Redshaw, L. J. Sequeira, K. B. Dillon, W. Clegg, M. R. J. Elsegood, *Chem. Commun.,* **1996**, 2151.

55 K. B. Dillon, V. C. Gibson, J. A. K. Howard, C. Redshaw, L. Sequeira, J. W. Yao, *J. Organomet. Chem.,* **1997**, *528*, 179.

56 A. S. Batsanov, K. B. Dillon, V. C. Gibson, J. A. K. Howard, L. J. Sequeira, J. W. Yao, *J. Organomet. Chem.*, **2001**, *631*, 181.

57 M. Belay, F. T. Edelmann, *J. Organomet. Chem.*, **1994**, *479*, C21.

58 G. M. Benedikt, B. L. Goodall, S. Iyer, L. H. McIntoshIII, R. Mimma, L. F. Rhodes, C. S. Day, V. W. Day, *Organometallics,* **2001**, *20*, 2565.

59 C. Bartolomé, P. Espinet, F. Villafañe, S. Giesa, A. Martín, A. G. Orpen, *Organometallics,* **1996**, *15*, 2019.

60 P. Espinet, S. Martín-Barrios, F. Villafañe, P. G. Jones, A. K. Fisher, *Organometallics,* **2000**, *19*, 290.

61 S. Brooker, N. Bertel, D. Stalke, M. Noltemeyer, H. W. Roesky, G. M. Sheldrick, F. T. Edelmann, *Organometallics,* **1992**, *11*, 192.

62 L. J. Sequeira, *Ph.D Thesis*, Durham, 1996.

63 M. P. Bigwood, P. J. Corvan, J. J. Zuckerman, *J. Am. Chem. Soc.*, **1981**, *103*, 7643.

64 A. S. Batsanov, S. M. Cornet, L. A. Crowe, K. B. Dillon, R. K. Harris, P. Hazendonk, M. D. Roden, *Eur. J. Inorg. Chem,* **2001**, 1729.

65 L. Heuer, P. G. Jones, R. Schmutzler, *J. Fluorine Chem.*, **1990**, *46*, 243.

66 A. Dubourg, J.-P. Declercq, H. Ranaivonjatovo, J. Escudié, C. Couret, M. Lazraq, *Acta Cryst.*, **1988**, *C44*, 2004.

67 M. Y. Eyring, E. C. Zuerner, L. J. Radonovich, *Inorg. Chem.*, **1981**, *20*, 3045.

68 M. Yoshifuji, I. Shima, N. Inamoto, K. Hirotsu, T. Higushi, *J. Am. Chem. Soc.*, **1981**, *103*, 4587.

69 K. B. Dillon, H. P. Goodwin, *J. Organomet. Chem.*, **1992**, *429*, 169.

70 M. Yoshifuji, K. Shibayama, N. Inamoto, T. Matsushita, K. Nishimoto, *J. Am. Chem. Soc.*, **1983**, *105*, 2495.

71 K. B. Dillon, V. C. Gibson, L. J. Sequeira, *J. Chem. Soc., Chem. Commun.*, **1995**, 2429.

72 K. B. Dillon, V. C. Gibson, J. A. K. Howard, L. J. Sequeira, J. W. Yao, *Polyhedron,* **1996**, *15*, 4173.

73 L. Weber, H. Schumann, *Chem. Ber.*, **1990**, *123*, 1779.

74 L. Weber, H. Schumann, *Chem. Ber.*, **1991**, *124*, 265.

75 A. H. Cowley, N. C. Norman, *Prog. Inorg. Chem.*, **1986**, *34*, 1.

Chapter 2

Group 13 Derivatives

In this work, we have been especially interested in the reactions between fluoromes or fluoroxyl compounds and boron trihalides. Attempts have also been made to prepare aluminium derivatives, but without success so far.

2.1 Introduction

There are three important methods to prepare alkyl (or aryl) boron dihalides or dialkyl (or diaryl) boron halides.[1,2]

- Interaction of organometallic compounds with boron halides or substituted boron halides:

$$Zn(C_6H_5)_2 + BF_3 \longrightarrow C_6H_5ZnF + C_6H_5BF_2$$

$$ArHgX + BX_3 \longrightarrow ArBX_2 + HgX_2$$

$$Al(Me)_3 + 3\ BBr_3 \longrightarrow 3\ MeBBr_2 + AlBr_3$$

$$Me_3SnC_6F_5 + 2\ BCl_3 \longrightarrow Me_2SnCl_2 + MeBCl_2 + C_6F_5BCl_2$$

- Reaction of triarylborons or aminodialkyl borons with a halogenating agent:

$$B(Bu_3) + HBr \xrightarrow{-BuH} Bu_2BBr$$

- Reaction of trimethyl boroxine with boron halides:

$$(MeBO)_3 + 2\ BF_3 \longrightarrow 3\ MeBF_2 + B_2O_3$$

- Arylhalogenoboranes

The chemistry of arylhalogenoboranes $ArBX_2$ (X=F, Cl, Br, I) is well-established. However, there are few communications concerning fluoro-containing aryldifluoroboranes [3,4]. Recently, Frohn *et al*[5], reported the preparation and NMR studies of some fluoroaryldifluoroboranes. The possible routes for the preparation of $C_6F_5BCl_2$ or $C_6F_5BF_2$ are as follow:

$$C_6F_5HgEt + BCl_3 \longrightarrow C_6F_5BCl_2 + EtHgCl$$

$$C_6F_5BCl_2 + 2\,HF \longrightarrow C_6F_5BF_2 + 2\,HCl$$

In the last decades, few examples have been published of boron compounds containing bulky and/or electron-withdrawing ligands such as mesityl[6] or very recently fluoromesityl.[7]

Boron trihalides (BX_3) can undergo rapid scrambling or redistribution reactions on being mixed, with formation of mixed halides BX_2Y and BXY_2. The related systems $RBX_2/R'BY_2$ (and $ArBX_2/Ar'BY_2$) also exchange X and Y but not R or Ar.[8] Goodwin[9] has also observed some fluorine/chlorine exchange in the reaction of BCl_3 with ArLi.

- Triarylboranes

The chemistry and particularly the conformation of triarylboranes have been studied;[10,11] their main features are the propeller-shaped conformations, and stereodynamics via the flip of aryl rings. The interest was to investigate the effect of bulky substituents such as mesityl or naphthyl groups on the conformation. More recently, Goodwin[9] synthesised Ar_3B (Ar: 2,4,6-tris(trifluoromethyl)phenyl) but no structure has been determined so far for this compound. Additionally, the structure of tris-[3,5-bis(trifluoromethyl)phenyl]borane has been briefly mentioned,[12] and structural

and dynamic NMR studies of tris[2-(trifluoromethyl)phenyl]borane have been carried out.[13]

Usually, in organoborane compounds the carbon link has a largely single σ B-C bond. Tri-coordinate organoboranes have a trigonal planar structure, with the potential for back bonding to the empty boron orbital from adjacent groups containing an unshared electron pair or a conjugated π-bond.[14]

2.2 Reaction with 2,4,6-tris(trifluoromethyl)phenyl lithium (ArLi)

This reaction was carried out following the method of Goodwin.[9] ArLi was added slowly to a $BCl_3.Et_2O$ solution at room temperature. The ^{19}F NMR spectra showed a number of peaks, including a doublet at –57.3 ppm ($^5J_{F\text{-}F}$ 14.3Hz) suggesting the presence of Ar_2BF. The ^{11}B NMR yielded signals at 45.1 and 26.0 ppm. ArLi was then added gradually into the solution, and ^{19}F and ^{11}B NMR spectra were recorded after each addition. The reaction was carried out until no further changes were observed in the NMR spectra. The final spectra exhibit the presence of a mixture of four different species: $ArBCl_2$, $ArBF_2$, Ar_2BF and Ar_3B. NMR data are listed in Table 2.1. $ArBF_2$ and Ar_3B could not be isolated, although $ArBCl_2$ was isolated by distillation under vacuum (Bp 60°C) as a yellow oil and Ar_2BF as a white solid. In addition, some typical boron halide species were observed in solution ($BFCl_2.Et_2O$, $BF_2Cl.Et_2O$, $BF_3.Et_2O$) (Table 2.2), confirming that halogen exchange had occurred. These values agree with the shifts found by Goodwin.[9]

	δ ^{19}F (ppm)	δ ^{11}B(ppm)
$ArBCl_2$	-56.3 (s, 6F, *o*-CF_3) -63.9 (s, 3F, *p*-CF_3)	56.8
$ArBF_2$	-54.1 (t, $^5J_{F-F}$15.8Hz, 6F, *o*-CF_3) -64.2 (s, 3F, *p*-CF_3) -107.3 (m, 2F, BF_2)	26.0
Ar_2BF	-57.3(d, $^5J_{F-F}$14.3Hz, 12F, *o*-CF_3) -64.0 (s, 6F, *p*-CF_3) -131.5 (m, 1F, BF)	45.1
Ar_3B	-60.2 (s, *o*-CF_3) -63.5 (s, *p*-CF_3)	?*

Table 2.1: *^{19}F and ^{11}B NMR data for the products of the reaction between ArLi and BCl_3*

	^{19}F (ppm)	^{11}B (ppm)
$BF_3.Et_2O$	-151.2 (s)	0
$BF_2Cl.Et_2O$	-128.4 (q, $^1J_{B-F}$ 30.0 Hz)	3.9 (t, $^1J_{B-F}$ 29.0 Hz)
$BFCl_2.Et_2O$	-114.3(q, $^1J_{B-F}$ 57.6 Hz)	7.9 (d, $^1J_{B-F}$ 58.1 Hz)
$BCl_3.Et_2O$		10.7

Table 2.2: *NMR Data for $BF_nCl_{3-n}.Et_2O$ adducts ($3 \leq n \leq 0$).*

* The ^{11}B NMR has been reported by Goodwin at 31.6 ppm. However, this shift does not agree with the literature values for R_3B compounds. In this work, no signal could be assigned with certainty.

The signal at –57.3ppm was confirmed as a doublet by recording the spectra were at different frequencies (188.16 and 376.35 MHz). This conclusion disagrees with the statements made by Goodwin[9] and Gibson *et al*,[15] where these signals were assigned to two different singlets for the *o*-CF_3 groups, due to non-equivalence of the aryl rings.

The presence of $ArBF_2$ and Ar_2BF can be explained by a chlorine/fluorine exchange while the reaction is taking place. The only sources of fluorine atoms in the solution are the CF_3 groups in the ArLi compound. The mechanism proposed for this exchange could be as shown below:

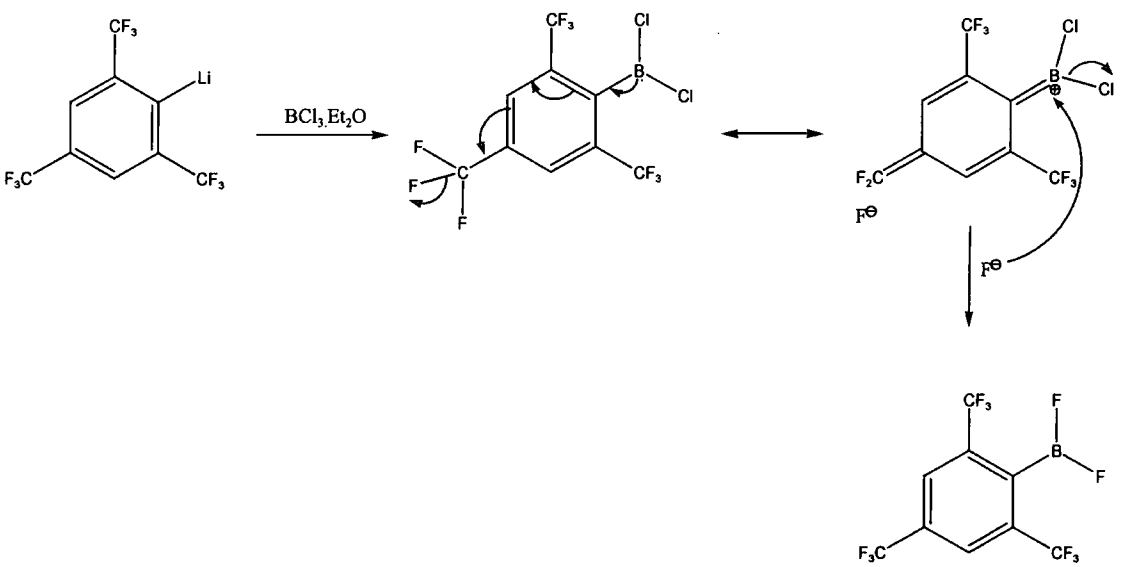

Equation 1.1: *Proposed mechanism for the fluorine/chlorine exchange.*

In order to identify the different species arising from the F/Cl exchange, a reaction between $BCl_3.Et_2O$ and $BF_3.Et_2O$ was carried out. ^{19}F and ^{11}B NMR spectra show the presence of $BCl_3.Et_2O$, $BF_3.Et_2O$, $BF_2Cl.Et_2O$ and $BFCl_2.Et_2O$. NMR data are listed in Table 2.2.

- X-ray structure of Ar_2BF:

Ar_2BF was isolated as a white solid which was purified by recrystallisation from dichloromethane. Crystals were submitted for X-ray diffraction. The structure was determined at 120 K by A.L. Thompson and is shown in Figure 2.1.

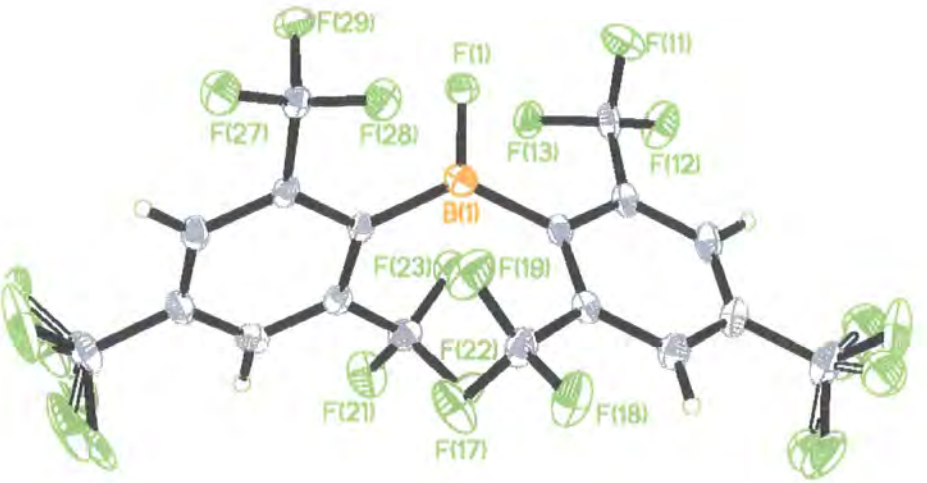

Figure 2.1: *Molecular structure of Ar_2BF*

Ar_2BF crystallises in the monoclinic space group P21/n with Z=4. Selected bond distances and angles are listed in Table 2.3 below:

Bond distance (Å)		Angles (°)	
B(1)-C(21)	1.588(4)	F(1)-B(1)-C(10)	115.2(2)
B(1)-C(11)	1.594(4)	F(1)-B(1)-C(21)	116.0(2)
B(1)-F(1)	1.313(3)		
B(1)-F(13)	2.763	C(21)-B(1)-C(11)	128.5(2)
B(1)-F(19)	2.792		
B(1)-F(23)	2.795		
B(1)-F(28)	2.785		
F(1)-F(11)	2.763		
F(1)-F(13)	2.583		
F(1)-F(28)	2.624		
F(1)-F(29)	2.711		

Table 2.3: *Selected Bond Distances and Angles for Ar_2BF*

The B(1)-C distances are 1.588(4) and 1.594(4) Å. Angles F(1)-B(1)-C(10) and F(1)-B(1)-C(21) are 115.2(2) and 116.0(2)° respectively. The two *para*-trifluoromethyl groups appear to be disordered, as often observed in compounds containing these substituents, for example Ar_2AsCl, Ar_2SbCl,[16] Ar_2BiCl and Ar_3Bi.[17]

The B-C distances are slightly shorter than those found in Ar_2BN_3 (1.62 Å) and $Ar_2B(OH)$ (1.60 Å)[7] the only structures containing B and Ar published so far. The C-B-C angle in 2,6-$(F_2C_6H_3)_2BCl$ is 123.1(2)°,[7] compared with 128.5(2)° for Ar_2BF. The latter is bigger due to the presence of the bulky CF_3 substituents in the *ortho* position.

Four short contacts between B---F are observed, for F(13), F(19), F(23) and F(28) (Table 2.3) at an average interatomic distance of ca. 2.78Å. This value is shorter than the sum of van der Waals radii of B (ca. 2.08 Å) and F (ca. 1.40 Å).[18] Moreover, some of the F(1)-F distances are found to be shorter than others, reflecting possible F---F interactions between some of the fluorines of the trifluoromethyl groups and the fluorine atom directly bonded to the central boron atom (Table 2.3).

2.3 Reaction with a 2,6-bis(trifluoromethyl)phenyl lithium / 2,4-bis(trifluoromethyl)phenyl lithium mixture (Ar'Li/Ar"Li)

A solution of Ar'Li/Ar"Li* was added to a BCl_3 solution in diethyl ether. The ^{19}F and ^{11}B NMR spectra indicated different species in solution ($Ar'BCl_2$, $Ar"_2BF$, $Ar"_3B$), and some species arising from direct fluorine/chlorine exchange ($BF_3.Et_2O$, $BFCl_2.Et_2O$, $BF_2Cl.Et_2O$), for which data are listed in Table 2.2. Compounds were separated by distillation under reduced pressure (0.05 Torr).

- $Ar'BCl_2$

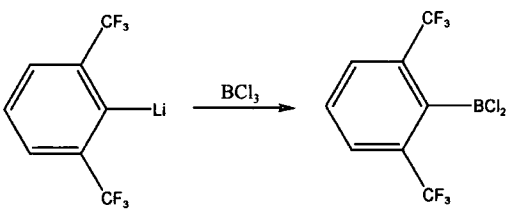

Equation 2.2: *Synthesis of $Ar'BCl_2$*

This fraction was collected at 48°C as a yellow oil. The ^{19}F NMR spectrum showed a singlet at –56.8 ppm corresponding to two *ortho*-CF_3 groups. The ^{11}B NMR consisted of one singlet at 57.5 ppm.

- $Ar"_2BF$

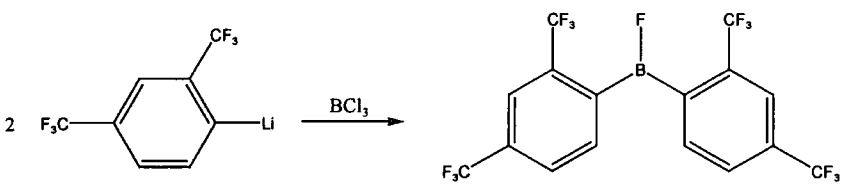

Equation 2.3: *Synthesis of $Ar"_2BF$*

* The Ar'Li/Ar"Li mixture was used because the lithiated compounds, Ar'Li and Ar"Li, could not be separated due to their close boiling points, caused by their similar molecular mass.

The ^{19}F NMR spectrum of the fraction collected at 92°C showed a doublet at -57.2 ($^{5}J_{F-F}$ 14.7 Hz, 6F, *o*-CF_3), a singlet at -63.3 (6F, *p*-CF_3), and a multiplet at -86.6 ppm (1F, B-F). The ^{11}B NMR exhibited a broad singlet at 47.8 ppm.

- $Ar"_3B$

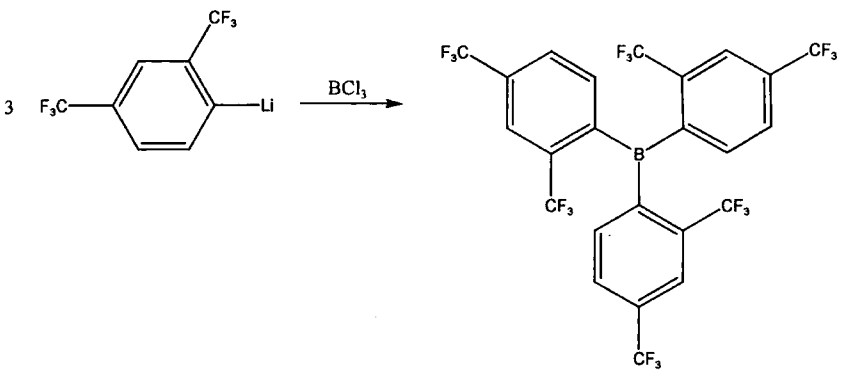

Equation 2.4: *Synthesis of $Ar"_3B$*

After distillation, a white solid remained in the flask. This was washed three times with hexanes and dried under vacuum. The ^{19}F NMR spectrum consisted of a singlet at -56.6 (9F, *o*-CF_3) and a singlet at -63.8 (9F, *p*-CF_3) ppm.

In order to investigate the rotation of the ring around the boron atom, ^{19}F NMR spectra of $Ar"_3B$ were recorded between 10°C and -80°C. No changes were observed until -40°C where a new set of signals started to appear. The spectrum at -80°C showed the signal corresponding to $Ar"_3B$ (e.g. two singlets at –56.6 and –63.8 ppm) and two singlets at -56.2 and -62.2 ppm. $Ar"_3B$ can exist in two different conformations as shown in Figure 2.3, so the second set of singlets could be explained by the rotation of an aryl ring to be in conformation B. However, these two sets of signals are in a 5.5:1 ratio (Figure 2.2). For conformation B, two sets of *o*-CF_3 signals and two sets for *p*-CF_3 signals are expected, both in a 2:1 intensity ratio, whereas for conformation A only one *o*-CF_3 and one *p*-CF_3

signal would be expected, giving an overall 3:3 *o/p* ratio. It therefore seems probable that the chemical shifts coincide for all three aryl rings in conformation A and for two of the rings in conformation B. Equal populations of both conformations would then lead to two *o*-CF_3 and two *p*-CF_3, in a 5:1 ratio for each set. The calculated energy difference between the two conformations is only 0.5 kcal/mol (value calculated by Dr M.A. Fox using the Gaussian 98 package) so this provides a reasonable explanation for the low-temperature results.

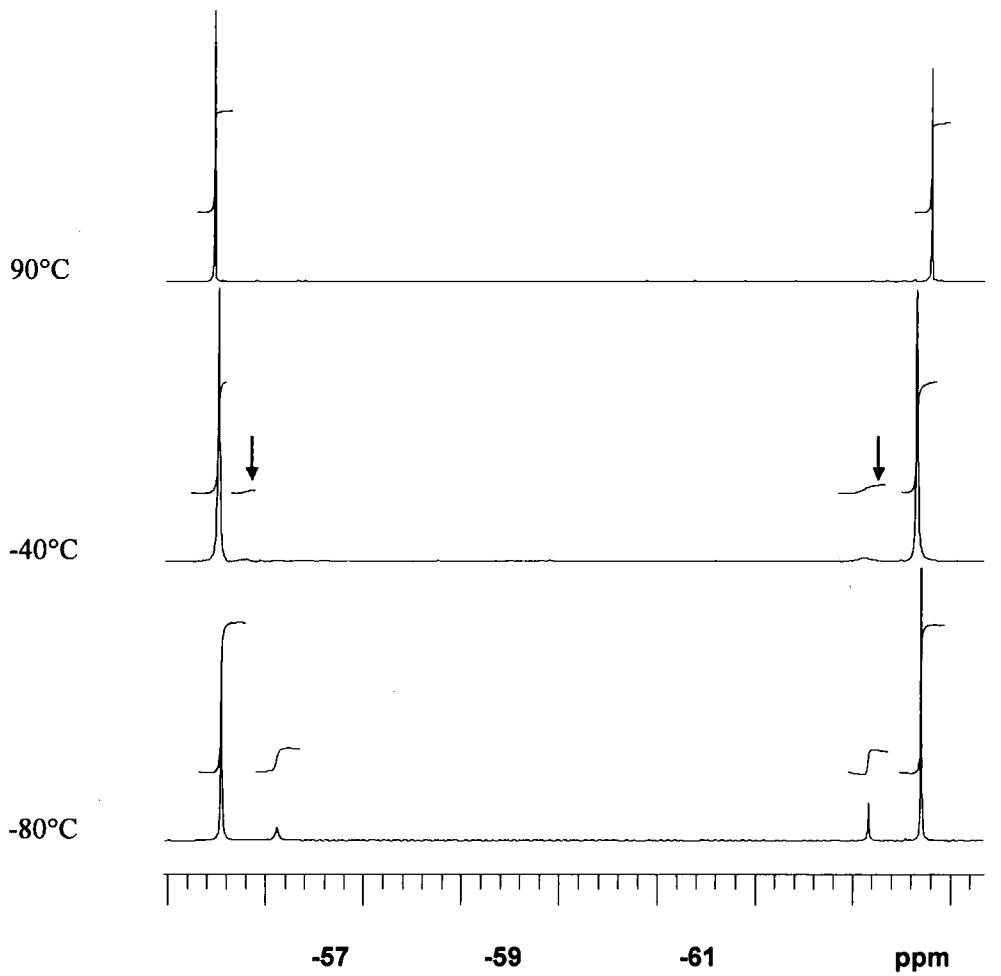

Figure 2.2: *Variable temperature ^{19}F NMR spectra of Ar"$_3$B*

In their studies on tris[2-(trifluoromethyl)phenyl]borane, Toyota *et al*[13] noticed that the singlet observed at room temperature was decoalesced at -100°C and separated into two singlets at -117°C. Unfortunately, due to solvent restrictions, it has not been possible to study Ar"$_3$B at a temperature below -80°C.

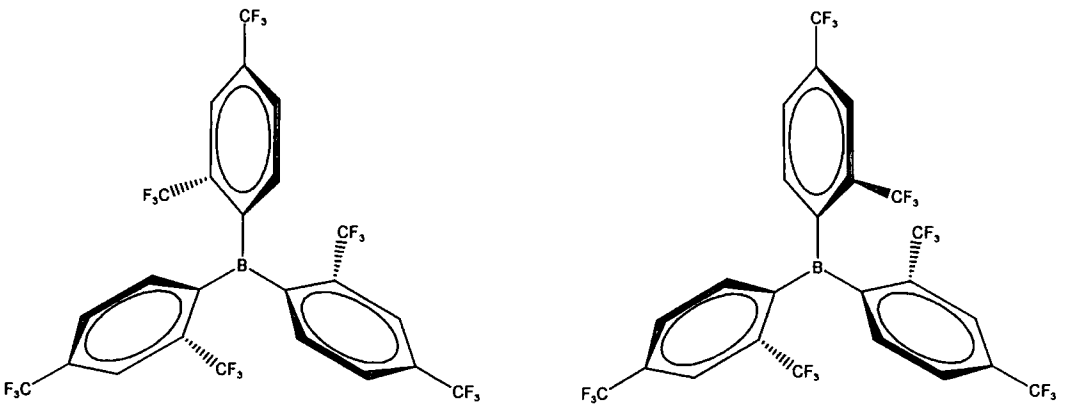

Conformation A Conformation B

Figure 2.3: *Different conformations for Ar"$_3$B*

The chemical shift in the ^{11}B NMR is 73.6 ppm and is within the typical range for tricoordinated boron atoms with three aryl substituents.[19]

A ^{13}C NMR spectrum was recorded at room temperature. Table 2.3 shows the assignments for each carbon.

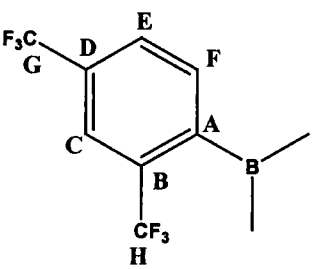

Figure 2.4: *Lettering scheme for Carbon Assignments in Ar$_3$"B*

Carbon	δ (ppm)	J (Hz)
A	143.7	broad singlet
B	133.5	q, $^2J_{C-F}$ 33.7
C	121.1	broad singlet
D	133.6	q, $^2J_{C-F}$ 33.7
E	135.2	s
F	127.3	s
G	123.1	q, $^1J_{C-F}$ 274.2
H	122.9	q, $^1J_{C-F}$ 274.2

Table 2.4: *$\delta^{13}C$ (ppm) for Ar''_3B*

The ^{13}C NMR spectrum shows the presence of only one *ipso* carbon, which confirms the symmetrical character of the molecule. These values are in agreement with those found for Mes_3B.[6]

The ^1H NMR shifts are given in Table 2.4 below:

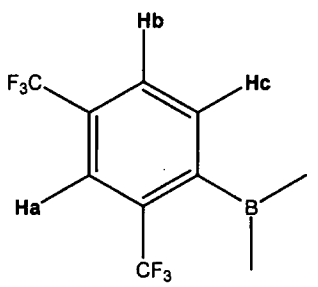

Figure 2.5: *Lettering scheme for Hydrogen Assignments in $Ar_3''B$*

H	δ (ppm)	J (Hz)
a	8.0	s
b	7.8	d, $^3J_{H-H}$ 7.75
c	7.4	d, $^3J_{H-H}$ 7.8

Table 2.5: *δ^1H (ppm) for Ar''_3B*

- X-ray structure of Ar''_3B

Crystals were grown by recrystallisation from dichloromethane. The molecular structure at 120 K, as determined by A.L Thompson, is shown in Figure 2.6.

Figure 2.6: *Molecular structure of Ar''_3B*

Ar"$_3$B crystallises in the triclinic P-1 space group with Z=2. Like Ph_3B[11] and Mes_3B[10], Ar"$_3$B exists in a propeller-like conformation in the ground state, with the three aryl groups twisted out of the plane defined by the three carbons attached to boron. The three rings are twisted by 46.7°, 53.7° and 68.9° towards the reference plane made by the three carbons bonded to the boron atom, C(11), C(21) and C(31). These angles are larger than those observed in triphenylborane (28.3°) and are more comparable to those found in mesitylborane (40°-60°)[11] and tris-[2-(trifluoromethyl)phenyl)]borane (40°-55°)[13], reflecting the steric size of the *ortho* substituents.

B-C distances are 1.582(4) Å and are similar to those found in Ar_2BF (1.59Å).

The C-B-C angles are 117.6°, 117.0° and 124.7° respectively for C(11)-B(1)-C(21), C(21)-B(1)-C(31) and C(1)-B(1)-C(31), reflecting the trigonal geometry of the boron atom. As in Ar_2BF, some short B---F contacts are observed with the fluorines of the *ortho*-CF_3 groups: F(13),F(32) and F(23) with an average interatomic distance of ca. 2.8Å (Table 2.7). The average distance is very similar to that found in tris-[2-(trifluoromethyl)phenyl]borane (see Table 2.7).[13] The distance F(32)---F(23) of 2.688 Å is shorter than the other F---F distances (3.921Å for F(32)-F(21), 3.125Å for F(11)-F(33), 4.601Å for F(31)-F(21) and 4.179Å for F(31)-F(23)). These short distances can be explained by a smaller C-B-C angle, which allows closer F---F interactions.

Another interesting feature is the bond angles at C(11), C(21), and C(31): a significant bending deformation, for example C(12)-C(11)-B(1) 126.7° and C(16)-C(11)-B(1) 116.8(2)°, results from the avoidance of steric interaction between B and the CF_3 moieties.

Table 2.6 shows selected bond lengths (Å) and angles (°) for Ph_3B[11] Mes_3B,[10] $(2\text{-}CF_3C_6H_4)_3B$[13] and Ar"$_3$B. The bonds and angles appear to be very similar, even though the presence of a more bulky group should bring more steric hindrance.

The molecular structure shows the molecule in conformation B (Figures 2.3 and 2.6) which is the more stable conformation. The short F---F interactions help to stabilise the molecule.

Ph_3B		Mes_3B		$(2\text{-}CF_3C_6H_4)_3B$		$Ar"_3B$	
B-C(1)	1.589(5)	B-C(1)	1.579(2)	B-C(1)	1.582(4)	B(1)-C(11)	1.582(4)
B-C(5)	1.571(3)	B-C(1')	1.579(2)	B-C(28)	1.576(4)	B(1)-C(21)	1.582(4)
B-C(5')	1.571(3)	B-C(10)	1.580(4)	B-C(15)	1.571(4)	B(1)-C(31)	1.582(4)
C(1)-B-C(5)	120.2	C(1)-B-C(1')	117.4(2)	C(1)-B-C(8)	119.7(2)	C(11)-B(1)-C(21)	117.6(2)
C(5)-B-C(5')	119.6	C(1)-B-C(10)	121.3(1)	C(1)-B-C(15)	118.6(2)	C(21)-B(1)-C(31)	124.7(2)
C(1)-B-(5')	120.2	C(1')-B-C(10)	121.3(1)	C(8)-B-C(15)	119.3(2)	C(21)-B(1)-C(31)	117.0(2)
Ref	10	9		12		This work	

Table 2.6: *Selected Bond Distances (Å) and Angles (°) for Ph_3B, Mes_3B, $Ar"_3B$ and $(2\text{-}CF_3C_6H_4)_3B$.*

Table 2.7 lists short B---F contacts in $(2\text{-}CF_3C_6H_4)_3B$ and $Ar"_3B$. The intramolecular B---F distances are similar, which is not surprising, the only difference between those two compounds being the presence of *para*-CF_3 groups in $Ar"_3B$ which do not interact with the boron central atom.

$(2\text{-}CF_3C_6H_4)_3B$		$Ar"_3B$	
B---F(1)	2.845(13)	B(1)---F(13)	2.800
B---F(4)	2.816(4)	B(1)---F(23)	2.802
B---F(7)	2.763(3)	B(1)---F(32)	2.815
Average	2.808		2.806

Table 2.7: *Short B---F contacts (Å) in $Ar*_3B$ and $Ar"_3B$*

2.4 Boronic Acids

Over the last decade, boronic acids have been found to be very good catalysts in the Suzuki-Miyaura cross-coupling reaction. Arylboronic acids containing electron-withdrawing substituents such as 2,4,6-tris(trifluoromethyl)phenyl or 3,5-bis(trifluoromethyl)phenyl groups act as highly efficient catalysts in the amidation of carboxylic acids by amines.[20]

2,4-Bis(trifluoromethyl)phenyl boronic acid ($Ar"B(OH)_2$) has been used as a powerful catalyst in the catalytic asymmetric allylation of aldehydes with allyltrimethylsilanes.[20]

- Bis[2,4,6-tris(trifluoromethyl)phenyl] boronic acid ($Ar_2B(OH)$):

$Ar_2B(OH)$ was obtained by hydrolysis of Ar_2BF. An NMR tube containing Ar_2BF was left standing for a few weeks.

- NMR

The ^{19}F NMR spectrum shows two singlets at -56.2 (12F, *o*-CF_3) and -63.8 (6F, *p*-CF_3) ppm. Unfortunately, the ^{11}B NMR could not be recorded, since the sample was not concentrated enough.

- X-ray structure of $Ar_2B(OH)$

Crystals were grown by slow hydrolysis of Ar_2BF. Long exposure of an NMR tube containing Ar_2BF to the air afforded white crystals of $Ar_2B(OH)$ suitable for X-ray diffraction. The molecular structure of $Ar_2B(OH)$ at 120 K was determined by A.L Thompson and is shown in Figure 2.7:

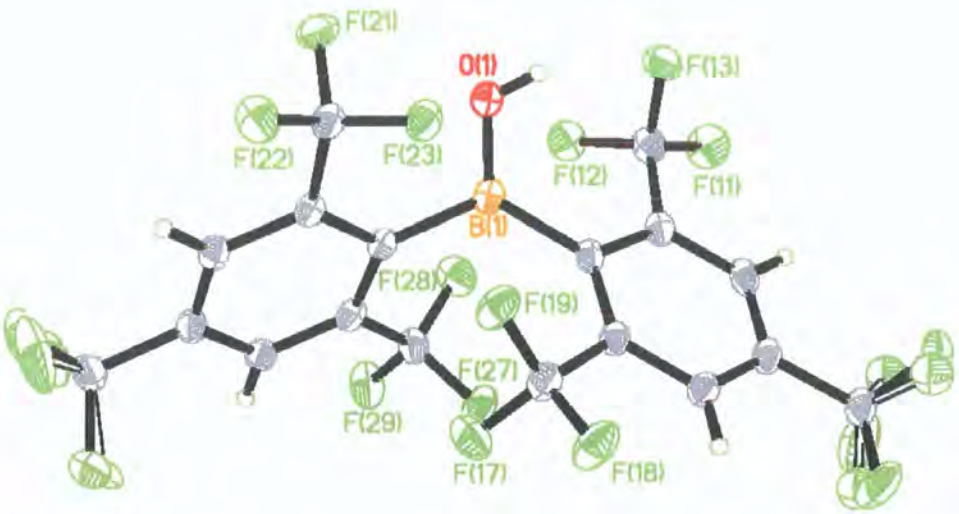

Figure 2.7: *Molecular structure of $Ar_2B(OH)$*

The structure of $Ar_2B(OH)$ at 200 K has already been determined by Fraenk *et al*[7] where it was obtained as a partially hydrolysed product, Ar_2BN_3 and Ar_2BOH. Their results are very similar to those obtained at 120 K in the present work; the discussion below refers to the data at 120 K. Selected bond distances and angles are included in Table 2.10.

The B-C distances average 1.61Å and are similar to those found in Ar_2BF. The O(1)-B(1)-C(21) angle is 112.65°, whereas O(1)-B(1)-C(11) is 121.62° An intramolecular OH---F bridge is found for the hydrogen atom of the OH group to one fluorine atom of a CF_3 group. The OH distance is 0.84 Å, while the H(1)---F(13) and H(1)---F(12) distances are 2.188 Å and 2.737 Å respectively. As in Ar_2BF and $Ar"_3B$, short B---F contacts are also observed: B(1)-F(12) 2.914 Å, B(1)-F(19) 2.816 Å, B(1)-F(23) 2.823 Å and B(1)-F(28) 2.829 Å (ca. 2.85 Å average).

- 2,6-Bis(trifluoromethyl)phenyl boronic acid ($Ar'B(OH)_2$)

$Ar'B(OH)_2$ was obtained by slow hydrolysis of $Ar'BCl_2$, leaving the flask exposed to air.

- NMR

The ^{19}F NMR spectrum exhibited a singlet at -55.2 (6F, *o*-CF_3) ppm.

- X-ray structure of $Ar'B(OH)_2$

$Ar'B(OH)_2$ crystals were grown in an NMR tube containing a solution of $Ar'BCl_2$ after one month of standing and were submitted for X-ray diffraction. The structure at 120 K was ascertained by A.L Thompson, and is shown in Figure 2.8:

Figure 2.8: *Molecular structure of $Ar'B(OH)_2$*

$Ar'B(OH)_2$ crystallises in the orthorhombic space group with Z=4. Selected bond distances and angles are included in Table 2.11. The B(1)-C(1) distance is 1.597(2) Å, and is slightly shorter than the one found in Ar_2BOH (1.613 Å). The average B-O distance is 1.35 Å. As in Ar_2BOH, some H---F intramolecular contacts were observed: F(6)-H(1B) 2.714 Å and F(3)-H(2B) 2.707 Å. Short B---F contacts from the CF_3 groups in the *ortho* position were detected as in all other compounds: B-F(2) 2.622 and B-F(4) 2.634 Å. Hydrogen atoms of the OH groups appeared to be disordered.

2.5 Discussion

2.5.1 Comparison of the chemical shifts

The ^{11}B NMR chemical shifts are listed in Table 2.8:

	$ArBCl_2$	**$ArBF_2$**	**Ar_2BF**	**$Ar_2B(OH)$**	**Ar_2BN_3**[7]	**Ar_3B**[9]
δ ^{11}B (ppm)	56.8	26.0	45.1	-	49.3	?
	$Ar'BCl_2$		**Ar''_2BF**	**$Ar'B(OH)_2$**		**Ar''_3B**
δ ^{11}B (ppm)	57.5		47.8	-		73.6
		$MesBF_2$[21]	**Mes_2BF**[6]	**$Mes_2B(OH)$**[6]	**Mes_2BNH_2**[22]	**Mes_3B**[6]
δ ^{11}B (ppm)		25.7	53	51.4	43.8	79.2

Table 2.8: *^{11}B NMR chemical shifts for RBX_2 or R_2BX compounds*

The chemical shifts for R_3B and R_2BX are at higher frequency than those for RBX_2. The overall order is $R_3B > R_2BX > RBX_2$. Trigonal boron is a good σ donor and π acceptor, whereas halogens are σ and π donor ligands (Figure 2.9). High electron density around the nucleus and the π donor effect causes shielding. The 2p π orbital rises in energy with an increase in fluorine substitution, but the combined inductive effect is greater and hence the boron becomes progressively more positively charged.[23]

Ar_3B compounds only have σ interactions and no pπ interactions (B-C bonds); the electron density on boron decreases, causing a deshielding effect. Replacement of an aryl ring by halogens creates a shielding effect due to π back donation to the boron, on which the electron density is higher. The more halogens are bonded to the boron, the higher the electron density becomes on boron and thus causes a shielding effect.

Furthermore, the proximity of fluorine atoms from the fluoromes or fluoroxyl ligand to the boron centre (Table 2.10) may allow pπ interactions, resulting in the partial occupation of the vacant orbital on boron, and an increase in shielding.

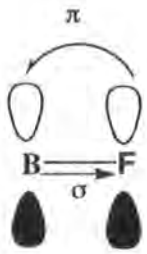

***Figure 2.9**: Electron donation from fluorine to boron*

A series of *ab initio* calculations has been carried out (at the GIAOHF/6-31G*//HF/6-31G* level) by M.A Fox using the Gaussian 98 package.[24] All calculations have been carried out on compounds containing no *para*-CF_3 groups (e.g. Ar or Ar" derivatives). Results are listed in Table 2.9:

Model Compounds (for calculations)	δ ^{11}B calc (ppm)	Compound	δ ^{11}B exp (ppm)
tris-(2-$CF_3C_6H_4$)	68.7	Ar"$_3$B	73.6
Ar'$_2$BF	44.1	Ar$_2$BF	45.1
Ar'$_2$B(OH)	41.2	Ar'B(OH)	
Ar'$_2$B(OH)	41.2	Ar$_2$B(OH)	
Ar'BF_2	22.6	$ArBF_2$	26.0
Ar'BCl_2	59.3	Ar'BCl_2	57.5
Ar'BCl_2	59.3	$ArBCl_2$	56.8
Ar'B(OH)	26.4	Ar'B(OH)$_2$	

Table 2.9: *Comparison between δ ^{11}B calculated and experimental*

Calculated values are in good agreement with to those found experimentally.

2.5.2 Comparison of the molecular structures

Table 2.10 lists selected bond lengths (Å) and angles (°) for Ar$_2$BF, Ar$_2$BOH and Ar$_2$BN$_3$.[7]

The B-X distance (X=F, OH or N_3) depends on the X substituents. The bigger the group X is, the longer the bonds will be. The same characteristics apply to the B-C distances: 1.620(6) Å for Ar$_2$BN$_3$, 1.61Å for Ar$_2$BOH and 1.59Å for Ar$_2$BF. Hence, the ligand X seems to have a direct effect on the B-C bond distances.

This is also observed in Ar'B(OH)$_2$ (Table 2.11), where the B-C distance is intermediate between those in Ar$_2$BN$_3$ and Ar$_2$BF.

Ar_2BF		Ar_2BOH		Ar_2BN_3	
B(1)-F(1)	1.313(3)	B(1)-O(1)	1.340(2)	B(1)-N(1)	1.404(6)
B(1)-C(21)	1.588(4)	B(1)-C(21)	1.608(2)	B(1)-C(11A)	1.620(6)
B(1)-C(11)	1.594(4)	B(1)-C(11)	1.618(2)	B(10)-C(11B)	1.620(6)
F(1)-B(1)-C(21)	116.0(2)	O(1)-B(1)-C(21)	112.65(13)	C(11A)-B(1)-N(1)	115.0
F(1)-B(1)-C(11)	115.5	O(1)-B(1)-C(11)	121.62	C(11B)-B(1)-N(1)	115.0
C(21)-B(1)-C(11)	128.5	C(21)-B(1)-C(11)	125.73	C(11A)-B(1)-C(11B)	

Table 2.10: *Selected Bond Lengths (Å) and Angles (°) for Ar_2BX compounds*

$Ar'B(OH)_2$		Ar''_3B	
B(1)-O(1)	1.355(2)	B(1)-C(11)	1.582(4)
B(1)-O(2)	1.360(2)	B(1)-C(21)	1.582(4)
B(1)-C(1)	1.597(2)	B(1)-C(31)	1.582(4)
C(1)-B(1)-O(1)	118.15(14)	C(11)-B(1)-C(21)	117.6(2)
C(1)-B(1)-O(2)	121.03(14)	C(11)-B(1)-C(31)	124.7(2)
O(1)-B(1)-O(2)	118.3(3)	C(21)-B(1)-C(31)	117.0(2)

Table 2.11: *Selected Bond Distances (Å) and Angles (°) for $Ar'B(OH)_2$ and Ar''_3B*

2.5.3 **Short contact distances**

In all the compounds, short B---F contacts are observed. The number of contacts depends of the number of CF_3 groups in the *ortho*-position. These are listed in Table 2.12. B---F contacts are shorter in compounds containing only one aryl ring. In $Ar_2B(OH)$, the range 2.829-2.914Å is broader, probably because of the F---H interaction discussed earlier.

	Ar_2BF	$Ar_2B(OH)$	$Ar'B(OH)_2$	Ar''_3B
B-F	2.763-2.796	2.829-2.914	2.622-2.634	2.800-2.815
No. of Contacts	4	4	2	3
No. of *ortho*-fluorines	12	12	6	9

Table 2.12: *Short B---F Contacts (Å)*

2.5.4 **Optimised geometry**

The geometry of the compounds structurally characterised has been optimised (at the HF/6-31G* level) by M.A. Fox with a Gaussian 98 package[24]. The structure was simulated and bond distances and angles evaluated (Appendix A).

Table 2.13 compares the calculated distances with the experimental data. Values are very similar. In each case, short B---F contacts are found. The optimised values for boronic acids ($Ar'B(OH)_2$ and $Ar'_2B(OH)$) also show the presence of an intramolecular F---H bridge.

2.6 Attempted reactions with Aluminium Chloride

Apparently, no previous attempts have been made to synthesise aluminium derivatives containing fluoromes or fluoroxyl ligands

2.6.1 Reaction with 2,6-bis(trifluoromethyl)phenyl lithium (Ar'Li) / 2,4-bis(trifluoromethyl)phenyl lithium (Ar"Li)

A solution of Ar'Li/Ar"Li in diethyl ether was added slowly to an $AlCl_3$ solution in diethyl ether. The ^{19}F NMR showed a set of signals corresponding to *ortho*-CF_3 and *para*-CF_3 but none of them has been assigned. This reaction appears to give rise to a mixture of mono- and di-substituted compounds.

2.6.2 Reaction with 2,4,6-tris(trifluoromethyl)phenyl lithium (Ar'Li)

A solution of ArLi was added to an $AlCl_3$ solution in diethyl ether at 0°C. A number of signals corresponding to *o*-CF_3 and *p*-CF_3 were observed, indicated the presence of a mixture of different products in solution. However, a peak of high intensity corresponding to the starting material ArLi showed that aluminium chloride does not react very well with ArLi.

$Ar'B(OH)_2$			$Ar_2B(OH)$			Ar_2BF			$Ar"_3B$		
			$Ar'_2B(OH)$			Ar'_2BF			tris(2		$-CF_3C_6H_4)$
	optimised	exp.		opt.	exp		opt.	exp.		opt.	exp
B-O	1.352	1.355	B-O	1.336	1.340	B-C	1.604	1.591	B-C	1.595	1.582
B-C	1.599	1.597	B-C	1.620	1.613	B-F	1.313	1.313			
B---F	2.606	2.628	B---F	2.836	2.845	B---F	2.785	2.670	B---F	2.850	2.806
F---H	2.384	2.710									
O-B-O	117.337	118.225	O-B-C	116.77	117.13	F-B-C	115.409				
O-B-C	125.325	121.03	C-B-C	126.455	125.73	C-B-C	129.186	128.500	C-B-C	119.9	119.8

Table 2.13: *Comparison between optimised and experimental structural data**

* all bond distances(Å) and angles (°) given in this table are average distances (in Å)

2.7 Experimental

2.7.1 **Introduction**

- NMR spectroscopy

All manipulations, including NMR sample preparation, were carried out either under an inert atmosphere of dry nitrogen or in vacuo, using standard Schlenk procedures or a glovebox. Chemicals of the best available commercial grades were used, in general without further purification. ^{19}F NMR spectra were recorded on a Varian Mercury 200, Varian VXR 400, or Varian Inova 500 Fourier-transform spectrometer at 188.18, 376.35, and 470.26 MHz respectively. ^{11}B NMR spectra were recorded on the Varian Mercury 300 or Varian Inova 500 spectrometer at 96.22 and 160.35 MHz respectively. ^{1}H and ^{13}C NMR spectra were recorded on the Varian VXR 400 instrument at 400 and 100.57 MHz respectively. Chemical shifts were measured relative to external $CFCl_3$ (^{19}F) or $BF_3.Et_2O$ (^{11}B), with the higher frequency direction taken as positive.

- C,H,N analysis

Microanalyses were performed by the microanalytical services of the Department of Chemistry, using micro-combustion on a Perrkin Elmer CE 440 Elemental Analyser.

- X-ray Crystallography

Single crystal structure determinations were carried out from data collected at 120 K, using graphite monochromated Mo Kα radiation (λ = 0.71073 Å) on a Bruker SMART-CCD detector diffractometer equipped with a Cryostream N_2 flow cooling device.[25] In each case, series of narrow ω-scans (0.3°) were performed at several φ-settings in such a way as to cover a sphere of data to a maximum resolution between 0.70 and 0.77 Å. Cell parameters were determined and refined using the SMART software,[26] and raw frame data were integrated using the SAINT program.[27] The structures were solved using direct methods and refined by full-matrix least squares on F^2 using SHELXTL.[28]

- **Computation section**

All *ab initio* computations were carried out with the Gaussian 98 package.[24] The geometries discussed here were optimised at the HF/6-31G* level with no symmetry constraints. Frequency calculations were computed on these optimised geometries at the HF/6-31G* level for imaginary frequencies. Theoretical ^{11}B chemical shifts at the GIAO-HF/6-31G*//HF/6-31G* level have been referenced to B_2H_6 (16.6 ppm[29]) and converted to the usual $BF_3.OEt_2$ scale: $\delta\ ^{11}B = 123.4 - \sigma(^{11}B)$.

2.7.2 Synthesis of ArH

The vacuum line used for this reaction was specifically designed for the use and manipulation of SF_4. The inside of the line was coated with Teflon to prevent corrosion of the steel from the highly reactive gas. The vacuum system is outlined below (see figure)

An upper reservoir of known volume (425 cm^3) was filled over a period of 15 min with SF_4 from a cylinder. The mass of this gas was equal to approximately 150g. This was subsequently transferred to a small sample bottle (Teflon lined steel), using vacuum transfer methods. From the initial tare of the bottle the quantity of SF_4 transferred could be determined. This process was then repeated until the desired quantity of SF_4 (550g, 5.1 moles) had been obtained. The bottle was then allowed to warm to room temperature

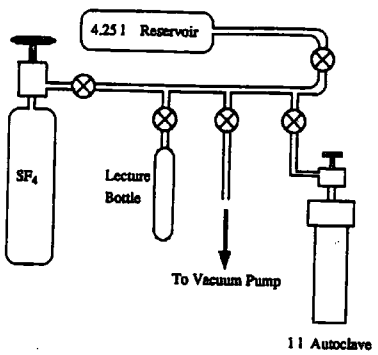

Figure 2.11 *Steel Vacuum Line for SF_4 Transfer*

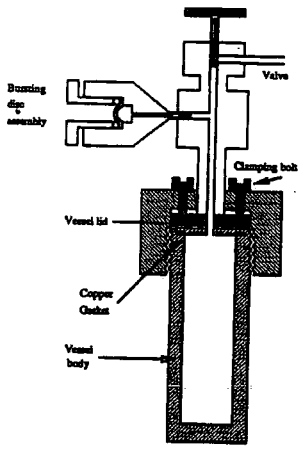

Figure 2.11: *Autoclave for SF_4 Fluorination Reactions*

Trimesic acid (benzene-1,3,5-tricarboxylic acid) (126g, 0.6 moles) was introduced into a 1000 cm^3 bomb. It was then evacuated and cooled to 76 K in liquid air.

The contents of the steel bottle were then carefully condensed into the bomb and the tare of the bottle checked to ensure that all the SF_4 had been transferred. The bomb was then place in a furnace, and heated with the help of thermocouples to a temperature of 150°C, which was maintained for the duration of the reaction (12 hours). The reaction was then allowed to cool to room temperature and the bomb was transferred to a fume cupboard.

$$C_6H_3(COOH)_3 \xrightarrow[423K \\ 130\ Atmos.Pressure]{SF_4} C_6H_3(CF_3)_3$$

The by-products of the reaction are SO_2, HF, and any unreacted SF_4. These gases need to be scrubbed, neutralised, and not allowed into the atmosphere. The gases were slowly passed over a funnel, which was placed in a big beaker filled with water.

After scrubbing the gases, the contents of the bomb were then tipped onto crushed ice to remove any unreacted trimesic acid and HF. The mixture was then filtered, and the filtrate washed three times with NaOH. The oily yellow compound was then separated and dried overnight over anhydrous magnesium sulphate.

The product was then purified by distillation using a fractionating column to yield a colourless oil (Bp 114°C). Yield 95g (75.4%)

^{19}F NMR ($CDCl_3$): δ -63.5 (singlet) ppm; **^{1}H NMR** ($CDCl_3$):δ 8.1 (singlet) ppm.

2.7.3 Preparation of ArLi

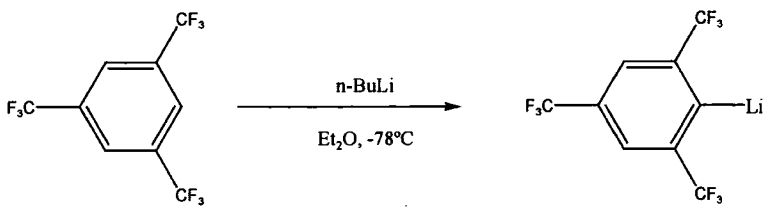

BuLi (41.75ml, 1.6 M in hexanes, 78 mmol) was added dropwise over 10 min to a solution of ArH (78 mmol) in diethyl ether at -78°C. The solution was allowed to warm to room temperature and stirred for 4 hours, giving a brown solution.

^{19}F NMR ($CDCl_3$): δ -53.6 (s, 6F, *o*-CF_3), δ-63.6 (s, 3F, *p*-CF_3)

2.7.4 Preparation of Ar'Li/Ar"Li

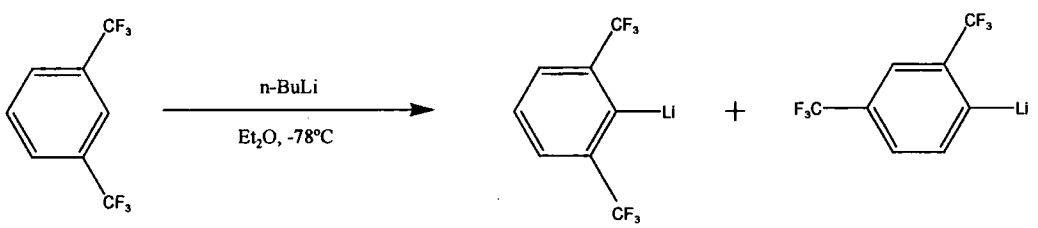

BuLi (57 ml, 1.6 M in hexanes, 91.2 mmol) was added dropwise over 10 min to a solution of Ar'H (91.2 mmol) in diethyl ether (200 ml) at -78°C. The solution was allowed to warm to room temperature and stirred for 4 hours, giving a dark brown solution.

^{19}F NMR ($CDCl_3$): Ar'Li δ -63.9 (s); Ar"Li δ-62.4 (s), -63.2 (s) ppm.

2.7.5 Synthesis of $ArBCl_2$

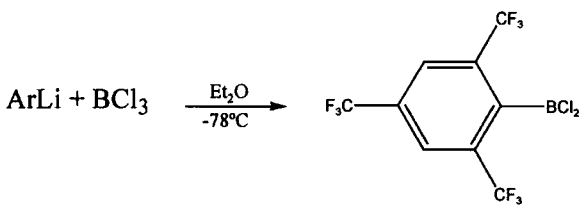

A solution of ArLi (50 ml, 20 mmol) was added dropwise to a BCl_3 solution (20 ml, 1M in p-xylene, 20 mmol) in diethyl ether at –78°C. A white precipate of LiCl immediately formed. The solution was stirred for 5 hours, giving a yellow solution. The solution was then filtered and solvents were removed under vacuum (0.01 Torr), leaving a yellow oil, which was distilled; a yellow oil was collected at 60°C.

^{19}F NMR ($CDCl_3$): δ -56.3 (s, 6F, *o*-CF_3), -63.9 (s, 3F, *p*-CF_3) ppm; **^{11}B NMR** ($CDCl_3$): δ 56.8 ppm (s).

2.7.6 Synthesis of Ar_2BF

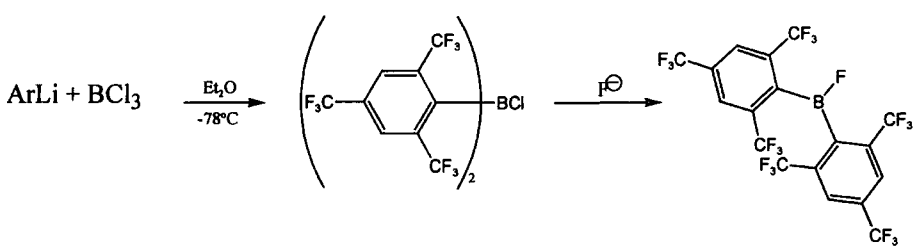

In the synthesis described previously for $ArBCl_2$, another product of the reaction is Ar_2BF. When the solvents were removed, a yellow oil and a white solid appeared. The latter was filtered off and washed three times with hexanes and dried in vacuo. Crystals were obtained by recrystallisation from dichloromethane. Yield 1.5g (13%).

Elemental analysis for $C_{18}H_4BF_{19}$ (592.02): Calc C 36.56, H 0.68%; Found C 35.04, H 0.98%.

^{19}F NMR: δ -57.3 (d, $^5J_{F\text{-}F}$ 14.3Hz, 12F, *o*-CF_3), -64.0 (s, 6F, *p*-CF_3), -131.5 (m, 1F, B-F) ppm; **^{11}B NMR**: δ 45.1 ppm (s).

2.7.7 Synthesis of Ar'BCl_2

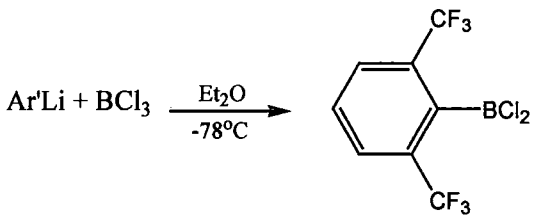

A solution of Ar'Li/Ar"Li mixture in Et_2O (100 ml, 45.6 mmol) was added dropwise to a solution of BCl_3 (22.8 ml, 1M in *p*-xylene, 22.8 mmol) at -78°C. The solution was allowed to warm to room temperature for 3 hours leaving a brown solution. A white solid of LiCl formed. The solution was filtered and the solvents removed under vacuum, leaving a brown oil, which was distilled under reduced pressure (0.05 Torr). A fraction was collected at 48°C.

^{19}F NMR ($CDCl_3$): δ -56.8 (s, 6F, *o*-CF_3) ppm; **^{11}B NMR** ($CDCl_3$): δ 57.5 ppm.

2.7.8 Synthesis of Ar"$_2$BF

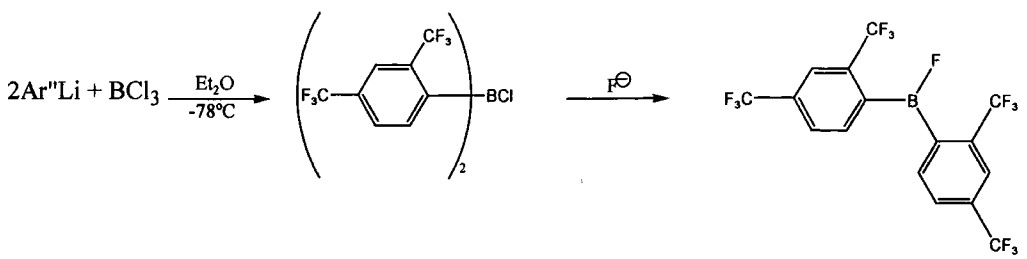

In the synthesis of Ar'BCl_2 described previously, another product of the reaction is Ar"$_2$BF. Using the same reaction, this compound was distilled under reduced pressure yielding a colourless oil [Bp=92°C (0.05 Torr)].

^{19}F NMR ($CDCl_3$): δ -57.2 (d, $^5J_{F\text{-}F}$ 14.7 Hz, 6F, *o*-CF_3), -63.3 (s, 6F, *p*-CF_3), -86.6 (m, 1F, B-F) ppm; **^{11}B NMR** ($CDCl_3$): δ 47.8 ppm.

2.7.9 Synthesis of Ar"$_3$B

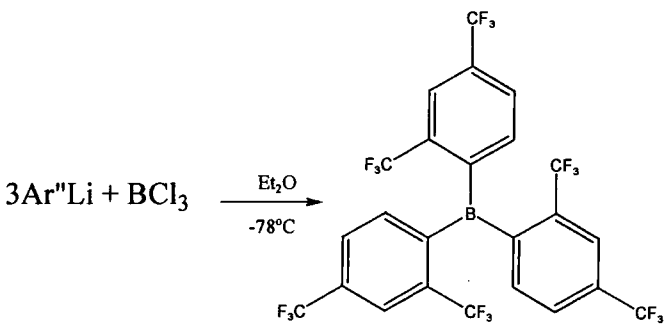

In the synthesis of Ar'BCl_2 described previously, a by-product of the reaction is Ar"$_3$B. After distillation, a white solid remained in the flask. This solid was washed 5 times with dichloromethane and purified by sublimation under vacuum. This afforded some white crystals.

^{19}F NMR ($CDCl_3$): δ -56.6 (s, 9F, *o*-CF_3), -63.8 (s, 9F, *p*-CF_3) ppm; **^{11}B NMR** ($CDCl_3$): δ 73.6 ppm; **^{13}C NMR** ($CDCl_3$): δ 143.7 9 (broad singlet), 135.2 (s), 133.6 (q, $^2J_{C-F}$ 33.7), 133.5 (q, $^2J_{C-F}$ 33.7) 127.3 (d, J 3.6), 123,1 (q, J_{C-F} 274.2), 122.9(q, J_{C-F} 274.2), (121.1 (broad singlet) ppm; **^{1}H NMR** ($CDCl_3$): δ 8.0 (s), 7.8 (d, $^3J_{H-H}$ 7.75), 7.4 (d, $^3J_{H-H}$ 7.8) ppm

References

1 M. F. Lappert, *Chem. Rev,* **1956**, *56*, 1024.

2 M. K. Majumdar, *J. Organomet. Chem.,* **1966**, *6*, 316.

3 R. T. C. Brownlee, R. W. Taft, *J. Am. Chem. Soc.,* **1970**, *92*, 7007.

4 R. D. Chambers, T. Chivers, *Proc. Chem. Soc.,* **1963**, 208.

5 H. J. Frohn, H. Franke, P. Fritzen, V. V. Bardin, *J. Organomet. Chem.,* **2000**, *598*, 127.

6 N. M. D. Brown, F. Davidson, R. McMullan, J. W. Wilson, *J. Organomet. Chem.,* **1980**, *193*, 271.

7 W. Fraenk, T. M. Klapötke, B. Brumm, P. Mayer, H. Nöth, H. Piotrowski, M. Suter, *J.Fluorine Chem.,* **2001**, *112*, 73.

8 T. D. Coyle, F. G. A. Stone, *J. Chem. Phys.,* **1960**, *32*, 1892.

9 H. P. Goodwin, *Ph.D Thesis*, Durham, 1990.

10 J. F. Blount, P. Finocchiaro, D. Gust, K. Mislow, *J. Am. Chem. Soc.,* **1973**, *95*, 7019.

11 F. Zettler, H. D. Hausen, H. Hess, *J. Organomet. Chem.,* **1974**, *72*, 157.

12 W. V. Konze, B. L. Scott, G. J. Kubas, *Chem. Commun.,* **1999**, 1807.

13 S. Toyota, M. Asakura, M. Oki, F. Toda, *Bull. Chem. Soc. Jpn.,* **2000**, *73*, 2357.

14 T. Onak, *Organoborane Chemistry*; Academic Press, New York, **1975**.

15 V. C. Gibson, C. Redshaw, W. Clegg, M. R. J. Elsegood, *Polyhedron,* **1997**, *16*, 2637.

16 N. Burford, C. L. B. Macdonald, D. J. LeBlanc, T. S. Cameron, *Organometallics,* **2000**, *19*, 152.

17 K. H. Whitmire, D. Labahn, H. W. Roesky, M. Noltemeyer, G. M. Sheldrick, *J. Organomet. Chem.,* **1991**, *402*, 55.

18 J. Emsley, *The Elements*; 2nd ed.; Oxford University Press, Oxford, **1991**.

19 H. Nöth, B. Wrackmeyer, *Nuclear Magnetic Resonance Spectroscopy of Boron Compounds*; Springer-Verlag, New York, **1978**; Vol. 9.

20 K. Ishihara, M. Mouri, Q. Gao, T. Maruyama, K. Furuta, H. Yamamoto, *J. Am. Chem. Soc.*, **1993**, *115*, 11490.

21 G. Bir, W. Schacht, D. Kaufmann, *J. Organomet. Chem.*, **1988**, *340*, 267.

22 R. A. Bartlett, H. Chen, H. V. R. Dias, M. M. Olmstead, P. P. Power, *J. Am. Chem. Soc.*, **1988**, *110*, 446.

23 M. E. Schwartz, L. C. Allen, *J. Am. Chem. Soc.*, **1970**, *92*, 1466.

24 Gaussian 98; Revison A.9, M. J. Frisch, G. W. Trucks, H. B. Schlegel, G. E. Scuseria, M. A. Robb, J. R. Cheeseman, V. G. Zakrzewski, J. A. Montgomery, Jr., R. E. Stratmann, J. C. Burant, S. Dapprich, J. M. Millam, A. D. Daniels, K. N. Kudin, M. C. Strain, O. Farkas, J. Tomasi, V. Barone, M. Cossi, R. Cammi, B. Mennucci, C. Pomelli, C. Adamo, S. Clifford, J. Ochterski, G. A. Petersson, P. Y. Ayala, Q. Cui, K. Morokuma, D. K. Malick, A. D. Rabuck, K. Raghavachari, J. B. Foresman, J. Cioslowski, J. V. Ortiz, A. G. Baboul, B. B. Stefanov, G. Liu, A. Liashenko, P. Piskorz, I. Komaromi, R. Gomperts, R. L. Martin, D. J. Fox, T. Keith, M. A. Al-Laham, C. Y. Peng, A. Nanayakkara, M. Challacombe, P. M. W. Gill, B. Johnson, W. Chen, M. W. Wong, J. L. Andres, C. Gonzalez, M. Head-Gordon, E. S. Replogle, and J. A. Pople, Gaussian, Inc., Pittsburg PA, 1998.

25 J. Cosier, A.M.Glazer, *J. Appl. Cryst.*, **1986**, *19*, 105.

26 SMART -NT; Data Collection Software, version 5.0, Bruker Analytical X-ray Instruments Inc., Madison, Wisconsin, USA, **1999**.

27 SAINT-NT; Data Reduction Software, version 6.0, Bruker Analytical X-ray Instruments Inc, Madison, Wisconsin, U.S.A., **1999**.

28 SHELXTL; version 5.1, Bruker Analytical X-ray Instruments Inc, Madison, Wisconsin, U.S.A., **1999**.

29 T. P. Onak, H.L.Landsman, R. E. Williams, *J. Phys. Chem.*, **1959**, *63*, 1533.

Chapter 3
Group 14 Derivatives

3.1 Introduction

Steric encumbrance in substituents bound to main group elements has led to kinetic stability in complexes. A number of bulky organic substituents has been used to stabilize compounds of group 14 elements, such as mesityl, t-butyl, bis(trimethylsilyl)methyl, tris(trimethylsilyl)methyl, 2,4,6-tri(t-butyl)phenyl and 2,4,6-tri(i-propyl)phenyl.[1,2] Surprisingly, little has been published about group 14 species containing fluoromes or fluoroxyl substituents. In this chapter, the preparation of a series of tetravalent group 14 derivatives (Si, Ge and Sn) is described.

3.1.1 **Organosilicons**

Organosilicon compounds have a considerable stability due to the strength of the Si-C bond. There are three general methods to form organosilicon compounds:

- reaction of $SiCl_4$ with organolithium, organoaluminium, or Grignard reagents:

$$RLi + SiCl_4 \longrightarrow RSiCl_3 + LiCl$$
$$R_3Al + 3\ SiCl_4 \longrightarrow 3\ RSiCl_3 + AlCl_3$$
$$RMgX + SiCl_4 \longrightarrow RSiCl_3 + MgClX$$

- hydrosilation of alkenes

Catalytic addition of Si-H across C=C double bonds (except for methyl and phenyl silanes)

$$RCH{=}CH_2 + HSiR_3 \longrightarrow RCH_2CH_2SiR_3$$

- direct reaction of RX or ArX with silicon in the presence of Cu as a catalyst (industrial method)[3]

$$2\ MeCl + Si \xrightarrow[300°C]{\text{Cu powder}} Me_2SiCl_2$$

3.1.2 Organogermanium derivatives

Preparative routes to organogermanium compounds parallel those for organosilicon compounds (see equations above), via an organolithium or Grignard reagent. Most of the several known organogermanium compounds can be considered as derivatives of R_nGeX_{4-n} or Ar_nGeX_{4-n} where X=hydrogen, halogen, OR, ...

3.1.3 Organotin compounds[4,5]

Organotin chemistry has been much more extensively investigated that those of germanium or silicon.
There are three synthetic routes:

- reaction with a Grignard reagent:

$$4\ RMgCl + SnCl_4 \longrightarrow SnR_4 + 4\ MgCl_2 \quad (\text{also with ArMgCl})$$

- reaction with an organoaluminium compound:

$$4\ AlR_3 + 3\ SnCl_4 \longrightarrow 3\ SnR_4 + 4\ AlCl_3$$

- direct reaction of RX with the element:

$$2\ RX + Sn \longrightarrow R_2SnX_2 \quad (\text{and } R_nSnX_{4-n}) \quad (\text{alkyl only})$$

A few examples containing the fluoromes substituent attached to group 14 elements have been reported in the literature: $ArSiMe_3$,[6] Ar_2SiF_2,[7] Ar_2SiHF, Ar_2SiH_2[8] and Ar_2GeH_2,[9] which was synthesised from the precursor Ar_2Ge. The reaction of ArLi with Ph_3SnCl gave $ArSnPh_3$.[10] Ar_2Sn can undergo oxidation reactions to lead to tin(IV) compounds. Thus, Ar_2SnF_2 is prepared by reaction of AsF_5 with Ar_2Sn. There are two general routes to prepare Ar_2SnCl_2:[11]

- Chlorination of Ar_2Sn:

$$Ar_2Sn + Cl_2 \longrightarrow Ar_2SnCl_2$$

- Reaction of ArLi with $SnCl_4$

$$2\ ArLi + SnCl_4 \longrightarrow Ar_2SnCl_2 + 2\ LiCl$$

The only examples containing Ar' or Ar" are tin derivatives: $Ar'SnMe_3$,[12,13] $Ar"SnMe_3$[12,13] and Ar'_2Sn.[14]

$$2\ ArLi + SiCl_4 \xrightarrow{F/Cl\ exchange} Ar_2SiF_2$$

$$2\ ArLi + HSiCl_3 \xrightarrow{F/Cl\ exchange} Ar_2SiHF$$

$$Ar_2SiHF + LiAlH_4 \longrightarrow Ar_2SiH_2$$

$$2\ Ar'Li.TMED + SnCl_2 \longrightarrow Ar'_2Sn$$

Preliminary work has been done on Si, Ge and Sn derivatives by Xue.[15] A general reaction between ArLi or Ar'Li/Ar"Li with ECl_4 (E=Si, Ge, Sn) was used. Tetravalent derivatives $Ar"_2SiCl_2$, $ArGeCl_3$, $Ar"_2GeCl_2$, Ar_2SnCl_2 and $Ar'SnCl_2$ were structurally characterised.

3.2 Silicon derivatives

3.2.1 Reaction of $SiCl_4$ with 2,4,6-tris(trifluoromethyl)phenyl lithium

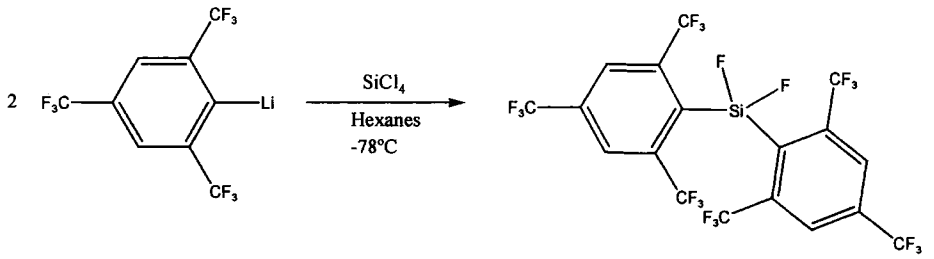

***Equation 3.1**: Synthesis of Ar_2SiF_2*

The reaction was carried out following the general method of reacting the lithiated compound ArLi with silicon tetrachloride $SiCl_4$.

ArLi was added slowly to a $SiCl_4$ solution in hexanes at -78°C. The ^{19}F NMR spectrum showed a triplet at –57.3 ($^5J_{F\text{-}F}$ 12.8 Hz), a singlet at – 64.2 and a multiplet at –124.5 ($^5J_{F\text{-}F}$ 12.8 Hz) ppm. The presence of a triplet at the chemical shift corresponding to the *o*-CF_3 suggests F-F coupling. This is confirmed by a multiplet at -124.5 ppm, assigned to the fluorines bonded directly to silicon. These signals suggest that only Ar_2SiF_2 can be isolated from the reaction. This has already been reported by Buijink *et al.*[7] The compound was isolated as a yellow oil (Bp 85° at 0.01 Torr).

The presence of Ar_2SiF_2 can be explained by a Cl/F exchange while the reaction takes place. This phenomenon has also been observed with the reaction with boron trichloride (Chapter 2), where a similar mechanism to the following has been proposed:

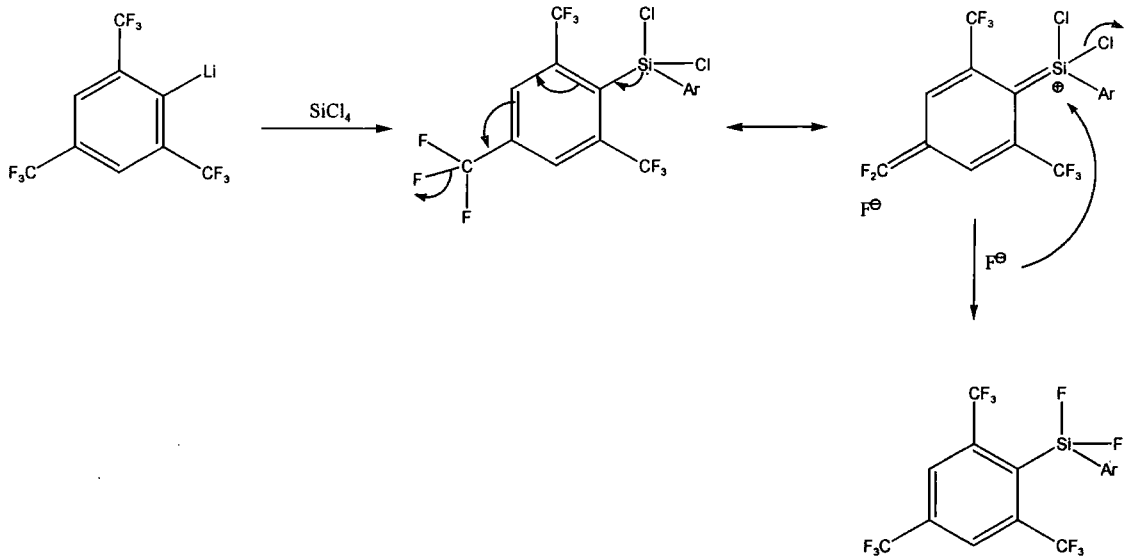

Scheme 3.1: *Possible mechanism of the formation of Ar_2SiF_2*

In order to check when the exchange occurs, an NMR tube reaction between ArH and $SiCl_4$ was attempted. The ^{19}F NMR spectrum only exhibited the presence of the starting material ArH at -63.5 ppm. This proves that the halogen exchange takes place once the Si (or B) atom is bonded to the ligand.

3.2.2 Reaction of $SiCl_4$ with a 2,6-bis(trifluoromethyl)phenyl lithium / 2,4-bis(trifluoromethyl)phenyl lithium mixture (Ar'Li/Ar"Li)

The mixture Ar'Li/Ar"Li was added to $SiCl_4$ in hexanes at -78°C. The ^{19}F NMR spectrum indicated the presence of different species in solution: Ar'_2SiCl_2, $Ar"_2SiCl_2$, Ar'_2SiF_2 and $Ar"_2SiF_2$ (Figure 3.1). Only $Ar"_2SiCl_2$ and $Ar"_2SiF_2$ have been isolated, as a yellow oil and a white solid respectively. Table 3.1 lists the chemical shifts of the different products of the reaction.

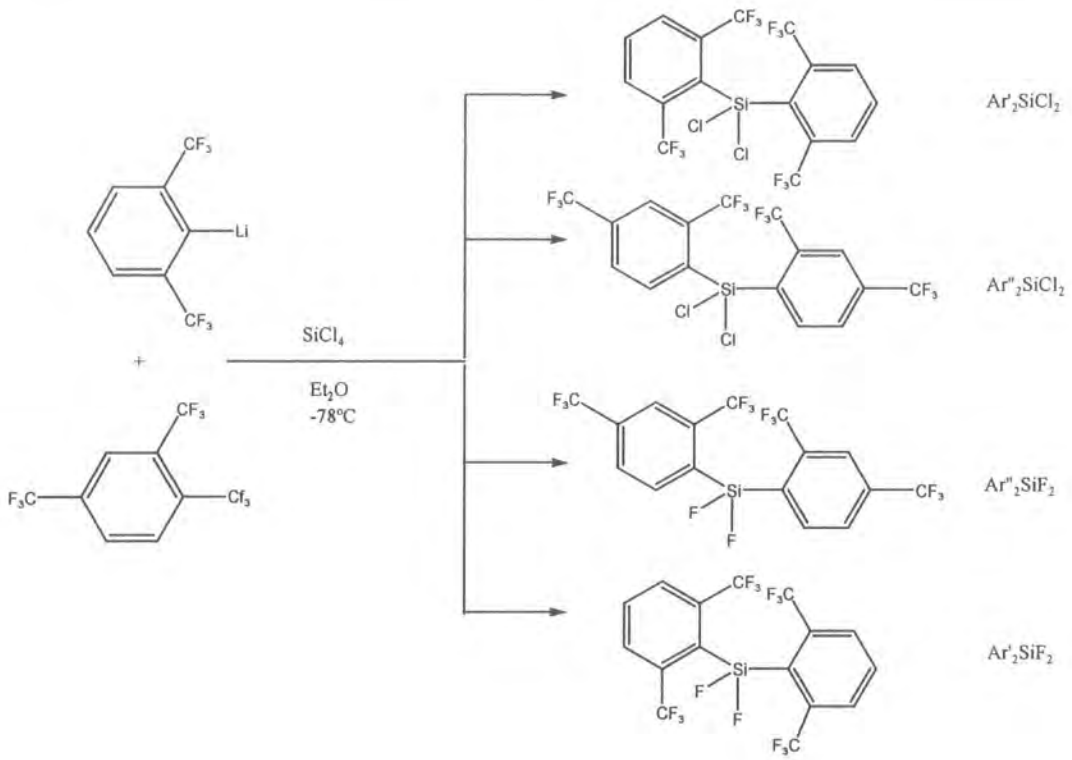

Scheme 3.2: *Different products of the reaction between Ar'Li/Ar"Li and $SiCl_4$*

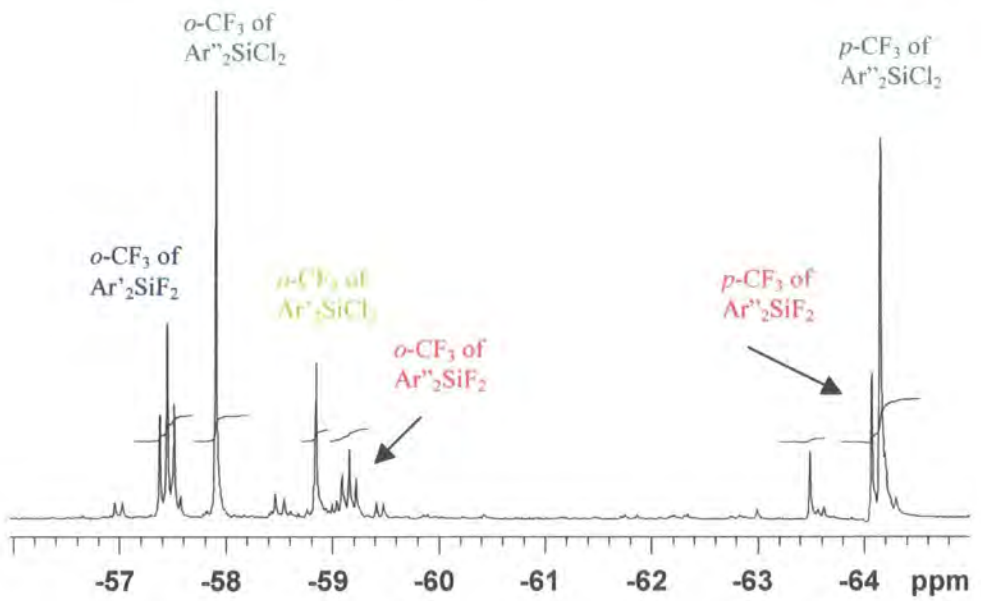

Figure 3.1: *^{19}F NMR spectrum of the reaction between Ar'Li/Ar"Li and $SiCl_4$*

Compound	δ for *o*-CF_3 (ppm)	δ for *p*-CF_3 (ppm)	δ for Si-F (ppm)
Ar''_2SiCl_2	-57.95 s (6F)	-64.2 s (6F)	
Ar'_2SiCl_2	-58.9 s (12F)		
Ar''_2SiF_2	-59.2 t, $^5J_{F-F}$ 12.4Hz (6F)	-64.1 s (6F)	-133.0 septet, $^5J_{F-F}$12.3Hz (2F)
Ar'_2SiF_2	-57.5 t, $^5J_{F-F}$ 12.3Hz (12F)		-125.5 m, $^5J_{F-F}$ 12.5Hz (2F)

Table 3.1: *$\delta^{19}F$ for the different products of the reaction between Ar'Li/Ar''Li and $SiCl_4$*

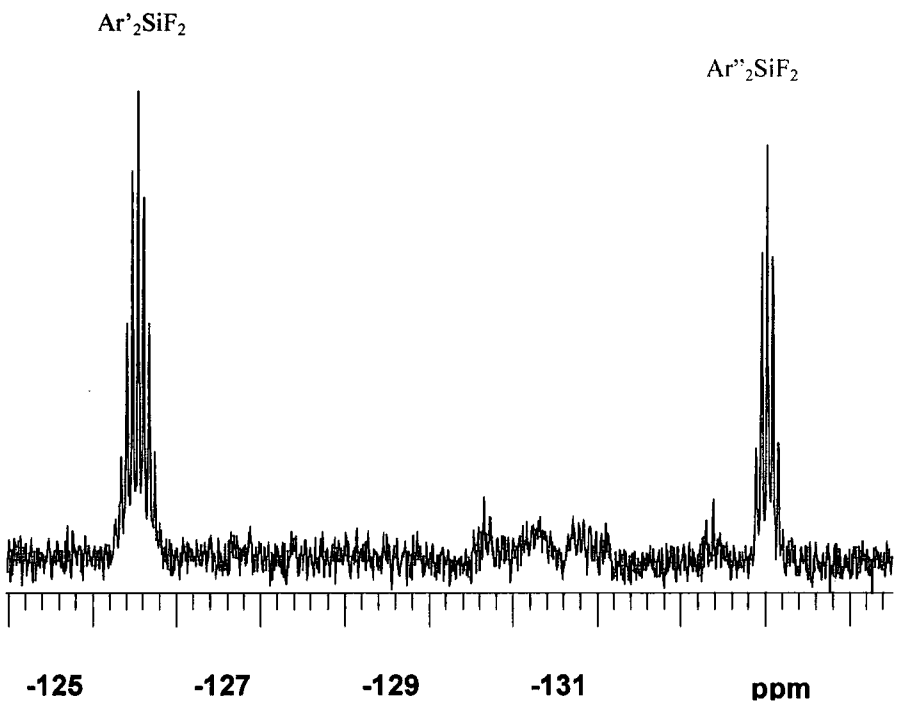

Figure 3.2: *^{19}F NMR region for the Si-F_2 signals in Ar'_2SiF_2 and Ar''_2SiF_2*

- $Ar"_2SiCl_2$

Crystals were obtained by recrytallisation from pentane by Xue.[15] The crystal structure has been determined by A.S. Batsanov (Figure 3.3).

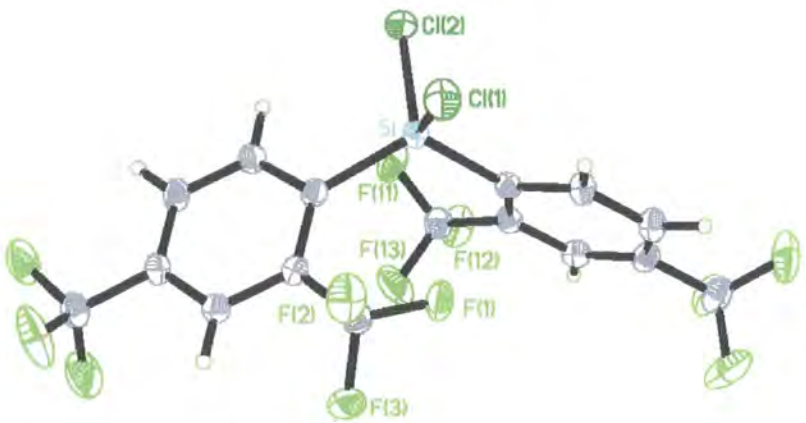

Figure 3.3: *Molecular structure of $Ar"_2SiCl_2$*

- Ar'_2SiF_2

Ar'_2SiF_2 was isolated as a white solid and purified by sublimation under vacuum (110°, 0.02 Torr). Crystals were submitted for X-ray diffraction. The structure was determined at 120K by A.L. Thompson and is shown in Figure 3.4:

Figure 3.4: *Molecular structure of Ar'_2SiF_2*

Ar'_2SiF_2 crystallises in the triclinic P-1 space group with Z=2. The compound exhibits an approximate tetrahedral geometry at the silicon with a C(11)-Si-C(21) angle of 115.53(8)°C. This angle is larger than normal for Si, and is due to the steric bulk of the aryl substituents. It is similar to the angle found in Ar_2SiHF (115.8(11)°),[8] and smaller than the one reported for Ar_2SiF_2 (119.1(2)°[7]). The F-Si-F angle in Ar_2SiF_2 was 105.8(2)°, and is 104.06(6)° in Ar'_2SiF_2. The Si-C distances, Si-C(11) 1.895(2) Å, Si-C(21) 1.8991(19) Å, are similar to those found in Ar_2SiHF and Ar_2SiF_2, and are within the range of values observed for other tetracoordinate silicon compounds (Si-C values in diarylsilicon dihalides reported to lie between 1.872(17) and 1.895(15) Å[16]).

The Si-F distances are 1.5790(3) and 1.5694(11) Å and are slightly longer than those found in Ar_2SiF_2. Table 3.2 lists selected bond distances (Å) for Ar_2SiHF,[8] Ar_2SiF_2[7] and Ar'_2SiF_2.

As found in Ar_2SiHF and Ar_2SiF_2, four short Si---F contacts are observed in Ar'_2SiF_2, within the range 2.745-3.073 Å, at an average interatomic distance of ca. 2.9162 Å. This value is shorter than the sum of van der Waals radii of 3.57 Å.[17]

Figure 3.6 shows the Si---F short contacts (covalent bonds are shown by a solid line and weaker interactions are designated by a dashed line).

Figure 3.7 shows the environment around the central atom.

This reveals a (4+4) coordination environment, which approaches a distorted tetracapped tetrahedron. The four Si---F contacts occupy approximate faces of the tetrahedron defined by the bonded atoms C(11), C(21), F(1) and F(2). This was also found for Ar_2SiF_2[8] and Ar_2SiHF as well as for bis[2,6-(dimethylaminomethyl)]silane, where the lone pair of each N was coordinated to Si.[18]

Ar_2SiHF		Ar_2SiF_2		Ar'_2SiF_2	
Si-F(1)	1.537(2)	Si-F(1)	1.557(3)	Si-F(11)	1.5790(13)
Si-H(1)	1.48	Si-F(2)	1.562(3)	Si-F(2)	1.5694911)
Si-C(1)	1.910(2)	Si-C(1)	1.913(5)	Si-C(11)	1.895(2)
Si-C(7)	1.911(2)	Si-C(10)	1.888(4)	Si-C(21)	1.8991(19)
Si-F(21)	2.974	Si-F(5)	2.715	Si-F(11)	2.793
Si-F(62)	2.773	Si-F(14)	3.056	Si-F(22)	3.073
Si-F(82)	3.075	Si-F(25)	2.728	Si-F(24)	2.745
Si-F(122)	2.713	Si-F(15)	3.006	Si-F(15)	3.054
C(1)-Si-C(7)	115.8(1)	C(10)-Si-C(1)	119.1(2)	C(11)-Si-C(21)	115.53(8)
H(1)-Si-F(1)	107.4	F(1)-Si-F(2)	105.8(2)	F(1)-Si-F(2)	104.06(6)
Ref	8	7		This work	

Table 3.2: *Selected Bond Distances (Å) and Angles (°) for Ar_2SiHF, Ar_2SiF_2 and Ar'_2SiF_2*

Figure 3.5: *Si---F Short Contacts (covalent bonds are shown by a solid line and weaker interactions are designated by a red line)*

Figure 3.6: *Coordination Environment around Silicon*

3.3 Germanium derivatives

3.3.1 Reaction of $GeCl_4$ with 2,4,6-tris(trifluoromethyl)phenyl lithium (ArLi)

ArLi was added to a solution of $GeCl_4$ in hexanes. The ^{19}F NMR spectrum showed the presence of two species in solutions: $ArGeCl_3$ and Ar_2GeCl_2. These were isolated as an oil and a solid respectively.

- $ArGeCl_3$

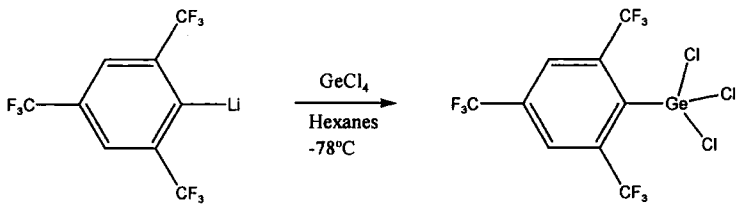

Equation 3.2: *Synthesis of $ArGeCl_3$*

This compound was purified by distillation under vacuum, leaving a yellow oil which crystallises on standing.

The ^{19}F NMR spectrum of $ArGeCl_3$ showed a singlet (6F) at –52.9 ppm for the *ortho*-CF_3 and a singlet (3F) at –63.5 ppm corresponding to the *para*-CF_3 groups.

$ArGeCl_3$ was previously synthesised by Xue,[15] and its crystal structure determined by A.S. Batsanov (Figure 3.7).

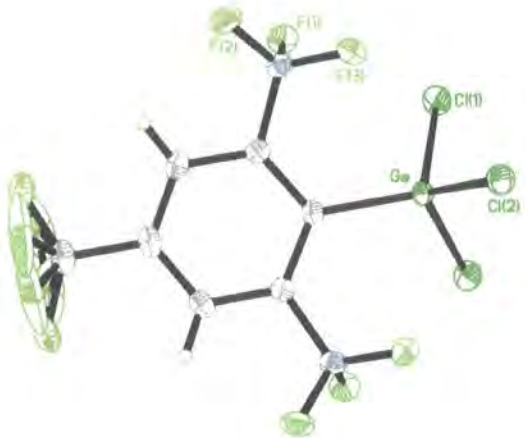

Figure 3.7: *Molecular structure of $ArGeCl_3$*

The geometry of the germanium atom is close to tetrahedral. There is a mirror plane through the molecule, with two of the chlorines and the *o*-CF_3 groups on the phenyl ring being symmetry-related. There is some asymmetry in the Cl-Ge-Cl bond angles which range from 99.82(3)° to 108.46(17)°. This probably arises from the Ge-F interactions with the fluorines in the *ortho* CF_3 groups. The Ge-C bond (Ge-C(1) 1.981(2)) distance is within the literature range for Ge-C bonds in Ar-Ge derivatives (1.942(1)-2.081(3)Å).[9,19] The *p*-CF_3 groups are found to be disordered.

- Ar_2GeCl_2

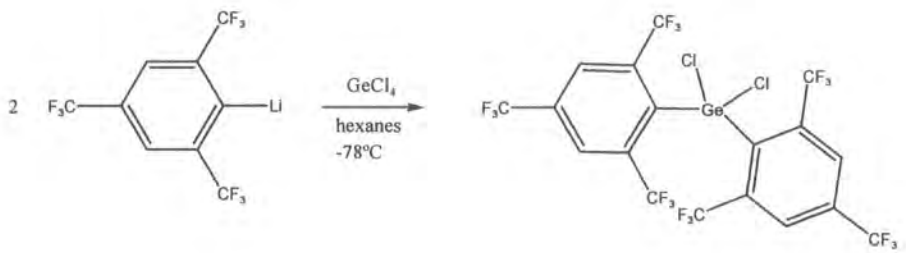

Equation 3.3: *Synthesis of Ar_2GeCl_2*

Ar_2GeCl_2 was isolated as a beige solid, which was purified by recrystallisation from dichloromethane. The ^{19}F NMR spectrum exhibited two singlets at –54.4 (12F) and –64.1(6F) ppm respectively, corresponding to the *o*-CF_3 and *p*-CF_3 groups.

- X-ray structure of Ar_2GeCl_2

Ar_2GeCl_2 was isolated as a beige solid and recrystallised from dichloromethame. Crystals were submitted for X-ray diffraction. The structure was determined at 120K by A.L. Thompson, and is shown in Figure 3.8:

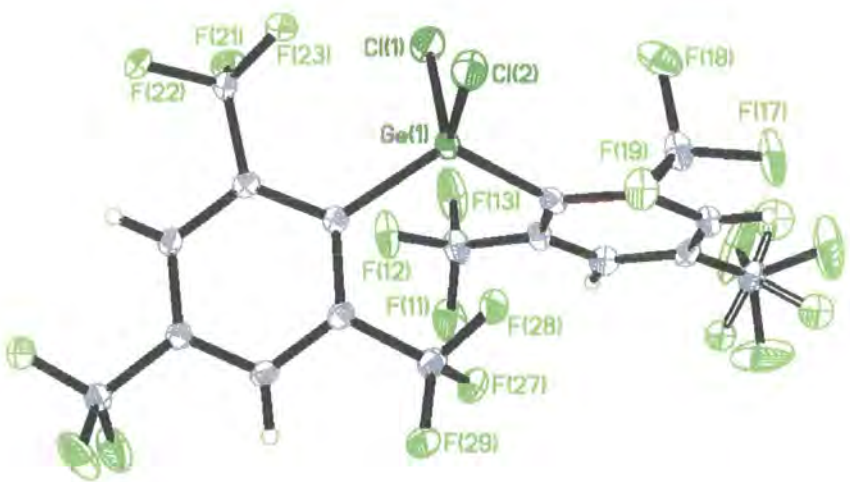

Figure 3.8: *Molecular structure of Ar_2GeCl_2*

Ar_2GeCl_2 crystallises in the monoclinic P2(1)/c space group with Z=4. One of the *para* CF_3 group is disordered. A distortion from tetrahedral geometry is observed, with a C-Ge-C angle of 120.07°. The Ge-C bond lengths are 1.997(3) Å for Ge-C(21) and 2.072(3) Å for Ge-C(11). These distances are similar to those found in Ar_2Ge (2.081(3) and 2.072(3) Å)[19] and are slightly longer than those in $ArGeCl_3$:[15] Ge-C(1) 1.981(2) Å. This is probably due to the steric hindrance imposed by a second fluoromes ligand. The Ge-Cl distances are in the same range as those found in $ArGeCl_3$ and slightly shorter than those

in $Ar"_2GeCl_2$.[15] However, this compound shows some asymmetry in the Ge-Cl distances, of 2.1174(9) Å and 2.1513(9) Å. Selected bond lengths (Å) and angles (°) for $ArGeCl_3$, Ar_2GeCl_2 and $Ar"_2GeCl_2$ are listed in Table 3.3 and Table 3.4. The four C-Ge-Cl angles in the disubstituted compounds vary between 96.65(9)° and 118.17(9)°.

Bond Distance (Å)		Angle (°)	
Ge-C(1)	1.981(2)	C(1)-Ge-Cl(2)	111.89(6)
Ge-Cl(12)	2.1117(8)	C(1)-Ge-Cl(1)	113.72(4)
Ge-Cl(1)	2.1277(4)	Cl(2)-Ge-Cl(1)	108.461(17)
Ge-Cl(1)#1	2.1277(4)	C(1)-Ge-Cl(1)#1	113.72(4)
		Cl(2)-Ge-Cl(1)#1	108.461(17)
		Cl(1)-Ge-Cl(1)#1	99.82(3)

Table 3.3: *Selected Bond distances (Å) and Angles (°) for* $ArGeCl_3$[15]

Bond Distance (Å)			Angle (°)		
	Ar_2GeCl_2	$Ar"_2GeCl_2$		Ar_2GeCl_2	$Ar"_2GeCl_2$
Ge(1)-C(1)	2.017(3)	1.957(2)	C(1)-Ge(1)-C(11)	120.07(12)	119.93(10)
Ge(1)-C(11)	1.997(3)	1.958(2)	C(1)-Ge(1)-Cl(1)	96.65(9)	108.30(7)
Ge(1)-Cl(1)	2.1513(9)	2.1483(8)	C(1)-Ge(1)-Cl(2)	118.17(9)	108.19(7)
Ge(1)-Cl(2)	2.1174(9)	2.1497(10)	C(11)-Ge(1)-Cl(1)	113.46(9)	107.76(7)
			C(11)-Ge(1)-Cl(2)	103.34(9)	108.67(7)
			Cl(1)-Ge(1)-Cl(2)	104.33(4)	102.65(4)

Table 3.4: *Selected Bond Distances (Å) and Angles (°) in Ar_2GeCl_2 and $Ar"2GeCl_2$*[15]

Three short Ge---F interactions are observed within the range 2.757-3.009Å, with an average interatomic distance of ca. 2.88Å. The distance is shorter than the sum of van der Waals radii of 3.66 Å.[17]

3.3.2 Reaction of $GeCl_4$ with a 2,6-bis(trifluoromethyl)phenyl lithium / 2,4-bis(trifluoromethyl)phenyl lithium mixture (Ar'Li/Ar"Li)

Ar'Li/Ar"Li was added to a solution of $GeCl_4$ in hexanes. The ^{19}F NMR spectrum showed predominantly the presence of $Ar"_2GeCl_2$, with two singlets at -58.7 (6F, *o*-CF_3) and -64.1 ppm (6F, *p*-CF_3). A single resonance at -53.8 ppm was assigned to the symmetrical molecule Ar'_2GeCl_2, since there were no signals of corresponding intensity for the *p*-CF_3. There were other low intensity peaks present in the spectrum however, and the signal at -53.8 ppm could possibly arise from $ArGeCl_3$, which should also give a single ^{19}F resonance (Figure 3.9).

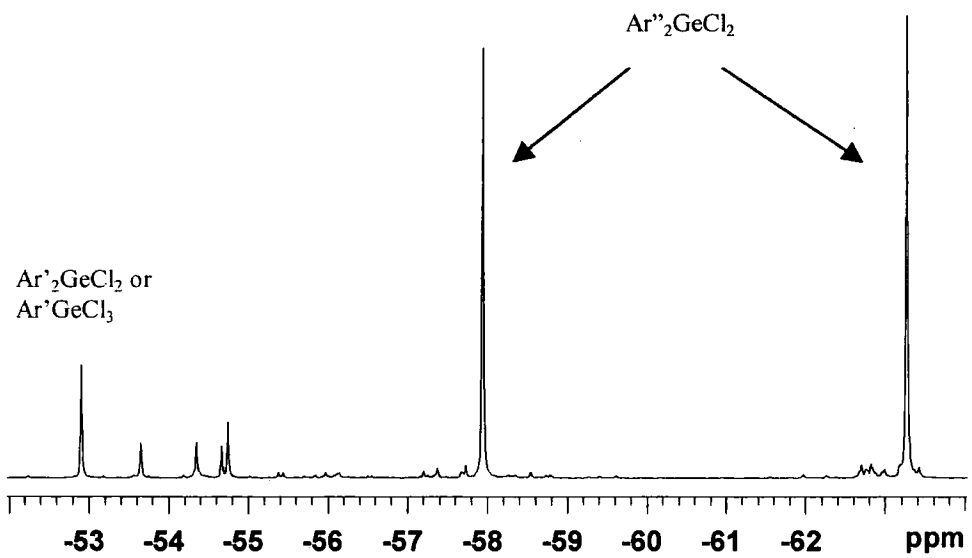

Figure 3.9: *^{19}F NMR spectrum of the reaction between Ar'Li/Ar"Li with $GeCl_4$*

3.4 Tin derivatives

3.4.1 Reaction of $SnCl_4$ with 2,4,6-tris(trifluoromethyl)phenyl lithium (ArLi)

A solution of ArLi was added to a $SnCl_4$ solution in hexanes. The ^{19}F NMR spectrum indicated the presence of $ArSnCl_3$ and Ar_2SnCl_2.

- $ArSnCl_3$

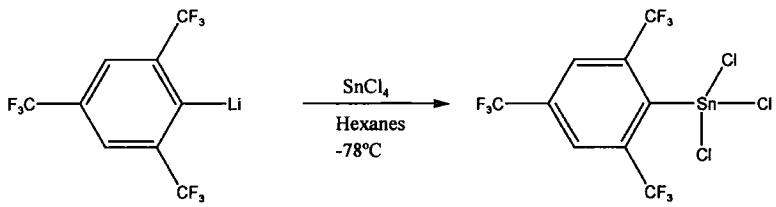

Equation 3.4: *Synthesis of $ArSnCl_3$*

This compound was isolated as an oil and purified by distillation under reduced pressure (0.01 Torr) (Bp 85°C).

The ^{19}F NMR spectrum consisted of two singlets, one with Sn satellites at –55.9 ($^4J_{Sn\text{-}F}$ 19.2Hz, 6F, *o*-CF_3) and one at –63.0 (3F, *p*-CF_3) ppm. The ^{119}Sn NMR spectrum showed a singlet at –140.7 ppm.

- Ar_2SnCl_2

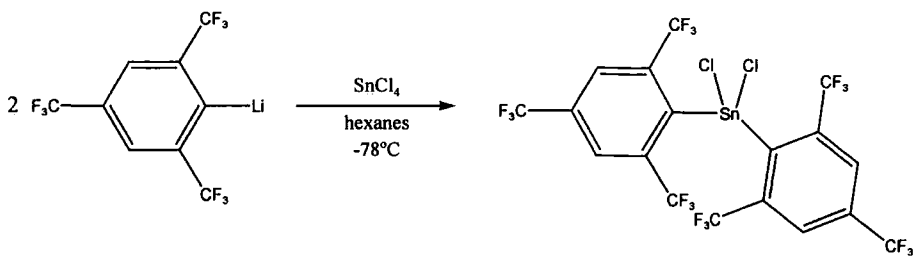

Equation 3.5: *Synthesis of Ar_2SnCl_2*

Ar_2SnCl_2 was isolated as a solid and recrystallised from diethyl ether.

The ^{19}F NMR spectrum exhibited singlets at -56.9 (with Sn satellites, $^4J_{Sn-F}$ 10.0Hz, 12F, *o*-CF_3) and -63.9 (6F, *p*-CF_3) ppm. The ^{119}Sn NMR spectrum consisted of a singlet at -146.7 ppm.

Ar_2SnCl_2 has already been synthesised by Xue,[15] and its crystal structure ascertained by A.E Goeta (Figure 3.10).

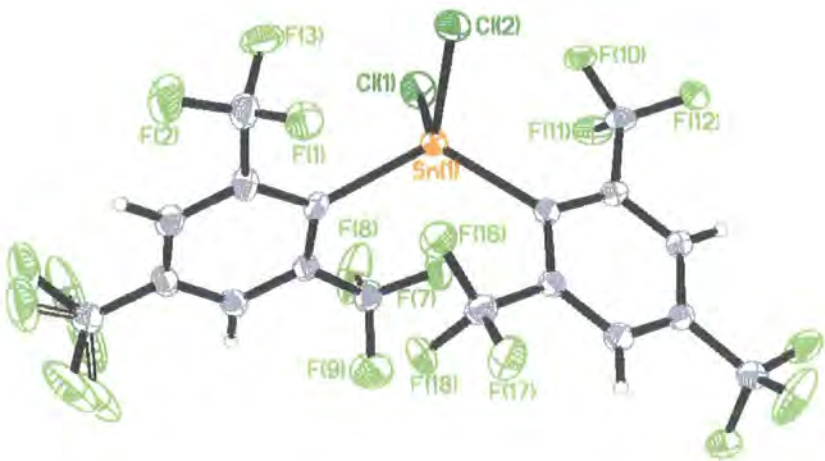

Figure 3.10: *Molecular structure of Ar_2SnCl_2*

The Sn-Cl bond lengths are similar (2.2977(17) and 2.3259(18) Å) to the values found for the only ArSnCl compound which has been structurally characterised, $Ar_2ClSn(\mu_2$-O)$SnClAr_2$, of 2.310(1) and 2.319(2) Å.[20]

3.4.2 Reaction of $SnCl_4$ with a 2,6-bis(trifluoromethyl)phenyl lithium / 2,4-bis(trifluoromethyl)phenyl lithium mixture (Ar'Li/Ar"Li)

An Ar'Li/Ar"Li solution in diethyl ether was added to a solution of $SnCl_4$ in hexanes at room temperature. The ^{19}F NMR spectrum showed the presence of two species in solution: Ar'_2SnCl_2 and $Ar"_2SnCl_2$ (Figure 3.11)

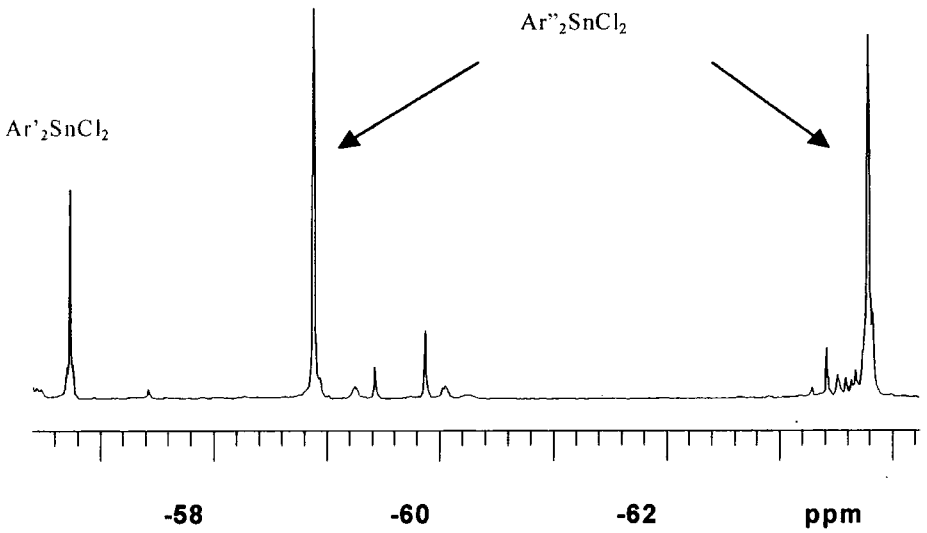

Figure 3.11: *^{19}F NMR spectrum of Ar'$_2$SnCl$_2$/Ar"$_2$SnCl$_2$*

- Ar'$_2$SnCl$_2$

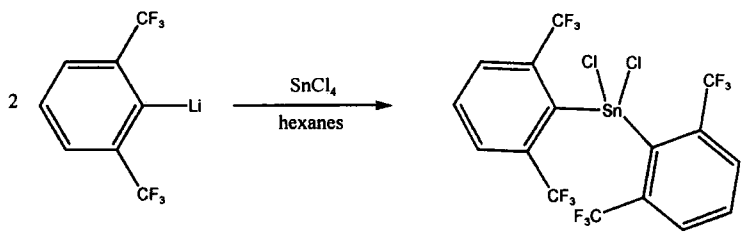

Equation 3.6: *Synthesis of Ar'$_2$SnCl$_2$*

Ar'$_2$SnCl$_2$ was isolated as a beige solid and recrystallised from pentane and diethyl ether.

One singlet with Sn satellites was observed in the ^{19}F NMR spectrum at -56.7 ppm ($^{4}J_{Sn-F}$ 10.0 Hz, 12F, *o*-CF_3). The ^{119}Sn NMR spectrum showed a singlet at -141.1 ppm.

The X-ray structure of Ar'_2SnCl_2 has been determined by A. E. Goeta from previous work by Xue (Figure 3.12).[15]

Figure 3.12: *Molecular structure of Ar'_2SnCl_2*

The Sn-C bond distance (2.176(2)) is slightly shorter than in ArSn(IV) and ArSn(II) derivative, which range from 2.179(6) to 2.316(9) Å.[21-23,10,20,24-26]

- Ar''_2SnCl_2

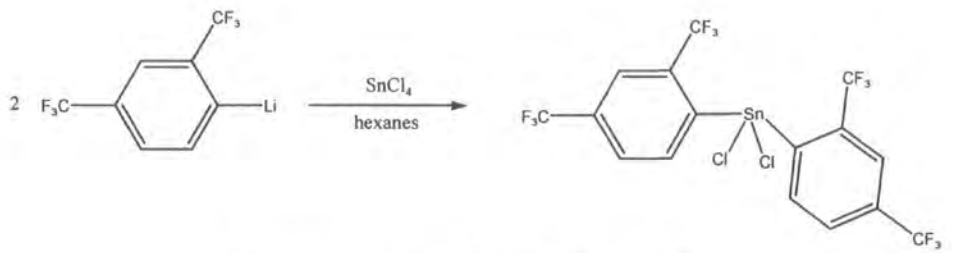

Equation 3.7: *Synthesis of Ar''_2SnCl_2*

This compound was synthesized as an oil, which was purified by distillation under reduced pressure. The ^{19}F NMR spectrum consisted of two singlets at –58.9 (6F, *o*-CF_3) and –63.8 (6F, *p*-CF_3) ppm. The ^{119}Sn spectrum showed a signal at –97.4 ppm.

3.5 Discussion

3.5.1 Solution-state NMR Spectroscopy

^{19}F NMR data for all the silicon derivatives are given in Table 3.5.

Compound	δ for *o*-CF_3 (ppm)	δ for *p*-CF_3 (ppm)	δ for Si-F (ppm)
Ar"$_2$SiCl$_2$	-57.9, s (6F)	-64.2, s (6F)	
Ar'$_2$SiCl$_2$	-58.9, s (12F)		
Ar"$_2$SiF$_2$	-59.2, t, $^5J_{F-F}$ 12.4Hz (6F)	-64.1, s (6F)	-133.0, septet, $^5J_{F-F}$ 12.3Hz (2F)
Ar'$_2$SiF$_2$	-57.5, t, $^5J_{F-F}$ 12.3Hz (12F)		-125.5 m, $^5J_{F-F}$ 12.5Hz (2F)
Ar$_2$SiF$_2$[7]	-57.3, t, $^5J_{F-F}$12.8Hz (12F)	-64.2, s (6F)	-124.5 m, $^5J_{F-F}$12.8H (2F)

Table 3.5: *^{19}F NMR data for Silicon (IV) Compounds*

With either ArLi or the mixture Ar'Li/Ar"Li a Cl/F exchange is observed. However, this exchange appeared to be slower for fluoroxyl since chloride compounds such as Ar'$_2$SiCl$_2$ and Ar"$_2$SiCl$_2$ could be identified in the ^{19}F NMR spectrum. Interestingly, there was more of the less sterically hindered chloride, Ar"$_2$SiCl$_2$ present than Ar'$_2$SiCl$_2$, but more Ar'$_2$SiF$_2$ than Ar"$_2$SiF$_2$ (Figure 3.1). This possibly indicates that Ar'$_2$SiCl$_2$

undergoes faster chlorine/fluorine exchange than $Ar"_2SiCl_2$. The overall order of exchange rate could then be: Ar_2SiCl_2>$Ar'SiCl_2$>$Ar"_2SiCl_2$.

No halogen exchange has been observed for Ge or Sn derivatives.

Table 3.6 lists the NMR data (^{19}F and ^{119}Sn) for Ge and Sn derivatives:

Compound	δ ^{19}F (ppm) for *o*-CF_3	δ ^{19}F (ppm) for *p*-CF_3	δ ^{119}Sn
$ArGeCl_3$	-52.9 s (6F)	-63.5 s (3F)	
Ar_2GeCl_2	-54.4 s (12F)	-64.1 s (6F)	
$Ar"_2GeCl_2$	-58.7 s (6F)	-64.1 s (6F)	
Ar'_2GeCl_2	-53.8 s (12F) [a]		
$ArSnCl_3$	-55.9 s with sats, $^4J_{Sn-F}$ 19.2 Hz (6F)	-63.0 s (3F)	-140.7
Ar_2SnCl_2	-56.9 s with sats, $^4J_{Sn-F}$ 10.0 Hz (12F)	-63.9 s (6F)	-146.7
Ar'_2SnCl_2	-56.7 s with sats, $^4J_{Sn-F}$ 10.0 Hz		-141.1
$Ar"_2SnCl_2$	-58.9 s (6F) [b]	-63.8 s (6F)	-97.4

Table 3.6: *^{19}F NMR and ^{119}Sn NMR data for Germanium (IV) and Tin (IV) Compounds*

The δ ^{19}F values are all in the same range for the three elements studied (Si, Ge, Sn) and correspond to the shifts found in all compounds containing *ortho* and *para* CF_3 group.

When these elements are reacted with the fluoroxyl mixture, the less sterically hindered compound $Ar"_2ECl_2$ is found to be predominant with E=Si or Ge. However, with Sn, the solution contains mainly the more sterically hindered disubstituted product Ar'_2SnCl_2.

[a] See text

[b] The Sn Satellites from this weak signal could not be observed

The larger size of the tin atom relative to silicon or germanium will reduce the steric hindrance between ligands in these ψ–tetrahedral structures, and probably explains the reversal in isomeric ratio between Ar'_2ECl_2 and Ar''_2ECl_2.

3.5.2 X-ray Crystallography

Ar_2GeCl_2 and Ar_2SnCl_2[15] are isostructural. Ar''_2GeCl_2 and Ar''_2SiCl_2[15] have also been found to be isostructural. Ar_2GeCl_2 and Ar_2SnCl_2 both have a very marked distortion from tetrahedral geometry as reflected in the C-E-C and C-E-Cl angles (Table 3.7). The largest angle around the E central atom is the C-E-C angle, being 120.07(12)° for C(11)-Ge-C(21) and 120.3(2)° for C(1)-Sn-C(11). In Ar_2GeCl_2, the C-Ge-Cl angles vary from 96.65(9) to 118.17(9)°, a variation of more than 21°. Similarly, in Ar_2SnCl_2 the C-Sn-Cl angles vary between 96.14 and 118.94°.

The structures of compounds containing fluoroxyl ligand have shown some disordered *para*-CF_3 groups.

Close E-F contacts are found to two or more fluorine atoms in all synthesised compounds, and are listed in Table 3.8. They are all shorter than the expected sum of the van der Waals radii for E and F. Similar secondary interactions between group 14 elements and fluorines in *o*-CF_3 groups have been described in the literature. In the case of Ar_2SiF_2, Ar_2SiHF, and $Ar'SiF_2$, four secondary Si---F interactions are observed between 2.715 and 3.056 Å, 2.713 and 3.075 Å, and 2.745 and 3.073 Å (Table 3.8) respectively. The coordination environment approaches a distorted tetracapped tetrahedron. Such a structure does not apply for tin or germanium compounds, which exhibit only three E---F short contacts, although in all instances there are further fluorines at longer distances. The secondary bonding appears to play a crucial role in determining the overall geometry of the compounds, and can lead to considerable distortion of the bond angles in the Ψ-tetrahedron.

	Ar_2GeCl_2		Ar_2SnCl_2	
Bond distances (Å)	Ge(1)-C(1)	2.0179(3)	Sn(1)-C(1)	2.1950(6)
	Ge(1)-C(11)	1.9970(3)	Sn(1)-C(11)	2.1810(6)
	Ge(1)-Cl(2)	2.1174(9)	Sn(1)-Cl(2)	2.2977(17)
	Ge(1)-Cl(1)	2.1513(9)	Sn(1)-Cl(1)	2.3259(18)
Angles (°)	C(1)-Ge(1)-C(11)	120.07(12)	C(1)-Sn(1)-C(11)	120.3(2)
	C(1)-Ge(1)-Cl(1)	96.65(9)	C(1)-Sn(1)-Cl(1)	96.14(7)
	C(1)-Ge(1)-Cl(2)	118.17(9)	C(1)-Sn(1)-Cl(2)	118.94(16)
	C(11)-Ge(1)-Cl(1)	113.46(9)	C(11)-Sn(1)-Cl(1)	113.89(17)
	C(11)-Ge(1)-Cl(2)	103.34(9)	C(11)-Sn(1)-Cl(2)	103.80(17)
	Cl(1)-Ge(1)-Cl(2)	104.33(4)	Cl(1)-Sn(1)-Cl(2)	102.58(7)

Table 3.7: *Selected Bond Distances(Å) and Angles (°) for Ar_2GeCl_2 and Ar_2SnCl_2*

Compound	Range(Å)	No of contacts	No of *o*-Fluorines
$Ar"_2SiCl_2$[15]	2.882-2.901	2	6
Ar'_2SiF_2	2.745-3.073	4	12
$ArGeCl_3$[15]	2.909	2	6
Ar_2GeCl_2	2.757-3.009	3	12
$Ar"_2GeCl_2$[15]	2.848-2.860	2	6
Ar_2SnCl_2[15]	2.722-3.014	3	12
Ar'_2SnCl_2[15]	2.688-3.002	3	12

Table 3.8: *Short E---F contacts*

3.6 Experimental

3.6.1 Introduction

- NMR spectroscopy

^{119}Sn NMR spectra were recorded on the Varian Inova 500 spectrometer at 186.37 MHz. Chemical shifts were measured relative to external Me_4Sn, with the higher frequency direction taken as positive.

- X-ray Crystallography

Single crystal structure determinations were carried out from data collected at 120 K, using graphite monochromated Mo Kα radiation (λ = 0.71073 Å) on a Bruker SMART-CCD detector diffractometer equipped with a Cryostream N_2 flow cooling device.[27] In each case, series of narrow ω-scans (0.3°) were performed at several φ-settings in such a way as to cover a sphere of data to a maximum resolution between 0.70 and 0.77 Å. Cell parameters were determined and refined using the SMART software,[28] and raw frame data were integrated using the SAINT program.[29] The structures were solved using direct methods and refined by full-matrix least squares on F^2 using SHELXTL.[30]

3.6.2 Synthesis of Ar_2SiF_2

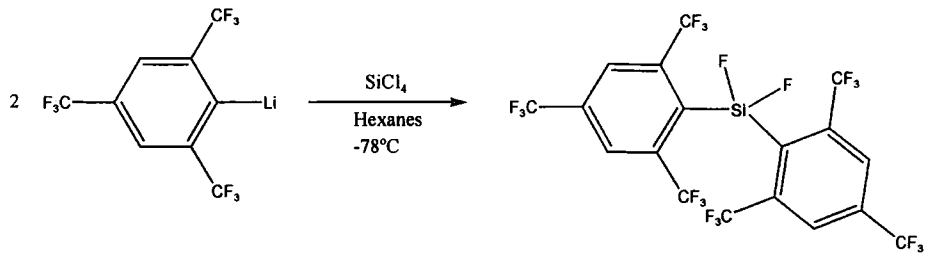

A solution of ArLi (100 ml, 30 mmol) in diethyl ether was added dropwise to a solution of $SiCl_4$ (2.5g, 1.72ml, 15 mmol) in hexanes at -78°C. The solution was allowed to warm to room temperature and stirred for 5 hours. A white precipitate formed. The solution was filtered and solvents were removed under vacuum, leaving a yellow oil. This oil was distilled under reduced pressure (0.01 Torr), giving a yellow oil, Bp 85°C.

Elemental analysis for $C_{18}H_4F_{20}Si$ (628.28), Calc: C 34.41, H 0.64%; Found: C 32.9, H 0.75%.

^{19}F NMR ($CDCl_3$): δ-57.3 (t, $^5J_{F\text{-}F}$12.8Hz), 12F, *o*-CF_3), -64.2 (s, 6F, *p*-CF_3), -124.5 (m, $^5J_{F\text{-}F}$12.8Hz, 2F).

3.6.3 Synthesis of Ar"$_2SiCl_2$

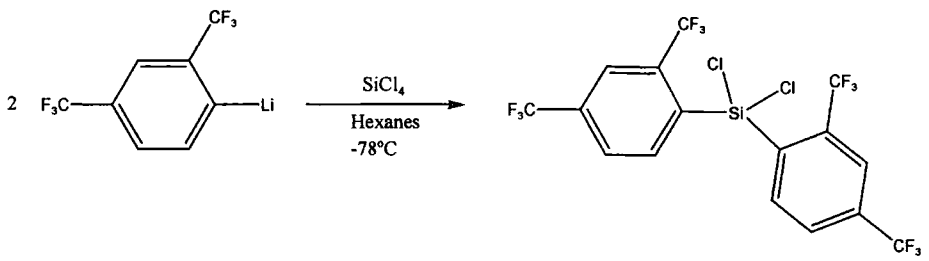

An Ar'Li/Ar"Li (50ml, 20 mmol) solution in diethyl ether was added dropwise to a solution of $SiCl_4$ (1.7g, 10 mmol) in pentane at -78°C. The solution was allowed to warm to room temperature and stirred for 3 hours. A precipitate of LiCl formed. This was filtered off and the solvents and excess $SiCl_4$ were removed under vacuum, leaving a yellow sticky oil which was distilled under reduced pressure (0.01 Torr). A fraction was collected at 120°C. Ar"$_2SiCl_2$ was purified by recrystallisation from pentane. Yield: 1.8g (32.4%).

Elemental analysis for $C_{16}H_6Cl_2F_{12}Si$ (525.20), Calc C 36.6, H 1.15%; Found C 36.8, H 1.24%

^{19}F NMR ($CDCl_3$): δ-57.9 (s, 6F, *o*-CF_3), -64.2 (s, 6F, *p*-CF_3) ppm.

3.6.4 Synthesis of Ar'_2SiF_2

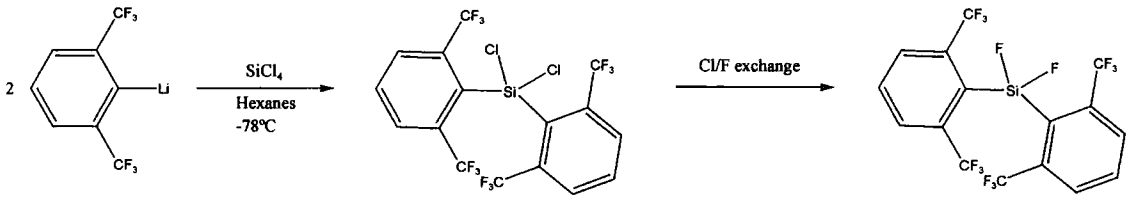

An Ar'Li/Ar"Li (50ml, 40 mmol) solution in diethyl ether was added dropwise to a solution of $SiCl_4$ (3.39g, 2.3 ml, 20 mmol) in hexanes at -78°C. The solution was allowed to warm to room temperature and stirred for 3 hours. A precipitate of LiCl formed. This was filtered off and the solvents and excess $SiCl_4$ were removed under vacuum, leaving a yellow oil ($Ar"_2SiCl_2$) and a white solid (Ar'_2SiF_2). This solid was washed three times with hexanes and purified by sublimation under vacuum, giving white crystals. Yield: 2.5g (12.7%).

Elemental analysis for $C_{16}H_6F_{14}Si$ (492.29), Calc C 39.04, H 1.23%; Found C 38.3, H 1.24%

^{19}F NMR ($CDCl_3$): δ-57.5 (t, $^5J_{F-F}$ 12.3Hz, 12F, *o*-CF_3), -125.5 (m, $^5J_{F-F}$ 12.5 Hz, 2F, Si-F)

3.6.5 Synthesis of $ArGeCl_3$

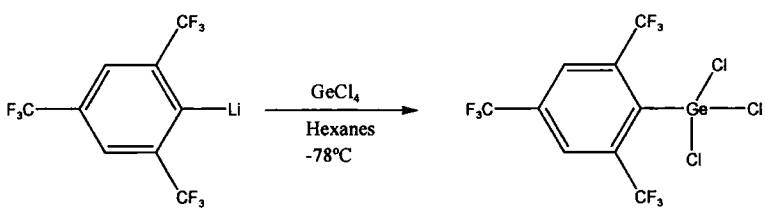

An ArLi (50 ml, 30 mmol) solution in diethyl ether was added dropwise to a $GeCl_4$ solution (3.2g, 1.71 ml, 15 mmol) in hexanes at -78°C. The solution was allowed to warm to room temperature and stirred for 4 hours. A white precipitate of LiCl appeared which

was filtered off. The solvents and excess $GeCl_4$ were removed under vacuum, leaving a yellow oil and a white solid. The yellow oil was filtered and then distilled under reduced pressure (0.01 Torr), giving a colourless oil of $ArGeCl_3$, bp 85°C. After one month, fine crystals formed. Yield: 2.6g (19%)

Elemental analysis for $C_9H_2Cl_3F_9Ge$ (460.07), Calc C 23.50, H 0.44%, Found C 24.1, H 1.16%

^{19}F NMR ($CDCl_3$): δ-52.9 (s, 6F, *o*-CF_3), -63.5 (s, 3F, *p*-CF_3) ppm.

3.6.6 Synthesis of Ar_2GeCl_2

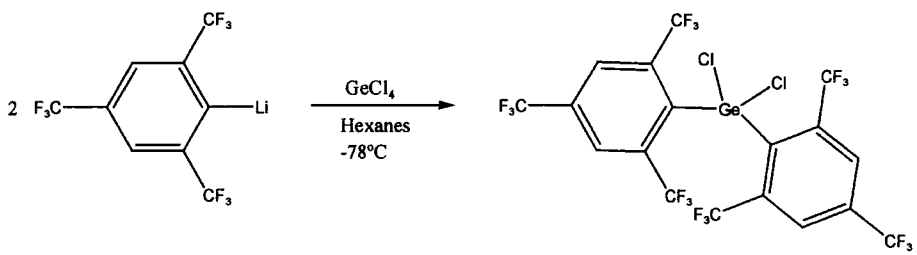

An ArLi (50 ml, 30 mmol) solution in diethyl ether was added dropwise to a $GeCl_4$ solution (3.2g, 1.71 ml, 15 mmol) in hexanes at -78°C. The solution was allowed to warm to room temperature and stirred for 4 hours. A white precipitate of LiCl appeared which was filtered off. The solvents and excess $GeCl_4$ were removed under vacuum, leaving a yellow oil and a white solid. The white solid was filtered off and washed 3 times with hexanes. Yield: 3.17g (30%). Crystals were grown by recrystallisation from dichloromethane.

Elemental analysis for $C_{18}H_4Cl_2F_{18}Ge$ (705.72), Calc C 30.64, H 0.57%, Found C 30.59, H 0.58%

^{19}F NMR ($CDCl_3$): δ-54.4 (s, 12F, *o*-CF_3), -64.1 (s, 6F, *p*-CF_3) ppm.

3.6.7 Synthesis of Ar"$_2$GeCl$_2$

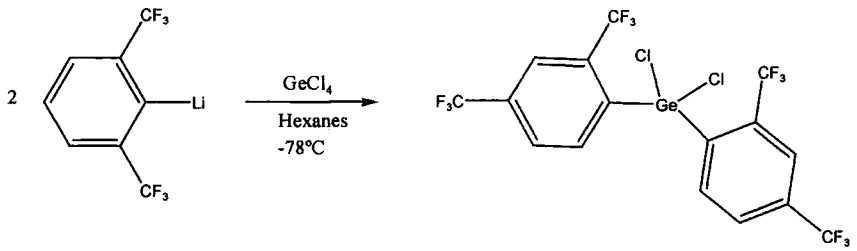

A solution of Ar'Li/Ar"Li (60 ml, 40 mmol) in diethyl ether was added dropwise to a solution of $GeCl_4$ (4.29g, 2.6 ml, 20 mmol) in diethyl ether at -78°C. The solution was allowed to warm to room temperature and stirred for 2 hours. A white precipitate of LiCl formed. The solution was filtered and the solvents were removed under vacuum, leaving a black oil. This oil was distilled under reduced pressure (0.01 Torr) and a fraction was collected at 80-90°C. Yield: 5.8g (51%). After one week, small crystals formed.

Elemental analysis for $C_{16}H_6Cl_2F_{12}Ge$ (569.72), Calc: C 33.7, H 1.06, Cl 12.45%; Found: C 32.4%, H 1.53, Cl 12.8%.

^{19}F NMR ($CDCl_3$): δ -58.7 (s, 6F, *o*-CF_3), -64.1 (s, 6F, *p*-CF_3) ppm.

3.6.8 Synthesis of ArSnCl$_3$/Ar$_2$SnCl$_2$

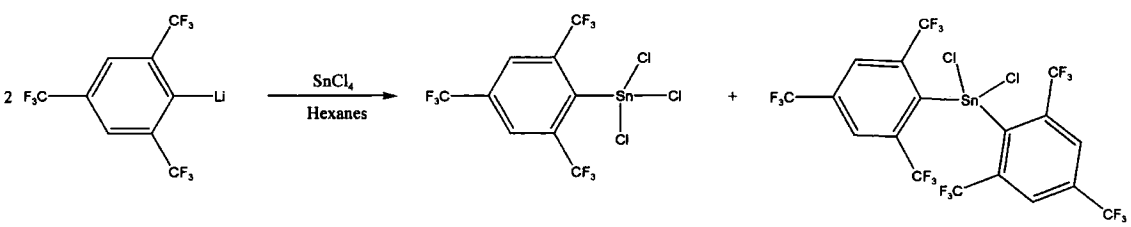

An ArLi (50 ml, 30 mmol) solution in diethyl ether was added slowly to a solution of $SnCl_4$ (3.90g, 2.75ml, 15 mmol) in hexanes at -78°C. The solution was then allowed to warm to room temperature and stirred for 5 hours. A white precipitate of LiCl appeared. The solution was filtered and the solvents were removed under vacuum, leaving a brown

oil and a solid. The oil was filtered and distilled under reduced pressure (0.01 Torr), giving a yellow oil of $ArSnCl_3$ (Bp 85°C) in a small quantity. The solid was washed 3 times with hexanes and dried under vacuum (Ar_2SnCl_2). Crystals were obtained by recrystallisation from diethyl ether. Yield 3.8g (51%).

Elemental analysis for $C_{18}H_4Cl_2F_{18}Sn$ (751.82), Calc: C 28.76, H 0.54%; Found: C 28.60, H 0.78%

^{19}F NMR ($CDCl_3$): $\underline{ArSnCl_3}$: δ-55.9 (s with Sn satellites, $^4J_{Sn\text{-}F}$ 19.2Hz, 6F, *o*-CF_3), -63.0 (s, 3F, *p*-CF_3) ppm; $\underline{Ar_2SnCl_2}$: δ -56.9 (s with Sn satellites, $^4J_{Sn\text{-}F}$ 10.0Hz, 12F, *o*-CF_3), -63.9 (s, 6F, *p*-CF_3) ppm; **^{119}Sn NMR** ($CDCl_3$): $\underline{ArSnCl_3}$: δ-140.7 ppm. $\underline{Ar_2SnCl_2}$: δ -146.7 ppm.

3.6.9 Synthesis of Ar'$_2$SnCl$_2$/Ar"$_2$SnCl$_2$

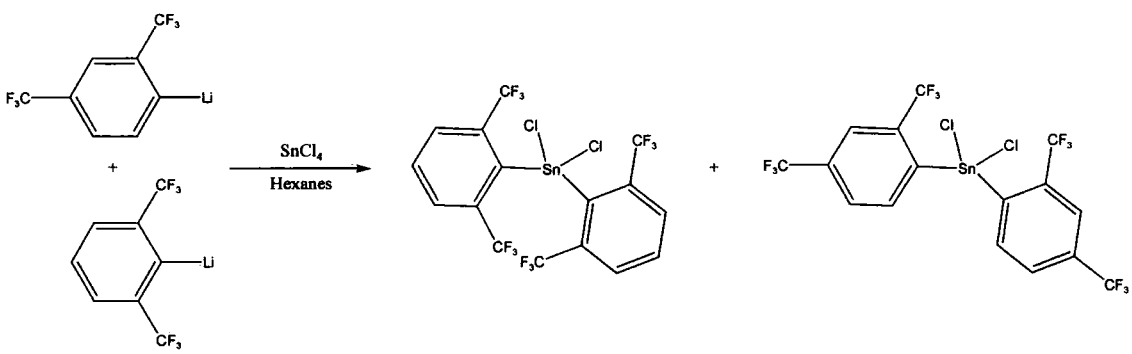

An Ar'Li/Ar"Li (250 ml, 94 mmol) solution in diethyl ether was added dropwise to a solution of $SnCl_4$ (12.24g, 8.63 ml, 47 mmol) at room temperature. The solution was stirred for 4 hours. A white precipitate of LiCl appeared. The brown solution was filtered and solvents and excess $SnCl_4$ were removed under vacuum, leaving a brown sticky oil and a brown solid. The oil was filtered (Ar"$_2$SnCl$_2$) and the solid washed with pentane and dichloromethane and dried in vacuo, giving a beige solid (Ar'$_2$SnCl$_2$). Crystals were grown by recrystallisation from pentane and diethyl ether.

Yield (Ar'_2SnCl_2) 3.48g (57%).

Elemental analysis for $C_{16}H_6Cl_2F_{12}Sn$ (615.82), Calc: C 31.21, H 0.98%; Found C 29.7, H 1.26%.

^{19}F NMR ($CDCl_3$): $\underline{Ar'_2SnCl_2}$: δ-56.7 (s with Sn satellites, $^4J_{Sn\text{-}F}$ 10.0Hz, 12F, *o*-CF_3) ppm; $\underline{Ar''_2SnCl_2}$: δ-58.9 (s, 6F, *o*-CF_3), -63.8 (s, 6F, *p*-CF_3) ppm; **^{119}Sn NMR** ($CDCl_3$): $\underline{Ar'_2SnCl_2}$: δ-141.1 ppm, $\underline{Ar''_2SnCl_2}$: δ-97.4 ppm.

References

1 N. Shimizu, N. Takesue, A. Yamamoto, T. Tsutsumi, S. Yasuhara, Y. Tsuno, *Chem. Lett.*, **1992**, 1263.

2 Y. Nakadaira, K. Oharu, H. Sakurai, *J. Organomet. Chem.*, **1986**, *309*, 247.

3 G. Wilkinson, F. G. A. Stone, E. W. Abel, *Comprehensive Organometallic Chemistry*; Pergamon Press, Oxford, **1982**; Vol. Vol.2.

4 I. Omae, *Organotin Chemistry*; Elsevier, Amsterdam, 1989.

5 A. G. Davies, P. J. Smith in *Comprehensive Organometallic Chemistry*; Pergamon Press, Oxford, **1982**, p 519-627.

6 G. E. Carr, R. D. Chambers, T. F. Holmes, D. G. Parker, *J. Organomet. Chem.*, **1987**, *325*, 13.

7 J. K. Buijink, M. Noltemeyer, F. T. Edelmann, *J. Fluorine Chem.*, **1993**, *61*, 51.

8 J. Braddock-Wilking, M. Schieser, L. Brammer, J. Huhmann, R. Shaltout, *J. Organomet. Chem.*, **1995**, *499*, 89.

9 J. E. Bender, M. M. B. Holl, A. Mitchell, N. J. Wells, J. W. Kampf, *Organometallics*, **1998**, *17*, 5166.

10 A. Vij, R. L. Kirchmeier, R. D. Willett, J. M. Shreeve, *Inorg. Chem.*, **1994**, *33*, 5456.

11 P. Poremba, H. Pritskow, F. T. Edelmann, *J. Fluorine Chem.*, **1997**, *82*, 43.

12 H. J. Kroth, H. Schumann, H. G. Kuivila, C. D. Shaeffer, J. J. Zuckerman, *J. Am. Chem. Soc.*, **1975**, *97*, 1754.

13 C. D. Schaeffer, J. J. Zuckerman, *J. Organomet. Chem.*, **1975**, *99*, 407.

14 M. P. Bigwood, P. J. Corvan, J. J. Zuckerman, *J. Am. Chem. Soc.*, **1981**, *103*, 7643.

15 B. Y. Xue, *M.Sc Thesis*, Durham, **1999**.

16 F. H. Allen, O. Kennard, R. Taylor, *Acc. Chem. Res.*, **1983**, *16*, 146.

17 A. Bondi, *J. Phys. Chem.*, **1964**, *68*, 441.

18 F. Carré, C. Chuit, R. J. P. Corriu, A. Mehdi, C. Reyé, *Angew. Chem., Int. Ed. Engl.*, **1994**, *33*, 1097.

18 F. Carré, C. Chuit, R. J. P. Corriu, A. Mehdi, C. Reyé, *Angew. Chem., Int. Ed. Engl.*, **1994**, *33*, 1097.

19 J. E. Bender, M. M. B. Holl, J. W. Kampf, *Organometallics,* **1997**, *16*, 2743.

20 S. Brooker, F. T. Edelmann, D. Stalke, *Acta Cryst.*, **1991**, *C47*, 2527.

21 H. Grützmacher, H. Pritzkow, F. T. Edelmann, *Organometallics,* **1991**, *10*, 23.

22 H. Grützmacher, H. Pritzkow, *Angew. Chem., Int. Ed. Engl.*, **1991**, *30*, 1017.

23 H. Grützmacher, H. Pritzkow, *Chem. Ber.*, **1993**, *126*, 2409.

24 V. Lay, H. Pritzkow, H. Grützmacher, *J. Chem. Soc., Chem. Commun.*, **1992**, 260.

25 J. F. Van Der Maelen Uría, M. Belay, F. T. Edelmann, G. M. Sheldrick, *Acta Cryst.*, **1994**, *C50*, 403.

26 S. Freitag, R. Herbst-Irmer, J. T. Alhemann, H. W. Roesky, *Acta Cryst.*, **1995**, *C51*, 631.

27 J. Cosier, A.M.Glazer, *J. Appl. Cryst.*, **1986**, *19*, 105.

28 SMART -NT; Data Collection Software, version 5.0, Bruker Analytical X-ray Instruments Inc., Madison, Wisconsin, USA, **1999**.

29 SAINT-NT; Data Reduction Software, version 6.0, Bruker Analytical X-ray Instruments Inc, Madison, Wisconsin, U.S.A., **1999**.

30 SHELXTL; version 5.1, Bruker Analytical X-ray Instruments Inc, Madison, Wisconsin, U.S.A., **1999**.

Chapter 4

Group 15 Derivatives

4.1 Introduction

Many researches have been devoted to low coordinate species of group 15 in the last 30 years. Since the preparation of the first stable diphosphene Ar*P=PAr* (Ar*: 2,4,6-tri-^{t}butylphenyl),[1] and phosphaalkyne, P≡C^{t}Bu[2] in 1981, the field of low coordinate organophosphorus chemistry has rapidly expanded. Low coordination P-chemistry is now a major area of study that has been the subject of numerous reviews[3-8] and several books.[9,10] Although low coordinate arsenic compounds are generally less stable than their phosphorus analogues, their chemistry has been well-developed,[11] and both arsenic and phosphorus are now widely used in organo-group 15 chemistry and as ligands in organometallic synthesis. Until recently, the organic chemistry of antimony and bismuth had been little investigated, mainly because of the decrease of stability of these compounds relative to those of P or As. However, some advances have been made in this field over the last five years.[12]

Group 15 elements (E) have three common oxidation states (I, III, V) and are known to have coordination numbers from one (RC≡E) to six ($[ECl_6]^-$). Low coordinate species are considered to be those with coordination number three or lower.

- Three coordinate species

There is a vast amount of E(III) chemistry (particularly of phosphorus and arsenic compounds), much of which is based around the derivatisation of EX_3 (X= Cl, Br, I) and the formation of E-F and E-H derivatives. A very common reaction is that between an organolithium species and EX_3 to form the lithium halide and the desired product REX_2.

$$RLi \xrightarrow[\text{ether}]{EX_3} REX_2 + LiX$$

Phosphorus and arsenic can also form R_2EX and R_3E, depending on the bulk of the R group. For example, PPh_3 can be synthesised but Ar_3P has never been prepared. The only

example containing three Ar ligands is Ar_3B,[13] which has a different geometry but which has not been structurally characterised.

The hydride derivatives REH_2 or R_2EH can be prepared by reduction of the chloride compounds with Bu_3SnH or $LiAlH_4$. Fluorination of $RECl_2$ or R_2ECl leads to the formation of fluoro-derivatives.

$$RECl_2 + 2\ Bu_3SnH \longrightarrow REH_2 + 2\ Bu_3SnCl$$

$$RECl_2 + 1/2\ LiAlH_4 \longrightarrow REH_2 + 1/2\ LiAlCl_4$$

$$RECl_2 + SbF_3 \longrightarrow REF_2$$

4.2 Phosphorus Derivatives

A number of phosphorus derivatives containing the Ar, Ar' or Ar" ligand has been reported in the literature: $ArPCl_2$,[14,15] Ar_2PCl,[14] ArPClF,[14] $ArPF_2$,[14] $ArPH_2$,[14,15] Ar_2PH,[16] $Ar'PCl_2$,[17] $Ar'PH_2$,[18] Ar'Ar"PCl,[19] Ar'Ar"PF[20] and $Ar"_2PF$.[20] A general method has been used in these syntheses, with PCl_3 or PBr_3 reacting directly with ArLi or Ar'Li/Ar"Li at low temperature with continuous stirring for a few hours.

4.2.1 Reaction with 2,4,6-tris(trifluoromethyl)phenyl lithium (ArLi)

4.2.1.1 $ArPCl_2$

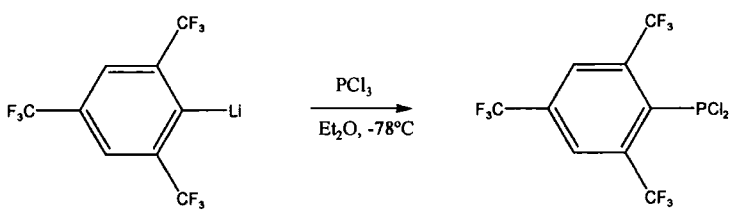

***Equation 4.1**: Synthesis of $ArPCl_2$*

$ArPCl_2$ was purified by distillation under reduced pressure (Bp 60°C), yielding a colourless liquid. The ^{31}P NMR spectrum gave a septet at 145.6 ppm ($^4J_{P-F}$ 61.3Hz) (Figure 4.1). The ^{19}F NMR showed a doublet and a singlet at –53.3 ($^4J_{P-F}$ 61.3 Hz, *o*-CF_3) and at –64.2 ppm (*p*-CF_3) respectively.

These values agreed with those found by Goodwin[13] and Roden.[21]

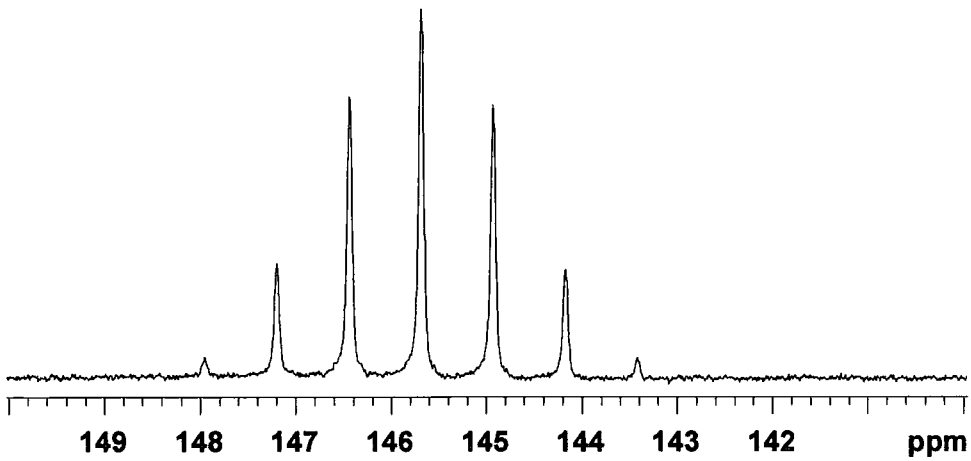

Figure 4.1: *^{31}P NMR spectrum of $ArPCl_2$*

4.2.1.2 Ar_2PCl

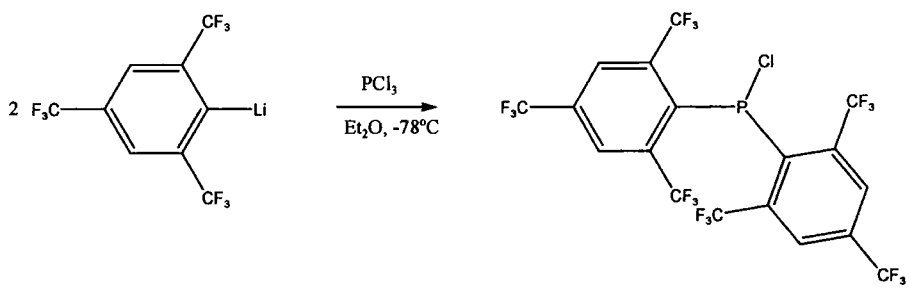

Equation 4.2*: Synthesis of Ar_2PCl*

This compound was obtained by reaction of two equivalents of ArLi with PCl_3. Ar_2PCl was distilled under reduced pressure (Bp 100°C) to give a clear yellow oil.

- NMR spectrscopy

The ^{31}P NMR spectrum exhibited a multiplet (13 lines) at 74.9 ppm ($^4J_{P-F}$ 41.9Hz, 12F). The ^{19}F NMR spectrum showed a doublet at –54.4 ($^4J_{P-F}$ 41.2Hz, 12F, *o*-CF_3) and a singlet at –64.1 (6F, *p*-CF_3) ppm.

- X-ray crystallography

Crystals were grown by recrystallisation from dichloromethane and submitted for X-ray diffraction. The structure was ascertained by A.L. Thompson at 120K and is shown in Figure 4.2:

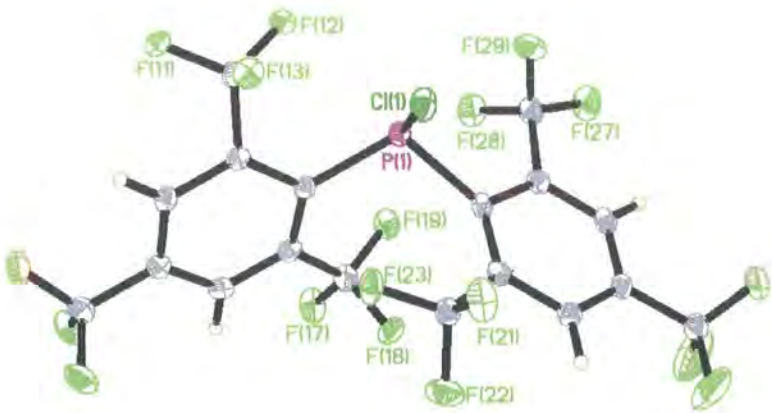

Figure 4.2: *Molecular Structure of Ar_2PCl*

Ar_2PCl crystallises in the monoclinic P2(1)/n space group with Z=4. Selected bond lengths (Å) and angles (°) are listed in Table 4.1 below:

Bond Distances (Å)		Angles (°)	
P(1)-Cl(1)	2.0628(10)	C(11)-P(1)-C(21)	109.87(12)
P(1)-C(11)	1.882(3)	C(11)-P(1)-Cl(1)	103.68(9)
P(1)-C(21)	1.885(5)	C(21)-P(1)-Cl(1)	92.95(9)

Table 4.1: *Selected Bond lengths (Å) and Angles (°) for Ar_2PCl*

P-C bond distances are slightly longer than those found in Ar'Ar"PCl,[19,21] the only Ar_2PCl compound structurally characterised so far [P-C(1) 1.854(2), P-C(11) 1.857(2) Å]. This is due to the steric hindrance imposed by the CF_3 groups in the *ortho* position. The P-Cl bond length is 2.0628(10) Å and is the similar to the P-Cl bond distance in Ar'Ar"PCl (2.061(1) Å). However, these P-Cl bond distances are relatively short in comparison with previously reported R_2PCl (where at least one of the R groups is alkyl) structures (CSD). This distance varies from 2.06 to 2.35 Å. The P-Cl distance is sensitive to electronic effects from other groups bonded to phosphorus, and its shortening here can be attributed to the electron-withdrawing properties of the CF_3 groups on the aromatic rings.

An interesting feature of the crystal structure is the asymmetry in the C-P-Cl bond angles, which differ by more than 10° (Table 4.1). Similar observations have been reported without comment in the literature for Ar_2AsCl,[22] Ar_2SbCl[22] and Ar_2BiCl[23] (Table 4.2). This asymmetry might arise as a consequence of secondary interactions between group 15 elements and fluorines of the *ortho*-CF_3 groups.

In Ar_2PCl, five short contacts are observed between phosphorus and the fluorine atoms of the *o*-CF_3: P---F(12) 2.843, P---F(13) 3.796, P---F(23) 3.111, P---F(28) 3.001, P---F(29) 2.954Å

Compound	Ar_2PCl	Ar_2AsCl*	Ar_2SbCl	Ar_2BiCl
E-Cl	2.0628(10)	2.1920(12)	2.358(11)	2.463(3)
E-C(1)	1.882(3)	2.023(4)	2.22(3)	2.356(8)
E-C(2)	1.885(3)	2.016(4)	2.25(3)	2.338(7)
C(1)-E-C(2)	109.87(12)	107.53(16)	107.0(12)	106.9(3)
C(1)-E-Cl	103.68(9)	100.57(12)	101.3(9)	99.5(2)
C(2)-E-Cl	92.95(9)	92.04(11)	88.4(9)	87.8(2)
Reference	This Work	22	22	23

Table 4.2: *Comparison of Key Bond Distances (Å) and Angles (°) for Ar_2ECl (E=P, As, Sb or Bi)*

* Data for the orthorhombic modification at 130 K

4.2.1.3 $ArPBr_2$

ArLi was added to a PBr_3 solution in diethyl ether at -78°C. $ArPBr_2$ was obtained as an orange oil which, after distillation under reduced pressure, gave colourless crystals.

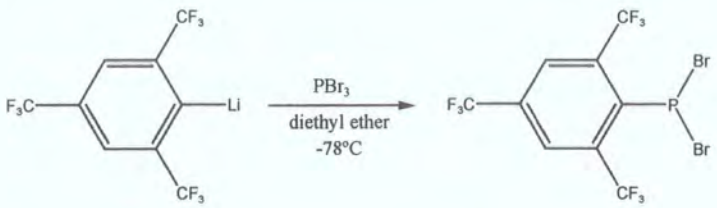

Equation 4.3: *Synthesis of $ArPBr_2$*

- NMR spectroscopy

The ^{31}PNMR spectrum consisted of a septet at 130 ppm ($^4J_{P\text{-}F}$ 62.3 Hz). The ^{19}F NMR spectrum showed a doublet at –53.1 ($^4J_{P\text{-}F}$ 62.4 Hz, 6F, *o*-CF_3) and a singlet at –64.1 (3F, *p*-CF_3) ppm.

- X-ray crystallography

Crystals were obtained after distillation and submitted for X-ray diffraction without any further purification. The structure was determined by A.S. Batsanov at 110K and is shown in Figure 4.3:

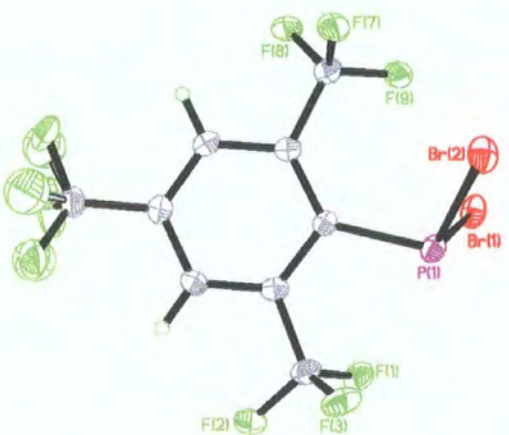

Figure 4.3: *Molecular structure of $ArPBr_2$*

$ArPBr_2$ crystallises in the triclinic $P\bar{1}$ space group with Z=4. It crystallises with two independent molecules in the asymmetric unit. Selected bond distances and angles are listed in Table 4.3.

Bond distances (Å)	P(1)-Br(1)	2.2228(8)	P(2)-Br(3)	2.2166(8)
	P(1)-Br(2)	2.2153(8)	P(2)-Br(4)	2.2194(8)
	P(1)-C(1)	1.879(3)	P(2)-C(11)	1.887(3)
Angles (°)	C(1)-P(1)-Br(2)	102.10(8)	C(11)-P(2)-Br(4)	102.41(8)
	C(1)-P(1)-Br(1)	102.52(9)	C(11)-P(2)-Br(3)	103.22(8)
	Br(2)-P(1)-Br(1)	105.35(3)	Br(3)-P(2)-Br(4)	104.90(3)

Table 4.3: *Selected Bond distances (Å) and Angles (°) for* $ArPBr_2$

The P-C bond length is similar to those found in Ar_2PCl and Ar'Ar"PCl.[19] These values are also in the same range as those found in other R_2PBr structures[24] (where P-C=1.885(6) and 1.891(6)). The Br-P-Br angles (Br(2)-P(1)-Br(1) 105.35(3); Br(3)-P(2)-Br(4) 104.90(3)) are slightly larger than the value reported in the literature for $Ph_3P{=}C(Me)PBr_2$,[25] $Ph_3P{=}C(Tms)PBr_2$,[25] (Table 4.4) and $C_5H(CHMe_2)_4PBr_2$[26] which range from 93.5(1)° to 96.06(7)°. The sum of the bond angles in $ArPBr_2$ (ca. 310°) is also larger when compared with the first two compounds mentioned above, where it varies from 295.8 to 305.7°, reflecting the greater steric demand of the *ortho*-CF_3 groups.

The P-Br bond lengths 2.2228(8), 2.2153(8), 2.2166(8), 2.2194(8) are slightly shorter than usually found in organophosphorus bromides (for example values between 2.268(2) and 2.489(3) Å),[24-30] although shorter distances have been observed in PBr_3 complexes

with $Cr(CO)_5$[31,32] and $W(CO)_5$[32]. This parallels the observation of a shorter P-Cl bond in Ar_2PCl and Ar'Ar"PCl.[19]

Short P---F secondary interactions are found in this compound in the range 2.865-3.208 Å for P(1) and 2.877-3.217 Å for P(2). The distance are shorter in all instances than the sum of the empirical van der Waals radii of P (1.91 Å) and F (1.40 Å),[33]as well as the theoretical ones (estimated as 2.05 and 1.42 Å respectively[34]).

The *para*-CF_3 groups are found to be disordered, as often observed in this kind of compound.

	$Ph_3P=C(Me)PBr_2$				$Ph_3P=C(Tms)PBr_2$	
Bond distances (Å)	P(1)-Br(1)	2.436(2)	P(2)-Br(3)	2.489(3)	P-Br(1)	2.401(2)
	P(1)-Br(2)	2.262(3)	P(2)-Br(4)	2.238(30	P(1)-Br(2)	2.2282(2)
	P(1)-C(1)	1.678(10)	P(2)-C(1)	1.728(9)	P(1)-C(1)	1.718(7)
Angles (°)	Br(1)-P-Br(2)	93.5(1)	Br(2)-P(2)-Br(3)	94.8(1)	Br(1)-P(1)-Br(2)	95.2(7)
	Br(1)-P(1)-C(1)	101.8(4)	Br(3)-P(2)-C(1)	109.4(3)	Br(1)-P(1)-C(1)	106.0(2)

Table 4.4: *Selected Bond distances and Angles for $RPBr_2$ compounds*[25,26]

4.2.1.4 Ar_2PBr

Attempts have been made to form Ar_2PBr from the reaction of two equivalents of ArLi and PBr_3. However, the formation of this product has never been observed in the solution state NMR spectroscopy. This is probably due to the steric hindrance of the Ar ligand and the bromine atom compared with the chlorine.

4.2.2 Reaction with 2,6-bis(trifluoromethyl)phenyl lithium (Ar'Li) / 2,4-bis(trifluoromethyl)phenyl lithium (Ar"Li)

When the Ar'Li/Ar"Li mixture reacts with PX_3, it can give rise to a series of five different mono- or disubstituted products.

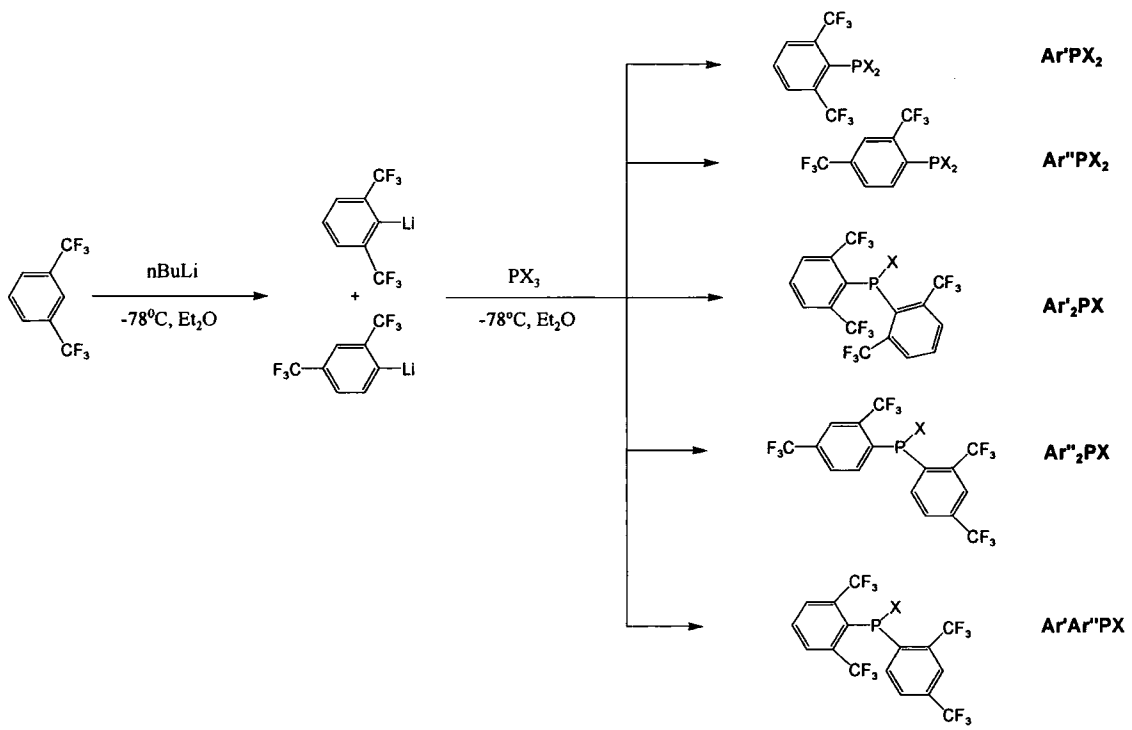

Scheme 4.1: *Different products of the reaction between Ar'Li/Ar"Li and PCl_3*

4.2.2.1 $Ar'PCl_2$

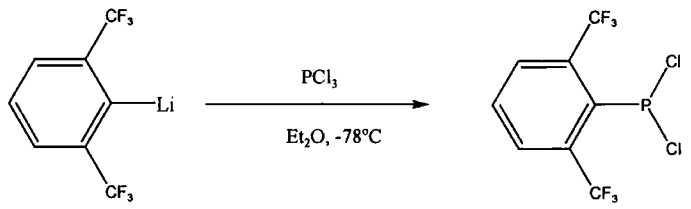

Equation 4.4: *Synthesis of $Ar'PCl_2$*

This compound was synthesised as a yellow oil.

The ^{31}P NMR of this compound consisted of a septet at δ148.4 ($^4J_{P-F}$=61.3 Hz). The ^{19}F NMR spectrum showed a doublet at δ-53.2 ($^4J_{P-F}$=61.3 Hz), corresponding to the two *ortho*-CF_3 groups.

4.2.2.2 $Ar''PCl_2$

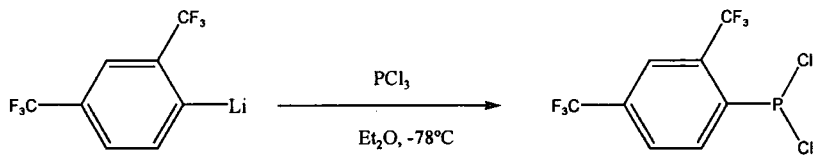

Equation 4.5: *Synthesis of $Ar''PCl_2$*

This product could not be separated from the first substitute $Ar'PCl_2$ because of their very close boiling points, caused by their identical molecular mass.

The ^{31}P NMR exhibited a quartet at δ151.6ppm ($^4J_{P-F}$ 83.8 Hz). This coupling constant is different than the one for $Ar'PCl_2$ because of the position of the CF_3 groups. In fact, in $Ar''PCl_2$, there is only one CF_3 in the *ortho*-position whereas there are two in $Ar'PCl_2$. Comparing the coupling constants between both compounds ($J_{Ar'PCl_2} < J_{Ar''PCl_2}$), it is possible to say that the *o*-CF_3 groups in $Ar''PCl_2$ interacts more with the phosphorus

atom. This could imply that the distance between the phosphorus atoms and the fluorine atom is shorter in Ar"PCl_2 than in Ar'PCl_2. The ^{19}F NMR spectrum showed two signals, a doublet at –56.5 ($^4J_{P-F}$ 83.8 Hz, *o*-CF_3) and a singlet at –63.6 (*p*-CF_3) ppm.

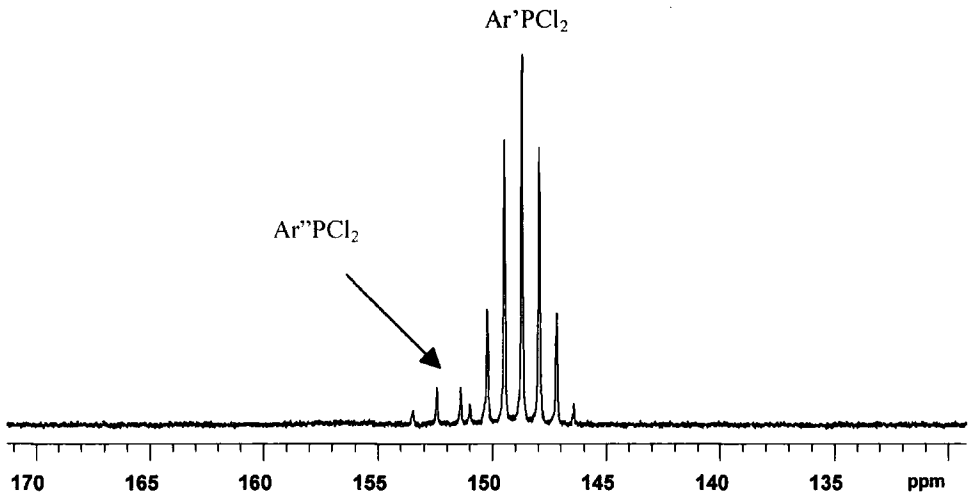

Figure 4.4: *^{31}P NMR of the mixture of Ar'PCl_2/Ar"PCl_2*

4.2.2.3 Ar"$_2$PCl

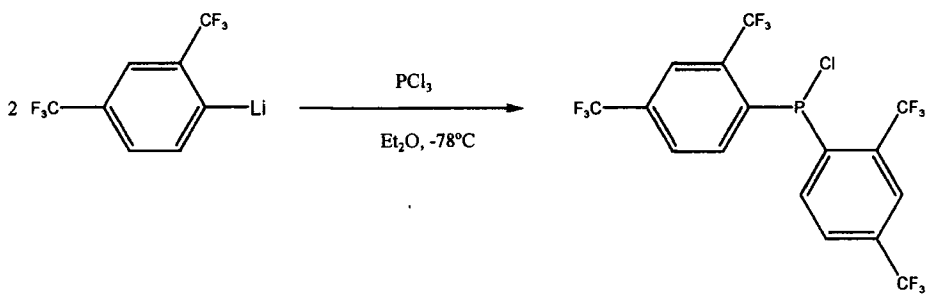

Equation 4.6*: Synthesis of Ar"$_2$PCl*

- NMR spectroscopy

The ^{31}P NMR spectrum shows a septet at 68.1 ppm ($^4J_{P-F}$ 65.6Hz), implying two CF_3 groups in *ortho* positions.

The ^{19}F NMR consists of a doublet at -57.3 ppm (6F, $^{4}J_{P-F}$ 65.6 Hz) and one singlet at δ -63.7 ppm (6F), corresponding to the two *para*-CF_3 groups.

The ^{19}F NMR spectrum of a solution of Ar"$_2$PCl in toluene-d_8 was recorded at -80°C and +95°C for comparison with the spectrum at ambient temperature described above.

Values of δ 56.9 ppm ($^{4}J_{P-F}$63.9Hz) were observed at -80°C and δ 57.4 ppm ($^{4}J_{P-F}$ 66.6 Hz) at +95°C. Only very small changes in either chemical shifts or coupling constants for the doublet were noticed, showing that the two Ar" groups remain equivalent over this temperature range

There is no steric hindrance between them. Ar" groups rotate and, due to the perfect symmetry of the molecule, they are always in an equivalent position. This explains why no changes are observed in the spectra.

The $^{13}C\{^{1}H\}$ NMR spectrum was recorded for a d_8-toluene solution at room temperature. Table 4.5 shows the assignments of each carbon. This spectrum only exhibits the existence of one type of *ipso* carbon, confirming that the molecule is perfectly symmetrical.

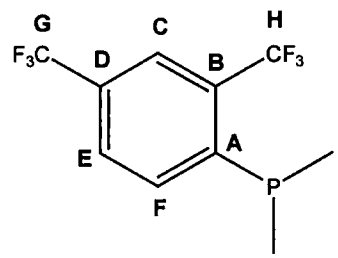

***Figure 4.5**: Lettering scheme for carbon atoms in Ar"$_2$PCl*

Carbon	δ (ppm)	J (Hz)
A	140.3	d, $^{1}J_{P-C}$ 56.8
B	133.1	q, $^{2}J_{C-F}$ 33.9
C	123.7	s (broad)
D	133.1	q, $^{2}J_{C-F}$ 33.9
E	129.1	s
F	123.6	d, $^{2}J_{P-C}$ 1.9
G	123.6	q, $^{1}J_{C-F}$ 275.8
H	123.4	qd, $^{1}J_{C-F}$ 273.05, $^{3}J_{P-C}$ 1.74

Table 4.5: *Signal assignments for ^{13}C spectrum of Ar"$_2$PCl*

- X-ray crystallography

Crystals were obtained by recrystallisation from hexanes. The structure was determined at 100 K by A.E. Goeta and is shown in Figure 4.6:

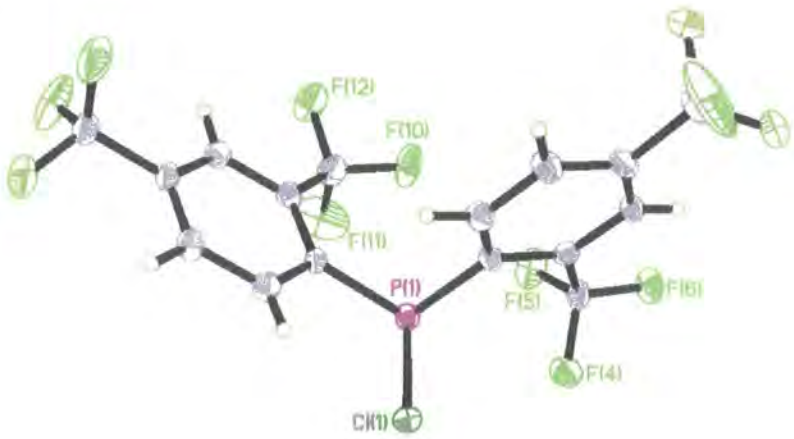

Figure 4.6: *Molecular structure of Ar"$_2$PCl*

Ar"$_2$PCl crystallises in the monoclinic I2/a space group with Z=8. Selected bond lengths and angles are listed Table 4.6.

Bond Distances (Å)		Angles (°)	
P(1)-Cl(1)	2.0619(9)	C(1)-P(1)-C(11)	100.37(10)
P(1)-C(1)	1.854(2)	C(1)-P(1)-Cl(1)	97.38(7)
P(1)-C(11)	1.885(2)	C(11)-P(1)-Cl(1)	100.95(7)

Table 4.6: *Selected Bond distances (Å) and Angles (°) for Ar"$_2$PCl*

P-C and P-Cl bond distances are similar to those found in Ar_2PCl, although the P-C bonds are slightly longer in Ar_2PCl, due to the steric demand of the four CF_3 groups in *ortho* positions in comparison to only two in Ar"$_2$PCl. The same feature applies to the C-P-C angles, being 100.37(10)° in Ar"$_2$PCl and 109.87(12)° in Ar_2PCl. Three P---F short contacts are observed: P---F(10) 2.874Å, P---F(4) 3.048Å, P---F(5) 3.124Å. The average

atomic distance is 3.015 Å, and is shorter than the sum of the van der Waals radii (3.31 Å).[33]

4.2.2.4 Ar'Ar"PCl

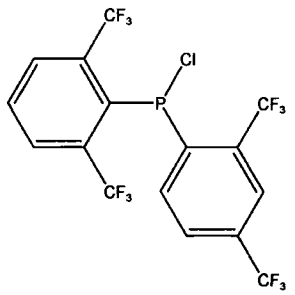

Figure 4.7: *The Ar'Ar"PCl molecule*

This compound was synthesised and crystallised by Roden.[21] The ^{31}P NMR spectrum showed a complex multiplet at δ67.3 ppm, caused by the presence of three *ortho*-CF_3 groups. (Figure 4.8)

The ^{19}F spectrum for a toluene solution was expected to be composed of two doublets, (one having double intensity) (from the Ar' group) and one singlet. At ambient temperature, however, a doublet at δ -59.3 ppm ($^4J_{P-F}$ 59.1 Hz) and two singlets (a broad double intensity line at –55.4 ppm and a sharp peak at –64.1 ppm) were observed (Figure 4.9)

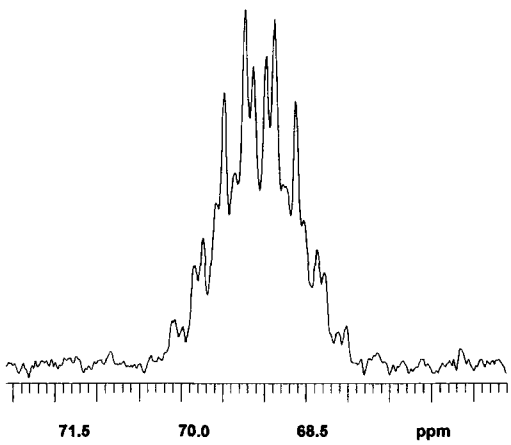

Figure 4.8: *^{31}P NMR spectrum of Ar'Ar"PCl*

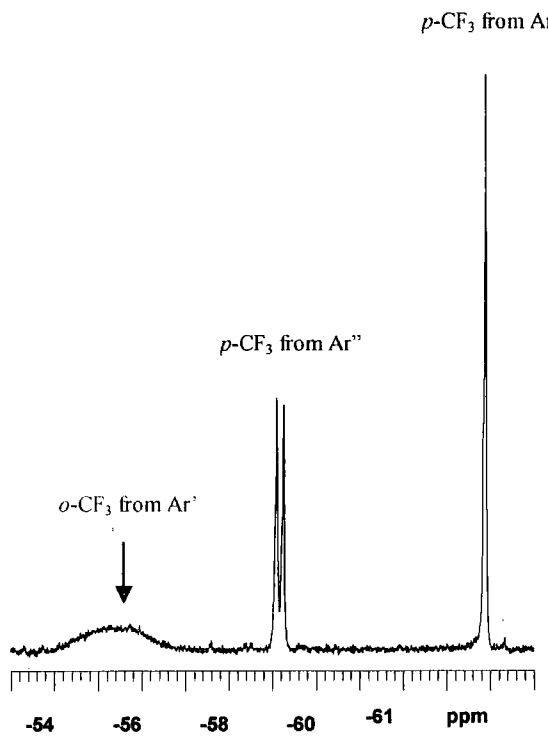

Figure 4.9: *^{19}F NMR spectrum of Ar'Ar"PCl*

The $^{13}C\{^{1}H\}$ NMR spectrum was also recorded for a toluene/$CDCl_3$ solution at ambient temperature. Probable assignments (Figure 4.10) are shown is Table 4.7, though some of these are necessarily tentative. The carbons to which the CF_3 groups were attached could not be assigned with confidence, since these signals were of low intensity and were overlapped with stronger signals. The presence of two distinct *ipso* carbon signals confirms the asymmetric nature of the Ar'Ar"PCl, as does the observation of three different CF_3 signals, one of double intensity.

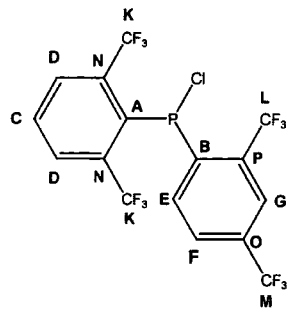

Figure 4.10: *Lettering Scheme for Carbon Atoms in Ar'Ar"PCl*

Carbon	δ (ppm)	J (Hz)
A	137.6	d, $^{1}J_{P-C}$ 67.9
B	136.7	d, $^{1}J_{P-C}$ 84.0
C	132.11[a]	s
D	131.1	s (broad, double intensity)
E	134.2	d, $^{2}J_{P-C}$ 8.7
F	128.0	d, J_{P-C} 3.4
G	123.7	m, $^{3}J_{P-C}$ 5.0
K	123.18[a]	q, $^{1}J_{C-F}$ 275.8 (double intensity)
L	123.24[a]	qd, $^{1}J_{C-F}$ 275.5, $^{3}J_{P-C}$ 3.4
M	123.1	q, $^{1}J_{C-F}$ 272.6
N	132.06[a]	m
O	132.3	m
P	131.8	m

Table 4.7*: $\delta^{13}C$ Assignments*

[a] Although the absolute accuracy of the chemical shifts is only quoted to one decimal place, a further digit is given when two signals are very close but resolved

- X-ray Crystallography

The structure was determined by A.S. Batsanov at 150K and is shown in Figure 4.11.[19,21] This compound was the first structurally characterised diarylchlorophosphane.

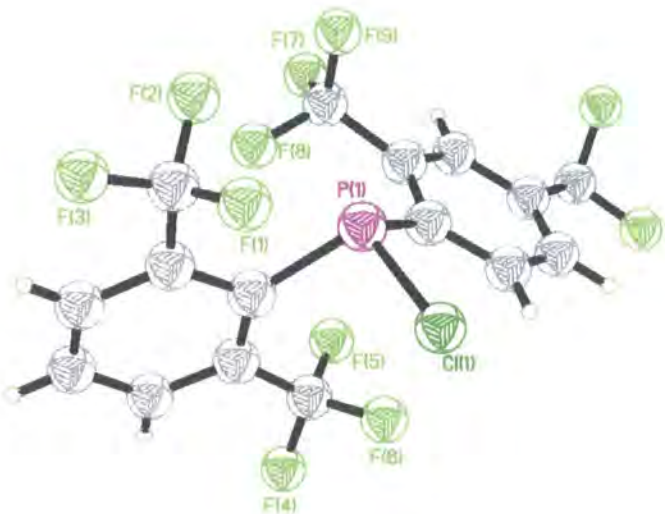

Figure 4.11: *Molecular structure of Ar'Ar"PCl*[21]

The P-C and P-Cl bonds distances (P-Cl 2.061(1), P-C(1) 1.875(1), P-C(9) 1.852(1) Å) are similar to those found in Ar_2PCl and $Ar"_2PCl$. The P-C(1) bond is longer than that for P-C(9), reflecting the steric demand of the two CF_3 groups in *ortho* positions of the Ar' moiety.

The three covalent bonds around the phosphorus have a pyramidal configuration, complemented by two short intramolecular interactions: P---F(1) 2.890(1) Å and P---F(8) 2.897(1) Å. Overall, four short P---F distances are found in the range 2.890-3.25Å. These contacts are shorter than the sum of the van der Waals radii of 3.31 Å.[33]

4.2.2.5 $Ar'PBr_2$

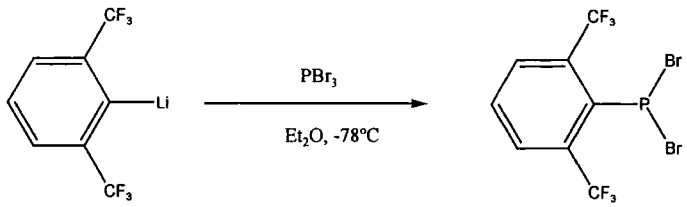

Equation 4.7: *Synthesis of $Ar'PBr_2$*

A solution of Ar'Li/Ar"Li was added to a PBr_3 solution in diethyl ether at -78°C. The resulting oil was distilled under reduced pressure (Bp 60°C) to give a yellow oil.

The ^{31}P NMR spectrum showed a septet at δ134.1 ($^4J_{P-F}$ 62.8Hz) ppm. The ^{19}F NMR spectrum consisted of a doublet δ -52.9 ($^4J_{P-F}$ 62.8Hz, 6F, *o*-CF_3) ppm.

4.2.2.6 $Ar"PBr_2$

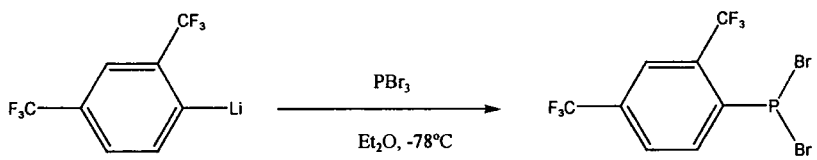

Equation 4.8: *Synthesis of $Ar"PBr_2$*

This product could not be separated from the first substitute $Ar'PBr_2$ because of their very close boiling point, caused by their identical molecular mass.

The ^{31}P NMR consisted of a quartet at 141.0 ($^4J_{P-F}$ 85.5Hz). The ^{19}F NMR showed a doublet at –56.9 ($^4J_{P-F}$ 85.8Hz, 3F, *o*-CF_3) and a singlet at -62.8 (3F, *p*-CF_3) ppm.

4.2.2.7 Ar"$_2$PBr

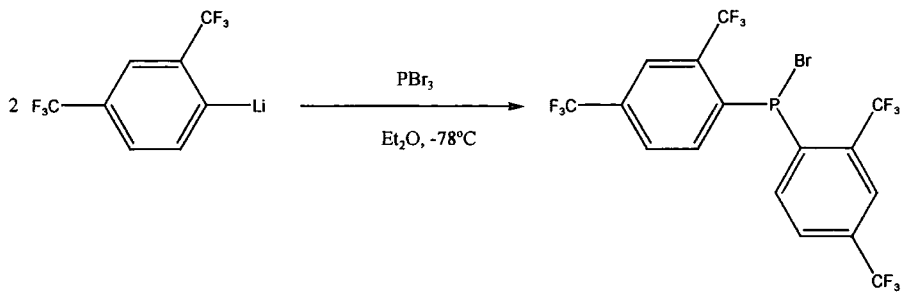

Equation 4.9: *Synthesis of Ar"$_2$PBr*

Two equivalents of the Ar'Li/Ar"Li mixture were added to a solution of PBr_3 at -78°C to give an brown oil, which was purified by distillation under reduced pressure (Bp 120°C). This afforded a yellow oil, which crystallised on standing.

- NMR spectroscopy

The ^{31}P NMR spectrum showed a doublet at 57.4 ($^4J_{P-F}$ 65.8 Hz) ppm and the ^{19}F NMR spectrum consisted of a doublet at –57.7 ($^4J_{P-F}$ 65.8 Hz, *o*-CF_3) and a singlet at –63.7 (*p*-CF_3) ppm.

- X-ray crystallography

Crystals were grown by recrystallisation from hexanes. The structure was determined by A.S. Batsanov at 103 K and is shown in Figure 4.12:

Figure 4.12: *Molecular structure of Ar"$_2$PBr*

Ar"$_2$PBr crystallises in the monoclinic I2/a space group with Z=8.
Selected bond distances and angles are listed in Table 4.8:

Bond Distances (Å)		Angles (°)	
P(1)-Br(1)	2.2340(5)	C(1)-P(1)-C(11)	100.51(8)
P(1)-C(1)	1.8572(18)	C(1)-P(1)-Br(1)	96.99(6)
P(1)-C(11)	1.8591(17)	C(11)-P(1)-Br(1)	101.31(6)

Table 4.8: *Selected Bond Distances (Å) and Angles(°) for Ar"$_2$PBr*

Bond distances and angles are very similar to those found in the analogous compound Ar"$_2$PCl. The P-Br bond distance is in the same range as the P-Br bond distances found in $ArPBr_2$. Ar"$_2$PCl and Ar"$_2$PBr are isostructural.
As in $ArPBr_2$ and Ar"$_2$PCl, short P---F contacts are found between the phosphorus and three of the fluorine atoms of the *ortho*-CF_3 groups: P---F(4) 3.067 Å, P---F(5) 3.122 Å,

P---F(10) 2.887 Å, with an interatomic average distance of ca. 3.025 Å. This distance is shorter than the sum of the van der Waals radii (3.31 Å).[33]

4.2.2.8 Ar'Ar"PBr

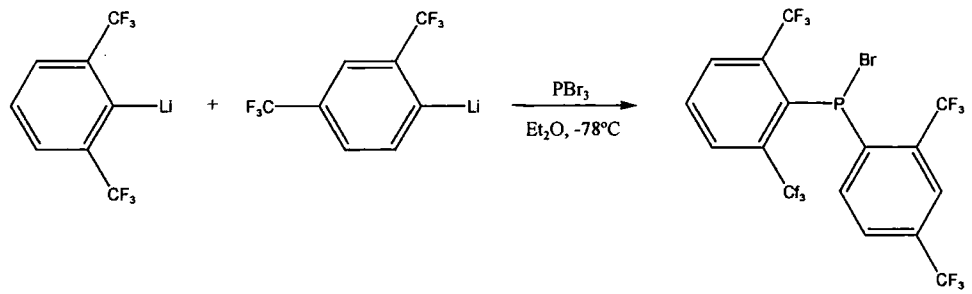

Equation 4.10: *Synthesis of Ar'Ar"PBr*

This compound was present in solution as a disubstituted product of the reaction between the Ar'Li/Ar"Li mixture and PBr_3. Distillation under reduced pressure of the solution gave at 120°C an oil, which NMR revealed to be a mixture of $Ar"_2PBr$ and Ar'Ar"PBr. Although $Ar"_2PBr$ could be isolated, Ar'Ar"PBr could not.

The ^{31}P NMR exhibited a multiplet (13 lines) at 58.9 ppm. The ^{19}F NMR showed three different signals: a broad singlet at -55.2 (6F, *o*-CF_3 in Ar'), a doublet at -58.8 ($^4J_{P-F}$ 56.6 Hz, 3F, *o*-CF_3 in Ar") and a singlet at -63.5 (3F, *p*-CF_3) ppm.

4.2.2.9 $Ar"_2PH$

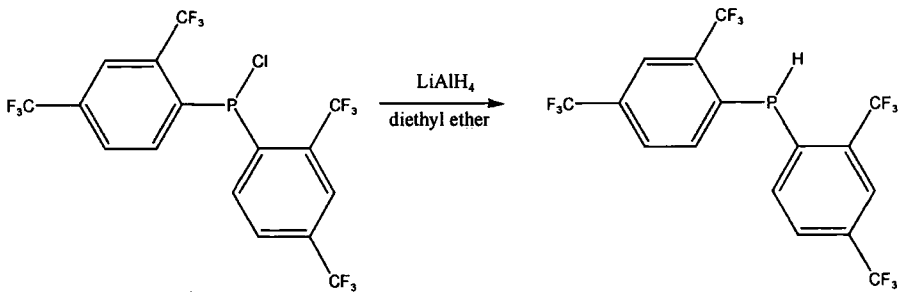

Equation 4.11: *Synthesis of $Ar"_2PH$*

$Ar"_2PH$ was obtained by reduction of $Ar"_2PCl$ with $LiAlH_4$, yielding a white solid. The $^{31}P\{^1H\}$ spectrum consisted of a septet at -48.7 ($^4J_{P-F}$ 36.7 Hz) ppm. The ^{31}P, ^1H coupled spectrum showed a doublet of septets at -49.0 ($^4J_{P-F}$ 36.8 Hz, $^1J_{P-H}$ 270.4 Hz) ppm.

The ^{19}F NMR spectrum exhibited a doublet at -60.0 ($^4J_{P-F}$ 37.1 Hz, 6F, *o*-CF_3) and a singlet at -63.8 (s, 6F, *p*-CF_3) ppm.

Four signals were found in the ^1H NMR spectrum. These are listed in Table 4.9 below.

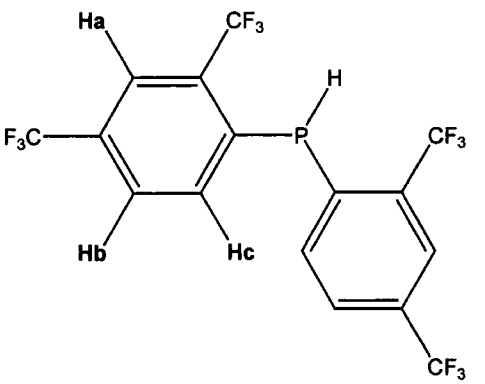

Figure 4.13: *Lettering Scheme for $Ar"_2PH$*

Hydrogen	δ ^1H (ppm)	J (Hz)
Ha	7.9	s
Hb	7.7	d, $^3J_{H-H}$ 7.8
Hc	7.4	d, $^3J_{H-H}$ 7.9
H	6.2	doublet, $^1J_{P-H}$ 274.5

Table 4.9: *δ^1H assignments for $Ar"_2PH$*

4.2.2.10 Ar'Ar"PH

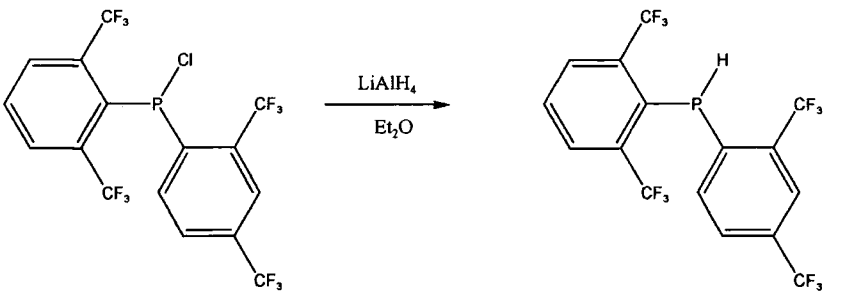

Equation 4.12: *Synthesis of Ar'Ar"PH*

Ar'Ar"PH was prepared by reduction of the chloride Ar'Ar"PCl with $LiAlH_4$. The product was isolated as a white solid.

The proton-decoupled ^{31}P NMR spectrum consisted of a multiplet at –67.2 ppm. The proton-coupled ^{31}P NMR spectrum showed a doublet of multiplets at –67.6 ($^1J_{P-H}$ 240.7 Hz) ppm. The $^1J_{P-H}$ coupling constant is in the same range as the one found in $Ar'PH_2$ ($^1J_{P-H}$ 216.7 Hz).[21]

The ^{19}F NMR spectrum exhibited a broad singlet at –57.7 ppm (6F, *o*-CF_3 in Ar'), a doublet at –61.2 ($^4J_{P-F}$ 43.7 Hz, 3F, *o*-CF_3 in Ar") and a singlet at -63.4 (3F, *p*-CF_3) ppm.

The ^1H NMR spectrum confirmed the presence of a P-H bond with a doublet at 5.7 ppm ($^1J_{P-H}$ 240.4Hz).

Crystals of Ar'Ar"PH were grown by recrystallisation from pentane. Data were collected, but the structure could not be solved.

4.2.2.11 Attempted synthesis of Ar'Ar"PF

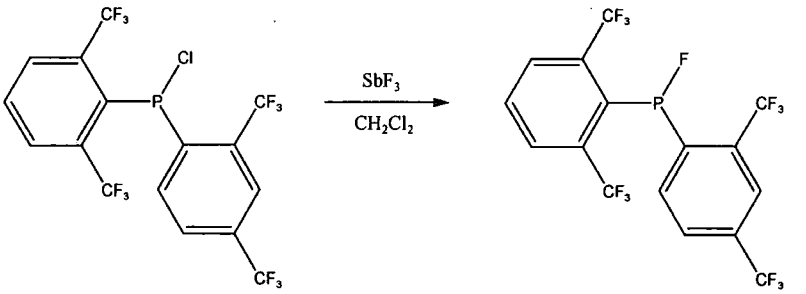

Equation 4.13: *Attempted Synthesis of Ar'Ar"PF*

SbF_3 was added to a solution of Ar'Ar"PCl in dichloromethane. No change was observed in the ^{19}F or ^{31}P NMR spectra, which showed only the presence of the starting material.

4.2.2.12 Attempted synthesis of $Ar"_2PF$

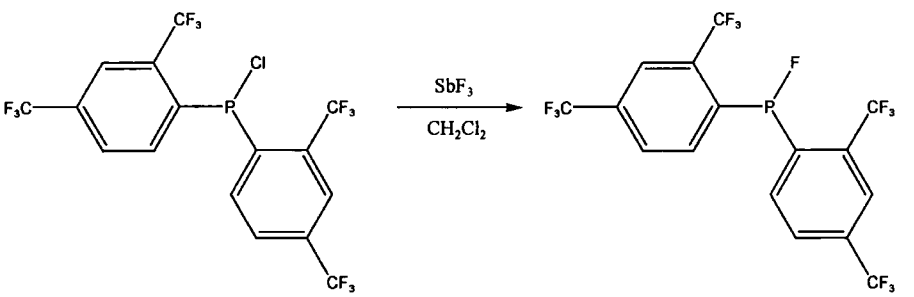

Equation 4.14: *Attempted Synthesis of $Ar"_2PF$*

SbF_3 was added to a solution of $Ar"_2PCl$ in CH_2Cl_2. The mixture was stirred for a few days and then refluxed for two weeks. No change was observed in the ^{19}F or ^{31}P NMR spectra.

The direct fluorination of the chloride derivatives containing two Ar' or Ar" groups does not seem to occur. Roden[21] noticed the same results with the reaction between Ar_2PCl

and SbF_3, where only a very small amount of Ar_2PF was obtained. The steric hindrance around the P-Cl bond, imposed by two fluoromes or fluoroxyl substituents, makes the substitution reactions difficult.

4.2.2.13 ArAr'PCl/ArAr"PCl

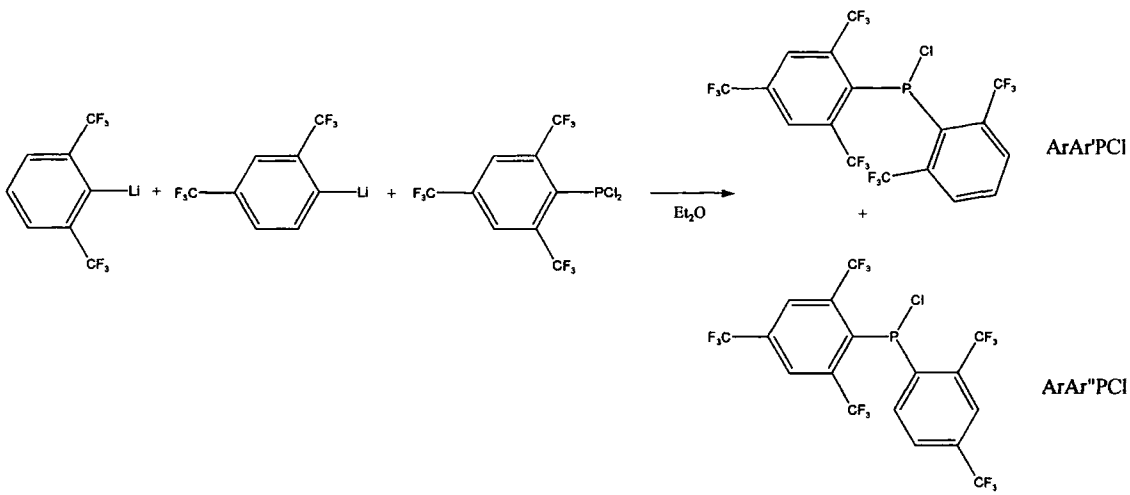

Equation 4.15: *Synthesis of ArAr'PCl/ArAr"PCl*

The mixture of the chloro-derivatives was obtained by reaction of Ar'Li/Ar"Li with $ArPCl_2$ in an overall 1:1 molar ratio. The mixture was purified by distillation giving a yellow oil, but the compounds could not be separated. Attempted recrystallisation from hexanes afforded a white powder of the mixture.

The ^{31}P NMR spectrum for ArAr'PCl showed a multiplet at 76.6 ppm. For ArAr"PCl a multiplet was also observed at 69.9 ppm. Three signals were observed in the ^{19}F NMR spectrum of ArAr'PCl: two doublets at –54.1 ($^4J_{P-F}$ 42.1Hz, 6F, *o*-CF_3) and –54.3 ($^4J_{P-F}$ 42.1Hz, 6F, *o*-CF_3) ppm, and a singlet at –64.0 (3F, *p*-CF_3). The ^{19}F NMR spectrum of ArAr"PCl consisted of a broad signal at –55.5 (6F, *o*-CF_3 in Ar), a doublet at –58.6 ($^4J_{P-F}$ 58.3Hz, 3F, *o*-CF_3 in Ar") and two singlets at –63.6 (3F, *p*-CF_3) and –64.1 (3F, *p*-CF_3).

This compound is the first synthesised product containing fluoromes and fluoroxyl ligands within the same molecule. The coupling constant in ArAr"PCl is larger than the

one in ArAr'PCl ($^4J_{P-F}$ 42.1Hz in ArAr'PCl, 58.1 Hz in ArAr"PCl). This has been observed in the monosubstituted products Ar'PCl_2 and Ar"PCl_2, reflecting the fact that one of the CF_3 groups in the *ortho* position interacts more with the phosphorus than the other one.

No evidence was found for the formation of Ar'$_2$PX. This is probably due to the steric demand of the two Ar' substituents containing two CF_3 groups in *ortho* position. However, Ar_2PX has been isolated. In the case of the reaction with Ar'Li/Ar"Li the formation of the less sterically hindered products Ar"$_2$PCl and Ar'Ar"PCl is preferred.

4.3 Arsenic Derivatives

Only a few arsenic derivatives containing fluoromes ligands have been reported. The first arsenic derivatives prepared were Ar_2AsF[15] by reaction of 2 equivalents of ArLi with AsF_3. ArAsF was reduced to Ar_2AsH via $LiAlH_4$.[15] More recently $ArAsCl_2$[35] and Ar_2AsCl[27] were synthesised. Ar_2AsCl is the only arsenic derivatives containing Ar to be structurally characterised. No examples of fluoroxyl-containing derivatives have been described. Xue[36] attempted the reaction between Ar'Li/Ar"Li and $AsCl_3$, which afforded a mixture of different mono- and di-substituted products. These could not be separated.

A general method has been used in these syntheses with $AsCl_3$ or $AsBr_3$ reacting directly with ArLi or Ar'Li/Ar"Li at low temperature with continuous stirring for a few hours.

4.3.1 Reaction with 2,4,6-tris(trifluoromethyl)phenyl lithium (ArLi)

4.3.1.1 $ArAsCl_2$

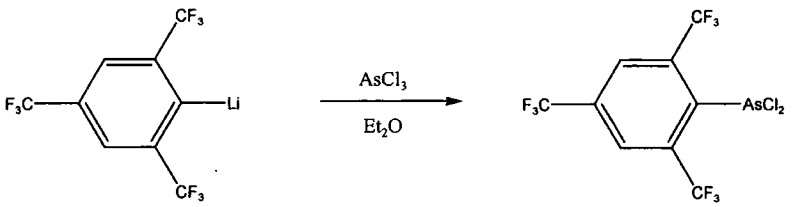

Equation 4.16: *Synthesis of $ArAsCl_2$*

$ArAsCl_2$ was isolated as a yellow oil and purified by distillation under reduced pressure (Bp 60°). The ^{19}F NMR showed two singlets at -53.5 (s, 6F, *o*-CF_3) and at -64.2 (3F, *p*-CF_3) ppm.

4.3.1.2 Ar_2AsCl

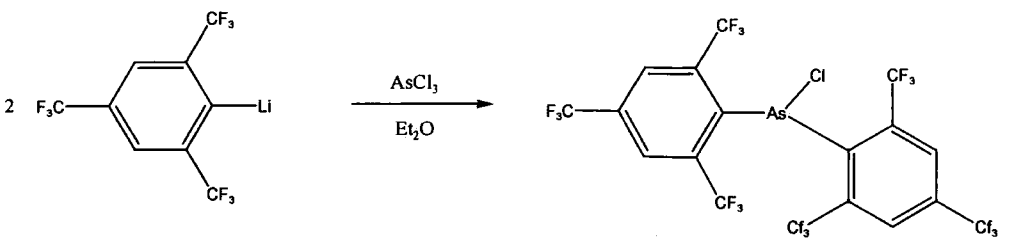

Equation 4.17: *Synthesis of Ar_2AsCl*

Ar_2AsCl is a di-substituted product from the reaction above. It has been isolated as a white solid.

The ^{19}F NMR consisted of two singlets at -54.6 (12F, *o*-CF_3) and at -63.9 (6F, *p*-CF_3) ppm respectively. The structure of this compound has recently been determined and reported by Burford *et al.*[22]

4.3.1.3 $ArAsBr_2$

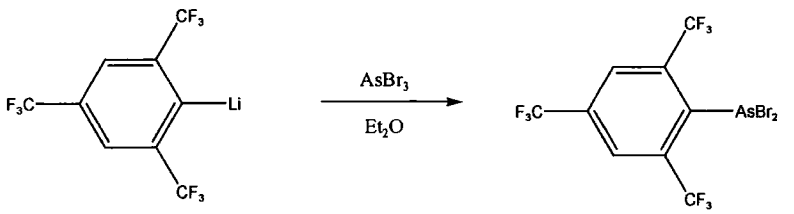

Equation 4.18: *Synthesis of $ArAsBr_2$*

This compound was isolated as a yellow oil after distillation under reduced pressure (Bp 120°C). Two different singlets were observed in the ^{19}F NMR spectrum at -53.2 (6F, *o*-CF_3) and -63.8 (6F, *p*-CF_3) ppm.

4.3.1.4 Ar_2AsBr

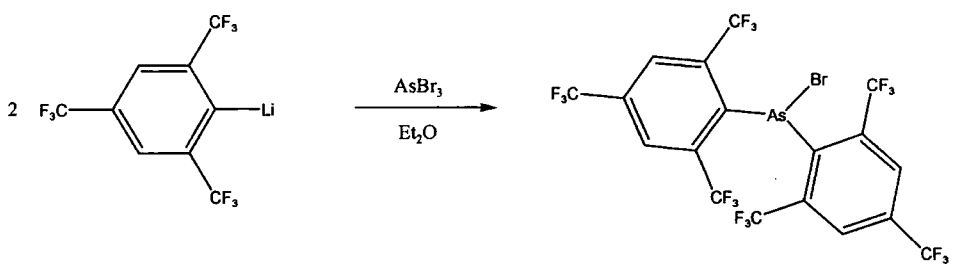

Equation 4.19: *Synthesis of Ar_2AsBr*

Ar_2AsBr is the disubstituted compound arising from the reaction of ArLi with $ArBr_3$ in a 2:1 molecular ratio. The compound was separated from $ArAsBr_2$ by distillation (Bp 150°C). The ^{19}F NMR spectrum exhibited two singlets at -54.4 (12F, *o*-CF_3) and -63.9 (6F, *p*-CF_3) ppm.

4.3.1.5 $ArAsH_2$

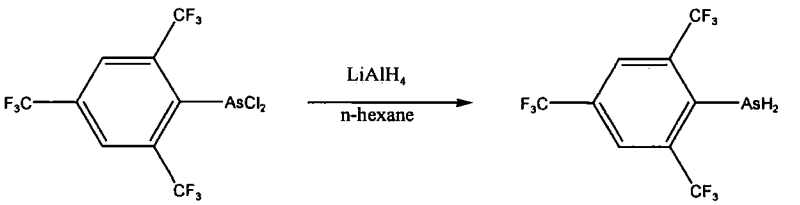

Equation 4.20: *Synthesis of $ArAsH_2$*

$ArAsH_2$ was prepared by reduction of $ArAsCl_2$ with $LiAlH_4$. This afforded a yellow oil. The ^{19}F NMR showed two signals: a triplet at -61.4 ($^5J_{F\text{-}H}$ 6.4 Hz, 6F, *o*-CF_3) and singlet at -64.2 (3F, *p*-CF_3) ppm. A broad singlet was observed at 6.2 ppm in the ^1H NMR spectrum, assigned to the H bonded to As.

4.3.1.6 Ar_2AsH

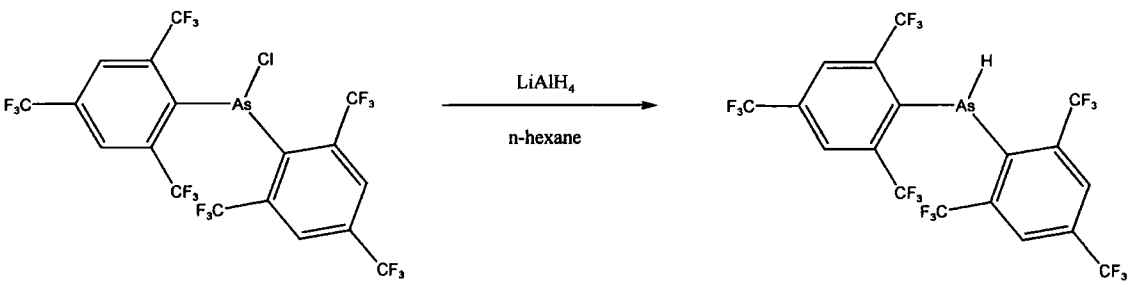

Equation 4.21: *Synthesis of Ar_2AsH*

Reduction of Ar_2AsCl by $LiAlH_4$ gave Ar_2AsH as a colourless oil. The ^{19}F NMR consisted of a doublet at -58.7 ($^5J_{F\text{-}H}$ 3.6 Hz, 12F, *o*-CF_3) and a singlet -64.2 (6F, *p*-CF_3) ppm. The ^1H NMR spectrum showed a broad singlet δ-6.4 ppm corresponding to H bonded to As.

These ^{1}H NMR chemicals shifts correspond to those found previously in the literature for for Ar_2AsH.[15] Scholz *et al* reported ^{19}F NMR data showing a doublet at –64.1 ppm corresponding to the ^{7}J coupling between the *para*-CF_3 groups and the hydrogen.[15] This coupling has not been noticed in the present work.

4.3.2 Reaction with 2,6-bis(trifluoromethyl)phenyl lithium (Ar'Li) / 2,4-bis(trifluoromethyl)phenyl lithium (Ar"Li)

As for phosphorus compounds, the reaction of Ar'Li/Ar"Li with $AsCl_3$ can give rise to a mixture of five different products, two monosubstituted ($Ar'AsCl_2$ and $Ar"AsCl_2$) and three disubstituted (Ar'_2ArCl, $Ar"_2AsCl$ and Ar'Ar"AsCl).

4.3.2.1 $Ar'AsCl_2/Ar"AsCl_2$

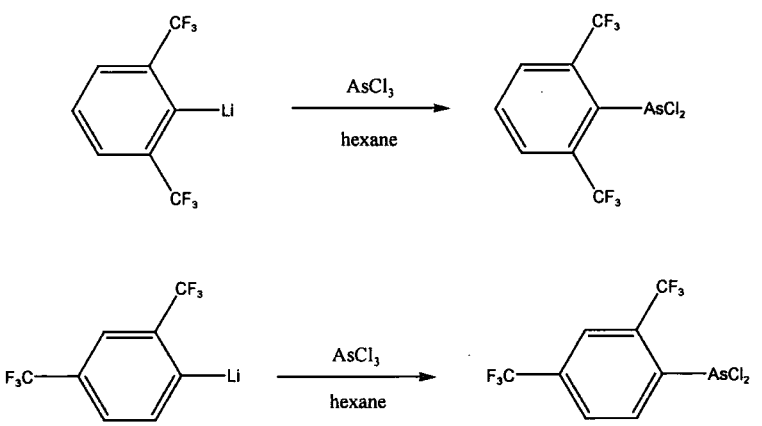

Equation 4.22: *Synthesis of $Ar'AsCl_2/Ar"AsCl_2$*

These two compounds could not be separated by distillation because of their close boiling points. The mixture was isolated as a yellow oil (Bp 115°C). The ^{19}F NMR spectrum of $Ar'AsCl_2$ consisted of a singlet at -52.9 (6F, *o*-CF_3) ppm; for $Ar"AsCl_2$ it showed two singlets at -57.7 (3F, *o*-CF_3) and -63.7 (3F, *p*-CF_3) ppm.

4.3.2.2 Ar'Ar"AsCl

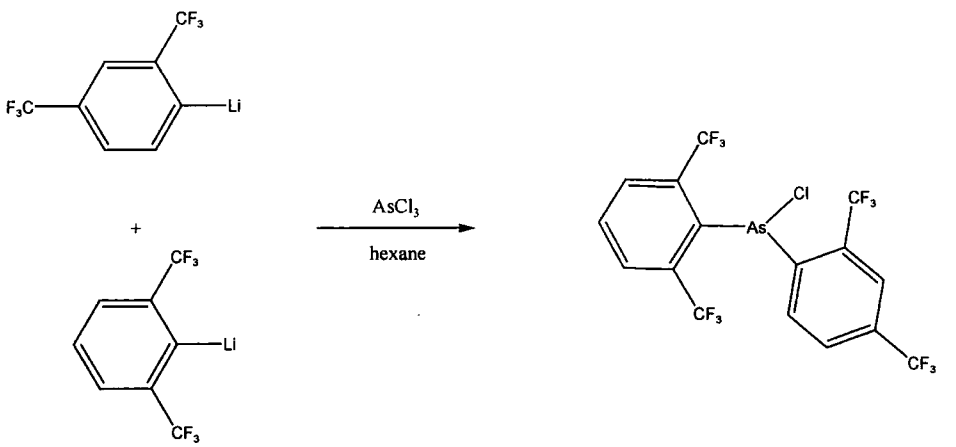

Equation 4.23: *Synthesis of Ar'Ar"AsCl*

Ar'Ar"AsCl was isolated by distillation under vacuum (Bp 150°C), and purified by recrystallisation from n-hexane.

- NMR spectroscopy

The ^{19}F NMR spectrum showed a broad singlet at –54.8 ppm (6F), corresponding to the *ortho*-CF_3 groups of the Ar' moiety, a singlet at –58.8 (3F) for the *ortho*-CF_3 of the Ar" substituent and a singlet at –63.5 (3F, *p*-CF_3) (Figure 4.14).

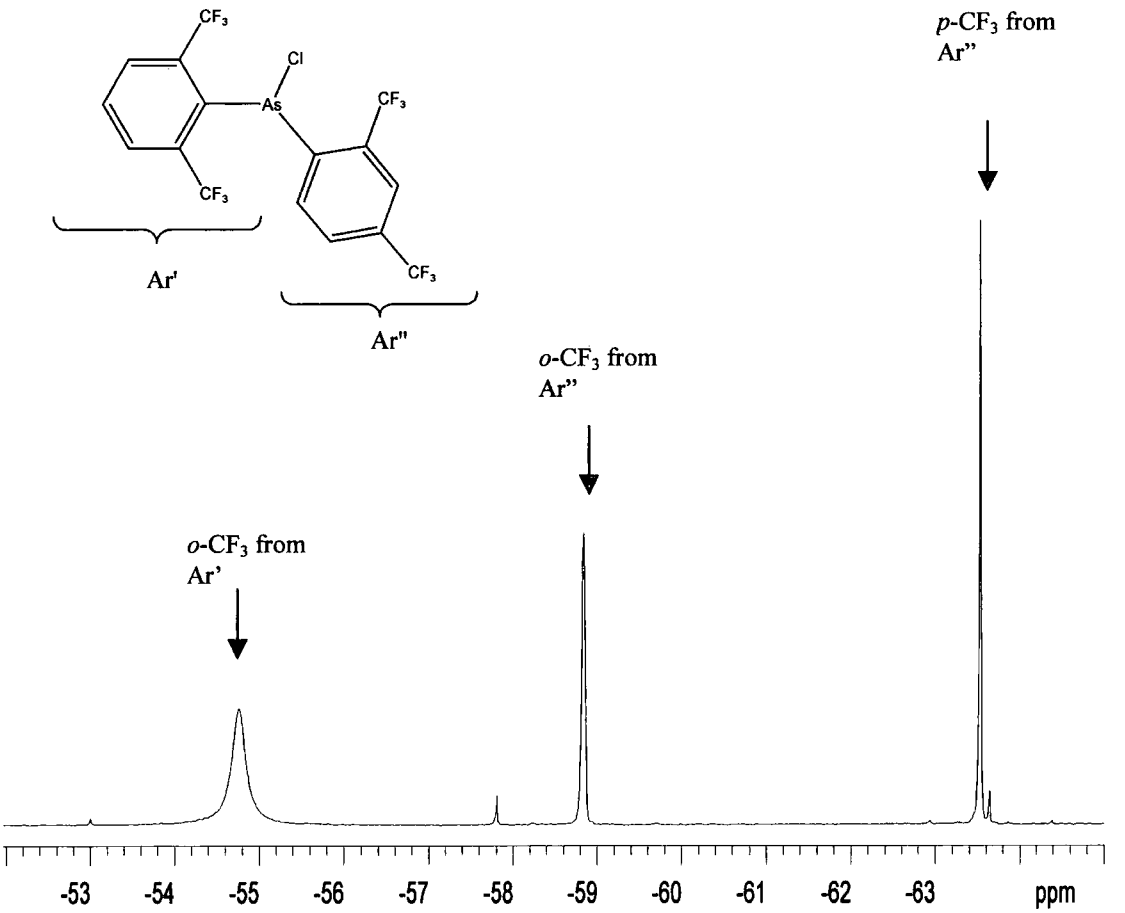

Figure 4.14: *^{19}F NMR spectrum of Ar'Ar"AsCl*

Data for the ^{1}H NMR are listed in Table 4.10.

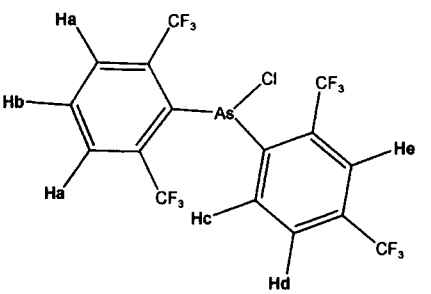

Figure 4.15: *Lettering scheme for Ar'Ar"AsCl*

Hydrogen	δ ^{1}H (ppm)	J (Hz)
Ha	7.28	d, $^3J_{H-H}$ 8
Hb	6.6	t, $^3J_{H-H}$ 7.6
Hc	8.1	d, $^3J_{H-H}$ 8
Hd	7.26	d, $^3J_{H-H}$ 7.6
He	7.7	

Table 4.10: *δ^1H Assignments*

- X-Ray crystallography

Crystals were grown by recrystallisation from hexane. The structure of Ar'Ar"AsCl was ascertained by A.E. Goeta at 100 K and is shown in Figure 4.16.

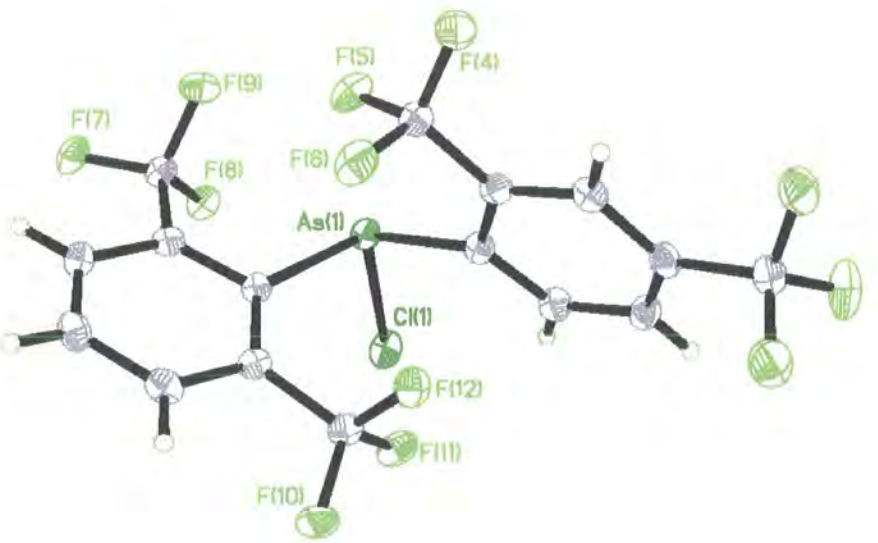

Figure 4.16: *Molecular structure of Ar'Ar"AsCl*

Selected bond distances and angles are listed Table 4.11, with those for Ar_2AsCl[22] for comparison.

	Bond distance (Å)		Angle(°)	
Ar'Ar"AsCl	As(1)-Cl(1)	2.2074(5)	C(1)-As(1)-C(11)	102.98(7)
	As(1)-C(1)	1.9880(18)	C(1)-As(1)-Cl(1)	100.08(6)
	As(1)-C(11)	2.0182(17)	C(11)-As(1)-Cl(1)	98.84(5)
Ar_2AsCl[22]	As(1)-Cl	2.1920(12)	C(1)-As(1)-C(2)	107.53(16)
	As(1)-C(1)	2.023(4)	C(1)-As(1)-Cl(1)	101.3(9)
	As(1)-C(2)	2.016(4)	C(2)-As(1)-Cl(1)	88.4(9)

Table 4.11: *Selected Bond Distances (Å) and Angles (°) in Ar'Ar"AsCl and* Ar_2AsCl[22]

The As-Cl bond length of 2.2074(5) Å is similar to that in the orthorhombic modification of Ar_2AsCl (2.1920(12) Å),[22] and slightly shorter than in $AsCl_3$[37] or other organo-derivatives with one As-Cl bond.[38-40] The As-C bond lengths are slightly longer in Ar_2AsCl. Angles are also larger in Ar_2AsCl than in Ar'Ar"Cl, reflecting the greater steric demand of the Ar ligands in comparison to the Ar" substituents.

Some short As---F contacts are found: As---F(5) 2.701 Å , As---F(8) 2.851 Å, As---F(9) 3.171 Å, As---F(11) 3.292 Å, with an average interatomic of ca. 3.003 Å. This is shorter than the sum of the van der Waals radii of As (2.00 Å) and F (1.40 Å).[41]

4.3.2.3 Ar'$AsBr_2$/Ar"$AsBr_2$

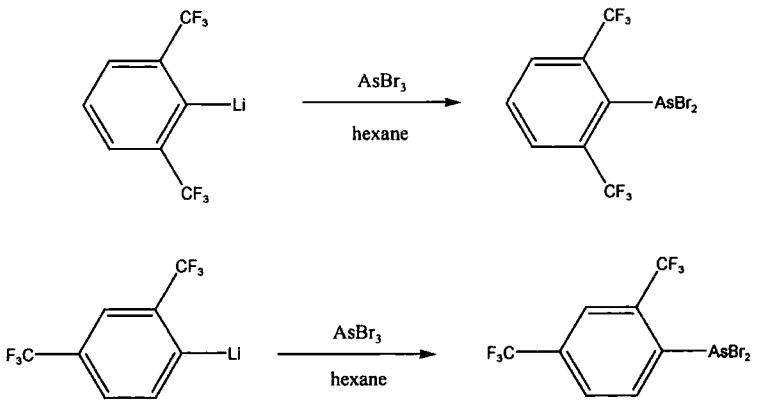

Equation 4.24: *Synthesis of Ar'$AsBr_2$/Ar"$AsBr_2$*

Ar'Li/Ar"Li was added to a solution of $AsBr_3$ in hexanes. The product was purified by distillation under reduced pressure (0.01 Torr), and a yellow oil was collected at 81°C. Ar'$AsBr_2$ and Ar"$AsBr_2$ could not be separated. The ^{19}F NMR exhibited a singlet at -52.7 (6F, *o*-CF_3) for Ar'$AsBr_2$. For Ar"$AsBr_2$ two singlets were observed at δ-58.5 (3F, *o*-CF_3) and -62.8 (3F, *p*-CF_3) ppm.

4.3.2.4 Ar'Ar"AsBr

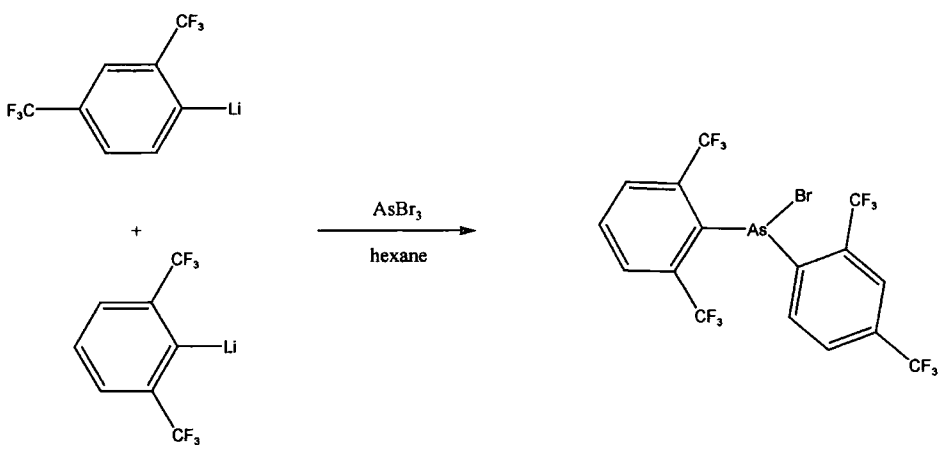

Equation 4.25: *Synthesis of Ar'Ar"AsBr*

Ar'Ar"AsBr was isolated by distillation (Bp 110°C) as a mixture with Ar"$_2$AsBr. The mixture was dissolved in hexanes and left in the freezer where, after a month, crystals of Ar'Ar"AsBr appeared.

- NMR spectroscopy

As found in the analogous compound Ar'Ar"AsCl, three signals were observed in the ^{19}F NMR spectrum: a broad signal at –54.9 (6F) corresponding to the *ortho*-CF_3 groups of the Ar' ligand; the *o*-CF_3 group of the Ar" moiety has a shift of –58.8 (3F) ppm, while a singlet at –63.5 (3F) ppm corresponds to the CF_3 group in the *para* position.

- X-ray crystallography

Crystals were formed by recrystallisation from hexanes. The structure was ascertained at 120 K by A.L. Thompson, and is shown in Figure 4.17.

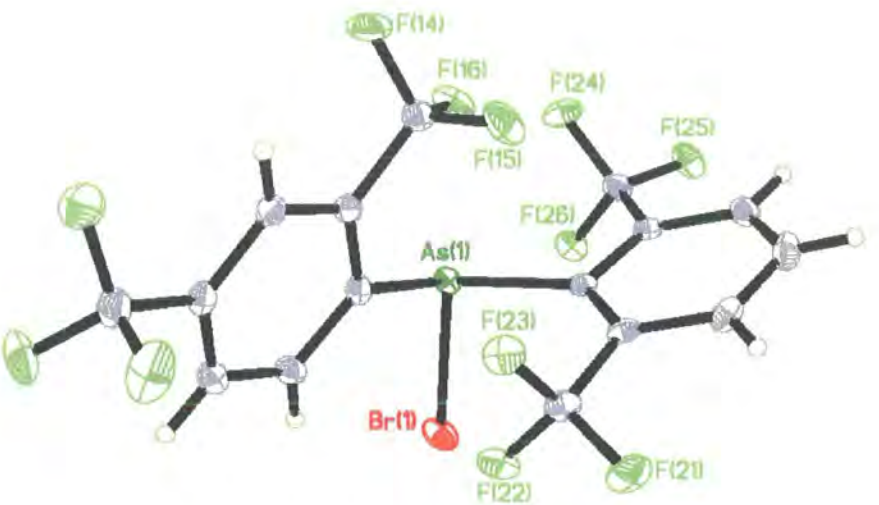

Figure 4.17: *Molecular structure of Ar'Ar"AsBr*

The As-Br bond distance of 2.3530(3) Å is similar to those found in the literature, lying between the values of 2.31 Å for $AsBr_3$[42] and 2.40(1) Å for Ph_2AsBr.[43]. It is similar to the corresponding bond length in Mes_2AsBr of 2.34(2) Å at low temperature and 2.3846(4) Å at higher temperature.[44]

The As-C bond lengths are similar to the ones found in Ar'Ar"AsCl, and the angles are in the same range too. Four short As---F contacts have been observed in this molecule: As---F(16) 2.707 Å, As---F(22) 3.277 Å, As---F(24) 3.157 Å, As---F(26) 2.840 Å, with an average interatomic distance of ca. 2.99 Å. This is shorter than the sum of the van der Waals radii (3.40 Å).[41] These intramolecular interactions are similar to those found in Ar'Ar"AsCl.

4.3.2.5 Ar"$_2$AsBr

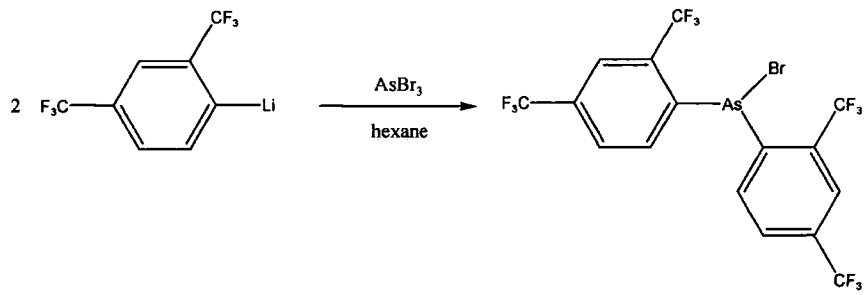

Equation 4.26: *Synthesis of Ar"$_2$AsBr*

Ar"$_2$AsBr is a product of the reaction of two equivalents of the Ar'Li/Ar"Li mixture with $AsBr_3$. This compound was obtained in a mixture with Ar'Ar"AsBr. Ar"$_2$AsBr was isolated as a yellow oil after recrystallisation of Ar'Ar"AsBr. The ^{19}F NMR spectrum showed two singlets at -58.4 (6F, *o*-CF_3) and -63.6 (6F, *p*-CF_3) ppm.

4.3.2.6 Ar'Ar"AsH

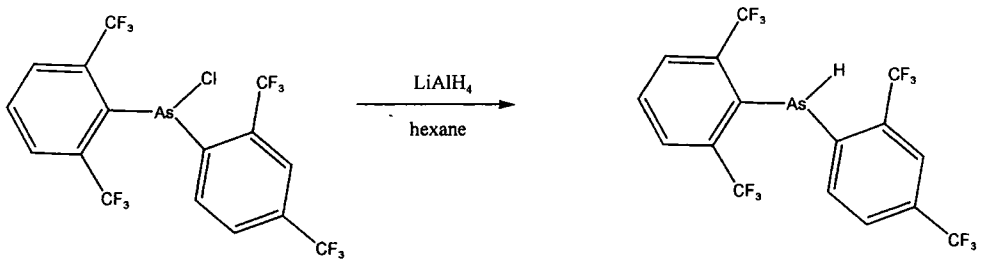

Equation 4.27: *Synthesis of Ar'Ar"AsH*

Reduction of Ar'Ar"AsCl by $LiAlH_4$ afforded a white solid of Ar'Ar"AsH.

- NMR Spectroscopy

Three signals were observed in the ^{19}F NMR spectrum: the *ortho*-CF_3 groups of the Ar' moiety appeared as a broad singlet at –58.2 ($^5J_{F-H}$ 7.1 Hz, 6F) ppm. The Ar" substituents showed two different signals, a singlet at -61.2 (3F) ppm corresponding to the *ortho*-CF_3 and a singlet at -63.8 (3F) ppm assigned to the *para*-CF_3 groups.

Data for the ^1H NMR spectrum in d_8-toluene are listed in Table 4.12:

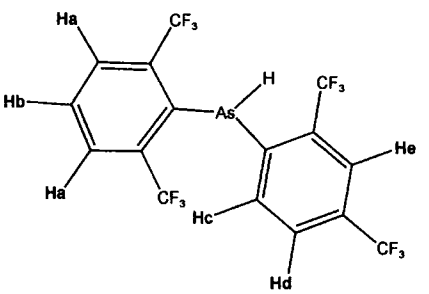

Figure 4.18: *Lettering scheme for Ar'Ar"AsH*

Hydrogen	δ ^{1}H (ppm)	J (Hz)
Ha	8.06	d, $^3J_{H-H}$ 8
Hb	7.7	t, $^3J_{H-H}$ 8
Hc	6.9	d, $^3J_{H-H}$ 7.6
Hd	7.4	d, $^3J_{H-H}$ 8
He	7.9	s
H	5.99	broad singlet, As-H

Table 4.12: *δ^1H assignments for Ar'Ar"AsCl*

- X-ray crystallography

Crystals suitable for X-ray diffraction were obtained by sublimation under vacuum. The structure of Ar'Ar"AsH was determined at 120 K by A.L. Thompson, and is shown in Figure 4.19:

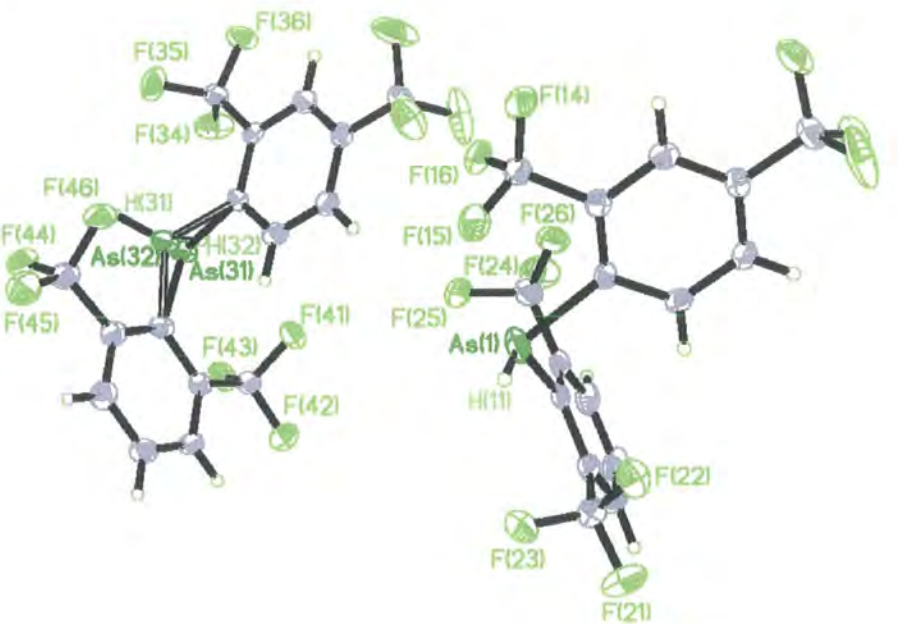

Figure 4.19: *Molecular structure of Ar'Ar"AsH*

There are two distinct molecules in each asymmetric unit, one of which has the arsenic disordered over two almost equally-populated sites (55% and 45% occupation respectively). Data for the non disordered As(1) atom are quoted in Table 4.13.

Bond distance (Å)		Angle (°)	
As(1)-H(11)	1.37(6)	C(11)-As(1)-C(21)	98.11(18)
As(1)-C(11)	1.980(5)	C(11)-As(1)-H(11)	102(2)
As(1)-C(21)	1.995(5)	C(21)-As(1)-H(11)	126(2)
As(31)-H(31)	1.63(12)	C(31)-As(31)-C(41)	96.5(2)
As(31)-C(31)	2.007(6)	C(31)-As(31)-H(31)	97(4)
As(31)-C(41)	2.006(6)	C(41)-As(31)-H(31)	94(4)
As(32)-H(32)	1.42(10)	C(31)-As(32)-C(41)	97.9(2)
As(32)-C(31)	1.984(5)	C(31)-As(32)-H(32)	94(4)
As(32)-C(41)	1.983(5)	C(41)-As(32)-H(32)	116(4)

Table 4.13: *Selected Bond distances (Å) and Angles (°) for Ar'Ar"AsH*

The As-C distances are similar to those found in the analogous compounds, Ar'Ar"AsCl and Ar'Ar"AsBr, ranging from 1.980(4) to 2.007(6) Å. It is not possible to be precise about distances and bond angles involving the H atom attached to As. The As(1)-H(11) bond length is 1.37(6) Å and in the disordered molecule 1.42(10) Å for As(32)-H(32) and 1.63(12) Å for As(31)-H(31). The As-H bond distances found for Ar'Ar"AsH are within the range of the values found for some structurally characterised compounds containing an As-H bond: 1.484(18) Å in a primary organoarsine,[45] 1.519 Å in AsH_3,[46] 1.520 Å in $[Cp^*Mn(CO)_2]AsH$[47] and 1.5(2) in $Cp_2Nb(HAsEt_2)(H_3BAsEt_2)$.[48] As in Ar'Ar"AsCl and Ar'Ar"AsBr, four short contacts between the As atom and some of the fluorines of

the *ortho*-CF_3 groups are found, lying between 2.934 and 3.186 Å for As(1), 2.859 and 3.326 Å for As(31), and between 2.880 and 3.247 Å for As(32).

4.4 Antimony and bismuth derivatives

Although the chemistry of low-coordinate phosphorus and arsenic is well developed, it has been little extended to low-coordinate organo-antimony or bismuth compounds. Only two Sb derivatives containing the fluoromes ligand are known: $ArSbCl_2$[14,22,49] and Ar_2SbCl.[22] The bismuth atom has proved large enough to be able to bear three aryl rings; Ar_2BiCl[23] and Ar_3Bi[23] have been reported.

4.4.1 Antimony derivatives

The Ar'Li/Ar"Li mixture was added to a solution of $SbCl_3$ in hexanes at room temperature in a 2:1 molecular ratio. Solution-state spectroscopy showed a mixture of five different products, which was separated by distillation under reduced pressure.

4.4.1.1 $Ar'SbCl_2/Ar"SbCl_2$

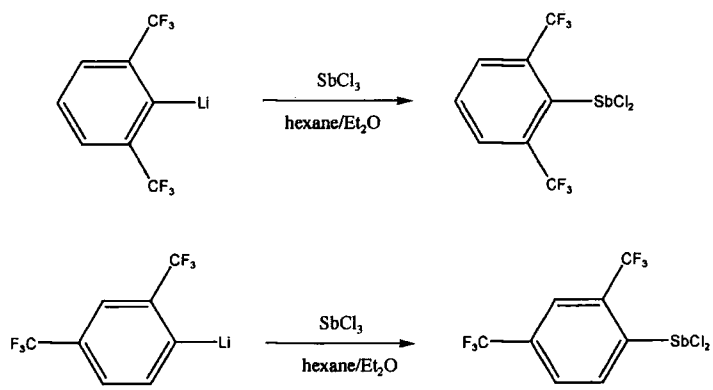

Equation 4.28: *Synthesis of $Ar'SbCl_2/Ar"SbCl_2$*

An orange oil was collected at 95°C. The ^{19}F NMR spectrum showed the presence of two products, which could not be separated. Ar'$SbCl_2$ exhibited a singlet at δ-53.2 (6F, *o*-CF_3) ppm. The spectrum of Ar"$SbCl_2$ showed two singlets at δ-54.9 (3F, *o*-CF_3) and -63.6 (3F, *p*-CF_3) ppm.

4.4.1.2 Ar'$_2$SbCl/Ar"$_2$SbCl

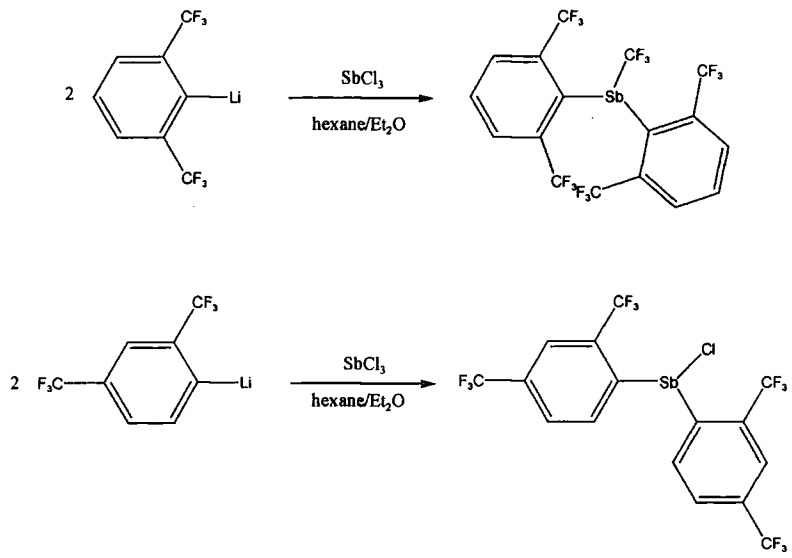

Equation 4.29: *Synthesis of Ar'$_2$SbCl/Ar"$_2$SbCl*

Another fraction was collected at 120°C as a yellow oil. This oil was dissolved in hexanes and cooled down to -30°C overnight. A white solid formed. The ^{19}F NMR spectrum of this solid showed the presence of two products.

A singlet at -55.1 (12F, *o*-CF_3) ppm was observed for Ar'$_2$SbCl. Two other singlets were found at -58.4 (6F, *o*-CF_3) and -63.7 (6F, *p*-CF_3) ppm, assigned to Ar"$_2$SbCl.

4.4.1.3 Ar'Ar"$_2$Sb

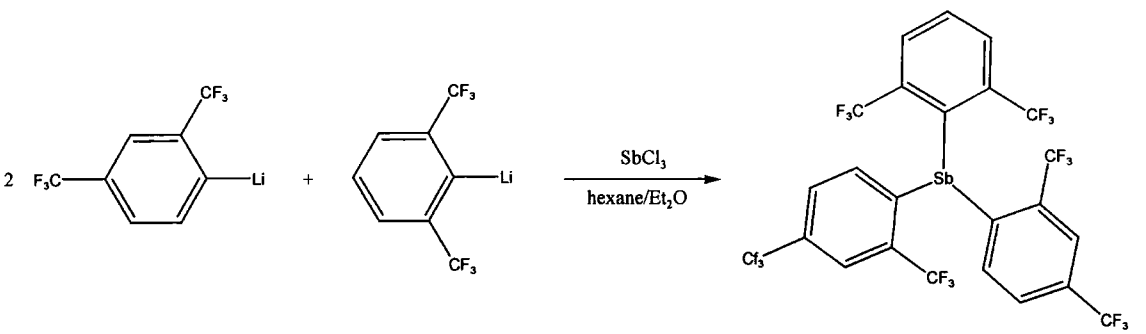

Equation 4.30: *Synthesis of Ar'Ar"$_2$Sb*

Ar'Ar"$_2$Sb appeared as a sticky solid, which was purified by recrystallisation from dichloromethane. This is the first antimony compound containing three fluoroxyl ligands prepared so far.

- NMR spectroscopy

The ^{19}F NMR spectrum exhibited three singlets at -55.5 (6F, *o*-CF_3 in Ar'), -58.4 (s, 6F, *o*-CF_3 in Ar") and -63.6 (s, 6F, *p*-CF_3) ppm.

Variable temperature ^{19}F NMR spectra were recorded at –50°C and 100°C, but no change was observed within the temperature range. As discussed for Ar"$_3$B (Chapter 2), any exchange probably occurs at a lower temperature. Because of solvent restrictions, a lower range of temperatures could not be run.

A ^{13}C{^{1}H} NMR spectrum was recorded in d_8-toluene. Data are quoted in Table 4.14

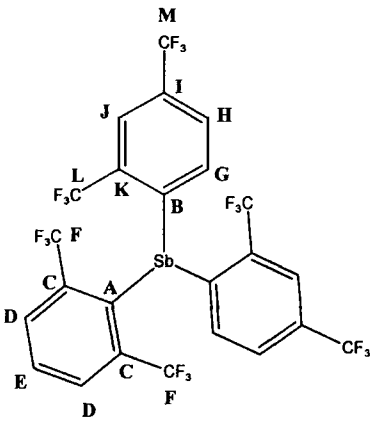

Figure 4.20: *Lettering scheme for Ar'Ar"$_2$Sb*

Carbon	δ (ppm)	J (Hz)
A	139.9	broad singlet
B	142.8	broad singlet, double intensity
C	132.1	q, $^2J_{C-F}$ 33.4
D	130.4	q, $^3J_{C-F}$ 5.9
E	139.9	s
F	124.5	q, $^1J_{C-F}$ 275.8
G	128.9	s
H	128.0	s
I	137.6	q, $^2J_{C-F}$ 31.5
J	123.1	m
K	136.7	q, $^2J_{C-F}$ 31.5
L	123.5	q, $^1J_{C-F}$ 275.8
M	124.1	q, $^1J_{C-F}$ 275.8

Table 4.14: *$\delta^{13}C$ for Ar'Ar"$_2$Sb*

- X-ray crystallography

Crystals of Ar'Ar"$_2$Sb were obtained by recrystallisation from dichloromethane. The structure was determined at 120 K by A.E. Goeta, and is shown in Figure 4.21:

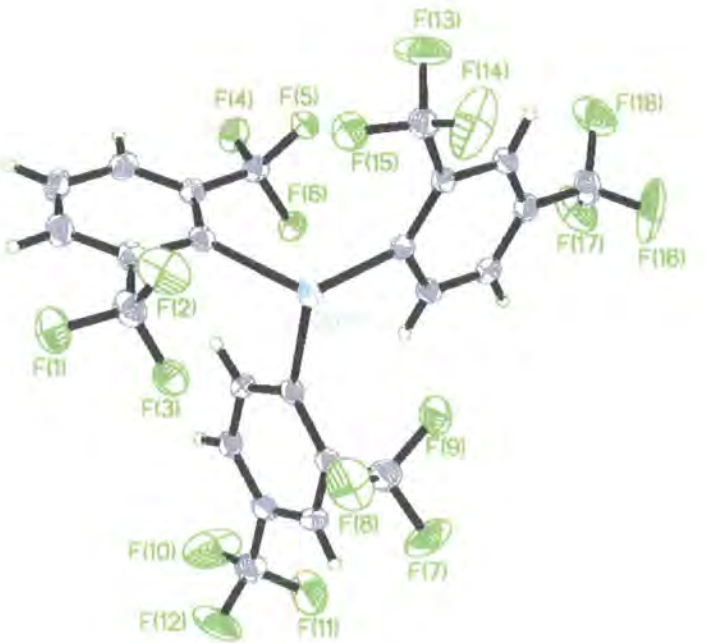

Figure 4.21: *Molecular structure of Ar'Ar"$_2$Sb*

The molecule crystallises in the monoclinic P2(1)/c space group with Z=4. The Sb atom exhibits a trigonal geometry with the C-Sb-C angles ranging from 92.46(10) to 108.31(10)°. This difference (~16°C) is probably due to the unsymmetrical character of Ar'Ar"$_2$Sb and the presence of bulky CF_3 groups in the *ortho* position. The C-Sb-C bond angles for triaryl antimony compounds described in the literature, range from 105.3° in Mes_3Sb,[50] 104.7° in (2,6-dimethylphenyl)$_3$Sb,[51] 97.3° in (*p*-tolyl)$_3$Sb,[52] 97.4° in (*o*-tolyl)$_3$Sb,[53] to 95° in Ph_3Sb.[54] Asymmetry in the bond angle was observed, which seems to occur with the Ar, Ar' or Ar" substituents. This can be explained by the presence of short Sb---F contacts between the fluorine of the CF_3 in the *ortho* position and the central Sb atom. Three intramolecular interactions are observed (Table 4.15) with an interatomic

average distance of ca. 2.94Å, which is shorter than the sum of the van der Waals radii of 3.74 Å.[41] These values are similar to those found in Ar_2SbCl.[22]

The geometry of the antimony atom (sum of the bond angles at Sb: 296.03°) is comparable to those observed in Ar_2SbCl[22] and $SbAr_2OSO_2CF_3$[22] (where the sums of the bonds angles are 296.7 and 287.8° respectively).

Two of the Sb-C (Sb(1)-C(21) 2.184(3) and Sb(1)-C(11) 2.194(3) Å) bond distances are shorter than those found in Ar_2SbCl and $SbAr_2OSO_2CF_3$.[22] This is due to smaller steric demand of the Ar" groups in comparison with the Ar substituents. The third Sb(1)-C(1) bond length is longer due to the presence of trifluoromethyl groups in the *ortho* position. The average Sb-C distances in tris(2,6-dimethylphenyl)stibine is 2.190Å [51]. Sb-C distances are longer than in Ph_3Sb (average 2.155(9) Å), probably as a result of steric interactions with the *o*-CF_3.

	Ar'Ar"$_2$Sb		Ar_2SbCl		$SbAr_2OSO_2CF_3$	
Bond distance (Å)	Sb(1)-C(21)	2.184(3)	Sb(1)-C(1)	2.22(3)	Sb(1)-C(1)	2.21(1)
	Sb(1)-C(11)	2.194(3)	Sb(1)-C(10)	2.25(3)	Sb(1)-C(10)	2.23(1)
	Sb(1)-C(1)	2.234(3)				
	Sb(1)-F(3)	2.911				
	Sb(1)-F(9)	3.024				
	Sb(1)-F(15)	2.889				
Angle (°)	C(21)-Sb(1)-C(11)	95.26(11)	C(1)-Sb(1)-Cl	101.3(9)	C(1)-Sb(1)-O	94.8(4)
	C(21)-Sb(1)-C(1)	108.31(10)	C(10)-Sb(1)-Cl	88.4(9)	C(10)-Sb(1)-O	87.7(4)
	C(11)-Sb(1)-C(1)	92.46(10)	C(1)-Sb(1)-C(10)	107.0(7)	C(1)-Sb(1)- C(10)	105.3(4)

Table 4.15: *Selected Bond distances (Å) and Angles (°) for Ar'Ar"$_2$Sb, Ar_2SbCl and $SbAr_2OSO_2CF_3$.*[22]

4.4.2 Bismuth derivatives

Several attempts have been made to react the Ar'Li/Ar"Li mixture with $BiCl_3$. The ^{19}F NMR spectrum showed the presence of different products in solution. Unfortunately, none has been separated from the mixture. It was difficult to assign any peak in the spectrum.

4.5 Discussion

4.5.1 Solution-state NMR spectroscopy

^{19}F NMR and ^{31}P NMR data for all phosphorus compounds are listed in Table 4.16.

^{19}F NMR chemical shifts are similar for all compounds containing the same Ar (or Ar' or Ar") substituents. However, a slight shielding is observed for the hydride derivatives where the shifts of the *ortho*-CF_3 groups of the Ar" moiety are –60.0 ppm in Ar"$_2$PH and –61.2 ppm in Ar'Ar"PH, being between –56.5 and –59.3 ppm for the other derivatives containing an Ar" substituent. The shielding is more noticeable in the ^{31}P NMR spectrum: 57.4 ppm for Ar"$_2$PBr and -48.7 ppm for Ar"$_2$PH.

The same shielding effect is observed in arsenic derivatives in the ^{19}F NMR data (Table 4.17). For example, the chemical shifts for the CF_3 groups in the *ortho* position are –53.5 ppm in $ArAsCl_2$ and -61.4 ppm in $ArAsH_2$. In the room temperature ^{19}F NMR spectra of all compounds containing one Ar" substituent and one Ar or Ar' substituent, a broad, unresolved resonance occurred for the two *ortho*-CF_3 groups of the Ar or Ar' moiety. Similar observations have been previously reported for Ar'Ar"PCl,[19] Ar'Ar"PF[20] and Cp*ArPCl,[55] with $^4J_{PF}$ not resolved, although interestingly a $^4J_{PF}$ value of 31.6 Hz was recorded for Cp*ArPH. These results suggest that there is a rotational barrier present in the more sterically hindered species. A detailed temperature-dependence study for some P and As derivatives, will be described in Chapter 5.

	^{19}F (δ ppm)				^{31}P (δ ppm)	
	Ar'	Ar"		Ar	^{1}H decoupled	^{1}H coupled
		ortho	*para*	*ortho* *para*		
$ArPCl_2$				-53.3 -64.2	145.6	
Ar_2PCl				-54.4 -64.1	74.9	
$Ar'PCl_2$	-53.2				148.4	
$Ar"PCl_2$		-56.5	-63.6		151.6	
Ar'Ar"PCl	-55.4	-59.3	-64.1		69.1	
$Ar"_2PCl$		-57.3	-63.7		68.3	
$ArPBr_2$				-53.1 -64.1	130.1	
$Ar'PBr_2$	-52.9				134.1	
$Ar"PBr_2$		-56.9	-62.8		141.0	
Ar'Ar"PBr	-55.2	-58.8	-63.5		58.9	
$Ar"_2PBr$		-57.7	-63.7		57.4	
$Ar"_2PH$		-60.0	-63.8		-48.7	-49.0
Ar'Ar"PH	-57.7	-61.2	-63.4		-67.2	-67.6

Table 4.16: *$\delta^{19}F$ and ^{31}P(ppm) for phosphorus compounds with Ar, Ar" and/or Ar" substituents*

	Ar'	Ar"		Ar	
		ortho	*para*	*ortho*	*para*
$ArAsCl_2$				-53.5	-64.2
Ar_2AsCl			-54.6	63.9	
$Ar'AsCl_2$	-52.9				
$Ar"AsCl_2$		-57.7	-63.7		
Ar'Ar"AsCl	-54.8	-58.8	-63.5		
$ArAsBr_2$			-53.2	63.8	
Ar_2AsBr			-54.4	-63.9	
$ArAsH_2$			-61.4	-64.2	
Ar_2AsH			-58.7	-64.2	
$Ar'AsBr_2$	-52.7				
$Ar"AsBr_2$		-58.5	-62.8		
Ar'Ar"AsBr	-54.9	-58.8	-63.5		
$Ar"_2AsBr$		-58.4	-63.6		
Ar'Ar"AsH	-58.2	-61.2	-63.8		

Table 4.17: *$\delta^{19}F$ chemicals shifts of arsenic compounds.*

4.5.2 X-ray Crystallography

Table 4.18 lists selected bond distances and angles for phosphorus compounds. The P-C bond lengths are all similar in $Ar"_2PCl$ and $Ar"_2PBr$. They are slightly longer in Ar_2PCl and $ArPBr_2$, due to the presence of two *ortho*-CF_3 groups instead of one in the $Ar"_2PX$ compounds.

A marked asymmetry in the C-P-Cl bond angles is noticed in Ar_2PCl (they differ by more than 10°), which is almost certainly due to the P---F secondary interactions. Only minor

differences in the C-P-X (X=Cl or Br) angles are apparent for the less sterically hindered compounds $Ar"_2PCl$, $Ar"_2PBr$, Ar'Ar"PCl[19] with a maximum value of ca. 4.6° in $Ar"_2PBr$.

Disorder was found for the *para*-CF_3 groups in $ArPBr_2$ and $Ar"_2PBr$. This is often observed in compounds containing these substituents, for example in Ar_2AsCl[22], Ar_2SbCl[22], Ar_2BiCl[23] and Ar_3Bi.[23]

Data for arsenic derivatives Ar'Ar"AsCl, Ar'Ar"AsBr and Ar'Ar"AsH are quoted in Table 4.19. The As-C distances are similar in all instances, ranging from 1.980(4) to 2.007(6) Å

The As-X distances are in the range of those reported in the literature for similar compounds.

Phosphorus or arsenic derivatives exhibit a pyramidal geometry around the central atom, with the sum of the bond angles ranging from 298.7 to 310.53°

$ArPBr_2$				Ar_2PCl		$Ar"_2PCl$		$Ar"_2PBr$	
P(1)-Br(1)	2.2228(8)	P(2)-Br(3)	2.2166(8)	P(1)-Cl(1)	2.0628(10)	P(1)-Cl(1)	2.0619(9)	P(1)-Br(1)	2.2340(5)
P(1)-Br(2)	2.2153(8)	P(2)-Br(4)	2.2194(8)	P(1)-C(11)	1.882(3)	P(1)-C(1)	1.854(2)	P(1)-C(1)	1.8572(18)
P(1)-C(1)	1.879(3)	P(2)-C(11)	1.887(3)	P(1)-C(21)	1.885(3)	P(1)-C(11)	1.857(2)	P(1)-C(11)	1.8591(17)
C(1)-P(1)-Br(2)	102.10(8)	C(11)-P(2)-Br(4)	102.41(8)	C(11)-P(1)-C(21)	109.87(12)	C(1)-P(1)-C(11)	100.37(10)	C(1)-P(1)-C(11)	100.51(8)
C(1)-P(1)-Br(1)	102.52(9)	C(11)-P(2)-Br(3)	103.22(8)	C(11)-P(1)-Cl(1)	103.68(9)	C(1)-P(1)-Cl(1)	97.38(7)	C(1)-P(1)-Br(1)	96.99(6)
Br(2)-P(1)-Br(1)	105.35(3)	Br(3)-P(2)-Br(4)	104.90(3)	C(21)-P(1)-Cl(1)	92.95(9)	C(11)-P(1)-Cl(1)	100.95(7)	C(11)-P(1)-Br(1)	101.63(6)

Table 4.18: *Selected Bond Distances (Å) and Angles (°) for Phosphorus Compounds*

Ar'Ar"AsCl		Ar'Ar"AsBr		Ar'Ar"AsH *	
As(1)-Cl(1)	2.2074(5)	As(1)-Br(1)	2.3530(3)	As(1)-H(11)	1.37(6)
As(1)-C(1)	1.9880(18)	As(1)-C(11)	1.9827(19)	As(1)-C(11)	1.980(5)
As(1)-C(11)	2.0182(17)	As(1)-C(21)	2.0099(19)	As(1)-C(21)	1.995(5)
C(1)-As(1)-C(11)	102.98(7)	C(11)-As(1)-C(21)	103.15(8)	C(11)-As(1)-C(21)	98.11(18)
C(1)-As(1)-Cl(1)	100.08(6)	C(11)-As(1)-Br(1)	101.43(6)	C(11)-As(1)-H(11)	102(2)
C(11)-As(1)-Cl(1)	98.84(5)	C(21)-As(1)-Br(1)	98.91(5)	C(21)-As(1)-H(11)	126(2)

Table 4.19: *Selected Bond Distances (Å) and Angles (°) for Arsenic Compounds*

* Data for As(1)

Secondary interactions between the group 15 elements and some of the fluorines of the *ortho*-CF_3 groups are found in all the compounds. This was observed previously in Ar_2AsCl, Ar_2SbCl and Ar'Ar"PCl. These short E---F contacts are given in Table 4.20. At least three such interactions are observed for six fluorines in *o*-CF_3 groups, four for nine fluorines and five for the only example studied with twelve fluorines (Ar_2PCl). The distances are shorter in all instances than the sum of the van der Waals radii. These secondary interactions play a vital role in the stabilisation of the molecule. They are also probably responsible of the large asymmetry found in the C-E-Cl angles in Ar_2ECl. Similar interactions for fluorines from *ortho*-CF_3 groups in Ar ligands have also been reported with transition metals V,[56] Cr,[18,57] and Mo.[18]

Compound	Range (Å)	No of contacts	No of fluorines	Ref.
$ArPBr_2$	P(1) 2.865-3.208	3	6	This work
		3	6	
	P(2) 2.877-3.217			
Ar_2PCl	2.843-3.111	5	12	This work
Ar'Ar"PCl	2.890-3.25	4	9	19
$Ar"_2PCl$	2.874-3.124	3	6	This work
$Ar"_2PBr$	2.887-3.122	3	6	This work
Ar_2AsCl	130(2)K 2.991-3.012	3	12	22
	296(1)K 2.935-3.110	3	12	22
Ar'Ar"AsCl	2.701-3.292	4	9	This work
Ar'Ar"AsBr	2.707-3.277	4	9	This work
Ar'Ar"AsH	As(1) 2.934-3.186	4	9	This work
	As(31) 2.859-3.326	4	9	
	As(32) 2.880-3.247	4	9	
Ar_2SbCl	2.821-3.107	4	12	22
$Ar'Ar"_2Sb$	2.911-3.024	3	12	This work

Table 4.20: *Short E-F Contacts (E=P, As or Sb)*

4.6 Experimental

4.6.1 Introduction

- NMR spectroscopy

The ^{31}P NMR spectra of phosphorus-containing starting materials were checked, to confirm the absence of any major impurities. ^{19}F NMR spectra were recorded on a Varian Mercury 200, Varian VXR 400, or Varian Inova 500 Fourier-transform spectrometer at 188.18, 376.35, and 470.26 MHz respectively. ^{31}P NMR spectra were recorded on the same instruments at 80.96, 161.91 or 202.32 MHz. ^{1}H and ^{13}C NMR spectra were recorded on the Varian VXR 400 instrument at 400 and 100.57 MHz respectively. Chemical shifts were measured relative to external $CFCl_3$ (^{19}F) or 85% H_3PO_4 (^{31}P), with the higher frequency direction taken as positive.

- X-ray crystallography

Single crystal X-ray diffraction experiments were carried out at low temperature, 100 to 120 K, using graphite monochromated Mo Kα radiation (λ = 0.71073) on a Bruker SMART (CCD 1 K area detector) diffractometer equipped with a Cryostream N_2 flow cooling device.[58] Series of narrow ω-scans (0.3°) were performed at several φ-settings in such a way as to cover a sphere of data to a maximum resolution between 0.70 and 0.77 Å. Cell parameters were determined and refined using the SMART software,[59] and raw frame data were integrated using the SAINT program.[60] The structures were solved by direct methods and refined by full-matrix least squares on F^2 using SHELXTL software.[61]

The reflection intensities were corrected by numerical integration based on measurements and indexing of the crystal faces for Ar"$_2$PBr and Ar'Ar"AsCl (using SHELXTL software).[61]For the remaining structures, the absorption corrections were carried out by the multi-scan method, based on multiple scans of identical and Laue equivalent reflections (using the SADABS software).[62]

Non-hydrogen atoms were refined anisotropically, except in some cases where there was disorder (see Results and Discussion). For structures $ArPBr_2$, $Ar"_2PCl$ and Ar'Ar"AsCl the hydrogen atoms were found in difference Fourier maps and in the case of $ArPBr_2$ constrained accordingly. For structures Ar_2PCl, $Ar"_2PCl$ and Ar'Ar"AsBr, the hydrogen atoms were positioned geometrically and refined using a riding model. In the special case of Ar'Ar''AsH, the hydrogen atoms were found in the Fourier difference map, one constrained and the other allowed to refine freely. The remaining hydrogen atoms were positioned geometrically and refined using a riding model

4.6.2 **Synthesis of $ArPCl_2$**

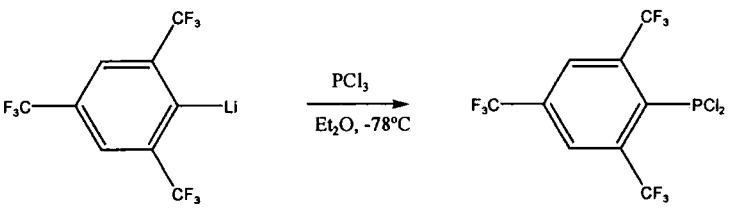

An ArLi (150 ml, 80 mmol) solution in diethyl ether was added dropwise over 20 minutes to a PCl_3 (7 ml, 80 mmol) solution in diethyl ether at -78°C. A precipitate of LiCl formed. The solution was allowed to warm to room temperature and stirred for 5 hours. The solution was filtered and the solvents and excess PCl_3 were removed under vacuum, leaving a yellow oil, which was distilled under reduced pressure (0.02 Torr) giving a colourless solution (Bp 60°C).

^{31}P NMR ($CDCl_3$): δ 145.6 (septet, $^4J_{P-F}$ 61.3 Hz) ppm; **^{19}F NMR** ($CDCl_3$): δ -53.3 (d, $^4J_{P-F}$ 61.3 Hz, 6F, *o*-CF_3), -64.2 (s, 3F, *p*-CF_3) ppm.

4.6.3 Synthesis of Ar_2PCl

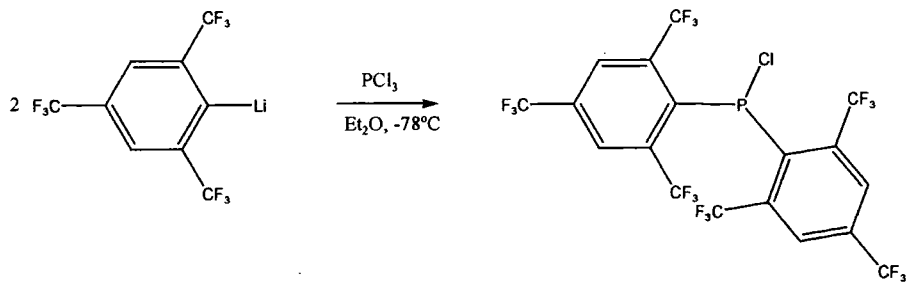

A solution of ArLi (100 ml, 48 mmol) was added dropwise to a solution of PCl_3 (2.09 ml, 24 mmol) in diethyl ether at -78°C. The solution was allowed to warm to room temperature and stirred for 2 hours. A white precipitate of LiCl appeared. The solution was filtered and the solvents and excess PCl_3 were removed under vacuum, leaving a yellow oil, which was distilled under reduced pressure (0.01 Torr). Fractions were collected at 60°C ($ArPCl_2$) and 100°C (Ar_2PCl). Crystals were grown by recrystallisation from dichloromethane.

Elemental Analysis for $C_{18}H_4ClF_{18}P$ (628.5), Calc: C 34.36, H 0.60 %, Found C 34.1, H 0.60 %.

^{31}P NMR ($CDCl_3$): δ74.9 (multiplet, $^4J_{P\text{-}F}$ 41.9Hz) ppm; **^{19}F NMR** ($CDCl_3$): δ-54.4 (d, $^4J_{P\text{-}F}$41.2Hz, 12F, *o*-CF_3), δ-64.1 (s, 6F, *p*-CF_3) ppm.

4.6.4 Synthesis of $ArPBr_2$

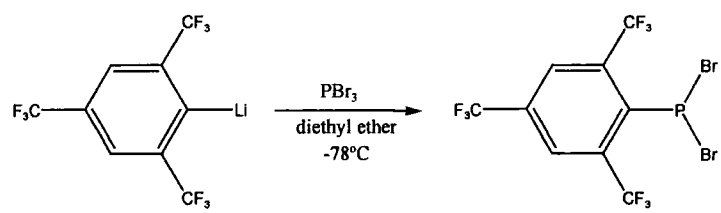

A solution of ArLi (100ml, 48 mmol) was added to a PBr_3 (2.25 ml, 24 mmol) solution in diethyl ether (100 ml) at –78°C. The solution was allowed to warm to room temperature and stirred for 2 hours. A white precipitate of LiBr appeared. The solution was filtered

and the solvents and excess PBr_3 were removed in vacuo, leaving an orange oil. This oil was distilled under reduced pressure (0.03 Torr), giving colourless crystals. Yield (based on ArH): 4.80g (20.3%).

Elemental Analysis for $C_9H_2Br_2F_9P$ (472), Calc: C 22.88, H 0.4 %; Found: C 22.76, H 0.45%.

^{31}P NMR ($CDCl_3$): δ130.1 (septet, $^4J_{P-F}$ 62.3Hz) ppm; **^{19}F NMR** ($CDCl_3$): δ-53.1 (doublet, $^4J_{P-F}$62.4Hz, 6F, *o*-CF_3), δ–64.1 (s, 3F, *p*-CF_3) ppm.

4.6.5 Synthesis of Ar'PCl_2/Ar"PCl_2

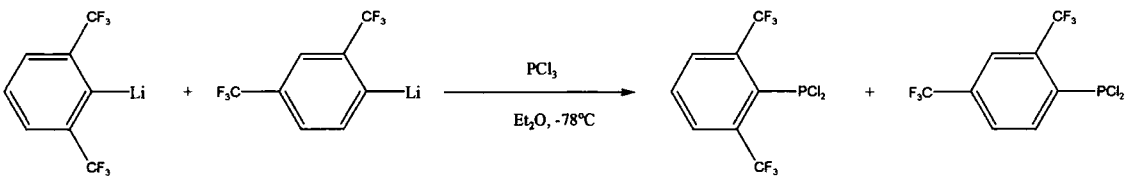

The Ar'Li/Ar"Li (96 mmol) solution was added dropwise over 20 min to a solution of PCl_3 (25.2g, 16 ml, 96 mmol) in diethyl ether (100 ml) at -78 °C. This solution was allowed to warm to room temperature and stirred for 4 hours. A white solid of LiCl appeared. The solution was filtered and solvent and PCl_3 in excess were removed in vacuo giving a brown oil. The product was purified by distillation under vacuum (Bp 86°C, 0.01 Torr). Yield (based on Ar'H): 15.7g (52.1%).

^{31}P NMR ($CDCl_3$): Ar'PCl_2 δ148.4 ppm (septet, $^4J_{P-F}$ 61.3), Ar"PCl_2 δ151.6 (q,$^4J_{P-F}$83.8); **^{19}F NMR** ($CDCl_3$) Ar'PCl_2 δ-53.2 (d,$^4J_{P-F}$ 61.3, 6F, *o*-CF_3), Ar"PCl_2:, δ-56.5 (d, $^4J_{P-F}$ 83.8, 3F, *o*-CF_3), δ-63.6 (singlet, 3F, *p*-CF_3).

4.6.6 Synthesis of Ar"$_2$PCl

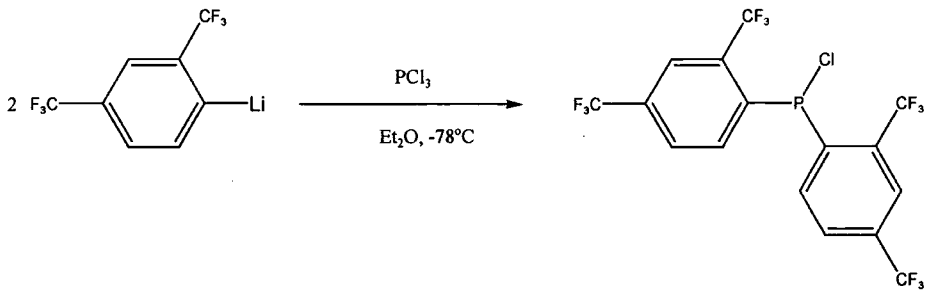

A solution of Ar'Li/Ar"Li (100 ml, 162 mmol) in diethyl ether was added dropwise over 20 min to a solution of PCl_3 (25.2g, 16 ml, 96 mmol) in diethyl ether (100 ml) at -78 °C. This solution was allowed to warm to room temperature and stirred for 4 hours. A white precipitate of LiCl appeared. The solution was filtered through a fine sinter, and solvent and PCl_3 in excess were removed in vacuo, giving a brown oil. The product was purified by distillation under vacuum (0.02 Torr), and two different fractions were collected at 86°C (Ar'PCl_2/Ar"PCl_2) and 140°C (Ar"$_2$PCl). Crystals were grown in hexanes. Yield (based on Ar'H) 11.68g (25%).

Elemental Analysis for $C_{16}H_6ClF_{12}P$ (492.5), Calc: C 38.97, H 1.22%; Found: C 38.96, H 1.35%.

^{31}P NMR ($CDCl_3$): δ68.3 (septet, $^4J_{P\text{-}F}$ 65.5Hz) ppm; **^{19}F NMR** ($CDCl_3$): δ-57.3 (d, $^4J_{P\text{-}F}$ 65.8Hz, 6F, o-CF_3), -63.7 (s, 6F, p-CF_3) ppm; **^{13}C NMR** (C_7D_8): δ140.3 (d, $^1J_{P\text{-}C}$ 56.8Hz), 133.1 (q, $^2J_{F\text{-}C}$ 33.9Hz), 133.1 (q, $^2J_{F\text{-}C}$ 33.9Hz), 129.1 (s), 123.7 (broad singlet), 123.6 (d, $^2J_{P\text{-}C}$ 1.9Hz), 123.6 (q, $^1J_{C\text{-}F}$ 275.8Hz), 123.4 (qd, $^1J_{P\text{-}C}$ 273.1Hz, $^3J_{C\text{-}F}$ 1.74Hz) ppm.

4.6.7 Synthesis of Ar'PBr_2/Ar"PBr_2, and Ar"$_2$PBr/Ar'Ar"PBr

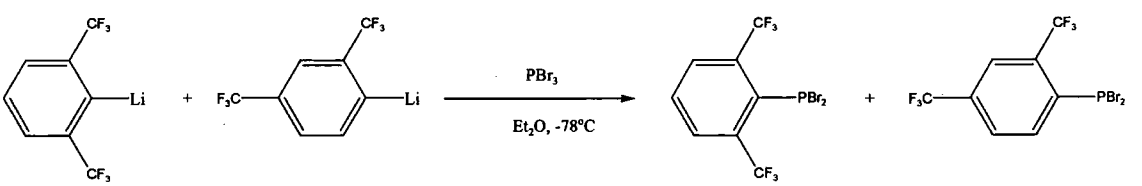

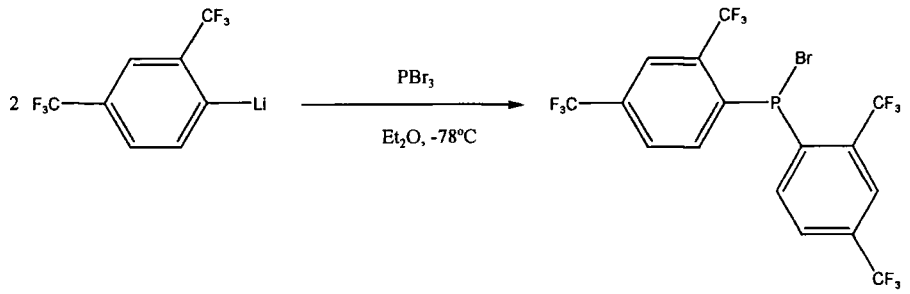

A solution of Ar'Li/Ar"Li (100 ml) was added slowly to a PBr_3 (8 ml, 85 mmol) solution in diethyl ether (100 ml) at -78°C. The solution was allowed to warm to room temperature and stirred for 5 hours. A white precipitate of LiBr appeared. The solution was filtered and the solvents and excess PBr_3 were removed in vacuo, leaving a brown oil. This oil was distilled under reduced pressure (0.01 Torr), and fractions were collected at 60°C (Ar'PBr_2/Ar"PBr_2) and 120°C (Ar"$_2$PBr/ Ar'Ar"PBr). Yield of Ar"$_2$PBr :(based on Ar'H): 4.52g (9%). It proved possible to isolate Ar"$_2$PBr but not Ar'Ar"PBr.

Elemental Analysis for $C_{16}H_6BrF_{12}P$ (537), Calc: C 35.78, H 1.13 %; Found: C 35.69, H 1.15%.

^{31}P NMR ($CDCl_3$): Ar'PBr_2: δ134.1 (septet, $^4J_{P-F}$ 62.8Hz) ppm; Ar"PBr_2: δ 141.0 (q, $^4J_{P-F}$ 85.5Hz); Ar"$_2$PBr: δ57.4 (septet, $^4J_{P-F}$ 65.8Hz) ppm; Ar'Ar"PBr: δ 58.9 ppm (m) ppm; **^{19}F NMR** ($CDCl_3$): Ar'PBr_2: δ -52.9 (d, $^4J_{P-F}$ 62.8Hz, 6F, *o*-CF_3) ppm; Ar"PBr_2: δ –56.9 (d, $^4J_{P-F}$ 85.8Hz, 3F, *o*-CF_3), -62.8 (s, 3F, *p*-CF_3); Ar"$_2$PBr: . δ-57.7 (d, $^4J_{P-F}$ 65.8Hz, 6F,*o*-CF_3), δ-63.7 (s, 6F, *p*-CF_3) ppm; Ar'Ar"PBr: δ -55.2 (broad singlet, 6F, *o*-CF_3 in Ar'), -58.8 (d, $^4J_{P-F}$ 56.6Hz, 3F, *o*-CF_3 in Ar"), -63.5 (s, 3F, *p*-CF_3) ppm.

4.6.8 Synthesis of Ar"$_2$PH

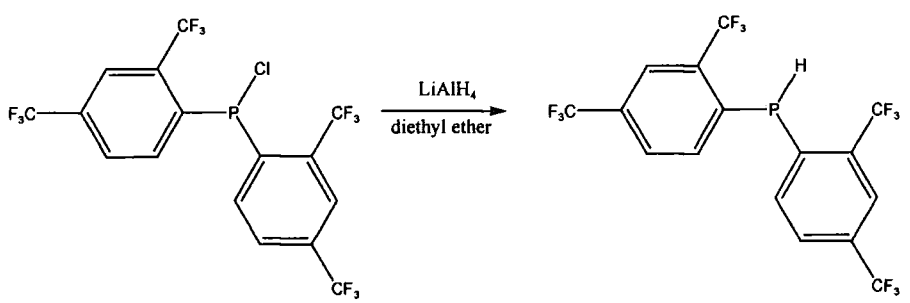

$LiAlH_4$ (0.57 ml, 0.57 mmol) was added dropwise to a solution of $Ar"_2PCl$ (0.56g, 1.13 mmol) in diethyl ether. The solution was stirred overnight. A white precipitate of LiCl appeared. The solution was filtered and solvents were removed under vacuum, leaving a yellow solid, which was washed twice with hexanes. Yield: 0.46g (89%).

Elemental Analysis for $C_{16}H_7F_{12}P$ (458): Cal C 41.92, H 1.52%; Found C 41.90, H 1.51%.

$^{31}P\{^1H\}$ NMR ($CDCl_3$): δ -48.7 (septet, $^4J_{P-F}$ 36.7 Hz) ppm; **^{31}P (^1H coupled)** ($CDCl_3$): δ -49.0 (d of septet, $^4J_{P-F}$ 36.8 Hz, $^1J_{P-H}$ 270.4 Hz) ppm; **^{19}F NMR** ($CDCl_3$): δ -60.0 (d, $^4J_{P-F}$ 37.1 Hz, 6F, *o*-CF_3), -63.8 (s, 6F, *p*-CF_3) ppm; **^1H NMR** ($CDCl_3$): δ 7.9 (s, Ha), 7.7 (d, $^3J_{H-H}$ 7.8 Hz, Hb), 7.4 (d, $^3J_{H-H}$ 7.9 Hz, Hc), 6.2 (d, $^1J_{P-H}$ 274.5) ppm.

4.6.9 Synthesis of Ar'Ar"PH

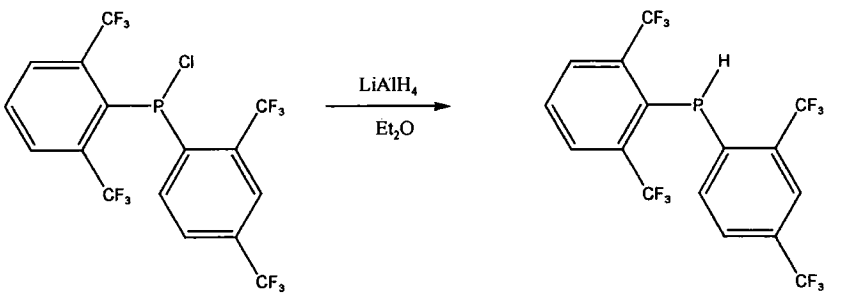

$LiAlH_4$ (0.09 ml, 1.0M in ether, 0.09 mmol) was added to an Ar'Ar"PCl (0.08g, 0.18mmol) solution in diethyl ether (5ml). The solution was stirred for one day. A white precipitate of LiCl appeared; the solution was then filtered and solvents were removed under vacuum, leaving a white solid, which was washed three times with diethyl ether. Yield 0.05g (60%).

Elemental analysis for $C_{16}H_7PF_{12}$ (458.2), Calc C 41.90, H 1.54%; Found C 39.95, H 2.12%.

^{19}F NMR ($CDCl_3$): δ –57.7 (broad singlet, 6F, *o*-CF_3 in Ar'), -61.2 (d, $^4J_{P-F}$ 43.7Hz, 3F, *o*-CF_3 in Ar"), -63.4 (s, 3F, *p*-CF_3) ppm; **$^{31}P\{^1H\}$ NMR** (C_7D_8): δ-67.2 (multiplet);

$^{31}P(^{1}H$ coupled) NMR (C_7D_8): δ-67.6 (d of multiplets, $^{1}J_{P-H}$ 240.7Hz); **^{1}H NMR** (C_7D_8): δ 7.5-6.2 (aromatic region), 5.7 (d, $^{1}J_{P-H}$ 240.4Hz, P-H) ppm.

4.6.10 Attempted synthesis of Ar"$_2$PF

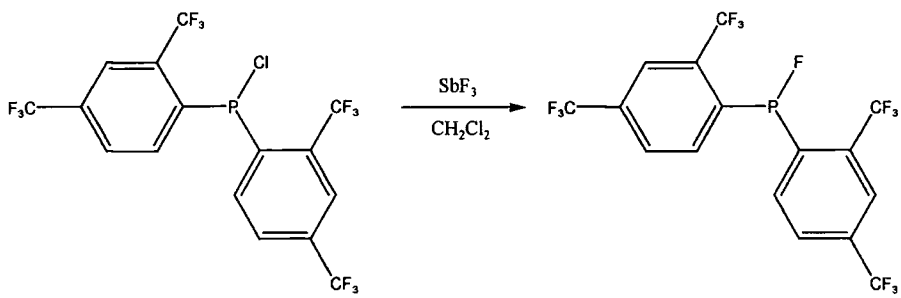

SbF_3 (0.35g, 1.9 mmol) was added to a solution of Ar"$_2$PCl (0.78g, 1.5 mmol) in CH_2Cl_2. The mixture was stirred for a few days and then refluxed for two weeks. No change was observed in the ^{19}F and ^{31}P NMR spectra.

4.6.11 Attempted synthesis of Ar'Ar"PF

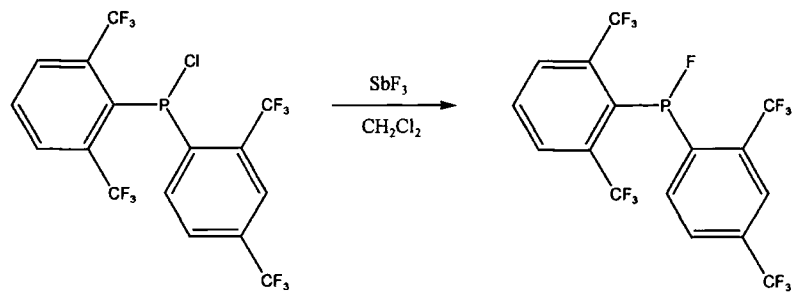

SbF_3 (0.27g, 1.5 mmol) was added to a solution of Ar'Ar"PCl (0.52g, 1.04 mmol) in dichloromethane. The solution was stirred at room temperature for a few days and then refluxed for a week. No change was observed in the ^{19}F and ^{31}P NMR spectra.

4.6.12 Synthesis of ArAr'PCl/ArAr"PCl

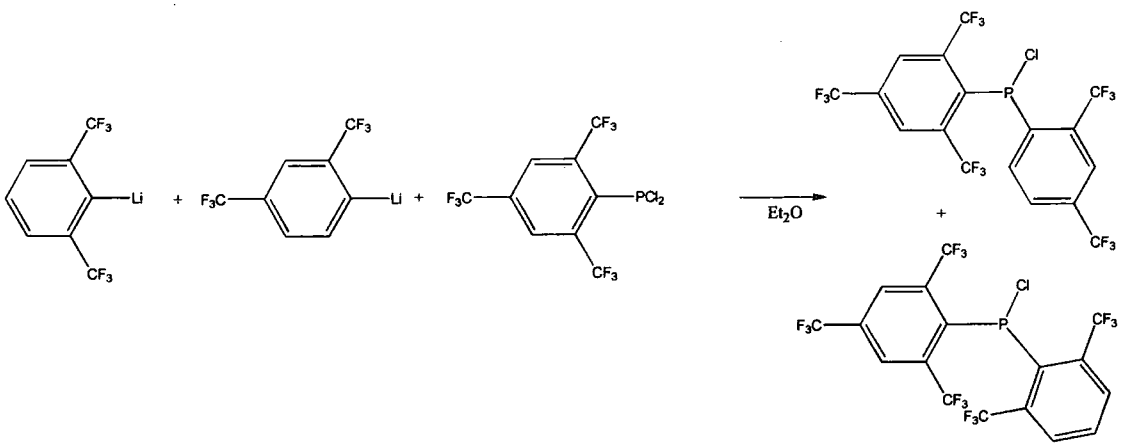

A solution of Ar'Li/Ar"Li (20 ml, 6.6 mmol) was added dropwise to a solution of $ArPCl_2$ (2.52g, 6.6mmol) in diethyl ether. A precipitate of LiCl immediately formed. The solution was filtered and distilled under reduced pressure (0.01 Torr), giving a yellow oil, (Bp110°C).

^{19}F NMR ($CDCl_3$): ArAr'PCl: δ -54.1 (d, $^4J_{P-F}$ 42.1Hz, 6F, *o*-CF_3), -54.3 (d, $^4J_{P-F}$ 42.1Hz, 6F, *o*-CF_3), -64 (s, 3F, *p*-CF_3) ppm; ArAr"PCl: δ-55.5 (broad singlet, 6F, *o*-CF_3 in Ar), -58.6 (d,$^4J_{P-F}$ 58.3Hz, 3F, *o*-CF_3 in Ar"), -63.6 (s, 3F, *p*-CF_3), -64.1 (s, 3F, *p*-CF_3) ppm; **^{31}P NMR** ($CDCl_3$): ArAr'PCl : δ76.6 (m) ppm; ArAr"PCl δ69.9 (m) ppm.

4.6.13 Synthesis of $ArAsCl_2$/Ar_2AsCl

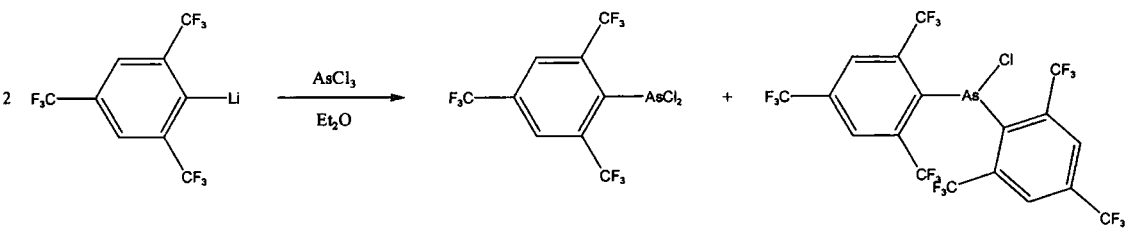

A diethyl ether solution of ArLi (100 ml, 35 mmol) was added dropwise to an $AsCl_3$ (6.45g, 3 ml, 35 mmol) solution in diethyl ether (50 ml) at -78°C. The solution was left to warm to room temperature and stirred for four hours. A white precipitate of LiCl

appeared. The solution was filtered and solvent and excess $AsCl_3$ were removed under vacuum, leaving a yellow solution and a white solid. The solution was filtered and distilled under reduced pressure (0.02 Torr), giving a yellow oil of $ArAsCl_2$, Bp 60°C. The white solid was washed twice with diethyl ether and dried under vacuum (Ar_2AsCl). The solid was purified by recrystallisation from dichloromethane. Yield: $ArAsCl_2$: 5.2g (34.8%); Ar_2AsCl: 4.8g (20.4%).

Elemental analysis for $C_{18}F_{18}H_4AsCl$ (612.4), Calc C 32.14, H 0.60%; Found C 32.19, H 0.62%.

^{19}F NMR ($CDCl_3$): $ArAsCl_2$: δ -53.5 (s, 6F, *o*-CF_3), -64.2 (s, 3F, *p*-CF_3) ppm; Ar_2AsCl: δ –54.6 (s, 12F, *o*-CF_3), -63.9 (s, 6F, *p*-CF_3) ppm.

4.6.14 Synthesis of $ArAsH_2$

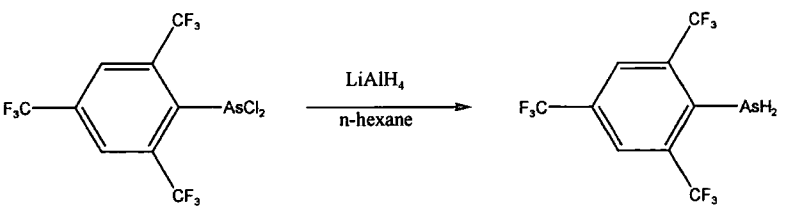

$LiAlH_4$ (1M in Et_2O, 1.08 ml, 1.08 mmol) was added dropwise to a solution of $ArAsCl_2$ (0.93g, 2.16 mmol) at room temperature. The solution was stirred for a few days. Solvents were removed under vacuum, giving a yellow oil.

^{19}F NMR ($CDCl_3$): δ-61.4 (t, $^5J_{F\text{-}H}$ 6.4 Hz, 6F, *o*-CF_3), -64.2 (s, 3F, *p*-CF_3) ppm.

4.6.15 Synthesis of $ArAsBr_2$/Ar_2AsBr

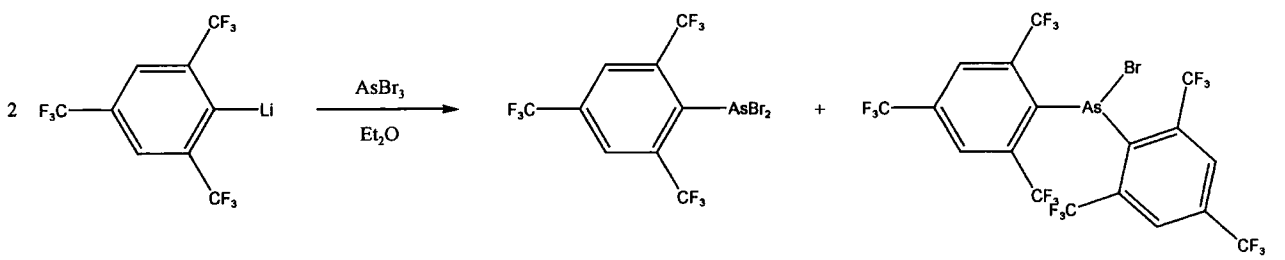

A diethyl ether solution of ArLi (10 mmol, 50 ml) was added dropwise to an $AsBr_3$ (1.36g, 5 mmol) solution in diethyl ether (50 ml) at -78°C. The solution was left to warm to room temperature and stirred for four hours. A white precipitate of LiBr appeared. The solution was filtered and solvent and excess $AsBr_3$ were removed under vacuum, leaving a brown solution. The solution was distilled under reduced pressure (0.02 Torr), giving a yellow oil. Fractions were collected at 120°C ($ArAsBr_2$) and 150°C (Ar_2AsBr).

^{19}F NMR ($CDCl_3$): $\underline{ArAsBr_2}$: δ -53.2 (s, 6F, *o*-CF_3), -63.8 (s, 6F, CF_3) ppm; $\underline{Ar_2AsBr}$: δ -54.4 (s, 12F, *o*-CF_3), -63.9 (s, 6F, *p*-CF_3) ppm.

4.6.16 Synthesis of Ar_2AsH

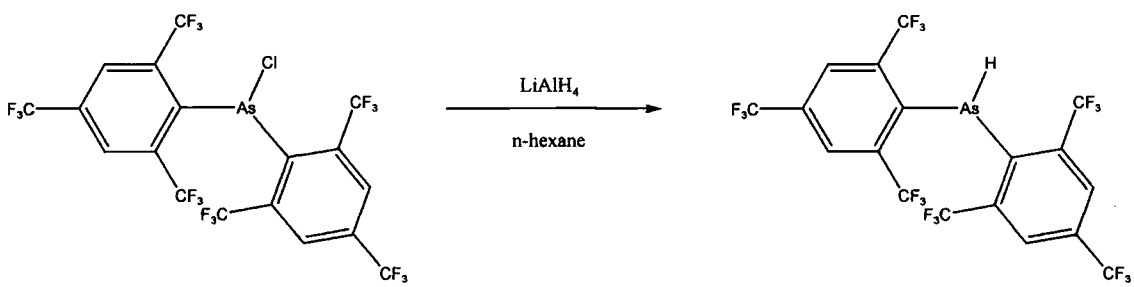

$LiAlH_4$ (1M in Et_2O, 3.1 ml, 3.13 mmol) was added dropwise to a solution of Ar_2AsCl (0.42g, 0.27 mmol) at room temperature. The solution was refluxed for two days. Solvents were removed under vacuum, giving a colourless oil.

^{19}F NMR ($CDCl_3$): δ-58.7 (d, $^5J_{F\text{-}H}$ 3.6 Hz, 12F, *o*-CF_3), -64.2 (s, 6F, *p*-CF_3) ppm; **^{1}H NMR** ($CDCl_3$): δ-6.4 (broad singlet, As-H) ppm.

4.6.17 Synthesis of Ar'$AsCl_2$/Ar"$AsCl_2$/Ar'Ar"AsCl

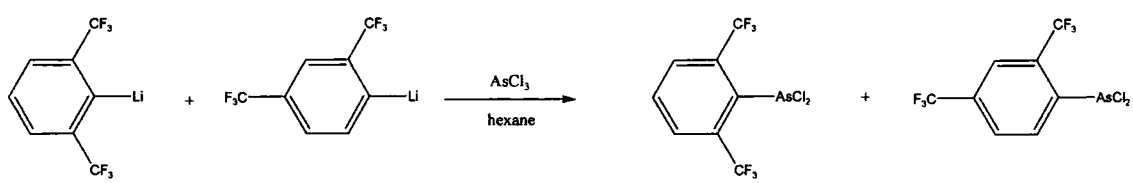

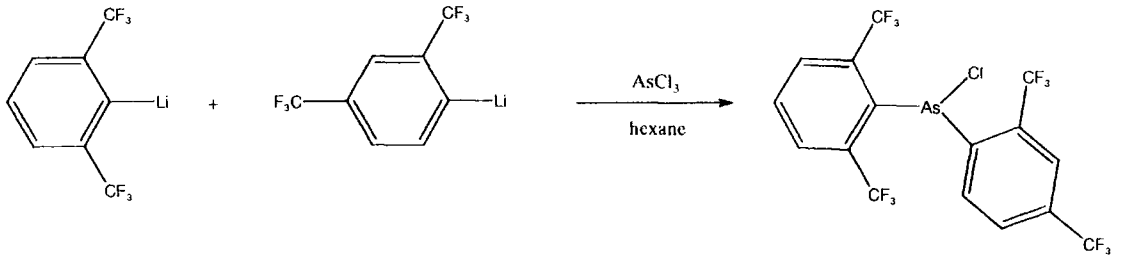

A solution of Ar'Li/Ar"Li (100 ml, 94 mmol) in diethyl ether was added dropwise to a solution of $AsCl_3$ (13.5 ml, 160 mmol) in hexanes (100 ml) over a period of 20 minutes at -78°C. The mixture was allowed to warm to room temperature and stirred for four hours. A precipitate of LiCl formed. This was filtered off and the solvents and excess $AsCl_3$ removed in vacuo, leaving a brown oil. . This oil was distilled under reduced pressure (0.01 Torr), and three different fractions were collected at 100°C (Ar'$AsCl_2$), 115°C (Ar"$AsCl_2$) and 145°C (Ar'Ar"AsCl). Ar'Ar"AsCl was purified by recrystallisation from hexanes. Yield (based on Ar'H): 4.5g (9%)

Elemental analysis for $C_{16}H_6AsClF_{12}$ (536.4), Calc C 35.79, H 1.12%; Found C 35.33, H 1.10%

^{19}F NMR ($CDCl_3$): Ar'$AsCl_2$: δ –52.9 (s, 6F, *o*-CF_3) ppm; Ar"$AsCl_2$: δ –57.7 (s, 3F, *o*-CF_3), -63.7 (s, 3F, *p*-CF_3), Ar'Ar"AsCl: -54.8 (broad singlet, 6F, *o*-CF_3 in Ar'), -58.8 (s, 3F, *o*-CF_3 in Ar"), -63.5 (s, 3F, *p*-CF_3) ppm; **^{1}H NMR** ($CDCl_3$): Ar'Ar"AsCl: 8.1 (d, $^3J_{H\text{-}H}$ 8Hz), 7.7 (s), 7.28 (d, $^3J_{H\text{-}H}$ 8Hz), 7.26 (d, $^3J_{H\text{-}H}$ 7.6Hz), 6.6 (t, $^3J_{H\text{-}H}$ 7.6Hz) ppm.

4.6.18 Synthesis of Ar'$AsBr_2$/Ar"$AsBr_2$, Ar"$_2$AsBr and Ar'Ar"AsBr

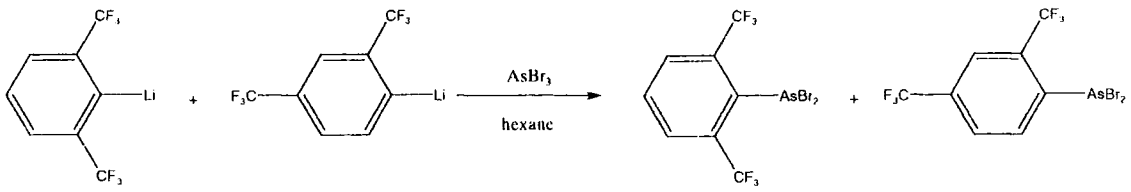

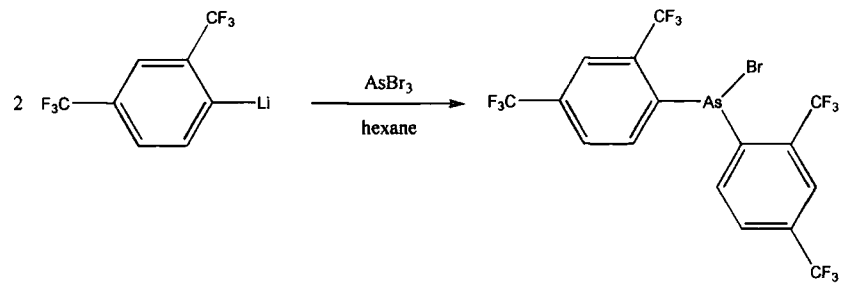

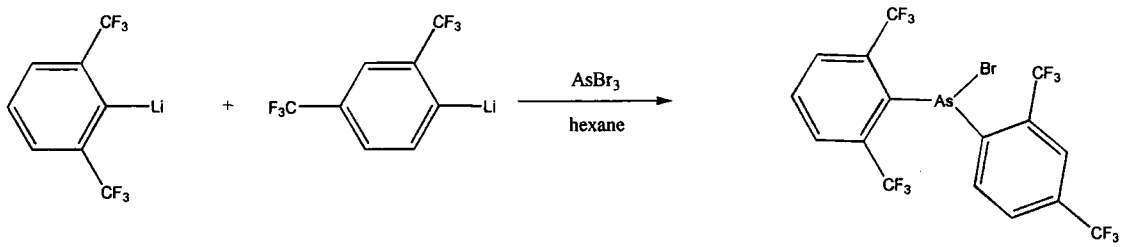

A solution of Ar'Li/Ar"Li (50 ml, 19 mmol) in diethyl ether was added dropwise to a solution of $AsBr_3$ (3.2 g, 10 mmol) in hexanes (25 ml) over a period of 20 minutes at room temperature. The mixture was allowed to warm to room temperature and stirred for four hours. Solvents and excess $AsBr_3$ were removed in vacuo, leaving a brown oil Solvents were removed under vacuum, leaving a brown oil which was distilled under reduced pressure (0.01 Torr). Fractions were collected at 81°C (Ar'$AsBr_2$/Ar"$AsBr_2$) and 110°C (Ar'Ar"AsBr/Ar"$_2$AsBr). Yield for Ar'$AsBr_2$/Ar"$AsBr_2$ 3.8g (42%)

The Ar'Ar"AsBr/Ar"$_2$AsBr mixture was dissolved in hexanes and left in the freezer. After one month colourless crystals of Ar'Ar"AsBr appeared. Yield for Ar'Ar"AsBr 0.98g (31%).

Elemental analysis for $C_{16}H_6AsBrF_{12}$ (581.03), Calc C 33.08, H 1.04%; Found C 33.46, H 1.04% Yield 3.8g (42%)

^{19}F NMR ($CDCl_3$): Ar'$AsBr_2$: δ-52.7 (s, 6F, *o*-CF_3); Ar"$AsBr_2$: δ-58.5 (s, 3F, *o*-CF_3), -62.8 (s, 3F, *p*-CF_3) ppm; Ar'Ar"AsBr: δ -54.9 (broad singlet, 6F, *o*-CF_3 in Ar'), -58.8 (s, 3F, *o*-CF_3 in Ar"), δ -63.5 (s, 3F, *p*-CF_3) ppm; Ar"$_2$AsBr: δ -58.4 (s, 6F, *o*-CF_3), -63.6 (s, 6F, *p*-CF_3) ppm .

4.6.19 Synthesis of Ar'Ar"AsH

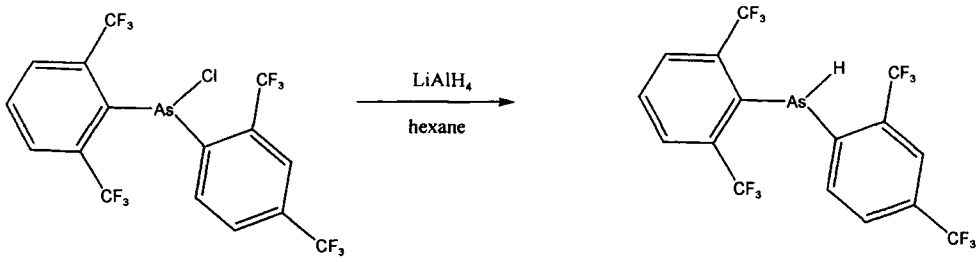

$LiAlH_4$ (0.2 ml, 1M in ether, 0.2 mmol) was slowly added at 0°C to an Ar'Ar"AsCl (0.2g, 0.4 mmol) solution in hexanes. The solution was left to warm to room temperature and stirred for four days. Solvents were removed in vacuo, and the resulting white solid washed three times with hexanes (3*2mL). Crystals were grown by sublimation under vacuum. Yield 0.15g (71%).

Elemental analysis for $C_{16}H_7AsF_{12}$ (502.1), Calc C 38.27, H 1.41%; Found C 37.98, H 2.03%

^{19}F NMR (C_7D_8): δ –58.2 (d, $^5J_{F-H}$ 7.1 Hz, 6F, *o*-CF_3 in Ar'), -61.2 (s, 3F, *o*-CF_3 in Ar"), -63.8 (s, 3F, *p*-CF_3) ppm; **^{1}H NMR** (C_7D_8): δ8.06 (d, $^3J_{H-H}$ 8Hz), 7.9 (s), 7.7 (t, $^3J_{H-H}$ 8Hz), 7.4 (d, $^3J_{H-H}$ 8Hz), 6.9 (t, $^3J_{H-H}$ 7.6Hz), 5.99 (broad singlet, As-H) ppm.

4.6.20 Synthesis of Ar'$SbCl_2$/Ar"$SbCl_2$/Ar'$_2$SbCl/Ar"$_2$SbCl/Ar'Ar"$_2$Sb

$$2\ Ar'Li + 2\ Ar''Li \xrightarrow[hexane/Et_2O]{SbCl_3} Ar'SbCl_2 + Ar''SbCl_2 + Ar'_2SbCl + Ar''_2SbCl + Ar'Ar''_2Sb$$

A solution of Ar'Li/Ar"Li (100 ml, 127 mmol) was added slowly to a $SbCl_3$ solution in hexanes/Et_2O at room temperature. A precipitate of LiCl formed. The solution was stirred for 5 hours. The solution was filtered and the solvents and excess $SbCl_3$ were removed under vacuum, leaving a brown oil, which was distilled under reduced pressure (0.02 Torr): fractions were collected at 95°C (orange oil, Ar'$SbCl_2$/Ar"$SbCl_2$), and 120°C (yellow sticky oil). The latter yellow oil was dissolved in hexanes and left in the freezer

overnight. A white solid formed, which was filtered off and washed twice with CH_2Cl_2 (Ar'_2SbCl/Ar''_2SbCl). Solvents were removed from the filtered yellow solution leaving a sticky solid, which was recrystallised, from dichloromethane giving white crystals of $Ar'Ar''_2Sb$.

Elemental analysis for $C_{24}H_9F_{18}Sb$ (761.06), Calc C 37.88, H 1.19%; Found C 37.72, H 1.19%.

^{19}F NMR ($CDCl_3$): $Ar'SbCl_2$: δ -53.2 (s, 6F, *o*-CF_3) ppm; $Ar''SbCl_2$: δ-54.9 (s, 3F, *o*-CF_3), -63.6 (s, 3F, p-CF_3) ppm; Ar'_2SbCl: δ -55.1 (s, 12F, *o*-CF_3) ppm; Ar''_2SbCl: δ -58.4 (s, 6F, *o*-CF_3), -63.7 (s, 6F, *p*-CF_3) ppm; $Ar'Ar''_2Sb$: δ -55.5 (s, 6F, *o*-CF_3 in Ar'), -58.4 (s, 6F, *o*-CF_3 in Ar''), -63.6 (s, 6F, *p*-CF_3) ppm.

4.6.26 Attempted reaction between Ar'Li/Ar''Li and $BiCl_3$

A solution of Ar'Li/Ar''Li (50 ml, 30 mmol) was added slowly to a $BiCl_3$ (4.922g, 15.6 mmol) solution in Et_2O at room temperature. A precipitate of LiCl formed. The solution was stirred for overnight. The solution was filtered and the solvents and excess $SbCl_3$ were removed under vacuum, leaving a beige solid. Attempt was made to dissolve this solid in CDCl3 but the material was only partially soluble, and no peaks could be assigned in the 19F NMR spectrum. The mixture was not further investigated.

References

1 M. Yoshifuji, I. Shima, N. Inamoto, K. Hirutsu, T. Higushi, *J. Am. Chem. Soc.*, **1981**, *103*, 4587.

2 G. Becker, G. Gresser, W. Uhl, *Z. Naturforsch,* **1981**, *36b*, 16.

3 J. F. Nixon, *Coord. Chem. Rev.*, **1995**, *145*, 201.

4 J. F. Nixon, *Chem. Rev.*, **1988**, *88*, 1327.

5 M. Regitz, *Chem. Rev.*, **1990**, *90*, 191.

6 L. Weber, *Chem. Rev.*, **1992**, *92*, 1839.

7 L. Weber, *Angew. Chem., Int. Ed. Engl.*, **1996**, *35*, 271.

8 A. C. Gaumont, J. M. Denis, *Chem. Rev.*, **1994**, *94*, 1413.

9 K. B. Dillon, F. Mathey, J. F. Nixon, *Phosphorus: The Carbon Copy*; Wiley, Chichester, **1998**.

10 M. Regitz, O. J. Scherer, *Multiple Bonds and Low Coordination in Phosphorus Chemistry*; Thieme, Stuttgart, **1990.**

11 L. Weber, *Chem. Ber.*, **1996**, *129*, 367.

12 C. Jones, *Coord. Chem. Rev.*, **2001**, *215*, 151.

13 H. P. Goodwin, *Ph. D Thesis*, Durham, **1990**.

14 K. B. Dillon, H. P. Goodwin, T. A. Straw, R. D. Chambers, Euchem Conference, *Phosphorus, Silicon, Boron, and Related Elements in Low Coordination States,* Paris-Palaiseau, **1988**.

15 M. Scholz, H. W. Roesky, D. Stalke, K. Keller, F. T. Edelmann, *J. Organomet. Chem.*, **1989**, *366*, 73.

16 M. G. Davidson, K. B. Dillon, J. A. K. Howard, L. J. Sequeira, J. W. Yao, *J. Organomet. Chem.*, **1998**, *550*, 481.

17 J. Escudié, C. Couret, H. Ranaivonjatovo, M. Lazraq, J. Satgé, *Phosphorus and Sulfur,* **1987**, *31*, 27.

18 A. S. Batsanov, K. B. Dillon, V. C. Gibson, J. A. K. Howard, L. J. Sequeira, J. W. Yao, *J. Organomet. Chem.*, **2001**, *631*, 181.

19 A. S. Batsanov, S. M. Cornet, L. A. Crowe, K.B.Dillon, R. K. Harris, P. Hazendonk, M. D. Roden, *Eur. J. Inorg. Chem,* **2001**, 1729.

20 L. Heuer, P. G. Jones, R. Schmutzler, *J. Fluorine Chem.*, **1990**, *46*, 243.

21 M. D. Roden, *Ph . D Thesis*, Durham, **1998**.

22 N. Burford, C. L. B. MacDonald, D. J. Leblanc, J. S. Cameron, *Organometallics,* **2000**, *19*, 152.

23 K. H. Whitemire, H. W. Roesky, S. Brooker, G. M. Sheldrick, *J. Organomet. Chem.*, **1991**, *402*, C4.

24 R. Peitschnig, J. Ebel, N. Zoche, M. Jansen, E. Niecke, *Bull. Soc. Chim. Fr.*, **1997**, *134*, 1039.

25 A. Schmidpeter, H. Nöth, G. Jochem, H.-P. Schrödel, K. Karaghiosoff, *Chem. Ber.*, **1995**, *128*, 379.

26 Y. Ehleiter, G. Wolmershäuser, H. Sitzmann, R. Boese, *Z. Anorg. Allgem. Chem.*, **1996**, *622*, 923.

27 N. Burford, A. I. Dipchand, B. W. Royan, P. S. White, *Inorg. Chem.*, **1990**, *29*, 4938.

28 A. N. Chernega, A. A. Korkin, N. E. Aksinenko, A. V. Ruban, V. D. Romanenko, *J. Gen. Chem. USSR,* **1990**, *60*, 2201.

29 G. Jochem, A. Schmidpeter, M. Thomann, H. Nöth, *Angew. Chem., Int. Ed. Engl.*, **1994**, *33*, 663.

30 H.-P. Schrödel, A. Schmidpeter, H. Nöth, M. Schmidt, *Z. Naturforsch.*, **1996**, *51b*, 1022.

31 H. Jelinek-Fink, E. N. Duesler, R. T. Paine, *Acta Cryst., Sect C,* **1987**, *C43*, 635.

32 M. S. Davies, M. J. Aroney, I. E. Buys, T. W. Hambley, J.L.Calvert, *Inorg. Chem.*, **1995**, *34*, 330.

33 Y. V. Zefirov, P. M. Zorkii, *Russ. Chem. Rev.*, **1989**, *58*, 421.

34 M. Franck, R. F. H. Jr., W. J. Hehre, *J. Am. Chem. Soc.*, **1984**, *106*, 563.

35 J. T. Alhemann, A. Kunzel, H. W. Roesky, M. Noltemeyer, L. Markovskii, H. G. Schmidt, *Inorg. Chem,* **1996**, *35*, 6644.

36 B. Y. Xue, *M.Sc. Thesis*, Durham, **1999**.

37 P. Kisluik, C. H. Townes, *J. Chem. Phys.*, **1950**, *18*, 1109.

38 J. Trotter, *Can. J. Chem.*, **1962**, *40*, 1590.

39 A. Camerman, J. Trotter, *J. Chem. Soc.*, **1965**, 730.

40 J. E. Stuckey, A. W. Cordes, L. B. Handy, R. W. Perry, C. K. Fair, *Inorg. Chem.*, **1972**, *11*, 8.

41 J. Emsley, *The Elements*; 2nd ed.; Oxford University Press, Oxford, 1991.

42 J. Trotter, *Z. Krist.*, **1965**, *122*, 230.

43 J. Trotter, *J. Chem. Soc.*, **1962**, 2567.

44 H. Nöth, R. Waldhör, *Z. Naturfosch.*, **1999**, *54b*, 603.

45 B. Twamley, C.-S. Hwang, N. J. Hardman, P. P. Power, *J. Organomet. Chem.*, **2000**, *609*, 152.

46 G. S. Blevins, A. W. Blake, W. Gordy, *Phys. Rev.*, **1955**, *97*, 684.

47 W. A. Hermann, B. Koumbouris, A. Schafer, T. Zahn, M. L. Ziegler, *Chem. Ber.*, **1985**, *118*, 2472.

48 G. I. Nikonov, A. J. Blake, J. Lorberth, D. A. Lemonovskii, S. Wocadlo, *J. Organomet. Chem.*, **1997**, *547*, 235.

49 J. K. Buijink, M. Noltemeyer, F. T. Edelmann, *J. Fluorine Chem.*, **1993**, *61*, 51.

50 M. Ates, H. J. Breunig, K. H. Erbert, R. Kaller, M. Drager, U. Behrens, *Z. Naturforsch. B Chem. Sci,* **1992**, *47*, 503.

51 A. N. Sobolev, I. P. Romm, V. K. Belsky, O. P. Syutkina, E. N. Guryanova, *J. Organomet. Chem.*, **1981**, *209*, 49.

52 A. N. Sobolev, I. P. Romm, V. K. Belsky, O. P. Syutkina, E. N. Guryanova, *J. Organomet. Chem.*, **1979**, *179*, 153.

53 P. Sharma, A. Cabrera, N. Rosas, R. L. Lagadec, S. Hernandez, J. Valdes, J.-L. Arias, C. V. Ambrouse, *Main Group Met. Chem.*, **1998**, *21*, 1998.

54 E. A. Adams, J. W. Collis, W. T. Pennington, *Acta Cryst. C,* **1990**, *C46*, 917.

55 H. Voelker, D. Labahn, F. M. Bohnen, R. Herbst-Irmer, H. W. Roesky, D. Stalke, F. T. Edelmann, *New J. Chem.*, **1999**, *97*, 1754.

56 V. C. Gibson, C. Redshaw, L. J. Sequeira, K. B. Dillon, W. Clegg, M. R. Elsegood, *J. Chem. Soc., Chem. Commun.*, **1996**, 2151.

57 K. B. Dillon, V. C. Gibson, J. A. K. Howard, C. Redshaw, L.Sequeira, J. W. Yao, *J. Organomet. Chem.*, **1997**, *528*, 179.

58 J. Cosier, A.M.Glazer, *J. Appl. Cryst.*, **1986**, *19*, 105.

59 SMART -NT; Data Collection Software, version 5.0, Bruker Analytical X-ray Instruments Inc., Madison, Wisconsin, USA, **1999**.

60 SAINT-NT; Data Reduction Software, version 6.0, Bruker Analytical X-ray Instruments Inc, Madison, Wisconsin, U.S.A., **1999**.

61 SHELXTL; version 5.1, Bruker Analytical X-ray Instruments Inc, Madison, Wisconsin, U.S.A., **1999**.

62 G. M. Sheldrick; SADABS,Empirical Absorption Correction Program., University of Göttingen, Germany, **1998**.

Chapter 5
^{19}F Variable Temperature NMR Studies

5.1 Introduction

Rotations of chemical bonds may involve some barrier to rotation. NMR is the most common method to determine energetic barriers to dynamic processes in molecules.

As described in the previous chapter, the ^{19}F NMR spectra of Ar'Ar"EX (E=P or As; X=Cl, Br, H) at room temperature exhibit a broad singlet of double intensity corresponding to the two CF_3 groups of the Ar' moiety in the *ortho* position.

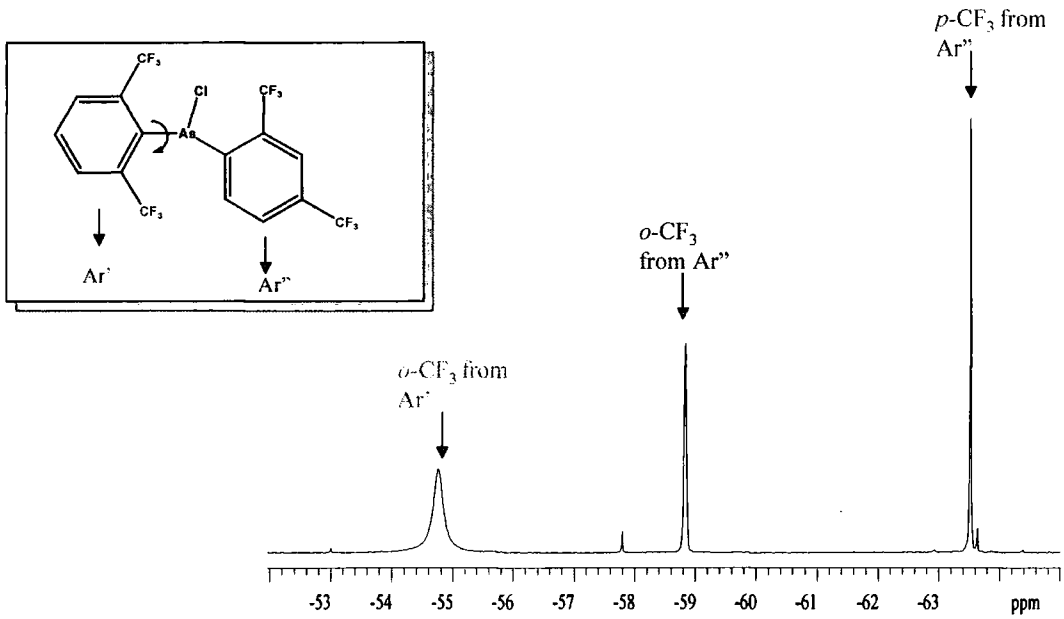

Figure 5.1: *Room Temperature ^{19}F NMR spectrum of Ar'Ar"AsCl*

This broad signal shows the inequivalence of the two CF_3 groups, due to hindered rotation of the aryl ring around the central atom (P or As). This signal was resolved using variable temperature NMR studies over the range –80 to 100°C. The rate at which the aromatic ring rotates is governed principally by the dynamics of neighbouring groups, which must move aside to allow the ring to flip. If the rate is comparable to the frequency difference between the lines (as for Ar'Ar"EX at room temperature), a broad signal is

shown. If the rate is very slow (low temperature), separate signals appear, and if the rate is very high (high temperature) a sharp single line is observed.

- Rate measurements

The temperature range over which measurements are made can be increased by using a combination of techniques. In the slow exchange regime, the exchange rate can be determined by selective inversion-recovery. When the rate is of the same order as the frequency difference between the lines in question, their appearance becomes strongly dependent on the exchange rate.

Some lineshape NMR experiments over a wide range of temperature have permitted determination of these rates in the slow, intermediate and fast exchange regimes. The temperature range has been extended to a point, where the free energy $\Delta G^{\ddagger}$ can be separated into two contributions: the enthalpy ($\Delta H^{\ddagger}$) and entropy ($\Delta S^{\ddagger}$) of activation.

When exchanges are comparable to chemical shift differences, characteristic line broadening and coalescence occur in the spectrum. This can be simulated using classic[1,2] or newer approaches,[3] in order to estimate the exchange rate.

Quoting the Gibbs free energy of activation, $\Delta G^{\ddagger}$, is equivalent to quoting the rate, since transition state theory says that the rate is given by the following equation;

$$\text{rate constant} = \frac{kT}{h} e^{-\Delta G^{*}/RT}$$

$$= \frac{kT}{h} e^{-\Delta H^{*}/RT} e^{-\Delta S^{*}/R}$$

Where k is Boltzmann's constant, h is Planck's constant and the transmission coefficient is assumed to be unity.

In order to separate the enthalpy and the entropy of activation, the rate constant is measured as a function of temperature, T, and an Eyring plot of ln(rate constant/T) vs (1/T) is constructed. This plot ($y=ax+b$) yields a slope a and intercept b. From this, the enthalpy and entropy can be easily determined:

$$\Delta G^{\ddagger} = \Delta H^{\ddagger} - T\,\Delta S^{\ddagger}$$

$$\Delta H^{\ddagger} = -aR$$

$$\Delta S^{\ddagger} = R\,(b\text{-}23.76)$$

To obtain reliable thermodynamic data, it is important to measure the rate over as wide a range of temperatures as possible.

5.2 Phosphorus compounds

5.2.1 Ar'Ar"PCl

- Variable temperature ^{19}F NMR measurements

At ambient temperature, a doublet at –59.3 ppm ($^{4}J_{P\text{-}F}$ 59.1 Hz) and two singlets (a broad double intensity line at –55.4 and a sharp peak at–64.1 ppm) were observed.

Spectra were recorded for a toluene solution, every 10°C from -80°C to +100°C. (Figure 5.2).

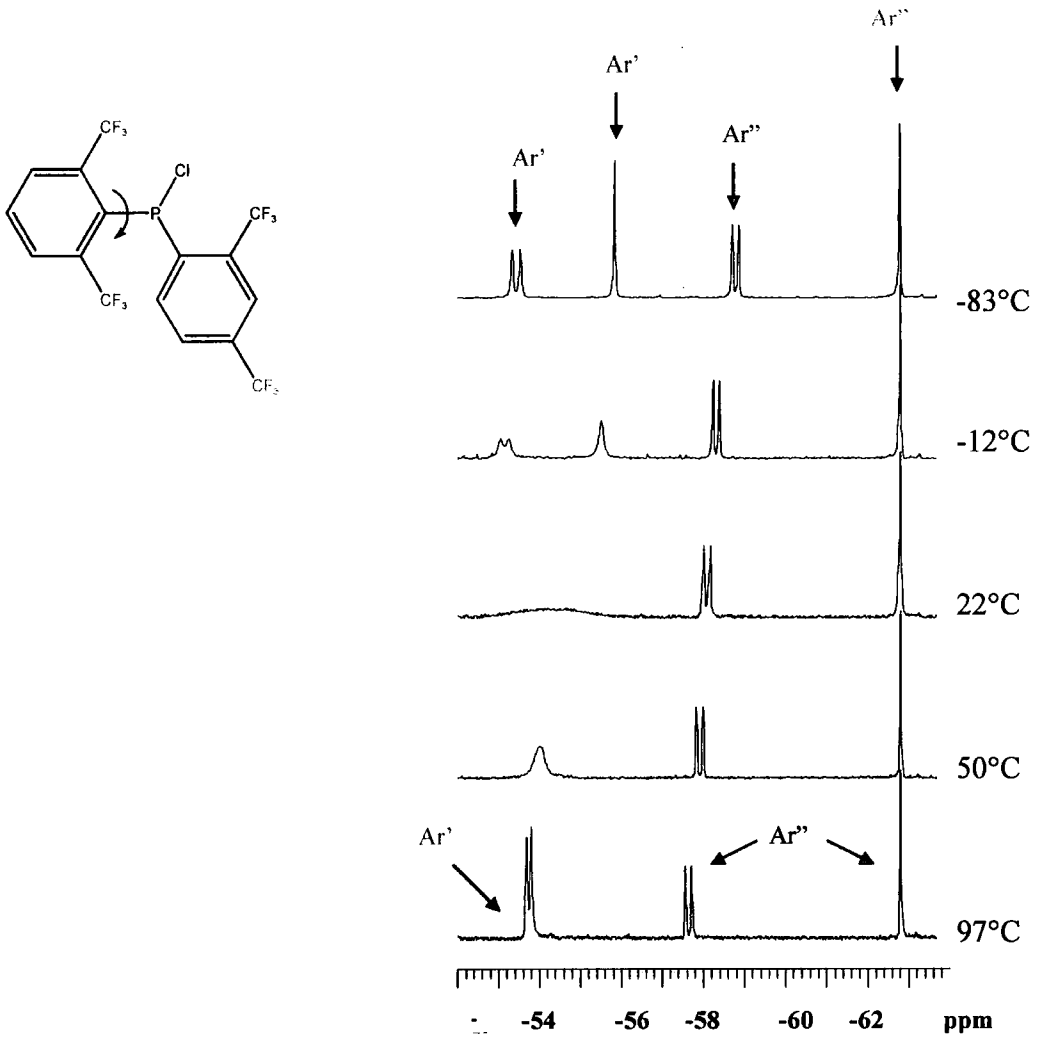

Figure 5.2: *Variable temperature ^{19}F NMR Spectra for Ar'Ar"PCl*

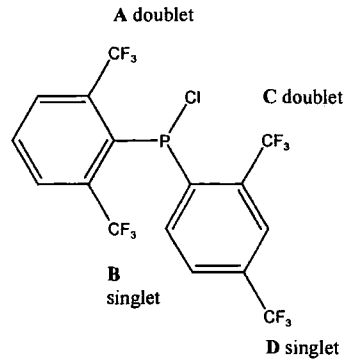

Figure 5.3: *Inequivalent CF_3 groups in the ^{19}F NMR at low temperature*

As the temperature is decreased, the peak broadens, then decoalesces near 10°C. The **A** and **B** signals then begin to resharpen.

At low temperature, two doublets and two singlets are observed. Signals assigned to the Ar" group are detected at similar positions to those at room temperature (δ -58.8, d, $^4J_{P-F}$ 59.1 Hz and δ -62.8 ppm), suggesting either that rotation about the P-Ar" bond is rapid on the NMR timescale even at low temperature, or that there is a single fixed conformation about the P-C bond. The Ar' moiety shows a doublet at -53.4 ppm ($^4J_{P-F}$ 76.7 Hz)at -83°C and a singlet at -55.8 ppm.

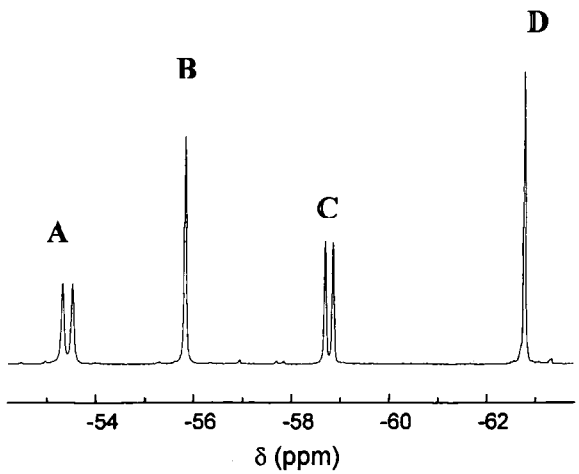

Figure 5.4: *^{19}F NMR spectrum at -90°C*

As the temperature is raised, the broad peak sharpens and the broad signal is resolved into a doublet (δ -54.9, $^4J_{P-F}$ 36.5 Hz) at 70°C. At 100°C, a sharp doublet is also observed at -54.9 ppm ($^4J_{P-F}$ 41.7 Hz). This shows that the rotation about the P-C bond is fast enough on the NMR timescale for the two CF_3 groups to become equivalent.

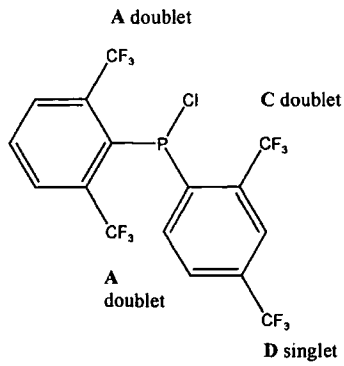

Figure 5.5: *Equivalent CF_3 groups in the ^{19}F NMR at high temperature*

Assignment	δ_a(ppm) Ar'		δ_b(ppm) Ar'	δ_c(ppm) Ar"	δ_d(ppm) Ar"(para)
high temp. 98°C		-54.9[a]		-58.8[b]	-64.0
ambient temp. 22°C		-55.5[c]		-58.9[d]	-63.6
low temp. -83°C	-53.4[e]		-55.8	-58.8[f]	-62.8

Table 5.1: *Comparison of fluorine chemical shift data at different temperatures*

[a] Doublet (double intensity) $^4J_{P-F}$ 41.7 Hz. [b] Doublet $^4J_{P-F}$ 56.8 Hz. [c] Broad, double intensity. [d] Doublet $^4J_{P-F}$ 58.3 Hz. [e] Doublet $^4J_{P-F}$ 76.7 Hz. [f] Doublet $^4J_{P-F}$ 59.5 Hz

The values of $^4J_{P-F}$ in this kind of system involving Ar'P or Ar"P bonds may contain a strong contribution from through space effects. Therefore, this implies that not only the two CF_3 groups in Ar' are not equivalent but also that one of them may be further away from the phosphorus atom. This was confirmed by the crystal structure, where intramolecular P---F interactions are observed (see chapter 4).

- Rotational barrier calculations

The Ar' group rotation was investigated in detail by bandshape fitting for temperatures between -80°C and +100°C. Lineshapes were simulated by P. Hazendonk using MATLAB (section 5.5.3) and compared visually with the experimental spectra (Figure 5.6).

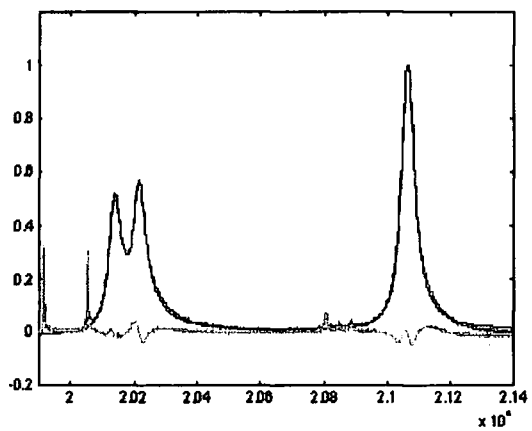

Figure 5.6: *Simulated (red line) and experimental (blue line) ^{19}F NMR spectrum at -20°C.*

The exchange rates are summarized in Table 5.2 and the Eyring Plot is shown in Figure 5.7.

Temp (°C)	Rate (s^{-1})	Temp (K)	1000/T	Ln(Rate/T)
-13.	125	260	3.852	-0.730
-1	390	272	3.683	0.362
2.	475	275	3.623	0.543
12	1130	285	3.508	1.377
21	2100	294	3.396	1.964
30	4250	303	3.300	2.640
38	7130	311	3.215	3.132
48	11800	321	3.115	3.604
58	22700	331	3.021	4.228
68	45000	341	2.932	4.882
78	81000	351	2.842	5.439
88	150000	361	2.766	6.028

Table 5.2: *Rates Determined by Lineshape Analysis.*

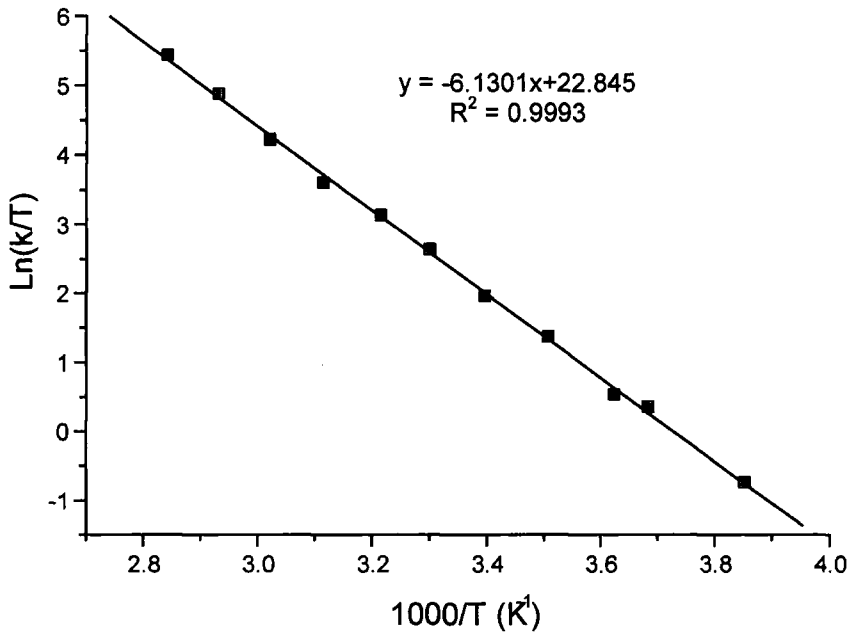

Figure 5.7: *Eyring Plot for Ar'Ar"PCl*

The Eyring Plot enables the enthalpy and entropy of the rotation to be determined. The ring flip process has a barrier of $\Delta H^{\ddagger} = 51.0$ kJ.mol^{-1}. The entropy $\Delta S^{\ddagger}$ is -7.6 J.mol^{-1}.K^{-1}.

5.2.2 Ar'Ar"PH

- NMR

As in Ar'Ar"PCl, at room temperature, the same kind of spectrum is observed, with a broad singlet at -57.6 ppm corresponding to the two CF_3 groups of the Ar' moiety. As the temperature decreases, the broad signal decoalesces near -20°C. The components then begin to resharpen. At -90°C, a doublet at -56.0 ppm ($^4J_{P-F}$ 57.8 Hz) and a singlet at -58.6 ppm are observed. At high temperature (90°C), the singlet sharpens as the two *ortho* trifluoromethyl groups of the Ar' ring become equivalent. A doublet is shown at -57.6 ppm ($^4J_{P-F}$ 29.3 Hz) (Figure 5.8).

Assignment	δ_a(ppm) Ar'		δ_b(ppm) Ar'	δ_c(ppm) Ar"	δ_d(ppm) Ar"(*para*)
high temp. 90°C		-57.6[a]		-61.0[b]	-63.8
ambient temp. 22°C		-57.6[c]		-61.1[d]	-63.4
low temp. -86°C	-56.0[e]		-58.6	-61.5[f]	-62.5

Table 5.3: *Comparison of fluorine chemical shift data at different temperatures*

[a] Doublet (double intensity) $^4J_{P-F}$ 29.15 Hz. [b] Doublet $^4J_{P-F}$ 45.1 Hz. [c] Broad, double intensity, [d] Doublet $^4J_{P-F}$ 43.7Hz. [e] Doublet $^4J_{P-F}$ 57.84 Hz. [f] Doublet $^4J_{P-F}$ 40.0 Hz

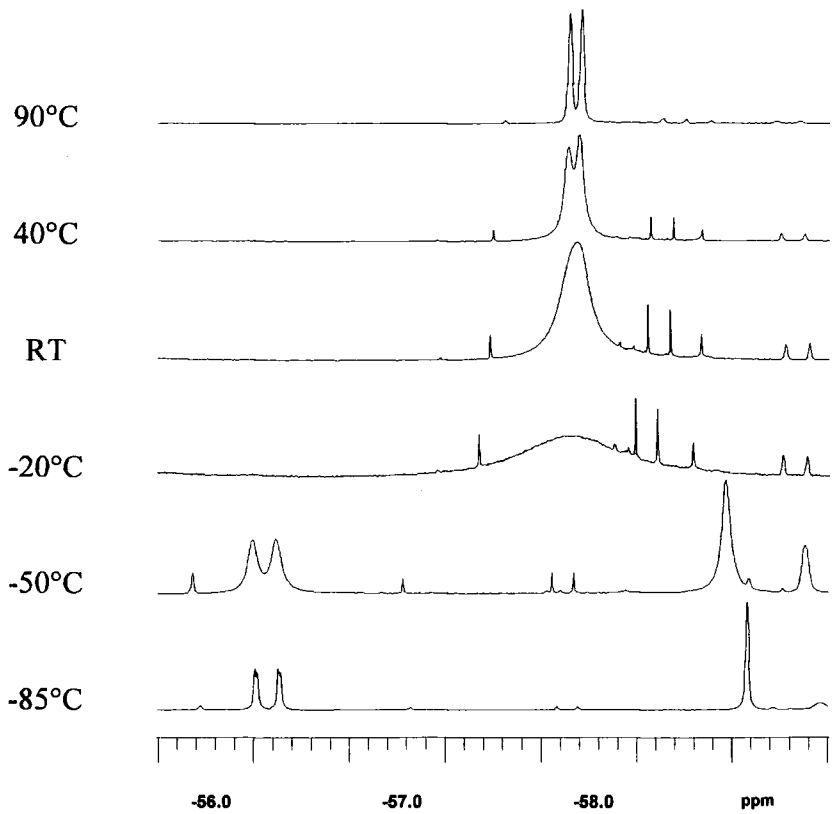

Figure 5.8: *Section of the VT ^{19}F NMR spectra of Ar'Ar"PH*

- Rotational barrier calculations

The Eyring plot of the rate derived from lineshape analysis gave the enthalpy and entropy: $\Delta H^{\ddagger} = 42.4$ kJ.mol^{-1} and $\Delta S^{\ddagger}$ -14.9 J.mol^{-1}.K^{-1}. Due to a smaller steric demand of the hydrogen atom in comparison with the chlorine atom, the energy required for the ring to rotate is larger in Ar'Ar"PCl.

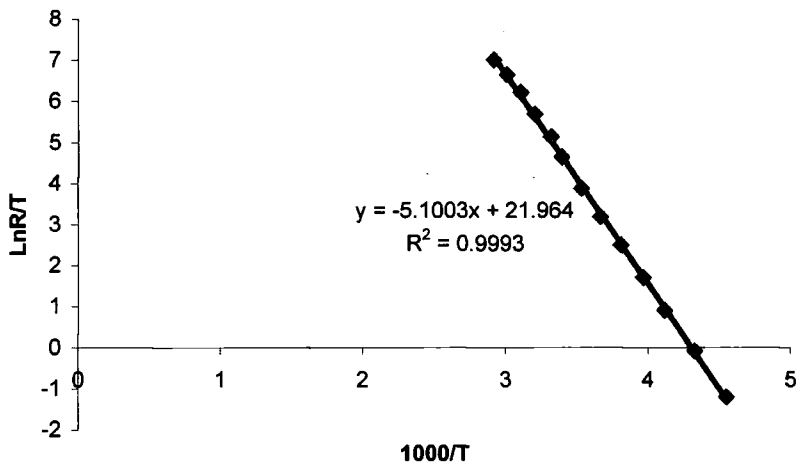

Figure 5.9: *Eyring plot for Ar'Ar"PH*

5.2.3 ArAr"PCl/ArAr'PCl

- NMR measurements

As explained in chapter 4, the products ArAr'PCl and ArAr"PCl could not be separated. The ^{19}F NMR spectrum at room temperature for ArAr'PCl shows two very close doublets at -54.1 ($^{4}J_{P-F}$ 42.1Hz) and -54.2 ppm ($^{4}J_{P-F}$ 42.1Hz), corresponding to the CF_3 groups in *ortho* positions for the Ar and Ar' moieties.

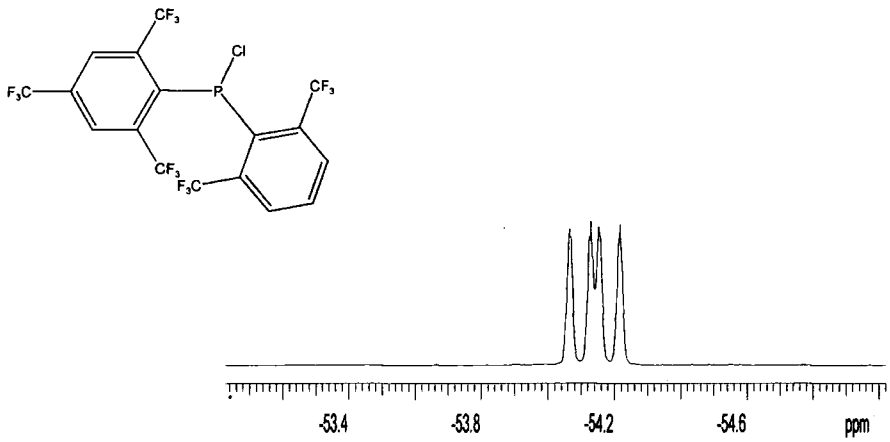

Figure 5.10: *^{19}F NMR spectrum of the ortho-CF_3 groups of ArAr'PCl at room temperature*

In ArAr"PCl, at ambient temperature, a broad singlet at -55.5 ppm is observed for the two *o*-CF_3 groups of the Ar moiety and, a doublet at -58.6 ($^4J_{P-F}$ 58.3 Hz) for the *o*-CF_3 groups in the Ar" moiety.

The broad singlet decoalesced near 0°C, and was resolved at -50°C into a doublet at -53.9 ppm ($^4J_{P-F}$ 80.9 Hz) and a singlet at -56.4 ppm (Table 5.4). At a lower temperature, the doublet overlapped the signals from the *ortho*-CF_3 of ArAr'PCl (Figure 5.11).

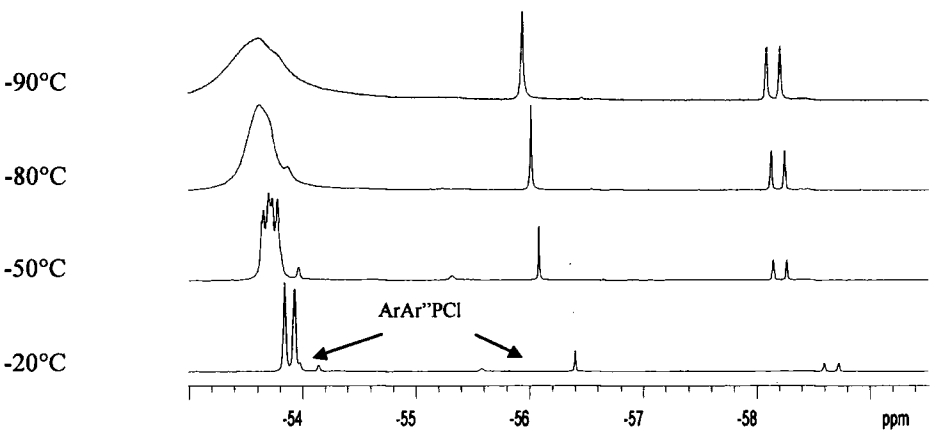

Figure 5.11: *Low temperature ^{19}F NMR spectra of ArAr"PCl/ArAr'PCl (the weaker peaks are those from ArAr"PCl)*

At high temperature, the broad singlet is resolved into a doublet at -55.7 ppm as the CF_3 groups of Ar become equivalent.

Fast fluorine exchange is also observed for ArAr'PCl. The two doublets at -54.1 and -54.3 ppm become a single doublet at -20°C and a broad singlet at -90°C. Unfortunately, due to solvent restrictions, it has not been possible to extend the series to lower temperature. At 60°C, the doublet becomes an apparent triplet due to overlapping of the two doublets (Figure 5.12). This overlapping is due to accidental degeneracy (the chemical shifts move with the temperature change). At low temperature the exchange occur.

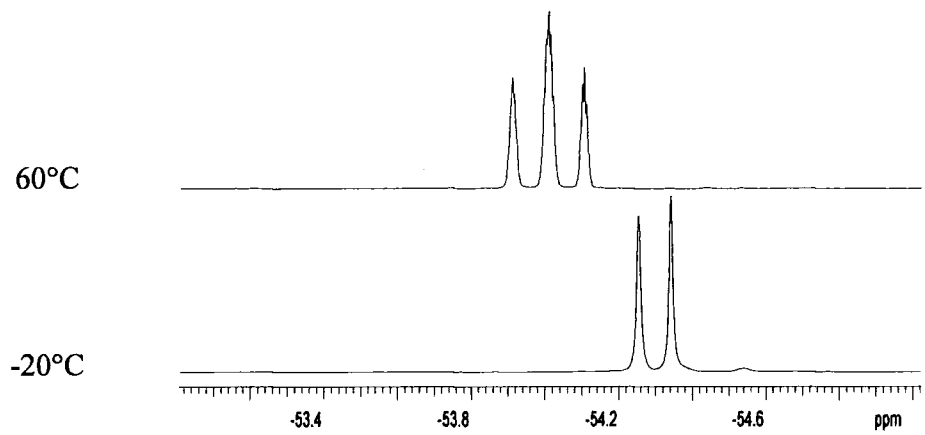

Figure 5.12: *Section of the ^{19}F NMR spectra of ArAr'PCl*

Assignment	δ_a(ppm) Ar'		δ_b(ppm) Ar'	δ_c(ppm) Ar"	δ_d(ppm) Ar"(*para*)
high temp. 59°C		-55.3[a]		-58.4[b]	-63.8
ambient temp. 22°C		-55.5[c]		-58.6[d]	-63.4
low temp. -63°C	-53.9[e]		-58.6	-58.5[f]	-62.5

Table 5.4: *Comparison of fluorine chemical shift data at different temperatures*

[a] Broad singlet, overlapped with signal from ArAr'PCl. [b] Doublet $^4J_{P-F}$ 59.7 Hz. [c] Broad, double intensity. [d] Doublet $^4J_{P-F}$ 58.3Hz. [e] Doublet $^4J_{P-F}$ 80.9 Hz. [f] Doublet $^4J_{P-F}$ 59.7 Hz

- Rotational barrier calculations

Simulations have only been done for ArAr"PCl. Calculations for ArAr'PCl would require variable temperature NMR spectra at a lower temperature than -90°C.

The Eyring plot of ArAr'PCl is shown in Figure 5.13.

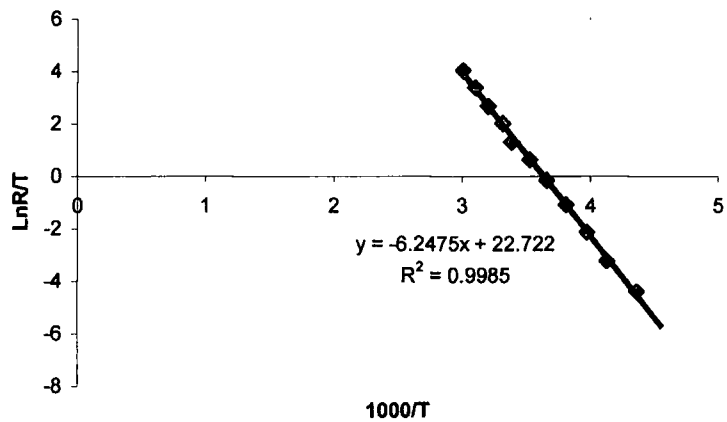

Figure 5.13: *Eyring Plot of ArAr"PCl*

The enthalpy and entropy determined from the Eyring plot are: $\Delta H^{\ddagger}$ = 51.9 kJ.mol^{-1} and $\Delta S^{\ddagger}$ = -8.6 J.mol^{-1}.K^{-1}. The enthalpy is similar to the one found in Ar'Ar"PCl. This is due to the fact that the two molecules only differ by the presence of one more *para*-CF_3 group from the Ar moiety. *Para*-CF_3 groups are not expected to have any influence on the rotational energy barrier. The $^4J_{P-F}$ coupling constants determined at different temperature also reflect the rotation of the molecule (Table 5.5). The molecule is in a different conformation and the *ortho*-CF_3 groups are closer or further away from the phosphorus atom. The presence of through space interactions (found in the crystal structure) contributes to the change in the coupling constants. As the molecule rotates, the CF_3 groups are closer or further away from the phosphorus atom.

	$^4J_{P-F}$ (Hz)					
	Ar'(or Ar)			Ar''		
	High Temp.	Room Temp.	Low Temp.	High Temp.	Room Temp.	Low Temp.
Ar'Ar"PCl	41.7		76.7	56.8	58.3	59.5
Ar'Ar"PH	29.1		57.5	45.1	43.7	40.0
ArAr"PCl		77	80.9	59.7	58.3	59.7

Table 5.5: *$^4J_{P-F}$ coupling constants at different temperatures*

At high temperature, the two CF_3 groups of the Ar' groups are equivalent; they are equidistant from the central atom. When the temperature decreases, they become inequivalent and one CF_3 is further away from the phosphorus atom. Only one P-F coupling is seen in the NMR spectrum, which shows a doublet and a singlet.

5.3 Arsenic compounds

5.3.1 Ar'Ar"AsCl

- NMR measurements

The room temperature ^{19}F NMR spectrum of Ar'Ar"AsCl is shown in Figure 5.1. As for the phosphorus derivatives, the spectrum exhibits a broad singlet corresponding to the two *o*-CF_3 groups of the Ar' moiety. Variable temperature spectra were recorded in d_8-toluene over the range -80°C to 60°C (Figure 5.14).

At the temperature is lowered, the signal broadens, then decoalesces near -5°C, and resharpens to give two distinct singlets from -60°C. As the temperature rises, the signal sharpens and a singlet is observed at 60°C. Table 5.6 summarises the fluorine chemical shifts at different temperatures.

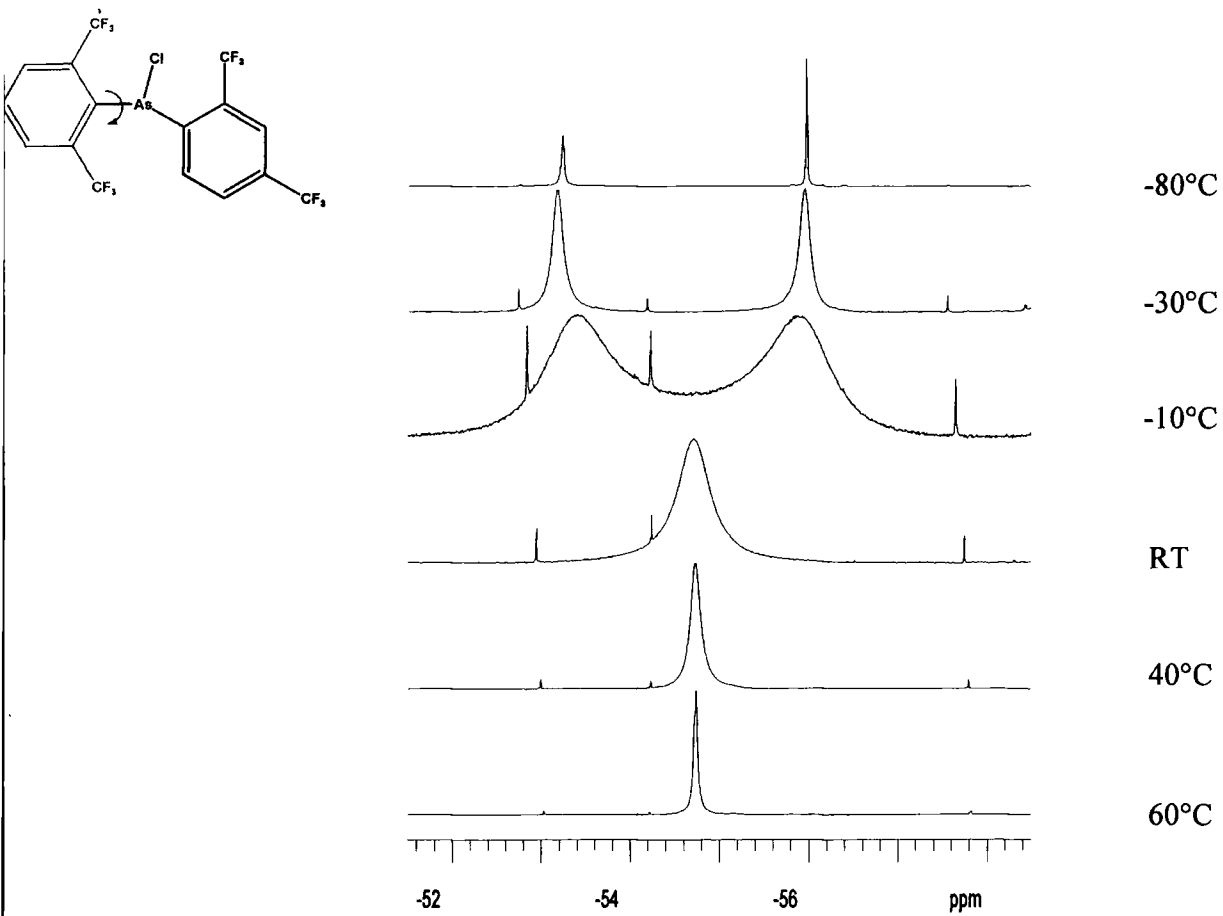

Figure 5.14: *Section of the Variable Temperature NMR spectra of Ar'Ar"AsCl*

At -80°C, the width of the two singlets differs. This can be explained by through-space interaction with some fluorines from one of the *o*-CF_3 groups and the arsenic atom (chapter 4).

Assignment	δ_a(ppm) Ar'		δ_b(ppm) Ar'	δ_c(ppm) Ar"	δ_d(ppm) Ar"(*para*)
high temp. 50°C		-54.7		-58.8	-63.6
ambient temp. 22°C		-54.7		-58.8	-63.5
low temp. -80°C	-52.9		-55.6	-58.2	-62.7

Table 5.6: *Comparison of fluorine chemical shifts at different temperatures for Ar'Ar"AsCl*

- Rotational barrier calculations

Rate constants were calculated by lineshape analysis and the Eyring plot was constructed (Figure 5.15). The Eyring plot gave $\Delta H^{\ddagger}$ = 48.7 kJ. mol^{-1} and $\Delta S^{\ddagger}$ = 0.4 $J.mol^{-1}.K^{-1}$.

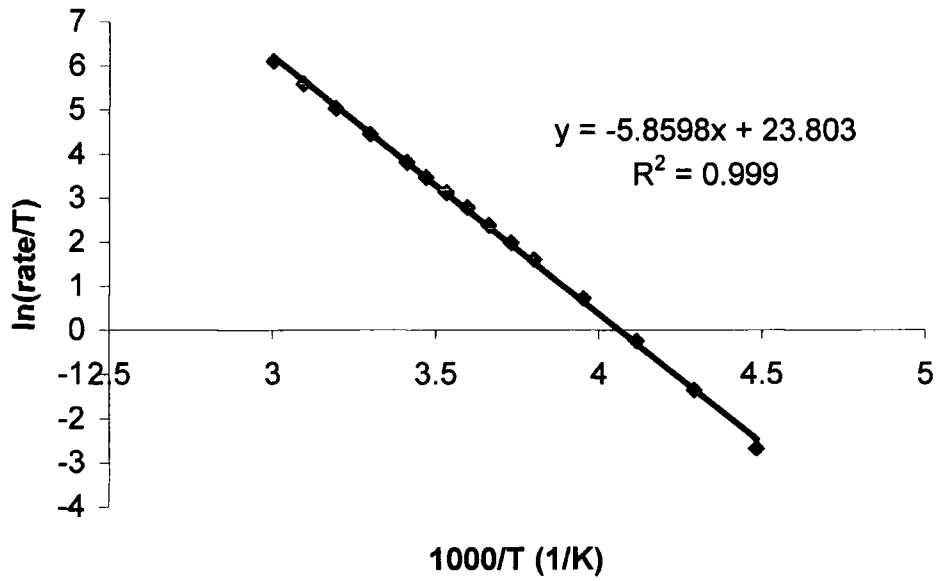

Figure 5.15: *Eyring Plot for Ar'Ar"AsCl*

The enthalpy is slightly lower than for the analogous phosphorus compound, Ar'Ar"PCl.

5.3.2 Ar'Ar"AsBr

- NMR measurements

Variable temperature ^{19}F NMR spectra showed the same behaviour as those for Ar'Ar"AsCl. The broad signal at room temperature broadens as the temperature decreases, and decoalesces at about 0°C to give two sharp singlets at -50°C (Figure 5.16). The *o*-CF_3 groups are then inequivalent.

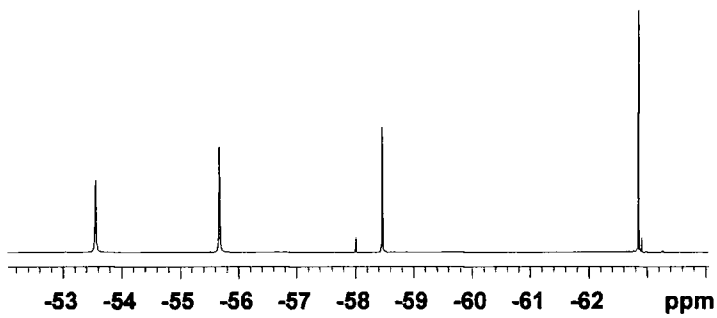

Figure 5.16: *^{19}F NMR spectrum of Ar'Ar"AsBr at -50°C*

When the temperature is increased, the broad singlet sharpens and a sharp singlet appears at 100°C, indicating the equivalence of the CF_3 groups in the *ortho* position.

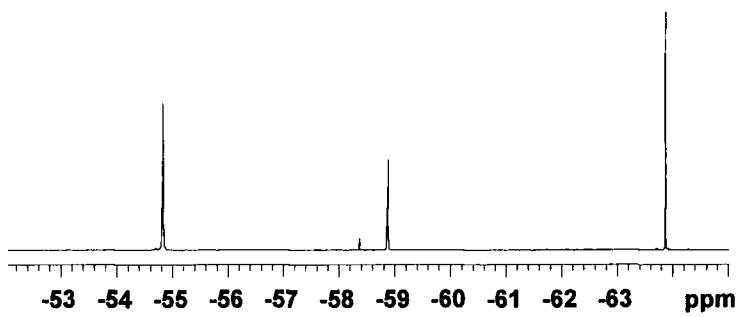

Figure 5.17: *^{19}F NMR spectrum of Ar'Ar"AsBr at 100°C*

Over the whole range of temperature, the signals from the CF_3 groups of the Ar" aryl ring are found at almost the same chemical shifts (Table 5.7).

Assignment	δ_a (ppm) Ar'	δ_b (ppm) Ar'	δ_c(ppm) Ar"	δ_d (ppm) Ar"(*para*)
high temp.100°C	-54.8		-58.9	-63.9
ambient temp. 23°C	-54.8		-58.7	-63.5
low temp. –50°C	-53.4	-55.6	-58.5	-62.8

Table 5.7: *^{19}F chemical shifts at different temperatures for Ar'Ar"AsBr*

- Rotational barrier calculations

The Eyring plot shown in Figure 5.18, gave $\Delta H^{\ddagger}$ = 49.0 kJ. mol^{-1} and $\Delta S^{\ddagger}$ = -3.0 $J.mol^{-1}$. K^{-1}.

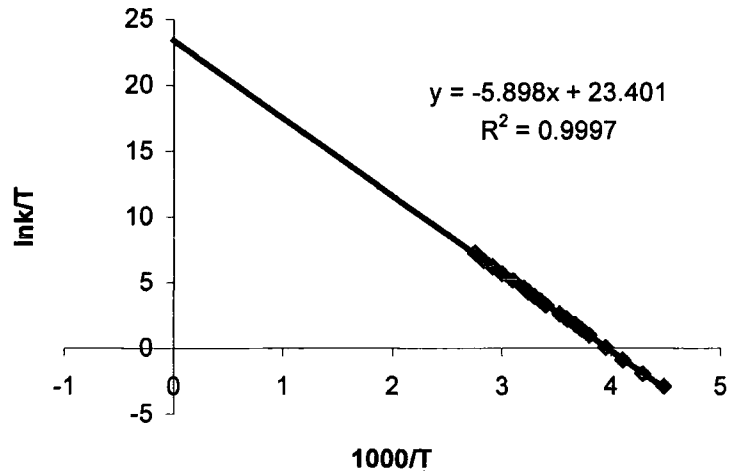

Figure 5.18: *Eyring plot for Ar'Ar"AsBr*

5.3.3 Ar'Ar"AsH

Spectra were recorded from -80°C to +100°C. The room temperature spectrum did not show a broad singlet but a sharp one for the *o*-CF_3 groups. This started to broaden at -10°C and decoalesced near -50°C. The spectrum at -80°C showed two singlets at -56.3 and -58.1 ppm (Figure 5.19). These two signals were still broad signals, and while studies at a lower temperature are expected to sharpen them, low temperature experiments were limited by the solvent, which freezes at –90°C. Spectra at high temperature showed a sharp singlet.

	δ_a(ppm)	δ_b(ppm)	δ_c(ppm)	δ_d(ppm)
Assignment	Ar'	Ar'	Ar"	Ar"(para)
high temp. 90°C	-57.6		-60.7	-63.8
ambient temp. 21°C	-57.6		-60.8	-63.4
low temp. -87°C	-56.3	-58.1	-61.0	-62.5

Table 5.8: *Comparison of the fluorine chemical shifts at different temperatures for Ar'Ar"AsH*

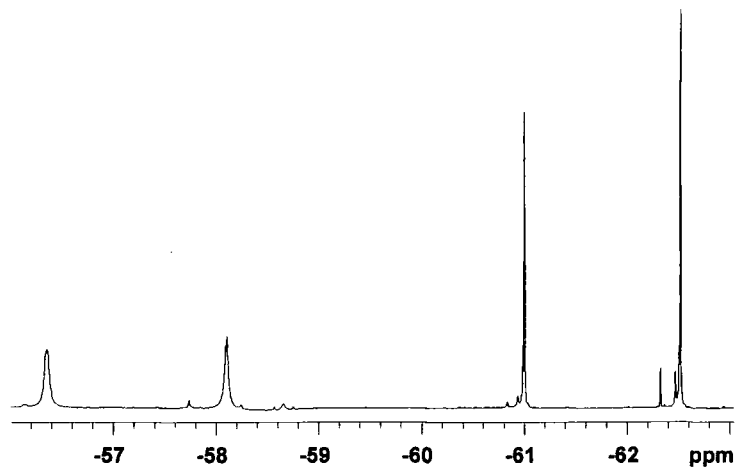

Figure 5.19*: ^{19}F NMR spectrum of Ar'Ar"AsH at -87°C*

- Rotational Barrier calculations

Simulated spectra (red line) are shown Figure 5.21. Those were compared with the experimental spectra (blue line).

The Eyring plot (Figure 5.20) derived from lineshape analysis gave $\Delta H^{\ddagger} = 37.8$ kJ. mol^{-1} and $\Delta S^{\ddagger} = -7.6$ J.mol^{-1}.K^{-1}.

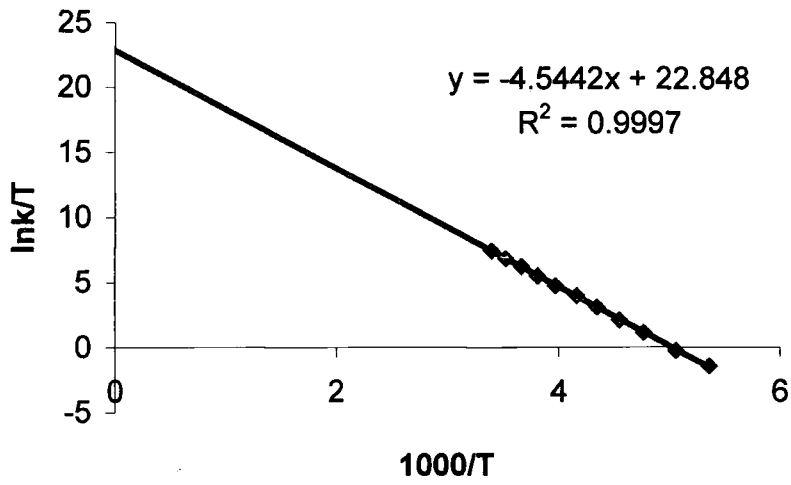

Figure 5.20: *Eyring Plot of Ar'Ar''AsH*

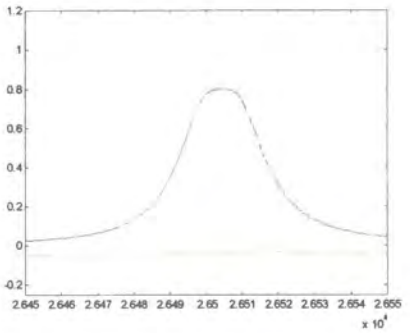

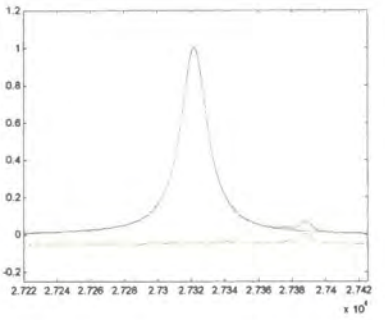

-87°C

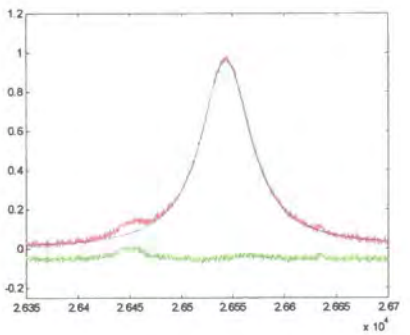

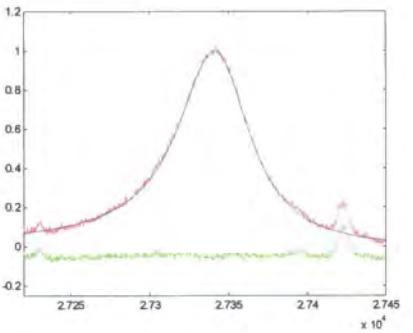

-75°C

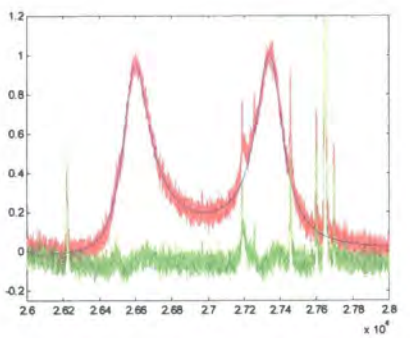

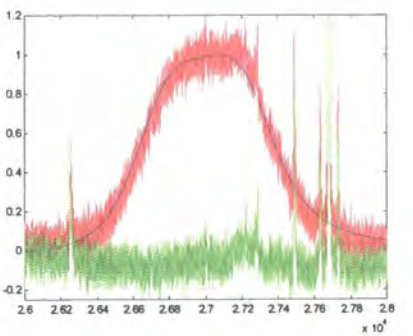

-64°C

-53°C

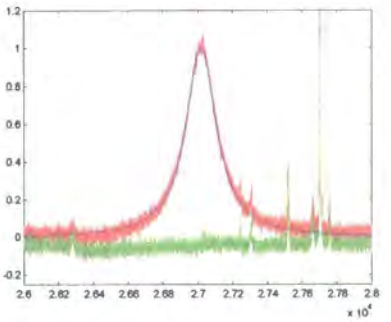

-43°C

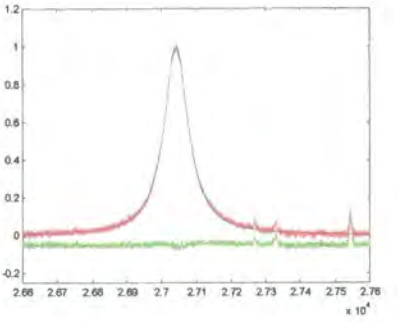

-33°C

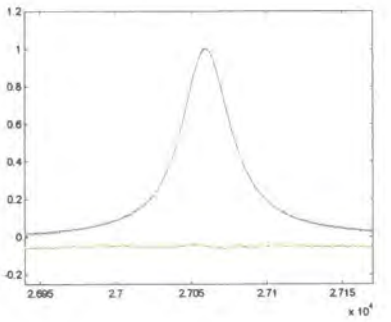

-21°C

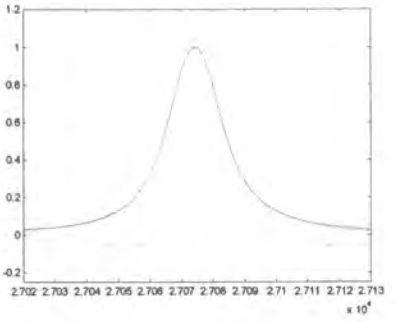

-11°C

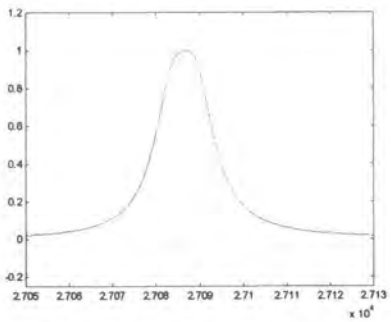

0°C

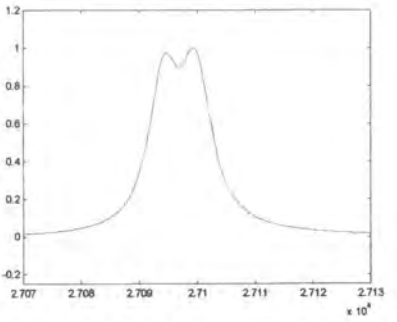

11°C

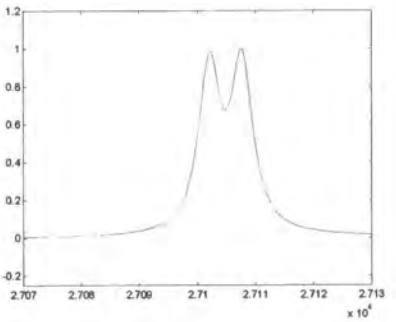

20°C

Figure 5.21: *Simulated (red line) and experimental (blue line) ^{19}F NMR Spectrum of Ar'Ar"AsH*

5.4 Discussions.

The thermodynamic parameters and the temperature of coalescence Tc, are listed in Table 5.9.

	$\Delta H^{\ddagger}$ (kJ.mol^{-1})	$\Delta S^{\ddagger}$ (J.mol^{-1}.K^{-1})	$\Delta G^{\ddagger}$ (298K)(kJ)	Tc (°C)
Ar'Ar"AsH	37.8±0.2	-7.6±1	40.0	-50
Ar'Ar"AsCl	48.7±0.4	0.4±2	48.6	0
Ar'Ar"AsBr	49.0±0.2	-3.0±1	50.0	-5
Ar'Ar"PH	42.4±0.5	-14.9±1	46.9	-20
Ar'Ar"PCl	51.0± 0.6	-7.6± 3	53.2	10
ArAr"PCl	51.9±0.4	-8.6±1	54.5	0

Table 5.9: *Thermodynamic parameters for Ar'Ar"EX and ArAr"PCl (E = P or As; X = H, Cl or Br)*

The enthalpy of activation of arsenic derivatives increases from Ar'Ar"AsH to Ar'Ar"AsBr: $\Delta H^{\ddagger}_{AsH} < \Delta H^{\ddagger}_{AsCl} < \Delta H^{\ddagger}_{AsBr}$. This is also observed in phosphorus compounds. $\Delta H^{\ddagger}_{PH} < \Delta H^{\ddagger}_{PCl}$. This reflects the steric demand of the bromine atom in comparison with the hydrogen atom. The bigger the atom X is, the more energy the molecule will need to rotate.

In analogous compounds, the enthalpy of activation is larger for phosphorus than for arsenic ($\Delta H^{\ddagger}_{AsCl} < \Delta H^{\ddagger}_{PCl}$) reflecting a greater space around the larger atom. This is confirmed in the crystallographic data (Table 5.10 and 5.11). Due to less steric demand of the hydrogen, bond distances and angles are shorter in Ar'Ar"EH derivatives. The longer the E-C' distance is, the less energy is required for the rotation. The same applies to the bond angles. They are much smaller in Ar'Ar"AsH than in all other compounds containing halogens. The C'-E-C" angle does not seem to play an important role in the rotational energy. In fact, angle C'-As-C" is smaller than C'-P-C" in the chlorine

derivatives and the enthalpies of activation are very close to each other ($\Delta H^{\ddagger}_{AsCl}$ = 48.7 kJ.mol^{-1} and $\Delta H^{\ddagger}_{PCl}$ = 51.0 kJ.mol^{-1}).

Bond distances (Å)	Ar'Ar"AsH	Ar'Ar"AsCl	Ar'Ar"AsBr	Ar'Ar"PCl
E-X	0.98	2.20	2.35	2.06
E-C'[a]	1.99	2.02	2.01	1.88
E-C"[a]	1.98	1.99	1.98	1.85

Table 5.10: *Bond distances (Å) in Ar'Ar"EX compounds.*

[a] C' is the *ipso* carbon from the Ar' moiety and C"is the one from the Ar" moiety.

Angles (°)	Ar'Ar"AsH	Ar'Ar"AsCl	Ar'Ar"AsBr	Ar'Ar"PCl
X-E-C'	79.20	98.00	98.91	100.23
X-E-C"	83.50	100.08	101.43	102.10
C'-E-C"	98.09	102.98	103.15	109.23

Table 5.11: *Bond Angles (°) in Ar'Ar"EX compounds*

Except for Ar'Ar"AsCl, all the entropy values are negative. This indicates that the transition state is more ordered than the optimum geometry, and that there is a preferred orientation of the ring. This orientation is due to the intramolecular interactions found in all the compounds structurally characterised, where four short E---F contacts are observed in each case (chapter 4). Two of those contacts come from the same CF_3 group in the Ar' moiety.

In Ar'Ar"AsCl, the entropy change is negligible and the rotational energy is just governed by the enthalpy factor. Entropy values are larger in the arsenic compounds than

in phosphorus derivatives. This can be explained by less steric constraint, due to a larger size of the As central atom.

5.5 Experimental

5.5.1 Syntheses

All the compounds have been prepared in the laboratory, and syntheses are described in Chapter 4.

5.5.2 NMR spectroscopy

NMR measurements were performed on a Varian VXR 400 (Ar'Ar"PCl) or a Varian Inova 500 spectrometer at 376.34 MHz and 470.26 MHz respectively. For low temperature, the probe was cooled using liquid N_2 and allowed to equilibrate for a few minutes at each temperature before each acquisition. All NMR spectra were recorded in d_8-toluene. Temperature calibration was done by chemical-shift difference between the OH resonances and CH_n resonances in either methanol (for low temperature) or ethylene glycol (for high temperature).

5.5.3 Lineshape analysis

The simulation program was written using MATLAB, assuming that the CF_3 groups were rotationally averaged to be equivalent. The phosphorous-containing compounds were simulated as an AX system exchanging with an MX, where the nuclei A and M are observed, representing the CF_3 groups. The chemical shift of A and M as well as the couplings J_{AX} and J_{MX} were used as free parameters, along with their spin lattice relaxation times, T_{2A} and T_{2B}.

Simulations were performed by varying the rate of exchange, and comparing the results with the experimental spectrum. The chi-squares (χ^2) were computed between the simulated and measured data points. The rate with the lowest chi-squares (χ^2) was taken as the measured rate.

References

1 G. Binsch, *J. Am. Chem. Soc.*, **1969**, *91*, 1304.

2 D. A. Kleier, G. Binsch, *J. Magn. Reson.*, **1970**, *3*, 146.

3 A. D. Bain, G. J. Duns, *Can. J. Chem.*, **1996**, *74*, 819.

Chapter 6
Synthesis of Platinum Complexes

6.1 Introduction

The chemistry of platinum has been widely developed over the last 50 years due to its nobility and catalytic properties. Its properties depend on the large number of valence d-electrons, which provide a series of orbitals of a range of energies and symmetries capable of bonding with a large range of compounds.

6.2 Platinum complexes

Platinum exists in different oxidation states, on which depends the geometry of the complexes (Table 6.1).

Oxidation states	Coordination number	Stereochemistry	Examples
0 (d^{10})	3	planar	$[Pt(PPh_3)_3]$
	4	tetrahedral	$[Pt(PF_3)_4]$
2 (d^8)	4	square planar	$[PtCl_4]^{2-}$
	5	trigonal bipyramidal	$[Pt(qas)I]^{+a}$
3 (d^7)	4	square planar	$[Pt(C_6Cl_5)_4]^{\cdot}$
4 (d^6)	6	octahedral	$[PtCl_6]^{2-}$
	8	"piano-stool"	$Pt(\eta^5\text{-}C_5H_5)Me_3]$
5 (d^5)	6	octahedral	$[PtF_6]^{\cdot}$
6 (d^4)	6	octahedral	PtF_6

Table 6.1: *Different oxidation states of platinum*

- Oxidation State 4 (d^6)

All complexes in this oxidation state which have been characterised, are octahedral and diamagnetic, with a low spin t_{2g}^6 configuration.

There are several Pt(IV) complexes. These compounds are thermodynamically stable and kinetically inert. Those with halides, pseudo-halides and N-donors are especially

[a] qas: tris-(2-diphenylarsinophenyl)arsine, $As(C_6H_4\text{-}2AsPh_2)_3$

numerous: $[PtX_6]^{2-}$, $[PtX_4L_2]$, $[PtL_6]$ have been characterised. O-donor ligands such as OH- also coordinate to Pt(IV), but S-, Se- , P- and As-donor ligands tend to reduce it to Pt(II).

- Oxidation state 3 (d^7)

This oxidation state is much less encountered. However, the most abundant examples of Pt(III) are dinuclear compounds of the type $[Pt_2(L\text{-}L)_4L_2]^{n-}$ [1] with single Pt-Pt bonds and a tetrabridged structure.

- Oxidation state 2 (d^8)

This is the most abundant oxidation state.

The complexes of Pt(II) are diamagnetic and square planar. The diagram below shows the change in energy of the d-orbitals on the metal as the axial ligands are removed from an octahedral complex. Any orbital containing "z" character (d_z^2, d_{xz}, d_{yz}) lowers in energy, and the other orbitals rise in energy accordingly. These effects cause the crystal field splitting pattern of the d orbitals to change dramatically, thus causing the pairing of the eight electrons.

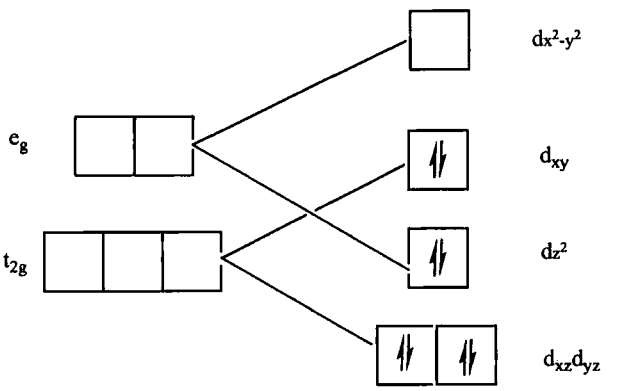

Figure 6.1: *Electron pairing in a square planar complex*

Not many complexes are formed with O-donor ligands, although complexes $[PtX_4]^{2-}$ (X = Cl, Br, I, SCN, CN) can easily be obtained. Complexes with ammonia and amines of the types $[PtL_4]^{2+}$ or PtL_2X_2 are also numerous.

- Oxidation state 0 (d^{10})

Complexes in oxidation state 0 are compounds of the type $[Pt(PR_3)_4]$. They are air stable with a tetrahedral geometry. Their most important property is their readiness to dissociate in solution to form three-coordinate planar $[Pt(PR_3)_3]$.

6.2.1 Platinum complexes as chemotherapeutic agents

The discovery of the cytotoxic properties of cis-dichlorodiammineplatinum(II) $[PtCl_2(NH_3)_2]$, now known as anticancer cisplatin, was made by the physicist Rosenberg and coworkers in 1965.[2] They also noticed that the active complexes $Pt(NH_3)_2Cl_2$ and $Pt(NH_3)_2Cl_4$ were only active in their *cis*-configuration.[3] Since then, the search for anti-tumour active platinum complexes has been intense and extensive, with a multiplicity of ligand combinations being studied. However, some attempts to replace nitrogen donors with phosphorus have not generally been successful. This has been attributed to a strong *trans* effect exerted in dichlorophosphane-Pt(II) compounds. Fluorophosphanes are believed to overcome this effect due to their strong σ-donor and π-acceptor properties.[4,5] The complex *cis*-$[Pt(ArP{=}PAr)(PEt_3)Cl_2]$, containing a low-coordinate phosphorus ligand, has shown anti-tumour properties, however, against a range of cancers.[6]

6.2.2 NMR spectroscopy

When considering characterisation of compounds using NMR, bonding any phosphorus species directly to platinum has one advantage. Both Pt(0) and Pt(II) are diamagnetic and do not broaden the signal due to unpaired electrons.

In square planar platinum(II) complexes containing phosphane ligands (PR_3), the ^{31}P NMR spectrum of the complex provides valuable information about the *cis* or *trans* arrangement of the ligands. The isotope ^{195}Pt, I=1/2, constitutes 33.8% of naturally

occurring platinum; in a ^{31}P NMR spectrum of a complex such as $[PtCl_2(PEt_3)]_2$, there is spin-spin coupling between the ^{31}P and the ^{195}Pt nuclei which gives rise to satellite peaks. If the PR_3 group are mutually *trans*, the value of $J_{P\text{-}Pt} \approx 2000\text{-}3000$ Hz but if the ligands are *cis*, the coupling constant is much larger, $\approx 3000\text{-}3500$ Hz.[7] While the values vary somewhat, comparison of the ^{31}P NMR spectra of *cis* and *trans* isomers of a given complex enables the configuration to be assigned.

When two different phosphorus donors are present, as in the present work where PEt_3 is usually ligated to platinum because of the starting material used (section 6.2), the ^2J coupling between the phosphorus atom of the new phosphane ligand and the phosphorus from PEt_3 ($^2J_{P\text{-}P}$) shows a great difference: for the *trans* isomer $^2J_{P\text{-}P}$ varies between 400 and 800 Hz, whereas it is very small in the *cis* isomer (about 15Hz). The coupling constant between the phosphorus and the platinum ($^1J_{Pt\text{-}P}$) is revealed to be greater in the *cis* isomer ($^1J_{Pt\text{-}P}$ from 3000 to 6000 Hz) than in the *trans* isomer ($^1J_{Pt\text{-}P}$ from 2000 to 3000 Hz). Goodwin[8] and Roden[9] demonstrated that the value of the coupling constant also depends on the groups attached to phosphorus. They showed that the largest coupling constants were formed in the compounds where there were the greatest electron withdrawal, for example $^1J_{Pt\text{-}P}$ for $Ar'PCl_2$ is bigger that that for $Ar'PH_2$.

6.3 The "platinum dimer"

The platinum(II) dimer has been used initially in previous work on fluoromes and fluoroxyl systems because the diphosphene ArP=PAr did not react with similar Pt(II) compounds ($PtCl_2$, $PtCl_2(PhCN)_2$). This dimer is prepared in three steps according to the reaction shown in Equation 6.1.[10]

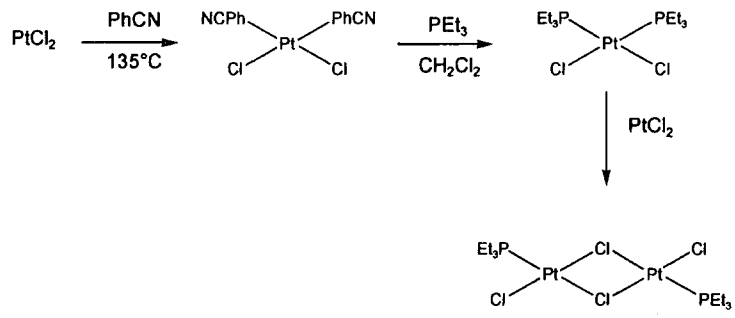

Equation 6.1: *Synthesis of Pt Dimer*

6.3.1 Reactions with low coordinate phosphorus species

The synthesis of this kind of complex involved the addition of one equivalent of Pt dimer to two equivalents of phosphorus compound in dichloromethane, at room temperature.

- with phosphanes

The platinum dimer can form complexes with phosphanes containing bulky electron-withdrawing substituents such as $ArPCl_2$, $ArPF_2$, $Ar'PCl_2$, etc. Goodwin[8] and Roden[9] have found that there are two possible isomeric products, the *cis* and *trans* complexes. The actual mechanism for the reaction is likely to be analogous to normal substitution in a square planar complex,[11] by formation of an initial five coordinate species, which then loses one of the original substituents to leave the square planar product. The mechanism proposed by Roden[9] is as follow:

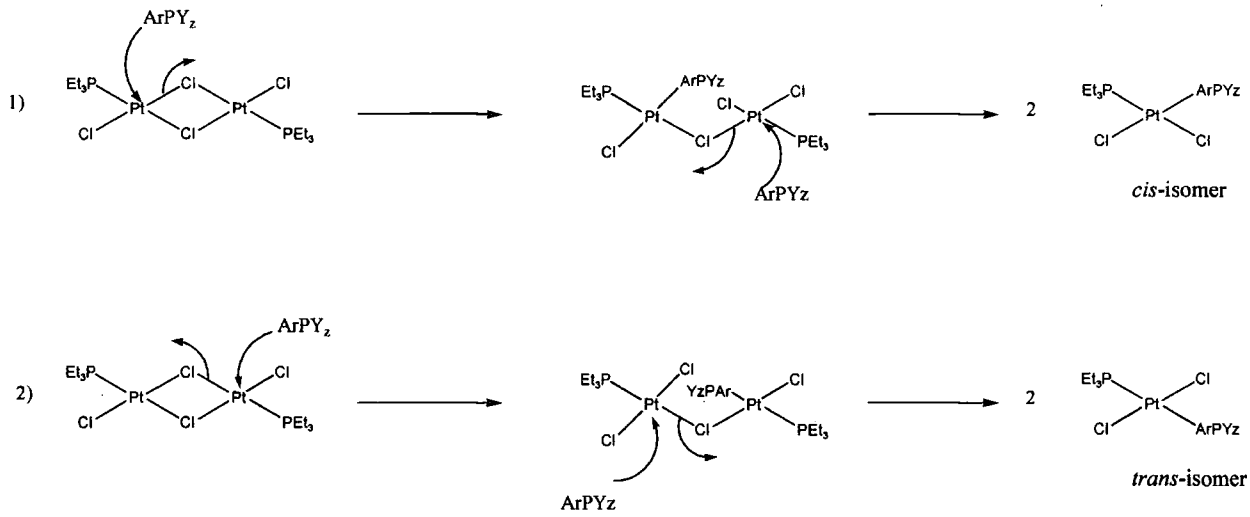

Figure 6.2: *Formation of the two possible isomers*

The initial product of the reaction is often the *trans* isomer but it rearranges to give the thermodynamically more favourable product, the *cis*-isomer. The formation of the *trans* isomer as the initial product is due to the *trans* effect, which is often seen in reactions of phosphanes with platinum complexes,[12] and this affects the reaction of the complex and the nature of the isomeric products.

Another factor could be that if the phosphane approaches on the opposite side of the molecule to the PEt_3 group, it is sterically more favourable to form the *trans* product first. It has been noticed that the time taken for the rearrangement varies with the phosphane. This could be due to:

- during the rearrangement, the steric bulk of the phosphane may influence the approach of the detached PEt_3 group. The larger the steric bulk of the phosphane, the more likely the PEt_3 group is to coordinate in the *trans* position. (Figure 6.3)
- the strength of the Pt-P bond may directly influence the formation of the necessary intermediate.

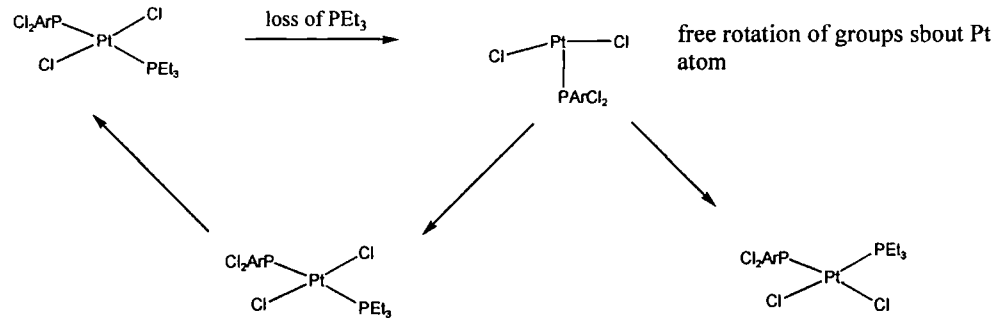

Figure 6.3: *Rearrangement of the initial trans product to give the thermodynamically more stable cis product.*

The intermediate species formed in these types of rearrangements has been shown to be three-coordinate.[9] This is formed by the loss of the most labile ligand on the platinum centre. The Pt-Cl bond are stronger than the Pt-P bonds, and X-ray studies on the compounds have shown that the PEt_3 groups bonded to the platinum are more weakly bound than electronegative phosphanes or phosphaalkenes.[9] This would imply that the Pt-PEt_3 bond is the weakest bond in the complex (the average Pt-PEt_3 bond length is 2.31Å, whereas it is ~2.18 Å for other phosphane ligands containing the strongly electronegative substituents Ar, Ar' or Ar"[9]).

- with diphosphenes

In complexation with diphosphenes, η^1-coordination is preferred.[13-15] The phosphorus atoms become inequivalent (even in a symmetrical diphosphene) so they are easily detectable in NMR spectroscopy. With unsymmetrical compounds, the coordination takes place at the less hindered phosphorus.[5]

6.4 *Synthesis of some Platinum-Phosphane Compounds*

6.4.1 Synthesis of the Pt dimer

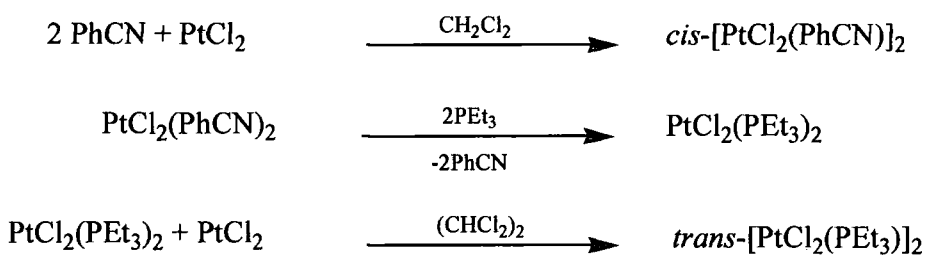

Equation 6.2: *Synthesis of trans-[$PtCl_2(PEt_3)]_2$*

$PtCl_2$ was dissolved in a CH_2Cl_2 solution of PhCN at 70°C, forming a yellow solution. As the solution cooled, yellow crystals formed and were isolated. The product $[PtCl_2(PhCN)_2]$ was then added to a solution of PEt_3 in dichloromethane. The resulting compound was dissolved at high temperature in a solution of $PtCl_2$ in $(CHCl_2)_2$ to form the Pt dimer. This was recrystallised from dichloromethane to give yellow crystals. The ^{31}P NMR of the Pt dimer showed a singlet at 11.6 ppm with platinum satellites ($^1J_{P\text{-}Pt}$ 3833.9 Hz) (Figure 6.4).

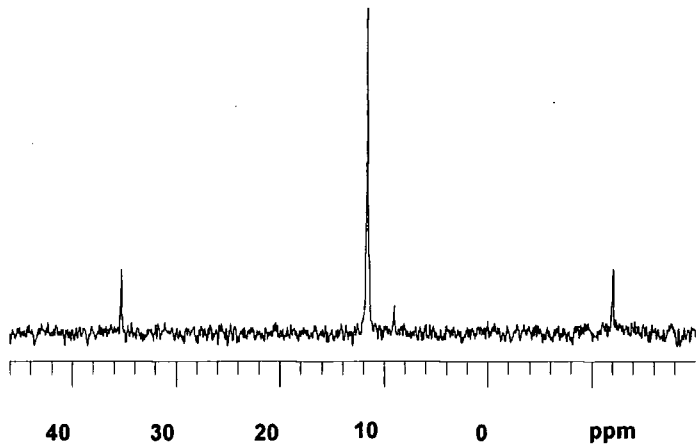

Figure 6.4: *^{31}P spectrum of $[PtCl_2(PEt_3)]_2$*

The structure has been determined in the department by A.S. Batsanov at 100K (Figure 6.5), but was also previously reported[16] at room temperature.

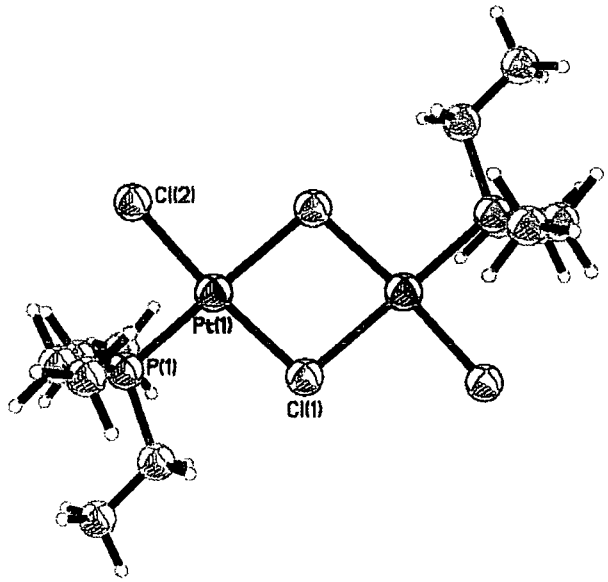

Figure 6.5: *Molecular structure of $[PtCl_2(PEt_3)]_2$*

As shown in Table 6.2, the difference in temperature has little effect on the structure.

	Room temperature[16]	100K
Pt-P	2.212(3)	2.2199(11)
Pt-Cl(1)	2.318(3)	2.3194(11)
Pt-Cl(2)	2.282(3)	2.2891(11)
P-Pt-Cl(1)	89.43(10)	89.03(4)
Cl(1)-Pt-Cl(2)	174.59(9)	175.00(4)
P-Pt-Cl(1)	179.07(9)	179.02(4)

Table 6.2: *Comparison of selected bond distances (Å) and angles (°) of $[PtCl_2(PEt_3)]_2$ at different temperatures.*

6.4.2 Reaction between Ar'Ar"PCl and Pt dimer

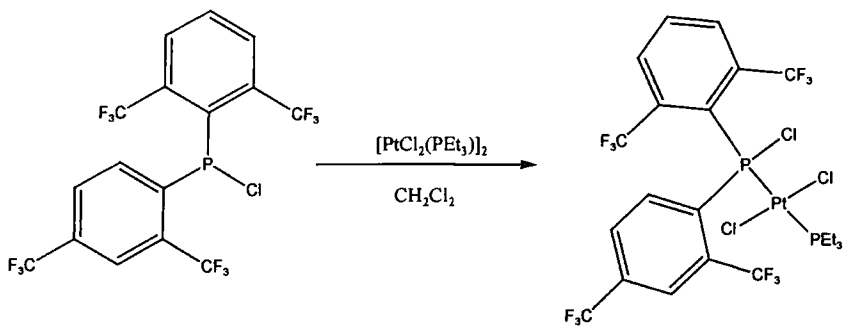

Equation 6.3: *Synthesis of trans-$[PtCl_2(PEt_3)(Ar'Ar"PCl)]$*

Ar'Ar"PCl was added to a solution of $[PtCl_2(PEt_3)]_2$ in $(CHCl_2)_2$ and the solution was allowed to stir for two days. The ^{31}P NMR shows a doublet with platinum satellites at 21.2 ppm ($^1J_{P\text{-}Pt}$ 2760.3Hz, $^2J_{P\text{-}P}$ 562.0 Hz) corresponding to the PEt_3 signal, and another doublet at 94.5 ppm ($^1J_{P\text{-}Pt}$ 2531.4 Hz, $^2J_{P\text{-}P}$ 562.0 Hz) for the phosphane. This reveals the complex to be a *trans* isomer.

The ^{19}F NMR spectrum exhibits two doublets at -53.4 (double intensity, $^{4}J_{P-F}$ 12.7 Hz) and -56.4 ($^{4}J_{P-F}$ 61.2 Hz) and a singlet at -62.8 ppm. As explained in chapter 4, there is a difference in the coupling from the CF_3 groups in the Ar' groups and the one in the Ar" moiety. All the CF_3 groups are inequivalent and this explains the difference in the coupling constant from one trifluoromethyl group to the other one. This confirms the results found by Roden.[9]

Stirring for a longer period did not allow the compound to rearrange to the *cis*-isomer. The NMR spectra did not show any change.

6.4.3 Reaction between Ar"$_2$PCl and [PtCl$_2$(PEt$_3$)]$_2$

The Pt dimer was added to a solution of Ar"$_2$PCl in dichloromethane and the resulting yellow solution was allowed to stir for a few days.

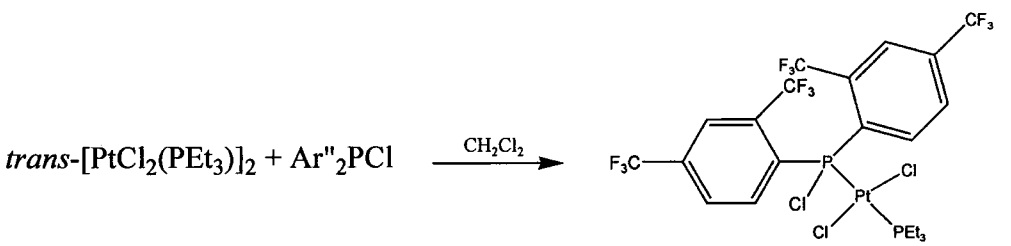

Equation 6.4: *Synthesis of trans-[PtCl$_2$(PEt$_3$)(Ar"$_2$PCl)]*

The ^{31}P NMR showed distinctive peaks with satellites, indicating the coordination of the phosphanes to the platinum. Resonances assignable to the PEt_3 group (δ 17.5 ppm, $^{2}J_{P-P}$ 562.2 Hz, $^{1}J_{Pt-P}$ 2752.4 Hz) showed the formation of a *trans* isomer. The signal for the phosphorus on the phosphane group was detected at 91.0 ppm as a doublet of septets ($^{2}J_{P-P}$ 563.3 Hz, $^{1}J_{Pt-P}$ 2685.9 Hz, $^{4}J_{P-F}$ 8.0 Hz).

The ^{19}F NMR spectrum exhibited a doublet at -55.7 ($^{4}J_{P-F}$ 7.3 Hz) and a singlet at -64.0 ppm.

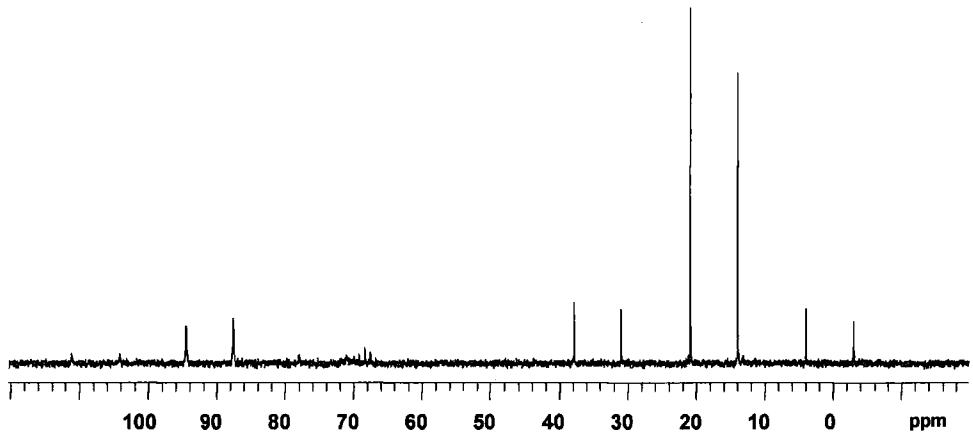

Figure 6.6: *^{31}P NMR spectrum of $[PtCl_2(PEt_3)(Ar''_2PCl)]$*

The solution was allowed to stir for two weeks to see if any rearrangement from a *trans* to a *cis* isomer occurred, but no changes were observed in the NMR spectrum.

6.4.4 Reaction between Ar''_2PH and $[PtCl_2(PEt_3)]_2$

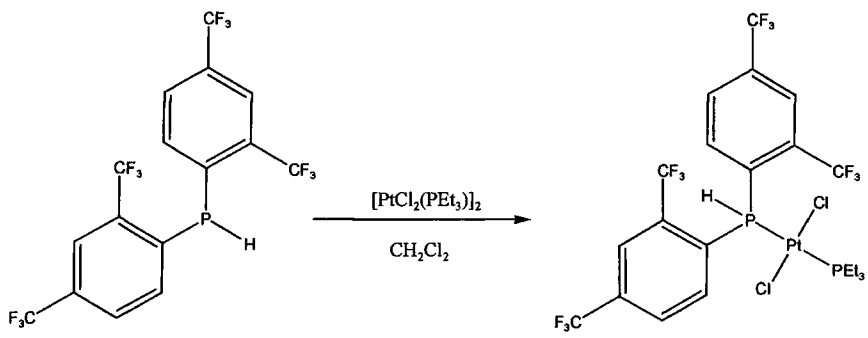

Equation 6.5: *Synthesis of $[PtCl_2(PEt_3)_2(Ar''_2PH)]$*

$[PtCl_2(PEt_3)]_2$ was added to an $Ar"_2PH$ solution in dichloromethane at room temperature. The resulting yellow solution was stirred for a few hours. The ^{31}P NMR spectrum showed the formation of the *trans* isomer, with two doublets with Pt satellites at 93.8 and 16.4 ppm.

	^{31}P		^{19}F	
	PEt_3	P	*o*-CF_3	*p*-CF_3
δ (ppm)	16.4	93.8	-57.8	-63.9
$^1J_{Pt-P}$ (Hz)	2551.7	2676.8	$^4J_{P-F}$ 2.8	
$^2J_{P-P}$ (Hz)	501.4	501.4		

Table 6.3: *$\delta^{31}P$ and ^{19}F NMR data for $[PtCl_2(PEt_3)(Ar"_2PH)]$*

6.4.5 Reaction between $ArPBr_2$ and $[PtCl_2(PEt_3)]_2$

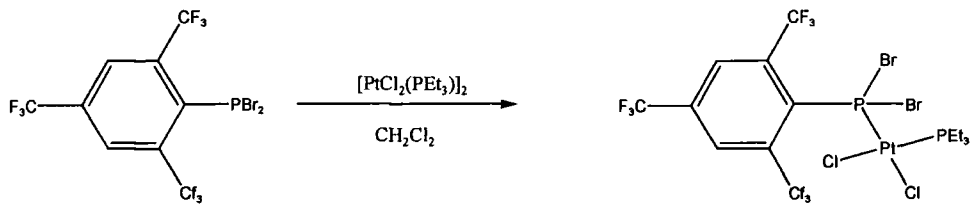

Equation 6.6: *Synthesis of $[PtCl_2(PEt_3)(ArPBr_2)]$*

The Pt dimer was added to a solution of $ArPBr_2$ in dichloromethane and the resulting yellow solution was allowed to stir for a month. NMR samples were made regularly to check any change in the reaction mixture.

The first complex formed was the *cis*-isomer. The ^{31}P NMR spectrum showed, for the PEt_3 group, a doublet with satellites at 16.6 ppm ($^1J_{Pt-P}$ 2966.4 Hz, $^2J_{P-P}$ 13.4 Hz), and the signal corresponding to the phosphorus from $ArPBr_2$ was a septet with platinum satellites at 90.5 ppm ($^1J_{Pt-P}$ 5287.5 Hz, $^4J_{P-F}$ 11.8 Hz). The ^{19}F NMR showed a doublet with

platinum satellites at -49.2 ppm ($^4J_{P-F}$ 12.4 Hz, $^5J_{Pt-F}$ 30.3 Hz, 6F, *o*-CF_3), and a singlet at -64.0 (3F, *p*-CF_3).

After a week new peaks started to appear in the spectra: in the ^{31}P NMR spectrum a doublet at 14.4 ppm ($^2J_{P-P}$791.8 Hz, $^1J_{P-Pt}$ 2731.6 Hz), indicating the presence of a *trans*-isomer, together with a weak doublet of multiplets at 92.4 ppm ($^2J_{P-P}$ 792.4 Hz). Unfortunately, the signal was too weak to be able to see any platinum satellites. The ^{19}F NMR spectrum displayed a doublet with platinum satellites at -49.8 ppm ($^4J_{P-F}$ 13.7 Hz, $^5J_{Pt-F}$ 30.5 Hz)

Spectra were recorded regularly and a number of new signals became visible in the phosphorus spectra, notably some multiplets at 145.8 ($^4J_{P-F}$ 61.0 Hz), 138.2 ($^4J_{P-F}$ 62.5 Hz), and 130.2 ($^4J_{P-F}$ 63.0 Hz) ppm. The chemical shifts and the coupling constants corresponding to these multiplets suggest the presence of $ArPCl_2$, ArPBrCl and $ArPBr_2$ respectively in solution. The ^{19}F NMR spectrum confirms this hypothesis, with the presence of doublets at -53.0, -53.4 and -53.5 ppm with coupling constants of 60.9, 61.6 and 62.9 Hz respectively. The existence of these species implies that halogen exchange occurs in solution between the chlorine of the platinum dimer and the bromine atoms of the phosphane.

Attempts to grow crystals out of the solution gave orange crystals (not suitable for X-ray diffraction). The ^{31}P NMR of these crystals consisted of a singlet at 10.9 ppm with Pt satellites ($^1J_{Pt-P}$ 3701 Hz) corresponding to the chemical shifts and coupling constant found in $[PtBr_2(PEt_3)]_2$. This also shows that a Br/Cl exchange has occurred.

Usually, a *cis*-complex is the most thermodynamically stable compound and does not rearrange itself to the *trans* isomer. Initial formation of a *cis*-complex, however, followed by halogen exchange, allows the formation of a *trans* complex.

6.4.6 Reaction between Ar'PBr_2/Ar"PBr_2 and $[PtCl_2(PEt_3)]_2$

$[PtCl_2(PEt_3)]_2$ was added to a solution of Ar'PBr_2/Ar"PBr_2 in dichloromethane. The solution was stirred for three weeks until no change was observed in the spectra.

Initially, the ^{31}P NMR spectrum showed the formation of two *cis*-isomers. (Table 6.4) Unfortunately, the signals from coordinated Ar"PBr_2 were to weak to allow determination of $^{1}J_{Pt\text{-}P}$.

	Ar'PBr_2		Ar"PBr_2	
	PEt_3	P	PEt_3	P
δ (ppm)	15.7	92.2	15.4	89.0
$^{1}J_{Pt\text{-}P}$ (Hz)	3004	5274.1	3174.7	
$^{2}J_{P\text{-}P}$ (Hz)	13.9	14.2	10.8	

Table 6.4: *Initial $\delta^{31}P$ NMR data for [$PtCl_2(PEt_3)$(Ar'PBr_2)] and [$PtCl_2(PEt_3)$(Ar"PBr_2)]*

In the ^{19}F NMR spectrum, two doublets and one singlet were observed.

	Ar'PBr_2	Ar"PBr_2	
		o-CF_3	*p*-CF_3
δ (ppm)	-49.0	-55.5	-63.4
$^{4}J_{P\text{-}F}$ (Hz)	10.6	6	
$^{5}J_{Pt\text{-}F}$ (Hz)	28.8	?	

Table 6.5: *δ^{19} F NMR data for [$PtCl_2(PEt_3)$(Ar'PBr_2)] and [$PtCl_2(PEt_3)$(Ar"PBr_2)]*

After a few days, many other peaks appeared in the spectrum. In the PEt_3 chemical shift area, (~11-17 ppm), six different signals with Pt satellites were distinguished but these could not be assigned (Table 6.6). The observation of new signals at 69.7 (septet) and 67.7 (quartet) ppm, with coupling constants of 65.5 and 61.3 Hz respectively, suggests the possible formation of Ar'PClBr and Ar"PClBr. The ^{19}F NMR spectrum also contained a number of new doublets.

δ (ppm)	$^{1}J_{Pt\text{-}P}$ (Hz)	$^{2}J_{P\text{-}P}$ (Hz)	Isomer
15.4	3210.2	13.7	*cis*
12.9	2573.5	561.12	*trans*
13.4	3204.1	15.2	*cis*
13.0	3204.1	10.7	*cis*

Table 6.6: *^{31}P chemical shifts and coupling constants of different products of the reaction between Ar'PBr_2/Ar"PBr_2 and $[PtCl_2(PEt_3)]_2$*

As already discussed in the reaction with $ArPBr_2$ some Cl/Br exchange seems to occur when reacting the Pt chloride dimer with a bromophosphane.

6.4.7 Reaction between Ar"$_2$PBr and $[PtCl_2(PEt_3)]_2$

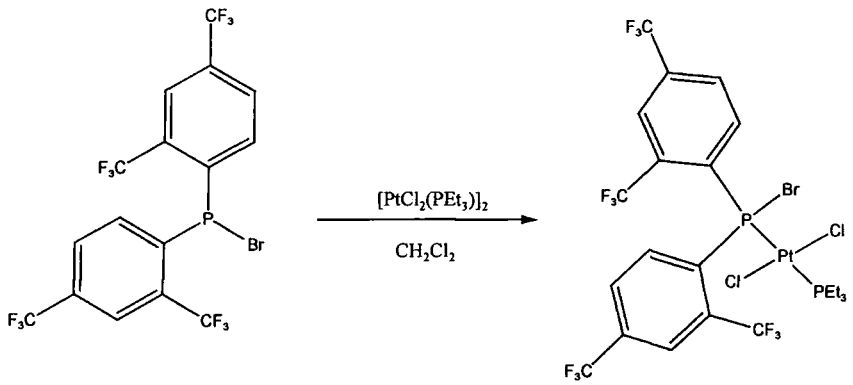

Equation 6.7: *Synthesis of $[PtCl_2(PEt_3)(Ar"_2PBr)]$*

A solution of $[PtCl_2(PEt_3)]_2$ in dichloromethane was added to a solution of Ar"$_2$PBr. The ^{31}P NMR spectrum showed the formation of a *trans* complex: δ 12.9 ppm (d, $^{2}J_{P\text{-}P}$ 562.5 Hz, $^{1}J_{P\text{-}Pt}$ 2654 Hz) (Figure 6.7); δ 86.3 ppm (d of septets, $^{2}J_{P\text{-}P}$ 562.3 Hz, $^{1}J_{Pt\text{-}P}$ 2637.6 Hz, $^{4}J_{P\text{-}F}$ 5.5 Hz) (Figure 6.8).

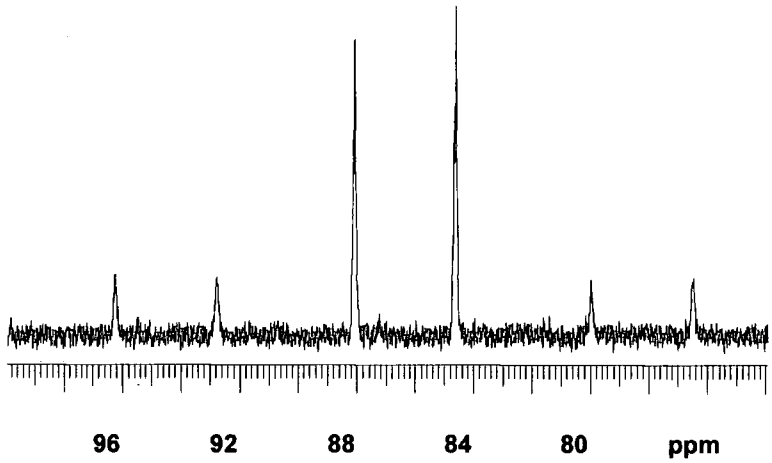

Figure 6.7: *^{31}P NMR spectrum of $[PtCl_2(PEt_3)(Ar"_2PBr)]$. (Phosphane region)*

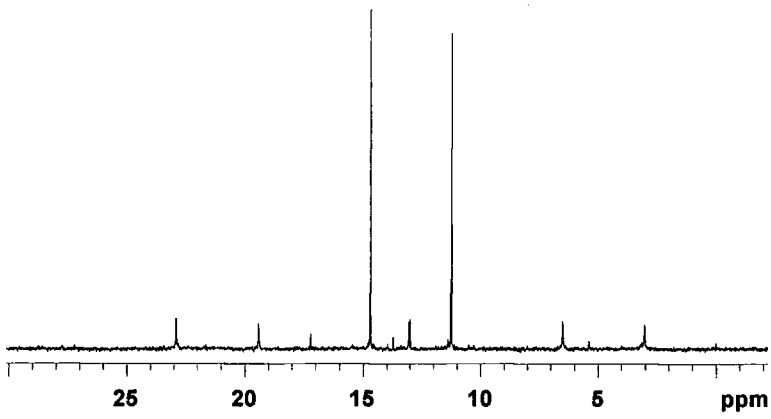

Figure 6.8: *^{31}P NMR spectrum of the reaction between $[PtCl_2(PEt_3)(Ar"_2PBr)](PEt_3$ region)*

The ^{19}F NMR spectrum displayed a doublet with platinum satellites at -55.3 ($^4J_{P-F}$ 6.0Hz) and a singlet at -63.8ppm.

This sample also showed some halogen exchange after being stirred for a while.

All the bromophosphane derivatives reacted with the "platinum dimer" seem to undergo some exchange between the bromine and the chlorine atoms of the platinum compounds. To prevent this exchange from happening, the bromophosphane compounds were reacted with the platinum bromide dimer $[PtBr_2(PEt_3)]_2$.

6.4.8 Synthesis of $[PtBr_2(PEt_3)]_2$

$PtBr_2$ was dissolved in a solution of PhCN at 70°C, forming a yellow solution. As the solution cooled yellow crystals formed and were isolated. The product, $[PtBr_2(PhCN)_2]$, was then added to a solution of PEt_3. The resulting compound was then dissolved at high temperature in a solution of $PtBr_2$ in $(CHCl_2)_2$ to form the Pt dimer. The ^{31}P NMR of the Pt dimer showed a singlet at 10.9 ppm with platinum satellites ($^1J_{P\text{-}Pt}$ 3701 Hz). The chemical shift and coupling constant are very similar to those found in $[PtCl_2(PEt_3)]_2$. Crystals were submitted for X-ray diffraction and the structure was ascertained at 120 K. (Figure 6.9). Selected bond distances and angles are listed in Table 6.7 and compared with the values found for $[PtCl_2(PEt_3)]_2$. The Pt-P bond distances are slightly longer in the bromide derivative, due to more steric demand.

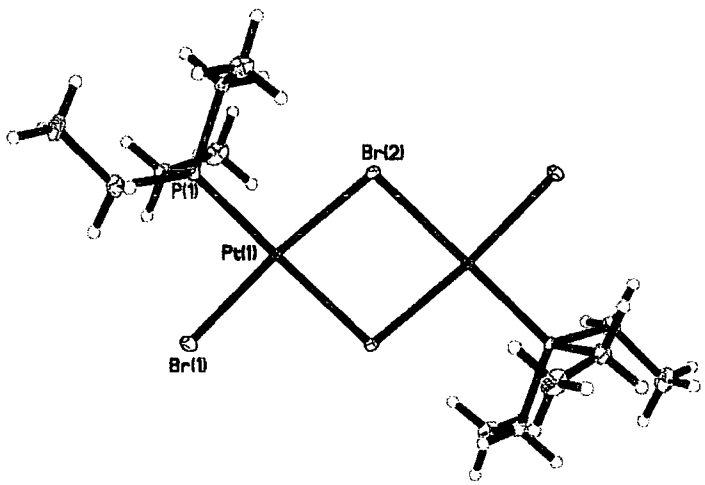

Figure 6.9: *Molecular structure of* $[PtBr_2(PEt_3)]_2$

	$[PtCl_2(PEt_3)]_2$ at 100K	$[PtBr_2(PEt_3)]_2$ 120K
Pt-P	2.2199(11)	2.2265(12)
Pt-X(1)	2.3194(11)	2.4229(7)
Pt-X(2)	2.2891(11)	2.4455(7)
P-Pt-X(1)	89.03(4)	90.54(3)
X(1)-Pt-X(2)	175.00(4)	173.294(17)
P-Pt-X(2)	95.91(4)	95.26(3)

Table 6.7: *Comparison of crystal data between $[PtCl_2(PEt_3)]_2$ and $[PtBr_2(PEt_3)]_2$*

6.4.9 Reaction between $ArPBr_2$ and $[PtBr_2(PEt_3)]_2$

A solution of $[PtBr_2(PEt_3)]_2$ in CH_2Cl_2 was added to a solution of $ArPBr_2$ in dichloromethane. The solution was stirred for 6 hours and NMR spectra were monitored regularly for four weeks. After just a few hours, the spectrum did not show any signs of the formation of a complex. After 10 days, the ^{31}P NMR spectrum displayed peaks corresponding to the presence of a *cis*-isomer.

	^{31}P		^{19}F	
	PEt_3	P	*o*-CF_3	*p*-CF_3
δ (ppm)	15.5	79.6	-52.9	-64.1
$^1J_{Pt-P}$ (Hz)	3221.1	5681.8	$^4J_{P-F}$ 4.5	
$^2J_{P-P}$ (Hz)	18.4	18.3		

Table 6.8: *$\delta^{31}P$ and ^{19}F NMR data for $[PtBr_2(PEt_3)(ArPBr_2)]$*

6.4.10 Reaction between $Ar"_2PBr$ and $[PtBr_2(PEt_3)]_2$

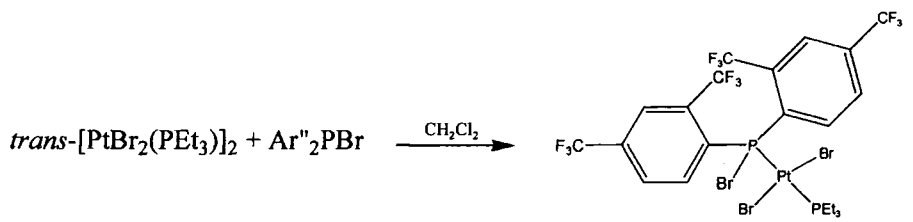

Equation 6.8: *Synthesis of $[PtBr_2(PEt_3)(Ar"_2PBr)]$*

A solution of $[PtBr_2(PEt_3)]_2$ in CH_2Cl_2 was added to a solution of $Ar"_2PBr$ in dichloromethane. The spectrum ran after just a few hours showed the formation of a *trans* complex but some peak from the starting material remained. After 10 days, the ^{31}P NMR spectrum displayed peaks corresponding to the presence of a *trans*-isomer

	^{31}P		^{19}F	
	PEt_3	P	*o*-CF_3	*p*-CF_3
δ (ppm)	12.0	72.0	-54.7	-63.9
$^1J_{Pt-P}$ (Hz)	2691.8	2516.5	$^4J_{P-F}$ 2.7	
$^2J_{P-P}$ (Hz)	562.8	562.4		

Table 6.9: *$\delta^{31}P$ and ^{19}F NMR data for $[PtBr_2(PEt_3)(Ar"_2PBr)]$*

The *cis*-isomer has not been formed.

6.4.11 Reaction between $Ar'PBr_2$/$Ar"PBr_2$ and $[PtBr_2(PEt_3)]_2$

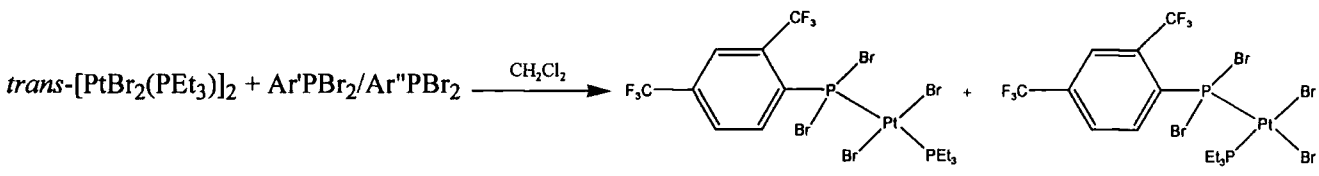

Equation 6.9: *Synthesis of $[PtBr_2(PEt_3)(Ar'PBr_2)]$ and $[PtBr_2(PEt_3)(Ar"PBr_2)]$*

A solution of $[PtBr_2(PEt_3)]_2$ in CH_2Cl_2 was added to a solution of $Ar'PBr_2/Ar''PBr_2$ in dichloromethane. The ^{31}P NMR spectrum showed a number of peaks, indicating the formation of at least three complexes, two *cis*-isomers and a *trans*-isomer.

	$Ar'PBr_2$ *cis*		$Ar''PBr_2$ *cis*		$Ar''PBr_2$ *trans*	
	PEt_3	P	PEt_3	P	PEt_3	P
δ (ppm)	13.5	113.4	14.1		11.9	108.6
$^1J_{Pt-P}$ (Hz)	3211.5		3201.7		2846.5	2756.7
$^2J_{P-P}$ (Hz)	11.5		11.6		682.7	682.3

Table 6.10: *δ ^{31}P NMR data for $[PtBr_2(PEt_3)(Ar''PBr_2)]$ and $[PtBr_2(PEt_3)(Ar'PBr_2)]$*

Because of weak signals, $^1J_{Pt-P}$ for the *cis* complexes could not be determined. The signals corresponding to the phosphorus of the phosphane ligands have not been observed for *cis*-$Ar''PBr_2$.

Signals corresponding to $Ar'PBr_2$ were still visible in the ^{31}P and ^{19}F NMR spectra. $Ar''PBr_2$ formed a *cis* and a *trans* complexes whereas $Ar'PBr_2$ only formed a *trans* complex. ^{19}F NMR data are listed in Table 6.11.

	$Ar'PBr_2$ *cis*	$Ar''PBr_2$ *trans*		$Ar''PBr_2$ *cis*	
	o-CF_3	*o*-CF_3	*p*-CF_3	*o*-CF_3	*p*-CF_3
δ (ppm)	-52.8	-47.6	-62.7	-50.8	-63.7
$^4J_{P-F}$ (Hz)	11.1	8.5		2.8	
$^5J_{Pt-F}$ (Hz)	30.3	32.5			

Table 6.11: *δ ^{19}F data for $[PBrl_2(PEt_3)(Ar''PBr_2)]$ and $[PBrl_2(PEt_3)(Ar'PBr_2)]$*

6.5 Attempted synthesis of Platinum-Arsane Compounds

$[PtBr_2(PEt_3)]_2$ was added to a series of arsenic derivatives such as $ArAsCl_2$, Ar_2AsCl and Ar'Ar"AsCl. No reaction was apparent from the ^{19}F NMR spectra, even after refluxing over a number of days.

The "platinum dimer" does not seem to coordinate to these arsenic derivatives, although many As-Pt complexes have been reported in the literature.

6.6 Discussion

6.6.1 Change in the chemical shifts

Chemical shifts upon bonding to platinum are listed in Tables 6.12 and 6.13.

Phosphane	Isomer	Phosphane	δ before bonding (ppm)	δ after bonding (ppm)
Ar'Ar"PCl	*trans*	Ar'Ar"PCl	67.3	94.5
$Ar"_2PCl$	*trans*	$Ar"_2PCl$	68.3	91.0
$Ar"_2PH$	*trans*	$Ar"_2PH$	-48.7	93.8
$Ar"_2PBr$	*trans*	$Ar"_2PBr$	57.4	86.3
$ArPBr_2$	*cis*	$ArPBr_2$	130.1	90.5
$Ar'PBr_2$	*cis*	$Ar'PBr_2$	134.1	92.2
$Ar"PBr_2$	*cis*	$Ar"PBr_2$	141.0	89.0

Table 6.12: *Comparison of the chemical shifts upon bonding to the chloro-dimer*

Phosphane	Isomer	Phosphane	δ before bonding (ppm)	δ after bonding (ppm)
$Ar"_2PBr$	*trans*	$Ar"_2PBr$	57.4	72.0
$ArPBr_2$	*cis*	$ArPBr_2$	130.1	79.6
$Ar'PBr_2$	*cis*	$Ar'PBr_2$	134.1	113.4
$Ar"PBr_2$	*trans*	$Ar"PBr_2$	141.0	108.6

Table 6.13: *Comparison of the chemical shifts upon bonding to bromo-dimer*

When bonding to platinum, the chemical shift of the monosubstituted phosphanes moves to a lower frequency. There is an increase of electron density at the phosphorus centre, due to the back donation of electrons from the platinum to the phosphorus.

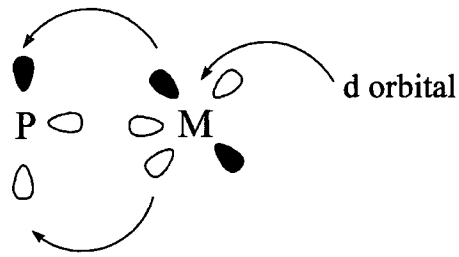

Figure 6.10: *Back donation of electrons from the metal to the phosphorus atom*

When the platinum dimer is coordinated to a disubstituted derivative, the chemical shift moves to a higher frequency. The presence of two aryl rings will increase the electron-withdrawing effect, and therefore decrease the electron density on the phosphorus.

The difference in chemical shifts for $Ar"_2PH$ is much larger than in the other cases. There, the dominant factor could be the σ-bonding. The hydrogen atom has approximately the same electronegativity as phosphorus,[17] and will not have back donation from the platinum atom.

All phosphorus compounds containing two bulky substituents (Ar' or Ar") form *trans*-isomers with the platinum dimer. No rearrangement to the *cis*-isomer has been observed. This is probably due to the steric hindrance imposed by the presence of the two fluoroxyl groups.

6.6.2 Comparison of the coupling constants

The coupling constants ($^1J_{Pt-P}$ and $^2J_{P-P}$) of the prepared complexes are listed in Table 6.14.

The magnitude of $^1J_{P-Pt}$ in phosphane complexes is proportional to the s-character of the phosphorus lone pair.[18] When the second phosphorus ligand is *cis* to PEt_3, the J_{Pt-P} value is larger than when the two phosphorus ligands have a *trans* configuration. In the latter case, the ligands compete for electrons, giving a *trans* influence[19] and hence reducing the $^1J_{P-Pt}$ coupling.

The sequence of phosphorus ligands, in term of increasing $^1J_{Pt-P}$ values, for the *cis* complexes is as follows:

$ArPH_2$	<Ar'Ar"PCl	$<Ar'PCl_2$	$<Ar'PBr_2$	$<Ar"PCl_2$	$<ArPBr_2$	$<ArPCl_2$	$<Ar'PF_2$	$<ArPF_2$
3809	4783	5260	5274	5488	5491	5511	6195	6252

H<Cl~Br<F

Ar'<Ar"<Ar

The coupling constant generally increases with the electronegativity of the atom(s) X bonded to the phosphorus atom. The largest coupling constant appears in the compounds where there is the greatest electron withdrawal from the groups attached to the phosphorus, with a $^1J_{Pt-P}$ range from 3800 to 6200 Hz. This increase is due to the amount of back donation occurring from the platinum to the phosphorus atom.

Compounds	Isomer	$^1J_{P-Pt}$ (Hz)	$^2J_{P-P}$ (Hz)	Ref
$ArPCl_2$	*cis*	5511.0		8
	trans	2885.8	679.0	
$ArPBr_2$	*cis*	5491.2	9.9	
	trans		792.4	8
$ArPF_2$	*cis*	6252.1		8
$ArPH_2$	*cis*	3809.1	20.6	8
$Ar'PCl_2$	*cis*	5260		9
$Ar"PCl_2$	*cis*	5488.1		9
$Ar'PBr_2$	*cis*	5274.1	14.2	This work
	trans			
$Ar"PBr_2$	*cis*		10.8	This work
$Ar'PF_2$	*cis*	6194.8	42.6	9
	trans	2723	690.6	
Ar'Ar"PCl	*cis*	4783.3		9
	trans	2531.4	562.0	This work
$Ar"_2PCl$	*trans*	2685.9	563.3	This work
$Ar"_2PH$	*trans*	2676.8	501.4	This work
$Ar"_2PBr$	*trans*	2637.6	562.3	This work

Table 6.14: *Coupling constant data for some Pt(II) complexes of phosphanes with Ar, Ar' or Ar" substituents*

For the first time in this kind of complex, coupling between fluorine atoms and the platinum has been observed in the ^{19}F NMR spectrum. The $^{5}J_{Pt\text{-}F}$ is about 30 Hz.

Some $J_{Pt\text{-}F}$ couplings constant have been reported in the literature. For a trifluoromethyl triphospholene[a] complex, a through space Pt---F interaction is observed with a coupling constant of 11 Hz.[20] Some short P---F contacts have been observed in all the structurally characterised phosphane complexes, and it is possible that the $J_{Pt\text{-}F}$ coupling come from some through space interaction between the fluorines of the *o*-CF_3 groups and the Pt atom. This could be confirmed by X-ray analysis, but unfortunately all crystals grown were not suitable.

6.7 Experimental

6.7.1 Introduction

- NMR spectroscopy

The ^{31}P NMR spectra of phosphorus-containing starting materials were checked, to confirm the absence of any major impurities. ^{19}F NMR spectra were recorded on a Varian Mercury 200 or Varian VXR 400 Fourier-transform spectrometer at 188.18 and 376.35 MHz respectively. ^{31}P NMR spectra were recorded on the same instruments at 80.96 or 161.91 MHz. Chemical shifts were measured relative to external $CFCl_3$ (^{19}F) or 85% H_3PO_4 (^{31}P), with the higher frequency direction taken as positive.

- X-ray crystallography

Single crystal X-ray diffraction experiments were carried out at low temperature, 100 to 120 K, using graphite monochromated Mo Kα radiation (λ = 0.71073) on a Bruker SMART (CCD 1 K area detector) diffractometer equipped with a Cryostream N_2 flow cooling device.[21] Series of narrow ω-scans (0.3°) were performed at several φ-settings in such a way as to cover a sphere of data to a maximum resolution between 0.70 and 0.77 Å. Cell parameters were determined and refined using the SMART software,[22] and raw

[a] triphospholene: $(CF_3)P(CF_3)P(CF_3)P(CF_3)C{=}C(CF_3)$

frame data were integrated using the SAINT program.[23] The structures were solved by direct methods and refined by full-matrix least squares on F^2 using SHELXTL software.[24]

6.7.2 Synthesis of *cis*-[$PtCl_2(PhCN)_2$]

$$2PhCN + PtCl_2 \longrightarrow \textit{cis}\text{-}[PtCl_2(PhCN)]_2$$

$PtCl_2$ (2.09, 7.8 mmol) was added to PhCN (20 ml) and was heated to 100°C for half an hour, yielding a bright yellow solution. This solution was cooled down and a yellow precipitate appeared. The solution was then filtered and the solid washed with petroleum ether and dried under vacuum. Yield 3.0g (95%).

Elemental analysis; Calc C 35.60, H 1.91, N 5.94%; Found C 35.63, H 2.10, N 5.93%

6.7.3 Synthesis of *cis*-[$PtCl_2(PEt_3)_2$]

$$PtCl_2(PhCN)_2 \xrightarrow[-2PhCN]{2PEt_3} PtCl_2(PEt_3)_2$$

$PtCl_2(PhCN)_2$ (2.2g, 4.66 mmol) was dissolved in CH_2Cl_2 (15ml). PEt_3 (1.1g, 2.86ml, 9.33 mmol) was added to the solution and the reaction was stirred during 3 hours. Solvent was removed in vacuo and the solid obtained washed twice with hexanes (20ml). A white solid appeared which was dried in vacuo. Yield 2.05g (88%)

Elemental analysis: Calc C 28.70, H 6.02 %; Found C 29.33, H 6.19 %

6.7.4 Synthesis of *trans*-$[PtCl_2(PEt_3)]_2$

$$PtCl_2(PEt_3)_2 + PtCl_2 \longrightarrow \textit{trans}\text{-}[PtCl_2(PEt_3)]_2$$

Cis-$PtCl_2(PEt_3)_2$ (2.04 g, 2.6 mmol) was added to a solution of $PtCl_2$ (1.46 g, 5.3 mmol) dissolved in $(CHCl_2)_2$ and heated to 150°C during 2 hours. After cooling, yellow crystals appeared. The solvent was removed under vacuum and the crystals were purified by recrystallisation from CH_2Cl_2. Yield 3.15g (77.5%)

Elemental analysis: Calc C 18.71, H 3.91%; Found C 18.74, H 3.95%

^{31}P NMR ($CDCl_3$): δ11.6 (singlet with Pt satellites, $^1J_{Pt\text{-}P}$ 3833.9 Hz) ppm.

6.7.5 Synthesis of *trans*-$[PtCl_2(PEt_3)_2(Ar'Ar''PCl)]$

$$Ar'Ar''PCl \xrightarrow{[PtCl_2(PEt_3)]_2} [PtCl_2(PEt_3)(Ar'Ar''PCl)]$$

A solution of $[PtCl_2(PEt_3)]_2$ (0.68 g, 0.10 mmol) in dichloromethane was added to a solution of Ar'Ar"PCl (0.1 g, 0.2 mmol) in dichloromethane. The solution was stirred overnight.

^{31}P NMR: δ 94.5 (d of septets with Pt satellites, $^1J_{P\text{-}Pt}$2531.4 Hz, $^2J_{P\text{-}P}$562.0 Hz), 21.2 (d with Pt satellites, $^1J_{Pt\text{-}P}$ 2760.3 Hz, $^2J_{P\text{-}P}$562.0 Hz) ppm; **^{19}F NMR**: δ -53.4 (d, $^4J_{P\text{-}F}$ 12.7 Hz, 6F, *o*-CF_3), -56.4 (d, $^4J_{P\text{-}F}$ 61.2, 3F, *o*-CF_3), -62.8 (s, 3F, *p*-CF_3) ppm.

6.7.6 Synthesis of *trans*-$[PtCl_2(PEt_3)(Ar''_2PCl)]$

$$Ar''_2PCl \xrightarrow{[PtCl_2(PEt_3)]_2} [PtCl_2(PEt_3)(Ar''_2PCl)]$$

A solution of $[PtCl_2(PEt_3)]_2$ (0.68 g, 0.10 mmol) in dichloromethane was added to a solution of $Ar"_2PCl$ (0.10 g, 0.20 mmol) in dichloromethane. The solution was stirred overnight.

^{31}P NMR: δ 91.0 (d of septets with Pt satellites, $^1J_{Pt\text{-}P}$ 2685.9 Hz, $^2J_{P\text{-}P}$ 563.3 Hz, $^4J_{P\text{-}F}$ 8.0 Hz), 17.5 (d with Pt satellites, $^1J_{Pt\text{-}P}$ 2752.4 Hz, $^2J_{P\text{-}P}$ 562.2 Hz) ppm; **^{19}F NMR:** δ-55.7 (d, $^4J_{P\text{-}F}$ 7.3 Hz, 6F, *o*-CF_3), -64.0 (s, 6F, *p*-CF_3) ppm.

6.7.7 Synthesis of *trans*-[$PtCl_2(PEt_3)(Ar"_2PH)$]

$$Ar"_2PH \xrightarrow{[PtCl_2(PEt_3)]_2} [PtCl_2(PEt_3)(Ar"_2PH)]$$

$[PtCl_2(PEt_3)]_2$ (0.36g, 0.43 mmol) was added to a solution of $Ar"_2PH$ (0.40g, 0.87 mmol) in dichloromethane. The solution was stirred overnight.

^{31}P NMR (CH_2Cl_2): δ 93.8 (d with Pt satellites, $^1J_{P\text{-}Pt}$ 2676.8 Hz, $^2J_{P\text{-}P}$ 501.4 Hz), 16.4 (d with Pt satellites, $^1J_{Pt\text{-}P}$ 2551.7 Hz, $^2J_{P\text{-}P}$ 501.4 Hz) ppm; **^{19}F NMR**: δ-57.8 (d, $^4J_{P\text{-}F}$ 2.8 Hz, 6F, *o*-CF_3), -63.9 (s, 6F, *p*-CF_3)

6.7.8 Synthesis of *cis*-[$PtCl_2(PEt_3)(ArPBr_2)$]

$$ArPBr_2 \xrightarrow{[PtCl_2(PEt_3)]_2} [PtCl_2(PEt_3)(ArPBr_2)]$$

$[PtCl_2(PEt_3)]_2$ (0.37 g, 0.48 mmol) was added to a solution of $ArPBr_2$ (0.45 g, 0.96 mmol). The solution was stirred for a month.

^{31}P NMR ($CDCl_3$): δ 90.5 (septet with Pt satellites, $^1J_{Pt\text{-}P}$ 5287.5 Hz, $^4J_{P\text{-}F}$ 11.8 Hz), 16.6 (d with Pt satellites, $^1J_{Pt\text{-}P}$ 2966.4 Hz, $^2J_{P\text{-}P}$ 13.4 Hz) ppm; **^{19}F NMR** ($CDCl_3$): δ-49.2 (d with Pt satellites, $^4J_{P\text{-}F}$ 12.4Hz, $^5J_{Pt\text{-}F}$ 30.3 Hz, 6F, *o*-CF_3), -64.0 (s, 3F, *p*-CF_3) ppm.

6.7.9 Synthesis of *cis*-[$PtCl_2(PEt_3)(Ar"PBr_2)$]and *cis*-[$PtCl_2(PEt_3)(Ar'PBr_2)$]

$$Ar'PBr_2 + Ar"PBr_2 \xrightarrow{[PtCl_2(PEt_3)]_2} [PtCl_2(PEt_3)(Ar'PBr_2)] + [PtCl_2(PEt_3)(Ar"PBr_2)]$$

$[PtCl_2(PEt_3)]_2$ (0.22 g, 0.42 mmol) was added to a solution of $Ar'PBr_2$/ $Ar"PBr_2$ (0.34g, 0.84 mmol) in dichloromethane. The solution was stirred during a few days. **^{31}P NMR** (CH_2Cl_2): *cis*-[$PtCl_2(PEt_3)(Ar"PBr_2)$]: δ 89.0 (s with Pt satellites, $^1J_{P\text{-}Pt}$? Hz), 15.4 (d with Pt satellites, $^1J_{P\text{-}Pt}$ 3174.7 Hz, $^2J_{P\text{-}P}$10.8 Hz) ppm; *cis*-[$PtCl_2(PEt_3)(Ar'PBr_2)$]: δ 92.2 (s with Pt satellites, $^1J_{P\text{-}Pt}$ 5274.1 Hz, $^2J_{P\text{-}P}$ 14.2 Hz), 15.7 (d with Pt satellites, $^1J_{P\text{-}Pt}$ 3004 Hz, $^2J_{P\text{-}P}$ 13.9 Hz); **^{19}F NMR** (CH_2Cl_2): *cis*-[$PtCl_2(PEt_3)(Ar"PBr_2)$]: δ-55.5 (d, $^4J_{P\text{-}F}$ 6Hz, 3F, *o*-CF_3), -63.4(s, 3F, *p*-CF_3) ppm; *cis*-[$PtCl_2(PEt_3)(Ar'PBr_2)$]: δ-49.0 (d, $^4J_{P\text{-}F}$ 10.6 Hz, $^5J_{Pt\text{-}F}$ 28.8 Hz, 6F, *o*-CF_3) ppm.

6.7.10 Synthesis of *trans*-[$PtCl_2(PEt_3)(Ar"_2PBr)$]

$$Ar"_2PBr \xrightarrow{[PtCl_2(PEt_3)]_2} [PtCl_2(PEt_3)(Ar"_2PBr)]$$

$[PtCl_2(PEt_3)]_2$ (0.17g, 0.24 mmol) was added to a solution of $Ar"_2PBr$ (0.26g, 0.48 mmol) in dichloromethane. The solution was stirred during three days.

^{31}P NMR (CH_2Cl_2): δ 86.3 (d of septets with Pt satellites, $^1J_{Pt\text{-}P}$ 2637.6 Hz, $^2J_{P\text{-}P}$ 562.3 Hz, $^4J_{P\text{-}F}$ 5.5 Hz), 12.9 (d with Pt satellites, $^1J_{Pt\text{-}P}$ 2654.0 Hz, $^2J_{P\text{-}P}$ 562.5 Hz) ppm; **^{19}F NMR**: δ-55.3 (d with Pt satellites, $^4J_{P\text{-}F}$ 7.5 Hz, $^5J_{Pt\text{-}F}$ 75.8 Hz, 6F, *o*-CF_3), -63.8 (s, 6F, *p*-CF_3)

6.7.11 Synthesis of *cis*-[$PtBr_2(PhCN)_2$]

$$2\ PhCN + PtBr_2 \longrightarrow \textit{cis}\text{-}[PtBr_2(PhCN)]_2$$

$PtBr_2$ (1.48g, 4.2 mmol) was added to PhCN (10ml) and was heated to 100°C for half an hour, yielding a bright orange solution. This solution was cooled down and a yellow precipitate appeared. The solution was then filtered and the solid washed with petroleum ether and dried under vacuum. Yield 1.89g (81%).

Elemental analysis for $C_{14}H_5Br_2N_2Pt$ (556): Calc C 30.27, H 1.44, N 5.01%; Found C 30.21, H 1.79, N 4.95%.

6.7.12 Synthesis of *cis*-[$PtBr_2(PEt_3)_2$]

$$PtBr_2(PhCN)_2 \xrightarrow[-2PhCN]{2PEt_3} PtBr_2(PEt_3)_2$$

$PtBr_2(PhCN)_2$ (1.77g, 3.18 mmol) was dissolved in CH_2Cl_2 (15ml). PEt_3 (1.75g, 2.18 ml, 6.36 mmol) was added to the solution and the reaction was stirred during 3 hours. Solvent was removed in vacuo and the solid obtained washed twice with hexanes (20 ml). A white solid appeared which was dried in vacuo. Yield 1.48g (83%).

Elemental analysis for $C_{12}H_{30}Br_2P_2Pt$ (591): Calc C 24.38, H 5.11%; Found C 28.26, H 6.30%.

6.7.13 Synthesis of *trans*-[$PtBr_2(PEt_3)]_2$

$$PtBr_2(PEt_3)_2 + PtBr_2 \longrightarrow \textit{trans}\text{-}[PtBr_2(PEt_3)]_2$$

Cis-$PtBr_2(PEt_3)_2$ (1.45g, 2.5 mmol) was added to a solution of $PtBr_2$ (1.03g, 2.9 mmol) dissolved in $(CHCl_2)_2$ and heated to 150°C during 4 hours. After cooling, yellow crystals

appeared. The solvent was removed under vacuum and the crystals were purified by recrystallisation from CH_2Cl_2. Yield 2.18 (79%).

Elemental analysis for $C_{12}H_{30}Pt_2Br_4P_2$ (946.09): Calc C 15.23, H 3.20%; Found C 15.27, H 3.23%

^{31}P NMR ($CDCl_3$): δ10.9 (singlet with Pt satellites, $^1J_{P\text{-}Pt}$ 3701 Hz) ppm.

6.7.14 Synthesis of *cis*-[$PtBr_2(PEt_3)(ArPBr_2)$]

$$ArPBr_2 \xrightarrow{[PtBr_2(PEt_3)]_2} [PtBr_2(PEt_3)(ArPBr_2)]$$

$[PtBr_2(PEt_3)_2]_2$ (0.45 g, 0.48 mmol) was added to a dichloromethane solution of $ArPBr_2$ (0.46 g, 0.97 mmol). The solution was stirred for one month.

^{31}P NMR (CH_2Cl_2): δ79.6 (d with Pt satellites, $^1J_{Pt\text{-}P}$ 5681.8Hz, $^2J_{P\text{-}P}$ 18.3Hz), 15.5 (d with Pt satellites, $^1J_{Pt\text{-}P}$ 3221.1 Hz, $^2J_{P\text{-}P}$ 18.4Hz) ppm; **^{19}F NMR** (CH_2Cl_2): δ-52.9 (d, $^4J_{P\text{-}F}$ 4.5Hz, 6F, *o*-CF_3), -64.1 (s, 3F, *p*-CF_3)

6.7.15 Synthesis of *trans*-[$PtBr_2(PEt_3)(Ar"_2PBr)$]

$$Ar"_2PBr \xrightarrow{[PtBr_2(PEt_3)]_2} [PtBr_2(PEt_3)(Ar"_2PBr)]$$

$[PtBr_2(PEt_3)]_2$ (0.14 g, 0.15 mmol) was added to a dichloromethane solution of $Ar"_2PBr$ (0.20g, 0.36 mmol). The solution was stirred overnight.

^{31}P NMR (CH_2Cl_2): δ 72.0 (d with Pt satellites, $^1J_{Pt\text{-}P}$ 2516.5 Hz, $^2J_{P\text{-}P}$ 562.4 Hz), 12.0 (d with Pt satellites, $^1J_{Pt\text{-}P}$ 2691.8 Hz, $^2J_{P\text{-}P}$ 562.8 Hz) ppm; **^{19}F NMR** (CH_2Cl_2): δ-54.7 (d, $^4J_{P\text{-}F}$ 2.7 Hz, 6F, *o*-CF_3), -63.9 (s, 6F, *p*-CF_3) ppm.

6.7.16 Synthesis of *cis*-[$PtBr_2(PEt_3)(Ar'PBr_2)$], *trans*-[$PtBr_2(PEt_3)(Ar"PBr_2)$] and cis-[$PtBr_2(PEt_3)(Ar"PBr_2)$]

trans-$[PtBr_2(PEt_3)]_2$ + Ar'PBr/$Ar"_2PBr$

$\downarrow$ CH_2Cl_2

cis-$[PtBr_2(PEt_3)(Ar'PBr_2)]$ + *trans*-$[PtBr_2(PEt_3)(Ar"PBr_2)]$ + *cis*-$[PtBr_2(PEt_3)(Ar"PBr_2)]$

$[PtBr_2(PEt_3)]_2$ (0.73 g, 078 mmol) was added to a dichloromethane solution of $Ar'PBr_2$/$Ar"PBr_2$ (0.63g, 1.56 mmol). The solution was stirred for three days.

^{31}P NMR (CH_2Cl_2): *trans*-$[PtBr_2(PEt_3)(Ar"PBr_2)]$: δ108.6 (d with Pt satellites, $^1J_{Pt\text{-}P}$ 2756.7Hz, $^2J_{P\text{-}P}$682.3 Hz), 11.9 (d with Pt satellites, $^1J_{Pt\text{-}P}$ 2846.5 Hz, $^2J_{P\text{-}P}$ 682.6 Hz) ppm; *cis*-$[PtBr_2(PEt_3)(Ar'PBr_2)]$: δ 113.4 ppm (m), 13.5 (d with Pt satellites, $^1J_{Pt\text{-}P}$ 3211.5 Hz, $^2J_{P\text{-}P}$ 11.5 Hz); *cis*-$[PtBr_2(PEt_3)(Ar"PBr_2)]$: δ 14.1 (d with Pt satellites, $^1J_{Pt\text{-}P}$ 3201.7 Hz, $^2J_{P\text{-}P}$ 11.6 Hz); **^{19}F NMR** (CH_2Cl_2): *trans*-$[PtBr_2(PEt_3)(Ar"PBr_2)$: δ-47.6 (d, $^4J_{P\text{-}F}$ 8.5 Hz, $^5J_{Pt\text{-}F}$ 32.5 Hz, 3F, *o*-CF_3), -62.7 (s, 3F, *p*-CF_3) ppm; *cis*-$[PtBr_2(PEt_3)(Ar'PBr_2)]$: δ -52.8 ppm (d with Pt satellites, $^4J_{P\text{-}F}$ 11.1 Hz, $^5J_{Pt\text{-}F}$ 30.3 Hz, 6F, *o*-CF_3); *cis*-$[PtBr_2(PEt_3)(Ar"PBr_2)]$: δ -50.8 ppm (d, $^4J_{P\text{-}F}$ 2.8 Hz, 3F, *o*-CF_3), -63.7 (s, 3F, *p*-CF_3) ppm

6.7.17 Attempted synthesis of $[PtCl_2(PEt_3)(ArAsCl_2)]$

$ArAsCl_2 \xrightarrow{[PtCl_2(PEt_3)]_2} [PtCl_2(PEt_3)(ArAsCl_2)]$

$[PtCl_2(PEt_3)]_2$ (0.25g, 0.33 mmol) was added to a $ArAsCl_2$ (0.28g, 0.66 mmol) solution in dichloromethane and allowed to stir. No reaction was apparent in the ^{19}F NMR spectrum, even after extended refluxing over a number of days.

6.7.18 Attempted synthesis of $[PtCl_2(PEt_3)(Ar_2AsCl)]$

$$Ar_2AsCl \xrightarrow{[PtCl_2(PEt_3)]_2} [PtCl_2(PEt_3)(Ar_2AsCl)]$$

$[PtCl_2(PEt_3)]_2$ (0.25g, 0.33 mmol) was added to a Ar_2AsCl (0.28g, 0.66 mmol) solution in dichloromethane and allowed to stir. No reaction was apparent in the ^{19}F NMR spectrum, even after extended refluxing over a number of days.

6.7.19 Attempted synthesis of $[PtCl_2(PEt_3)(Ar'Ar''AsCl)]$

$$Ar'Ar''AsCl \xrightarrow{[PtCl_2(PEt_3)]_2} [PtCl_2(PEt_3)(Ar'Ar''AsCl)]$$

$[PtCl_2(PEt_3)]_2$ (0.08g, 0.12 mmol) was added to a Ar_2AsCl (0.13g, 0.23 mmol) solution in dichloromethane and allowed to stir. No reaction was apparent in the ^{19}F NMR spectrum, even after extended refluxing over a number of days.

References

1 K. Umakoski, Y. Sasaki, *Adv. Inorg. Chem.*, **1994**, *40*, 187.

2 B. Rosenberg, L. Vancamp, T. Krigas, *Nature*, **1965**, *205*, 698.

3 T. G. Spiro, *Nucleic Acid-Metal Ion Interactions*; Wiley, New York, 1980.

4 M. Fild, *Z. Naturforsch*, **1968**, *23b*, 604.

5 L. J. Sequeira, *Ph.D. Thesis*, Durham, **1996**.

6 K. B. Dillon, H. P. Goodwin, B. Murrer, *unpublished work*, .

7 C. E. Housecroft, A. G. Sharpe, *Inorganic Chemistry*; Prentice Hall, Harlow, England, **2001**.

8 H. P. Goodwin, *Ph. D. Thesis*, Durham, **1990**.

9 M. D. Roden, *Ph. D. Thesis*, Durham, **1998**.

10 L. M. Venanzi, J. Chatt, *J. Am. Chem. Soc.*, **1955**, 2787.

11 N. N. Greenwood, A. Earnshaw, *Chemistry of the Elements*; 2nd ed., Oxford, 1997.

12 J. E. Huheey, *Inorganic Chemistry*; 3rd ed.; Harper and Row, **1983**.

13 D. Fenske, K. Merzweiler, *Angew. Chem., Int. Ed. Engl.*, **1986**, *25*, 338.

14 A. G. Del Pozo, A. M. Caminade, F. Dahan, J.-P. Majoral, R. Mathieu, *J. Chem. Soc., Chem. Commun.*, **1988**, 574.

15 K. B. Dillon, H. P. Goodwin, *J. Organomet. Chem.*, **1992**, *429*, 169 and references therein.

16 A. J. Blake, R. O. Gould, A. M. Marr, D. H. W. Rankin, M. Schröder, *Acta Cryst.*, **1989**, *C45*, 1218.

17 R. Appel, C. Casser, M. Immelkeppel, F. Knoch, *Angew. Chem., Int. Ed. Engl.*, **1984**, *23*, 895.

18 H. W. Kroto, J. F. Nixon, M. J. Taylor, A. A. Frew, K. W. Muir, *Polyhedron*, **1982**, *1*, 89.

19 E. Cartmell, G. W. A. Fowles in *Valency and Molecular Structure*; 4th ed.; Butterworths, **1983**; Chapter 11.

20 I. G. Phillips, R. G. Ball, R. G. Cavell, *Inorg. Chem.*, **1987**, *26*, 4074.

21 J. Cosier, A.M.Glazer, *J. Appl. Cryst.*, **1986**, *19*, 105.

22 SMART -NT; Data Collection Software, version 5.0, Bruker Analytical X-ray Instruments Inc., Madison, Wisconsin, USA, **1999**.

23 SAINT-NT; Data Reduction Software, version 6.0, Bruker Analytical X-ray Instruments Inc, Madison, Wisconsin, U.S.A., **1999**.

24 SHELXTL; version 5.1, Bruker Analytical X-ray Instruments Inc, Madison, Wisconsin, U.S.A., **1999**.

Chapter 7
Synthesis of multiple bonded phosphorus compounds

7.1 Double bonded compounds between heavier group14 and 15 elements

7.1.1 Diphosphenes

The history of diphosphenes started in 1877, when Kohler and Michaelis[1] first synthesised, by reacting $PhPH_2$ with $PhPCl_2$, what they called "phosphobenzene" by analogy with azobenzene. Some researches continued in this field, but chemists were discouraged by the emergence of the "classical double bond rule".[2] This rule stipulated that elements possessing a principal quantum number greater than 2 should not be able to form P_π-P_π bonds with themselves or other elements. "Phosphobenzene" has since been shown not to be a diphosphene, but a polymer.

However, in 1981, Yoshifuji *et al*,[3] reported the synthesis of the first stable diphosphene (by reaction between Ar^*PCl_2 and magnesium metal), containing a bulky substituent as a protecting group (2,4,6-tri-^{t}butylphenyl = supermesityl (Ar*))

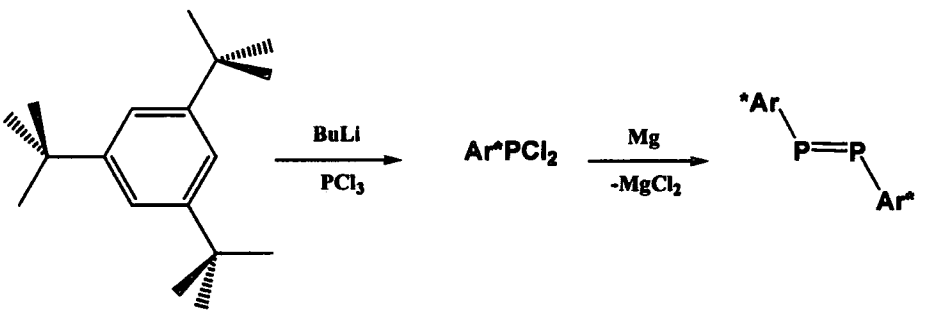

Subsequently, much research has been carried out in this area and other synthetic routes have been discovered in order to form double bonds between heavier group 14 and 15 elements.

7.1.2 Other multiple-bonded main group derivatives

These species are less common than diphosphenes. The first disilene $Mes_2Si{=}SiMes_2$ was obtained by West *et al,*[4] and in 1982, Satgé *et al*[5] reported the first heteronuclear double bonds in a germanophosphene [$Me_2Ge{=}PPh$] and a stannaphosphene [$Me_2Sn{=}PPh$]. Both phosphaarsenes [e.g. $(Me_3Si)_3C\text{-}As{=}P\text{-}C(SiMe_3)_3$][6] and diarsenes have also been generated, although only a few structures have been published of diarsenes.[7-10]

7.1.3 Synthetic routes

There are several synthetic methods to prepare double bond dipnictenes of heavier main groups elements.

- Thermolysis[11]

$$P_2H_4 \longrightarrow P_2H_2 + H_2$$

P_2H_2 is not a stable derivative.

- Photochemical elimination[4]

$$2\ Mes_2Si(SiMe_3)_2 \xrightarrow{-Me_3SiSiMe_3} Mes_2Si{=}SiMes_2$$

- Dehalogenation of R_nEX_2[6,12-16]

R_nEX_2 will react with a halide-abstracting agent such as elemental magnesium, potassium or an alkyllithium.

$$2\,RECl_2 + 2\,Mg(K) \longrightarrow RE{=}ER + 2\,MgCl_2 \qquad (E = P, As, Sb, Bi)$$

$$2\,R_2GeCl_2 + LiNap \longrightarrow R_2Ge{=}GeR_2$$

$$3\,(Me_3Si)_3C\text{-}PCl_2 + 3\,(Me_3Si)_3C\text{-}AsCl_2 \xrightarrow{BuLi} (Me_3Si)_3C\text{-}P{=}P\text{-}C(SiMe_3)_3 + (Me_3Si)_3C\text{-}As{=}As\text{-}C(SiMe_3)_3 + (Me_3Si)_3C\text{-}P{=}As\text{-}C(SiMe_3)_3$$

- Dehydrohalogenation of $R_nEX\text{-}HER'_m$[17-20]

This is a widely used method to synthesise symmetrical and unsymmetrical compounds. It consists of reacting R_nEX_2 and R'_mEH_2 in the presence of a base.

$$ArPCl_2 + ArPH_2 + 2\,DBU \xrightarrow{-2\,DBU.HCl} ArP{=}PAr$$

$$RPCl_2 + R'PH_2 + 2\,DBU \xrightarrow{-2\,DBU.HCl} RP{=}PR'$$

$$ArPH_2 + Mes(Bu)GeCl_2 + BuLi \longrightarrow Mes(Bu)Ge{=}PAr$$

$$RPH_2 + R'R''SiCl_2 + BuLi \longrightarrow RP{=}SiR'R''$$

This reaction has proved to be the most useful for the formation of symmetrical double bonds between main group 14 and 15 elements, and has occasionally been used to prepare unsymmetrical double bond compounds.

- Transition metal "catalysed" metathesis of double bonds[21,22]

$$RPCl_2 + W(PMe_3)_6 \longrightarrow RP{=}PR$$

Dillon *et al*[21] used the highly reducing nature and labile coordination sphere of the zerovalent tungsten complex, $W(PMe_3)_6$, as an efficient chloride ion abstractor. Dichlorophosphanes react with $W(PMe_3)_6$ in benzene smoothly over several hours to give the diphosphene RP=PR [R: 2,4,6-tris-^{t}butylphenyl, 2,4,6-tris(trifluoromethyl)phenyl, 2,6-bis(trifluoromethyl)phenyl]. The proposed mechanism is shown below (Figure 7.1).

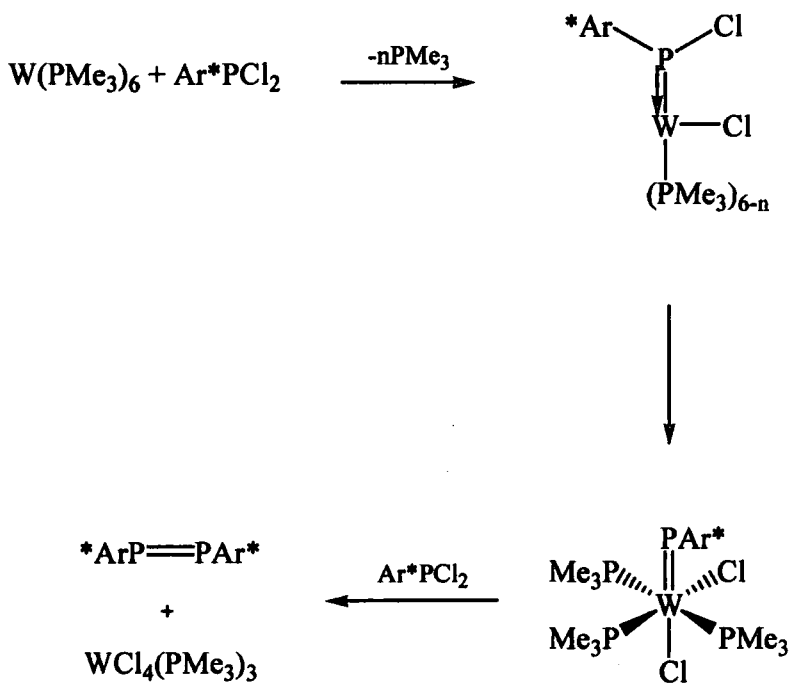

Equation 7.1: *Mechanism of the formation of diphosphenes with $W(PMe_3)_6$*

The key intermediate that is proposed in this mechanism is the tungsten phosphinidene complex. Although a few have been characterised, double bond transition metal phosphinidene complexes are relatively rare.[23-26]

Surprisingly, when different starting materials $ArPCl_2$ and Ar^*PCl_2 reacted with $W(PMe_3)_6$, only the unsymmetrical diphosphene ArP=PAr* was produced in a good yield. During the reaction, it was seen that the symmetrical diphosphene ArP=PAr was formed first, but was then converted to the unsymmetrical diphosphene ArP=PAr*. However, upon removal of the reaction solvent, the symmetrical diphosphenes were precipitated with the unsymmetrical signal almost lost from the ^{31}P NMR spectrum, as shown in Figure 7.1 below:

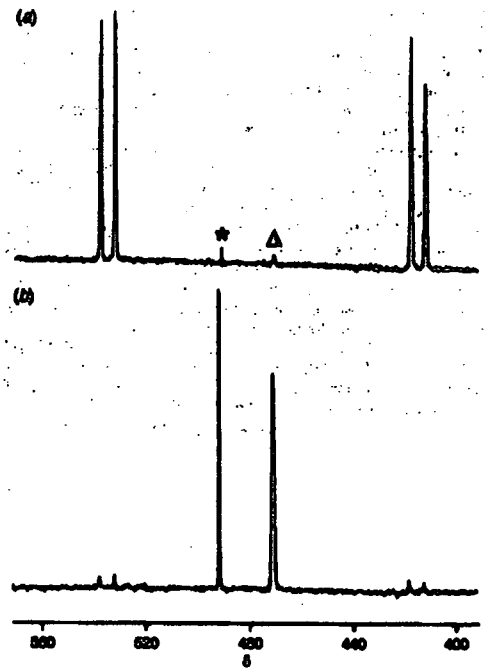

***Figure 7.1**: (a) ^{31}P NMR spectrum of $R^1P=PR^2$, generated upon treatment of a 1:1 mixture of R^1PCl_2 and R^2PCl_2 with $W(PMe_3)_6$ in benzene (* and Δ indicate resonances due to the symmetrical diphosphenes, $R^1P=PR^1$ and $R^2P=PR^2$, respectively. (b) ^{31}P NMR spectrum of the precipitated solids.*[21]

The result indicates that the presence of a particular species in solution is capable of rapidly catalysing the exchange of the diphosphene PR end-groups. This exchange does not occur in the absence of the tungsten species, since on addition of a $W(PMe_3)_6/ArPCl_2$ mixture to the symmetrical diphosphenes ArP=PAr and Ar*P=PAr*, they changed into the unsymmetrical diphosphene ArP=PAr*. The possible mechanism for this reaction could be PR end-group exchange that involves a phosphinidene intermediate.

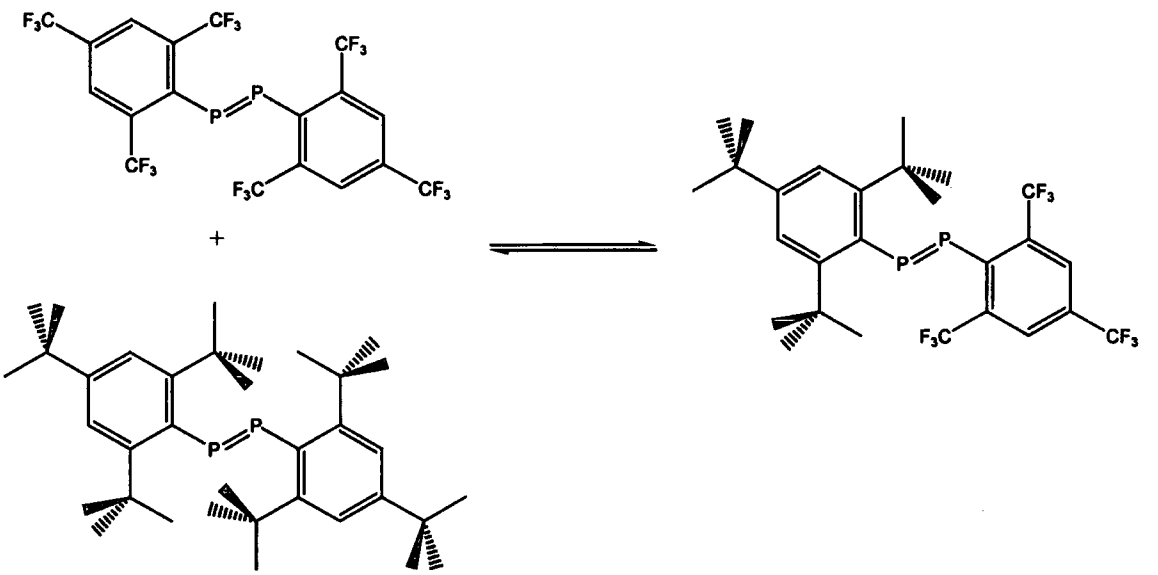

Figure 7.2: *Metathesis mechanism*

To isolate the unsymmetrical compound, it is first necessary to destroy the catalyst. The most convenient method is to treat the solution with benzaldehyde, a procedure analogous to that used to destroy well-defined alkylidene olefin metathesis catalysts.
This is the only route so far using different dichlorophosphanes to prepare unsymmetrical diphosphenes.

7.1.4 Synthetic routes and Chemical shifts of RP=ER' systems

- Phosphasilenes

Many synthetic routes have been found to synthesise Si=P derivatives:

- dechlorination of a chlorophosphane by alkyllithium[27,28]
- dehydrofluorination of a fluorosilylphosphane by an alkylithium[27,28]
- reaction of water or an alkyl halide with a diphosphasilaallylanion[29]
- addition of two equivalents of butyllithium to a mixture of primary phosphane and dichlorosilane[28]

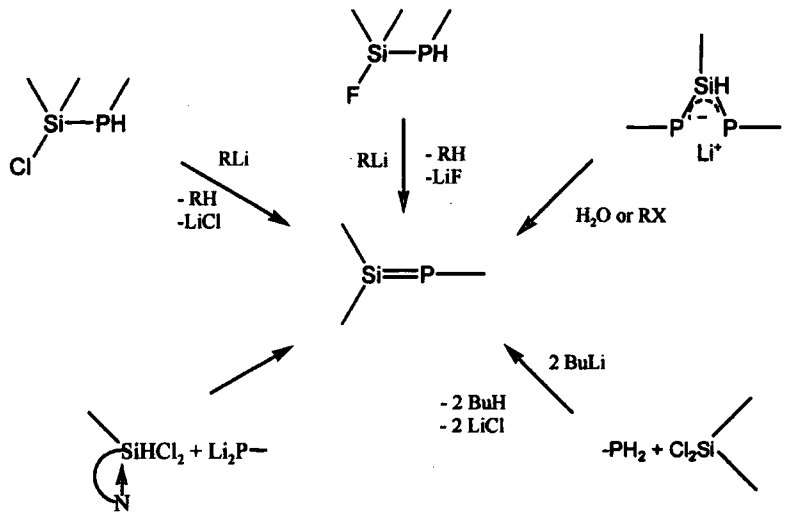

Equation 7.2: *Synthetic routes to phosphasilenes*

- Germaphosphenes

Germaphosphenes species can be prepared as follows:

- dehydrofluorination of a fluorogermylphosphane by tert-butyllithium[30-36]

- dehydrochlorination of a chlorogermylphosphane by a phosphorus ylide or DBU[30-36]
- reaction of a difluorogermane with a dilithium phosphanide[34,35]

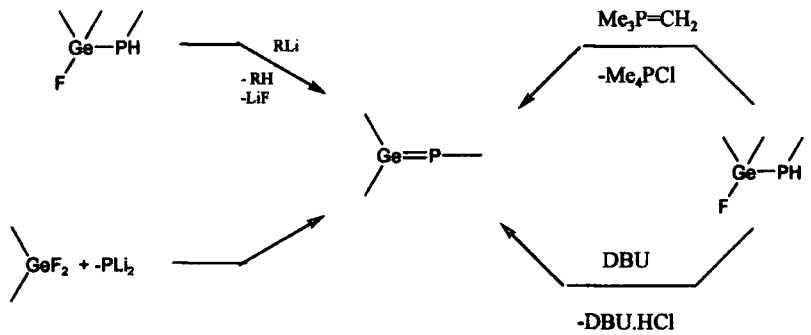

Equation 7.3: *Synthetic routes to germaphosphenes*

- Stannaphosphenes

There are two different routes to prepare stannaphosphenes:

- dehydrofluorination of a fluorostannylphosphane by tert-butyllithium[32,35-37]
- defluorosilylation of a fluorostannyl(silyl)phosphane[32,35-37]

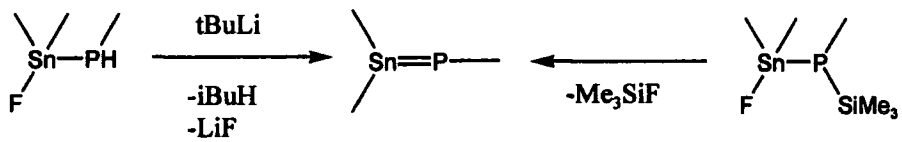

Equation 7.4: *Synthetic routes to stannaphosphenes*

^{31}P chemicals shifts of selected M=P compounds are listed in Table 7.1:

Phosphasilenes			
	δ ^{31}P (ppm)	δ ^{29}Si (ppm) $^{1}J_{P\text{-}Si}$ (Hz)	Reference
Mes_2Si=PMes*	136	151 148.5	27
Is(Mes)Si=PMes*	122.7	148.7 152	28
Germaphosphenes			
Mes_2Ge=PMes*	175		30,31,36,38
$^{t}Bu_2Ge$=PMes*	157		33
Mes(^{t}Bu)Ge=PMes*	*cis* Mes 169 *trans* Mes 157		33
Stannaphosphenes			
		δ ^{119}Sn (ppm) $^{1}J_{^{119}Sn\text{-}P}$ (Hz)	
$[(Bis)_2CH]_2Sn$=PMes*	205	658 2295	38,39
Is_2Sn=PMes*	171	500 2208	35,37
Is_2Sn=PIs	125	601 2182	40
Is_2Sn=PBis	169	606 2264	40

Mes = 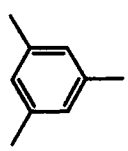 Mes* = 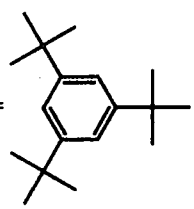 Is = 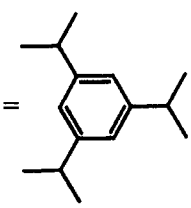 Bis = $(Me_3Si)_2CH$

Table 7.1: *$\delta^{31}P$, ^{29}Si and ^{119}Sn for metallaphosphenes*

7.2 Disphosphenes and related species

The reactions were carried out following the method described above, using the tungsten compound $W(PMe_3)_6$ as a chlorine abstractor.[21] Because of a very small amount of the catalyst being available, reactions have been attempted on an NMR scale or a very small scale.

7.2.1 Reaction of $ArPCl_2$ with $W(PMe_3)_6$

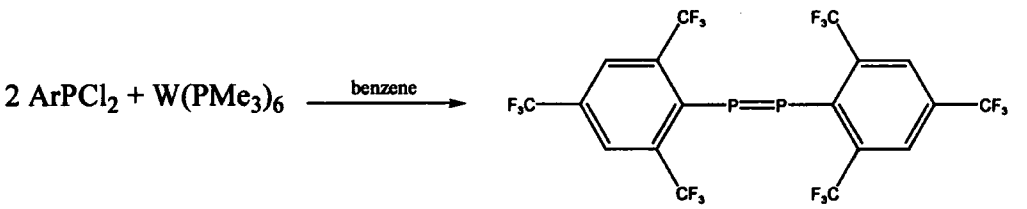

Equation 7.5: *Synthesis of ArP=PAr*

Two equivalents of $ArPCl_2$ were added to a solution of $W(PMe_3)_6$ in benzene-d_6 at room temperature. The reaction immediately turned from yellow to red. The mechanism of the formation of the diphosphene is shown in Equation 7.1. The ^{31}P NMR spectrum showed a multiplet (13 lines, $^1J_{P\text{-}P}$ 22.7 Hz) at 473 ppm, corresponding to ArP=PAr. A signal assigned to the W(IV) by-product $WCl_4(PMe_3)_3$ was found at 32.2 ppm and a singlet at -61.1 ppm indicated the presence of free PMe_3.

The characteristic ^{31}P chemical shift of the diphosphene is due to an increase in the paramagnetic shielding term caused by the existence of low-lying excited states. The ^{19}F NMR spectrum displayed a triplet at -55.9 ppm ($^4J_{P\text{-}F}$ 22.7 Hz) and a singlet at -63.1 ppm. This triplet has been observed in similar systems, for example Ar'P=PAr'.[38]

7.2.2 Reaction of Ar'PCl_2/Ar"PCl_2 with $W(PMe_3)_6$

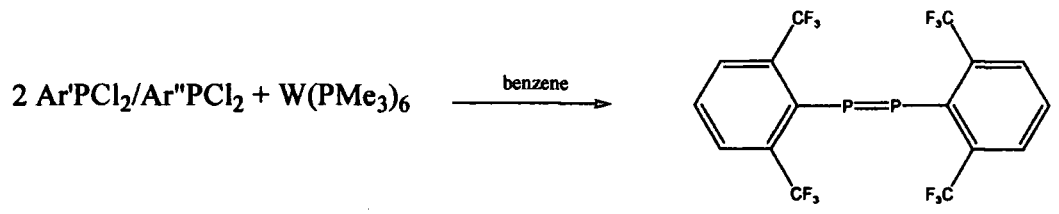

Equation 7.6: *Attempted synthesis of Ar'P=PAr'*

Two equivalents of the mixture Ar'PCl_2/Ar"PCl_2 were added to a solution of $W(PMe_3)_6$ in benzene-d_6 at room temperature. After stirring overnight, the solution turned red. The ^{31}P NMR spectrum exhibited a multiplet at 479.8 ppm ($^1J_{P-P}$ 45.2 Hz). This confirms the formation of the symmetrical diphosphene.[38] The quartet corresponding to Ar"PCl_2 was still visible in the spectrum. The ^{31}P NMR spectrum run after a week showed the appearance of a small multiplet at 506.0 ppm (the coupling constant could however not be determined for this signal). This signal could arise from the symmetrical species Ar"P=PAr".

7.2.3 Reaction between $ArPCl_2$, $ArAsCl_2$ and $W(PMe_3)_6$

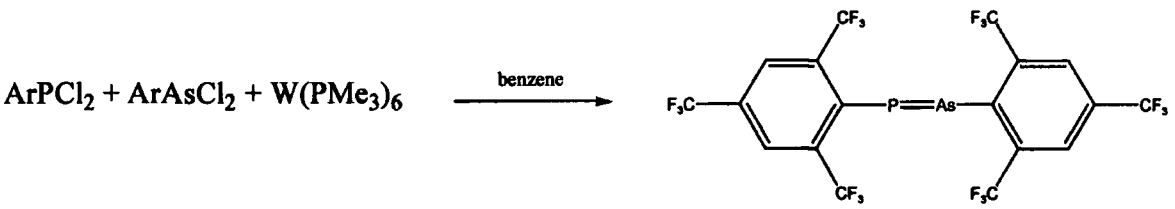

Equation 7.7: *Attempted synthesis of ArP=AsAr*

$ArPCl_2$ and $ArAsCl_2$ were added to a $W(PMe_3)_6$ solution in benzene-d_6 at room temperature. The solution was stirred overnight and a red coloration appeared. Only the signal corresponding to ArP=PAr at 473.9 ppm was observed in the ^{31}P NMR. No apparent signal of ArAs=PAr has been detected. However, no signal of the starting material $W(PMe_3)_6$ remained in the spectrum.

7.2.4 Reaction between $ArPCl_2$, Ar_2GeCl_2 and $W(PMe_3)_6$

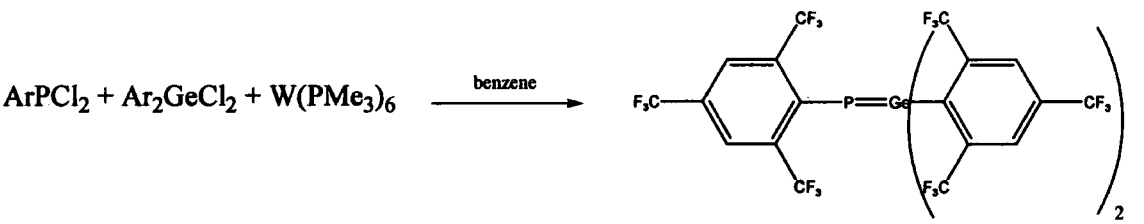

***Equation 7.8:** Attempted synthesis of ArP=GeAr*

$ArPCl_2$ and Ar_2GeCl_2 were added to a $W(PMe_3)_6$ solution in benzene-d_6 at room temperature. A red coloration appeared immediately. Only the signal corresponding to ArP=PAr at 473.9 ppm was observed in the ^{31}P NMR. No apparent signal of Ar_2Ge=PAr has been detected. The ^{19}F NMR spectrum only showed the presence of ArP=PAr and the starting material Ar_2GeCl_2

7.2.5 Reaction between $ArPCl_2$, Ar_2SnCl_2 and $W(PMe_3)_6$

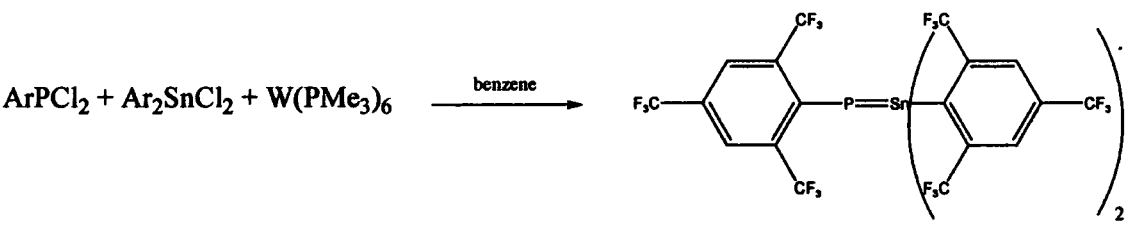

***Equation 7.9:** Attempted synthesis of ArP=SnAr*

$ArPCl_2$ and Ar_2SnCl_2 were added to a $W(PMe_3)_6$ solution in benzene-d_6 at room temperature. The reaction was stirred for three days. The only signal visible in the ^{31}P NMR spectrum was the one corresponding to ArP=PAr.

7.2.6 Conclusion

As previously described in the literature, ArP=PAr and Ar'P=PAr' were prepared. The attempt at making some ArP=EAr (E = As) or $ArP=EAr_2$ (E = Ge or Sn) does not seem to have been successful. The $W(PMe_3)_6$ catalyst might not be able to withdraw the chlorine atom from those elements.

However, all the reactions have been done on an NMR scale using very small quantities, which were not always very accurate. It would be interesting to scale up some of these, in order to check and confirm these results. In case the tungsten catalyst reacts very slowly to remove the chlorine atoms from arsenic, reacting two equivalents of $ArAsCl_2$ with $W(PMe_3)_6$ would be the next step. The study could not be done due to the unavailability of ^{19}F NMR spectroscopy at the time, and lack of more $W(PMe_3)_6$ catalyst.

7.3 Phosphaalkenes and Phosphaalkynes

7.3.1 Phosphaalkenes

The chemistry of phosphaalkenes has only been developed in the last 25 years. In 1960, Dimroth and Hoffman first reported the synthesis of compounds containing a P=C double bond.[41,42] In 1976, the first stable acyclic species was described.[43] However, these compounds were only stable in the absence of air and moisture. Kinetic stabilisation using bulky substituents on phosphorus has facilitated the development of several synthetic routes to prepare stable phosphaalkenes.[44]

The first phosphaalkene containing the Ar ligand, $ArP=CR^1R^2$ ($R^1=R^2=Cl$; $R^1=SiMe_3$, $R^2=H$; $R^1=Ph$, $R^2=H$), were reported by Dillon and Goodwin.[17,45] The method used for the first of these syntheses consists of two reactions:

$$CH_2Cl_2 + BuLi \longrightarrow CHLiCl_2$$

$$CHLiCl_2 + ArPCl_2 \longrightarrow ArP(CHCl_2)Cl \xrightarrow{DBU} Ar{=}PCCl_2$$

The coordination chemistry of these compounds with platinum has also been studied[45] and indicated the formation of η^1-bonded complexes.

7.3.2 **Phosphaalkynes**

The first phosphaalkyne HCP was synthesised in 1961 by Gier[46] but appeared to be very unstable. Twenty years later, the first stable phosphaalkyne, BuCP was prepared.[47] Since, a variety of stable phosphaalkynes has been synthesised.

The inorganic and organic chemistry of phosphaalkynes has been extensively developed in the recent years and numerous routes to prepare phosphaalkynes have been found.[44] Among them, the synthesis of RCP (where R=Supermes), by the reaction of the phosphaalkene $RP{=}CCl_2$ with $Pd(PPh_3)_4$, was described by Sanchez *et al*,[48] with a mechanism involving the rearrangement of the intermediate species [RP=C:]

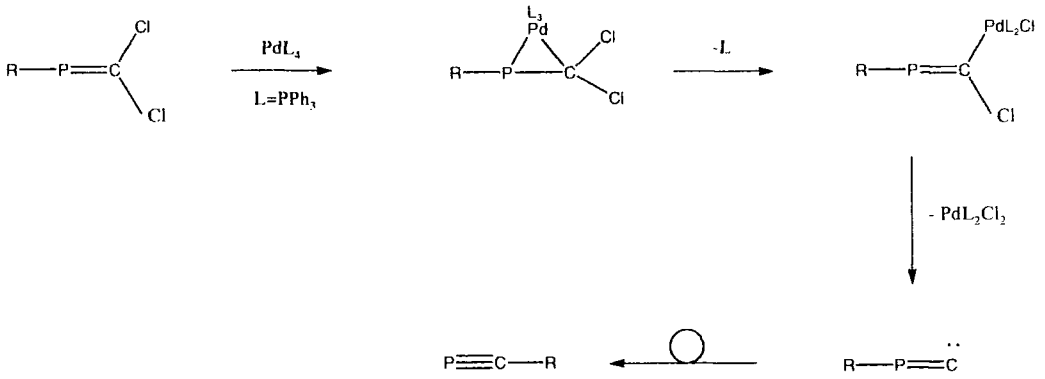

Equation 7.10: *Proposed mechanism for the synthesis of a phosphaalkyne using PdL_4 and $RP{=}CCl_2$*

This reaction is identical to the one published by Angelici *et al*[49] in which some crystal structures of the intermediates are shown. They described the formation of a four-membered ring between a C=C bond in the aryl ring and the P=C phosphaalkene bond (Equation 7.11).

The chemistry of phosphaalkynes is quite diverse and work has mainly been done with aryl and alkyl substituents on C. The alkyl group used, such as ^{t}Bu, tend to be electron-donating ligands, and increase the electron density at the C≡P triple bond. So far, no phosphaalkyne containing fluoromes or fluoroxyl substituents has been reported. However, some attempts have been made by Goodwin[17] and Roden[50] but have not been successful. Using "Angelici's method", Roden found that $ArP{=}CCl_2$ reacts with $Pt(PPh_3)_4$ to form a stable complex *trans*-$[Pt(PPh_3)_2Cl(C(Cl){=}PAr')]$ which has been structurally characterised.[50]

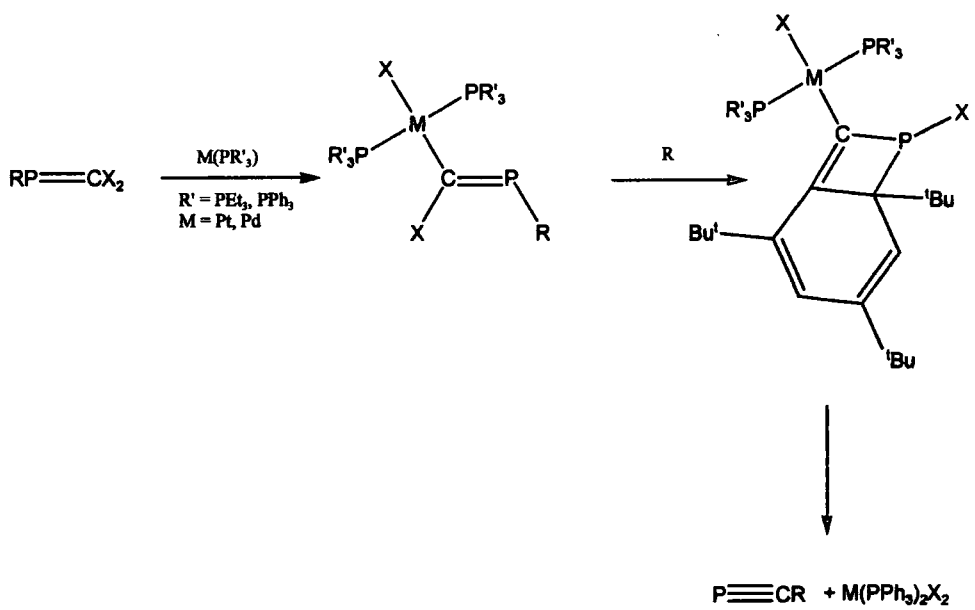

Equation 7.11: *Mechanism demonstrated by Angelici et al*[49]

7.3.3 Preparation of Phosphaalkenes

7.3.3.1 Synthesis of $ArP(Cl)CHCl_2$

This compound was synthesised by reaction of $ArPCl_2$ with a solution of lithiated CH_2Cl_2, $CHCl_2Li$, at -130°C. $ArP{=}CCl_2$ was purified by distillation, yielding a colourless oil.

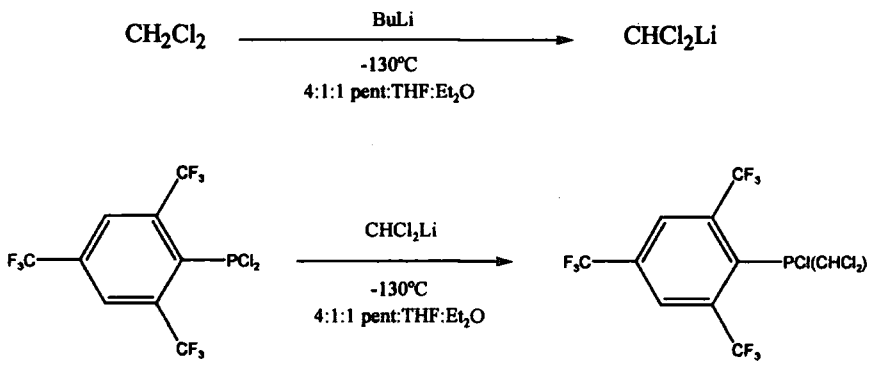

Equation 7.12: *Synthesis of $ArP(Cl)CHCl_2$*

The ^{31}P NMR spectrum showed a septet at 63.1 ppm ($^4J_{P\text{-}F}$ 49.3 Hz). The ^{19}F NMR spectrum displayed a doublet at -55.3 ppm ($^4J_{P\text{-}F}$ 49.3 Hz) corresponding to the *o*-CF_3 groups, and a singlet at -64.5 ppm (*p*-CF_3). These values agree with those found by Goodwin and Roden.[17,50]

7.3.3.2 Synthesis of $ArP{=}CCl_2$

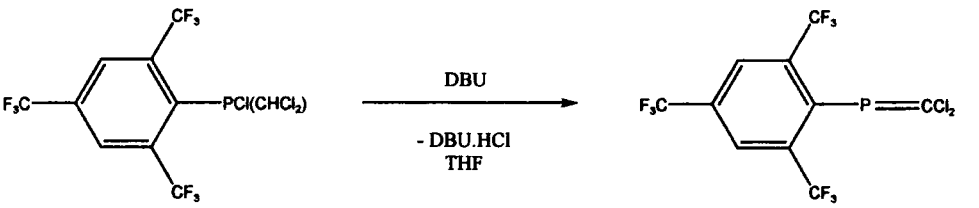

Equation 7.13: *Synthesis of $ArP{=}CCl_2$*

This phosphaalkene was prepared by addition of DBU to an $ArP(Cl)CHCl_2$ solution in THF at -78°C. The product was purified by distillation, giving a colourless oil.

A septet at 202.4 ppm was observed in the ^{31}P NMR spectrum ($^4J_{P\text{-}F}$ 20.6 Hz). The ^{19}F NMR spectrum exhibited a doublet at –60.0 ppm ($^4J_{P\text{-}F}$ 21 Hz, *o*-CF_3) and a singlet at -63.9 ppm (*p*-CF_3).

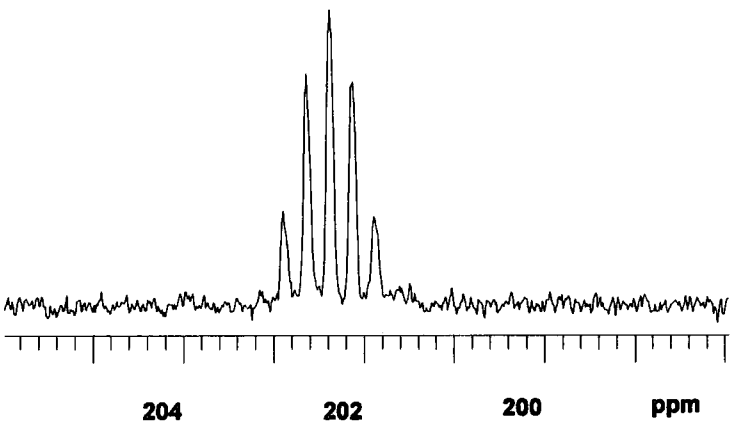

Figure 7.3: *^{31}P NMR spectrum of $ArP{=}CCl_2$*

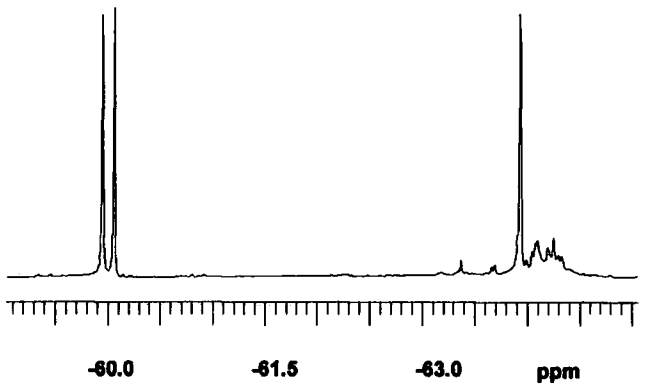

Figure 7.4: *^{19}F NMR spectrum of $ArP{=}CCl_2$*

7.3.3.3 Synthesis of Ar'P(Cl)$CHCl_2$

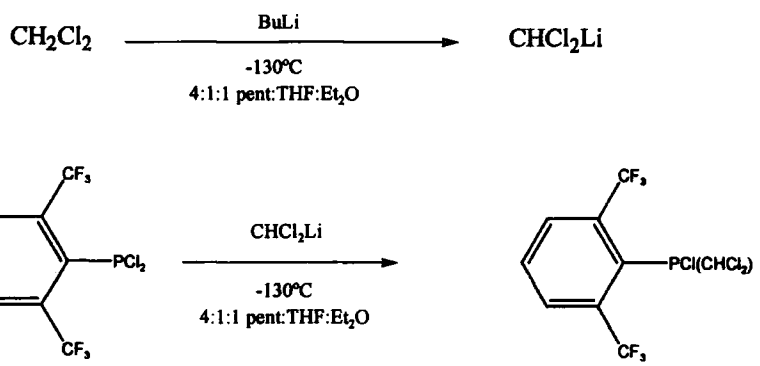

Equation 7.14: *Synthesis of Ar'P(Cl)$CHCl_2$*

This product was prepared following the same synthesis as described above for the preparation of ArP(Cl)$CHCl_2$.. The mixture Ar'Li/Ar"Li was reacted with a solution of

lithiated CH_2Cl_2 at -130°C. This compound was purified by distillation under reduced pressure.

The ^{31}P NMR spectrum showed a septet at 65.3 ppm ($^4J_{P-F}$ 48.8 Hz). A doublet at -53.9 ppm ($^4J_{P-F}$ 48.9 Hz) was observed in the ^{19}F NMR spectrum.

As observed by Roden, Ar"PCl_2 does not form the product Ar"P(Cl)$CHCl_2$. The signals from the starting material Ar"PCl_2 are still visible in both ^{31}P and ^{19}F NMR spectra.

7.3.3.4 Synthesis of Ar'P=CCl_2

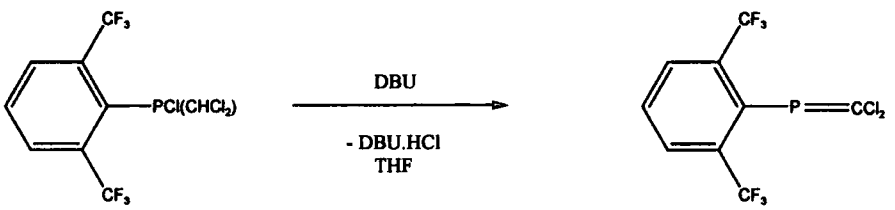

Equation 7.15: *Synthesis of Ar'P=CCl_2*

NMR spectroscopy showed a septet at 207.6 ppm ($^4J_{P-F}$ 20.7 Hz) in the ^{31}P spectrum and a doublet at –59.6 ppm ($^4J_{P-F}$ 21.1 Hz) in the ^{19}F spectrum.

These results are similar to those found by Roden. [50]

Comparison of the chemical shifts between the starting material $ArPCl_2$ or Ar'PCl_2 and the final products ArP=CCl_2 and Ar'P=CCl_2 shows that δ ^{19}F values are at lower frequency for the phosphaalkenes than for the phosphanes, and that δ ^{31}P moves to a higher frequency. This implies more shielding and electron density on the CF_3 groups. The electron-withdrawing effect is facilitated by the formation of the P=C double bond.

The P-F coupling constant is significantly smaller in the phosphaalkene than in the phosphane. The formation of the P=C bond decreases the p character of the phosphorus hybrid orbitals. The phosphorus becomes more positive and the chemical shifts move to higher frequency. In the meantime, the electron density in the CF_3 groups increases, moving the fluorine shifts to a lower frequency (Table 7.2).

	$\delta^{31}P$	$\delta^{19}F$		$^4J_{P-F}$
		o-CF_3	*p*-CF_3	
$ArPCl_2$	145.6	-53.3	-64.2	61.3
$ArP(Cl)CHCl_2$	63.1	-55.3	-64.5	49.3
$ArP{=}CCl_2$	202.4	-60.0	-63.9	20.6
$Ar'PCl_2$	148.4	-53.2		61.3
$Ar'P(Cl)CHCl_2$	65.3	-53.9		48.8
$Ar'P{=}CCl_2$	207.6	-59.6		21

Table 7.2: *Comparison of $\delta^{31}P$ and ^{19}F between phosphanes and phosphaalkenes*

7.4 Attempted preparation of phosphaalkynes

According to Angelici's report,[49] reaction of phosphaalkenes with Pt(0) or Pd(0) compounds leads to an intermediate Pt or Pd complex, which undergoes rearrangement to give a phosphaalkyne.

7.4.1 Reaction between $ArP{=}CCl_2$ and $Pt(PPh_3)_4$

- NMR spectroscopy

$ArP{=}CCl_2$ was added to a solution of $Pt(PPh_3)_4$ in toluene at room temperature.
The ^{31}P NMR spectrum exhibited two multiplets with Pt satellites at 203.7 ($^2J_{Pt-P}$ 282.6 Hz, $^4J_{P-F}$ 22.6 Hz) and 198.1 ($^2J_{Pt-P}$ 369.2 Hz, $^3J_{P-P}$ 45.4 Hz, $^4J_{P-F}$ 22.6 Hz) ppm, assigned

to the phosphaalkene ligand. Three different signals were assignable to PPh_3 bonded to platinum: a doublet at 24.6 ($^3J_{P-P}$ 27.5 Hz, $^1J_{Pt-P}$ 2963.5 Hz), a doublet of doublets at 17.3 ($^3J_{P-P}$ 48.4 Hz, $^3J_{P-P}$ 17.8 Hz, $^1J_{Pt-P}$ 1897.2) and a pseudo triplet at 14.1 ppm ($^2J_{P-P}$ /$^3J_{P-P}$ 15.3 Hz, $^1J_{Pt-P}$ 4063.8 Hz). A signal for the free PPh_3 was also observed at -6 ppm. The multiplets in the phosphaalkene region should, in fact, be a doublet of doublets of septets for the *cis*-isomer, due to the coupling with the fluorines of the two *o*-CF_3 groups (7 lines) and the phosphorus from the PPh_3, groups and a triplet of septets for the *trans*-isomer. The signal at 198.1 ppm has a greater intensity than the one at 203.7 ppm. The resonance at 14.1 ppm appeared as a triplet but should be a doublet of doublets. The $^2J_{P-P}$ and $^3J_{P-P}$ coupling constants are very similar and could not be distinguished. These results indicate the presence of two complexes in solution.

The ^{19}F NMR spectrum exhibited two close doublets at -57.8 ($^4J_{P-F}$ 23.7 Hz) and -57.9 ($^4J_{P-F}$ 23.0 Hz) ppm, and two singlets at -62.9 and -63.0 ppm.

^{19}F NMR spectroscopy also indicated the presence of two different species in solution. Neither of these corresponds to the starting material, and comfirms that two new complexes have been prepared, ascribed to *cis*- and *trans*-isomers. In the case of the *trans* isomer, the two PPh_3 groups are equivalent, and should only give a doublet in the ^{31}P NMR spectrum. The *cis* complex should give two different doublets of doublets for the PPh_3 groups with a *cis* and a *trans* coupling. Resonances in the ^{19}F NMR spectrum were assigned according to their relative intensities when compared with the ^{31}P NMR spectrum. Suggested assignments are listed in Table 7.3.

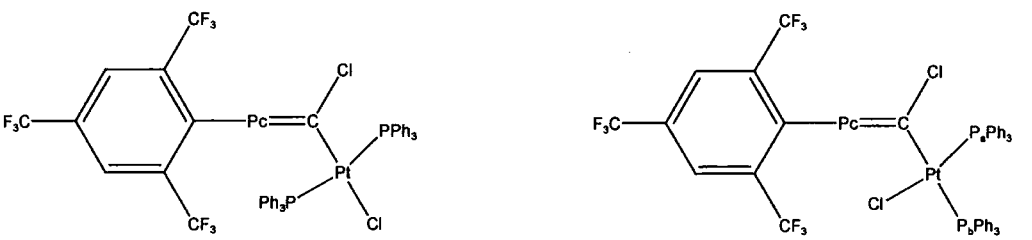

trans-isomer *cis*-isomer

Figure 7.5: *Trans and cis –[PtCl(PEt$_3$)$_2$(ArP=CCl)]*

		cis				*trans*		
		δ (ppm)	$J_{Pt-P}{}^a$	$^3J_{P-P}{}^a$	$^2J_{P-P}{}^a$	δ (ppm)	$J_{Pt-}{}^aP$	$^3J_{P-P}{}^a$
	P_a	14.1	4063.8	15.3				
^{31}P						24.6	2963.5	27.5
NMR	P_b	17.3	1897.2	48.4	17.8			
	P_c	198.1	369.2	45.4	22.6 ($^4J_{P-F}$)	203.7	?	22.6 ($^4J_{P-F}$)
			$^4J_{P-F}{}^a$				$^4J_{P-F}{}^a$	
^{19}F	*o*-CF_3	-57.9	23.7			-57.8	23.0	
NMR	*p*-CF_3	-63.0				-62.9		

[a] all coupling constants are given in Hz; $^1J_{Pt-P}$ for P_a and P_b; $^2J_{Pt-P}$ for P_c

Table 7.3: *Assignments for cis and trans isomers*

The solution containing those two isomers was stirred in dichloromethane in order to try and obtain a phosphaalkyne. No changes were observed in the ^{31}P NMR spectrum.

- X-ray crystallography

After standing for two month, orange crystals formed. They were submitted for X-ray analysis. The structure was determined by A.L. Thompson at 120K and is shown in Figure 7.6.

Trans-[PtCl(CCl=PAr)(PPh_3)$_2$] crystallises in the triclinic P-1 space group with Z=2. Selected bond angles (°) and distances (Å) are listed in Table 7.4. They are similar to those found in *trans*-[PtCl(CCl=PAr')(PPh_3)$_2$].[50]

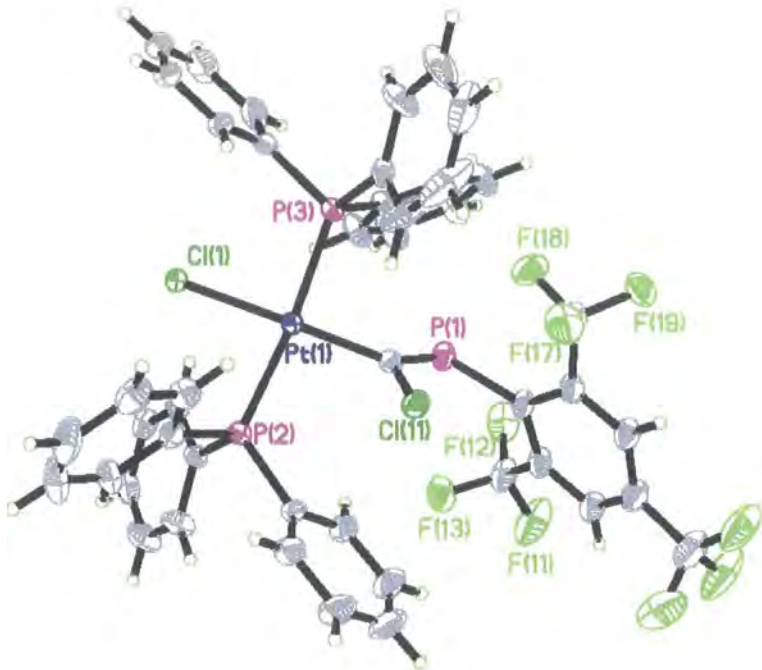

Figure 7.6: *Molecular structure of trans-[PtCl(CCl=PAr)(PPh$_3$)$_2$]*

Bond distances (Å)		Angles (°)	
Pt(1)-C(10)	2.0143(4)	C(10)-Pt(1)-P(3)	92.43(5)
Pt(1)-P(3)	2.3205(4)	C(10)-Pt(1)-P(2)	93.93(50
Pt(1)-P(2)	2.3284(4)	P(3)-Pt(1)-P(2)	173.693(16)
Pt(1)-Cl(1)	2.3629(5)	C(10)-Pt(1)-Cl(1)	173.63(5)
P(1)-C(10)	1.6882(19)	P(3)-Pt(1)-Cl(1)	89.043(16)
P(1)-C(11)	1.874(2)	P(2)-Pt(1)-Cl(1)	84.603(16)
Cl(11)-C(10)	1.7653(19)	C(10)-P(1)-C(11)	123.021(11)

Table 7.4: *Selected bond angles (°) and distances (Å)*

The platinum is in a square planar environment which is defined by the two PPh_3 (*trans* to each other), Cl, and [C(=PAr)Cl] ligands. The atoms Pt, P(2), P(3), Cl(1) and C(10) are

nearly coplanar. The C(10)-P(1) distance (1.6882(19) Å) is very similar to that of a C=P bond, as found in $[Pt(PEt_3)_2C(Cl)=PMes^*)Cl]$[49] (1.678(5) Å)and $Ph(Me_3Si)C=P\text{-}Mes^*$ (1.676(6) Å).[51] Three short contacts between some fluorines of the *o*-CF_3 groups and the phosphorus atom are found: P(1)---F(12) 3.039, P(1)---F(13) 3.160, P(1)---F(18) 2.911 Å. They are all shorter than the expected sum of the van der Waals radii for P(1.91 Å) and F(1.40 Å).

7.4.2 Reaction between Ar'P=CCl_2 and $Pt(PPh_3)_4$

Ar'P=CCl_2 was added to a $Pt(PPh_3)_4$ solution in benzene and the resulting yellow solution stirred. The initial ^{31}P NMR showed a multiplet with platinum satellites at 202.4 ($^2J_{Pt\text{-}P}$ 376.5 Hz, $^3J_{P\text{-}P}$ 46.1 Hz, $^4J_{P\text{-}F}$ 24.4 Hz), a doublet of doublets with Pt satellites at 17.1 ($^1J_{Pt\text{-}P}$ 1954.1 Hz, $^2J_{P\text{-}P}$ 16.7 Hz, $^3J_{P\text{-}P}$ 47.1 Hz) and a pseudo triplet at 13.5 ppm ($^1J_{Pt\text{-}P}$ 3936.1 Hz, $^2J_{P\text{-}P}$ / $^3J_{P\text{-}P}$ 18.7 Hz). A doublet at -57.8 ppm ($^4J_{P\text{-}F}$ 21.1 Hz) was observed in the ^{19}F NMR spectrum. These resonances indicate the formation of the *cis*-complex.
Half of the solvent was removed from the solution, and a white solid was isolated which displayed a resonance at 15.3 ppm ($^1J_{Pt\text{-}P}$ 3272.6 Hz) in the ^{31}P NMR spectrum. This compound is *cis*-$[Pt(PPh_3)_2Cl_2]$.[49] The solid was filtered off and spectra of the filtrate were recorded regularly to see any change occurring. After two weeks, new peaks appeared in the ^{31}P and ^{19}F NMR spectra. In addition to the signals described above, a multiplet at 208.3 ppm ($^2J_{Pt\text{-}P}$ 456.7 Hz), and a doublet with Pt satellites at 24.3 ppm ($^1J_{Pt\text{-}P}$ 2989.9 Hz, $^3J_{P\text{-}P}$ 27.5 Hz) were found. *Cis*- and *trans*-isomers were present in solution. The ^{19}F NMR exhibited two sets of doublets at –57.6 ($^4J_{P\text{-}F}$ 23.9 Hz) and –57.8 ($^4J_{P\text{-}F}$ 21.1 Hz) ppm. Assignments of these signals were made according to the relative intensities of the peaks, in comparison with the resonances in the ^{31}P NMR.

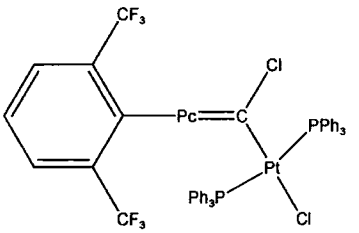

trans-isomer

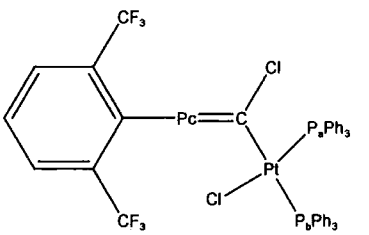

cis-isomer

Figure 7.7: *Trans and cis –[PtCl(PEt$_3$)$_2$(Ar'P=CCl)]*

		cis				*trans*		
		δ (ppm)	$J_{Pt\text{-}P}{}^a$	$^3J_{P\text{-}P}{}^a$	$^2J_{P\text{-}P}{}^a$	δ (ppm)	$J_{Pt\text{-}P}{}^a$	$^3J_{P\text{-}P}{}^a$
^{31}P NMR	P_a	13.5	3936.1	18.7		24.3	2989.9	27.5
	P_b	17.1	1954.1	47.1	16.7			
	P_c	202.4	376.5	45.4		208.3	456.7	
^{19}F NMR		-57.8	$^4J_{P\text{-}F}{}^a$ 21.1			-57.6	$^4J_{P\text{-}F}{}^a$ 23.9	

[a] all coupling constants are given in Hz

Table 7.5: *Assignments for cis and trans isomers*

Solvent was removed under vacuum, leaving a yellow/brown oil which was dissolved in toluene.

The ^{31}P NMR did not show the presence of the *cis* and *trans* isomers, but new signals of small intensity were observed in the spectrum: a multiplet at 131.5 and a peak at 26.3 ppm. No platinum satellites were found, probably due to the low intensity of the signals.

The ^{19}F NMR spectrum displayed a doublet at –58.6 ($^{4}J_{P-F}$ 8.1 Hz) and a singlet at –63.2 ppm. These could be assigned to an intermediate parallel to the one described by Angelici[49] (Figure 7.8).

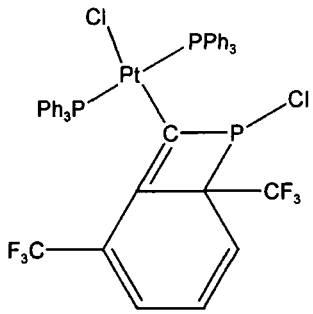

Figure 7.8: *Possible intermediate in the reaction*

Spectra of this intermediate were monitored after a month to see if any rearrangement to phosphaalkyne had occurred. A number of new peaks appeared in the spectra but none of them could be assigned. This could be due to degradation of the compound in the NMR tube.

No apparent signal corresponding to the phosphaalkyne has been found, but the presence of an intermediate species has been proved.

7.5 Experimental

7.5.1 **Introduction**

All manipulations, including NMR sample preparation, were carried out either under an inert atmosphere of dry nitrogen or in vacuo, using standard Schlenk procedures or a glovebox. Chemicals of the best available commercial grades were used, in general without further purification. We thank Johnson Matthey for the loan of platinum salts.

- NMR spectroscopy
  - diphosphenes and related species

^{31}P NMR spectra were recorded on a Bruker 300 spectrometer at 121.5 MHz.

  - phosphaalkenes

^{19}F NMR spectra were recorded on a Varian Mercury 200 or Varian VXR 400 Fourier-transform spectrometer at 188.18 and 376.35 MHz respectively. ^{31}P NMR spectra were recorded on the same instruments at 80.96 or 161.91 MHz. Chemical shifts were measured relative to external $CFCl_3$ (^{19}F). or 85% H_3PO_4 (^{31}P), with the higher frequency direction taken as positive.

- $W(PMe_3)_6$ was prepared by J. Grundy and Dr M. P. Coles at the University of Sussex. All manipulations with this catalyst were carried out at the University of Sussex.

7.5.2 **Synthesis of ArP=PAr**

$$2\ ArPCl_2 + W(PMe_3)_6 \xrightarrow{C_6D_6} ArP{=}PAr$$

$ArPCl_2$ (0.1g, 0.45 mmol) and $W(PMe_3)_6$ (0.1g, 0,21 mmol) were placed in an NMR tube and dissolved in C_6D_6. The solution changed colour from yellow to red. The resulting solution was stirred for 18 hours.

^{31}P NMR (C_6D_6): δ 473.0 (m, $^1J_{P\text{-}F}$ 22.7 Hz) ppm, **^{19}F NMR** (C_6D_6): δ -55.9 (t, $^4J_{P\text{-}F}$ 22.7 Hz, 12F, *o*-CF_3), -63.1 (s, 6F, *p*-CF_3) ppm.

7.5.3 Synthesis of Ar'P=PAr'

$$2\ Ar'PCl_2/Ar''PCl_2 + W(PMe_3)_6 \xrightarrow{C_6D_6} Ar'P{=}PAr'$$

$Ar'PCl_2/Ar''PCl_2$ (0.01g, 0.045 mmol) and $W(PMe_3)_6$ (0.01g, 0.021 mmol) were placed in an NMR tube and dissolved in C_6D_6. The solution changed colour from yellow to red. The resulting solution was stirred for 18 hours.

^{31}P NMR (C6D6): δ 479.8. (m, $^{1}J_{P\text{-}F}$ 22.7 Hz) ppm.

7.5.4 Attempted synthesis of ArP=AsAr

$$ArPCl_2 + ArAsCl_2 + W(PMe_3)_6 \xrightarrow{C_6D_6} ArP{=}AsAr$$

$ArPCl_2$ (0.05g, 0.022 mmol), $ArAsCl_2$ (0.006g, 0.022 mmol) and $W(PMe_3)_6$ (0.01g, 0.021 mmol) were placed in an NMR tube and dissolved in C_6D_6. The solution changed colour from yellow to red. The resulting solution was stirred for 3 days. The ^{31}P NMR spectrum only showed the formation of ArP=PAr.

7.5.5 Attempted synthesis of ArP=GeAr$_2$

$$ArPCl_2 + Ar_2GeCl_2 + W(PMe_3)_6 \xrightarrow{C_6D_6} ArP{=}GeAr_2$$

$ArPCl_2$ (0.01g, 0.022 mmol), Ar_2GeCl_2 (0.015g, 0.022 mmol) and $W(PMe_3)_6$ (0.01g, 0.021 mmol) were placed in an NMR tube and dissolved in C_6D_6. The solution changed colour from yellow to red. The resulting solution was stirred for 3 days. The ^{31}P NMR spectrum only showed the formation of ArP=PAr.

7.5.6 Attempted synthesis of ArP=SnAr$_2$

$$ArPCl_2 + Ar_2SnCl_2 + W(PMe_3)_6 \xrightarrow{C_6D_6} ArP{=}SnAr_2$$

$ArPCl_2$ (0.01g, 0.022 mmol), Ar_2SnCl_2 (0.016g, 0.022 mmol) and $W(PMe_3)_6$ (0.01g, 0.021 mmol) were placed in an NMR tube and dissolved in C_6D_6. The solution changed colour from yellow to red. The resulting solution was stirred for 3 days. The ^{31}P NMR spectrum only showed the formation of ArP=PAr.

7.5.7 Synthesis of $Pt(PPh_3)_4$

$$K_2[PtCl_4] + 2\ KOH + 4\ PPh_3 + EtOH \longrightarrow Pt(PPh_3)_4 + 4\ KCl + CH_3CHO + 2\ H_2O$$

PPh_3 (15.4g, 5.9 mmol) was dissolved in 200 ml of absolute ethanol at 65°C. When the solution was clear, a solution of 1.4g of KOH in a mixture of 32 ml of ethanol and 8 ml of water was added. Then, a solution of potassium tetrachloroplatinate (II) (5.24g, 1.26 mmol) in water was slowly added to the alkaline triphenylphosphine solution while stirring at 65°C. The addition was completed in about 20 min. A pale yellow compound began to separate within a few minutes of the first addition. After cooling, the compound was recovered by filtration, washed with warm ethanol (150 ml), then with cold water (60 ml) and again with cold ethanol (50 ml). The resulting pale yellow powder was dried under vacuum.

Elemental analysis for $PtC_{72}H_{60}P_4$ (1243.08): Calc C 69.50, H 4.86 %, Found: C 69.8, 4.75%.

7.5.8 Synthesis of $ArP(Cl)CHCl_2$

$$CH_2Cl_2 + BuLi \longrightarrow CHLiCl_2$$

$$CHLiCl_2 + ArPCl_2 \longrightarrow ArP(CHCl_2)Cl$$

BuLi (7.4 ml, 11.8 mmol, 1.6M in hexanes) was added dropwise to a solution of CH_2Cl_2 (0.85 ml, 11.8 mmol) in a 4:1:1 mixture of pentane:THF:Et_2O at -130°C with vigorous stirring. The mixture was allowed to stir for one hour and was then added rapidly through

a pre-cooled cannula to a solution of $ArPCl_2$ (4.52g, 11.8 mmol) in diethyl ether at -130°C. The solution was allowed to warm up and stirred for 4 hours. A precipitate of LiCl formed. The solution was filtered and the solvent removed under vacuum. The product was purified by distillation under reduced pressure, giving a colourless oil, Bp 70°C (0.03 Torr).

^{31}P NMR ($CDCl_3$): δ 63.1 (septet, $^4J_{P-F}$ 49.3 Hz) pm; **^{19}F NMR** ($CDCl_3$): δ –55.3 (d, $^4J_{P-F}$ 49.3 Hz, 6F, *o*-CF_3), -64.5 (s, 3F, *p*-CF_3) ppm.

7.5.9 Synthesis of $ArP{=}CCl_2$

$$ArP(CHCl_2)Cl \xrightarrow{DBU} Ar{=}PCCl_2$$

DBU (1.05g, 0.97 ml, 7 mmol) was added dropwise to a solution of $ArP(Cl)CHCl_2$ (3g, 7 mmol) in THF. The solution was stirred for two hours giving an orange solution. The solvent was removed under vacuum, and the product purified by distillation under reduced pressure. (Bp 60°C).

^{31}P NMR ($CDCl_3$): δ 202.4 (septet, $^4J_{P-F}$ 20.6 Hz); **^{19}F NMR** ($CDCl_3$): δ –60.0 (d, $^4J_{P-F}$ 21 Hz, 6F, *o*-CF_3), -63.9 (s, 3F, *p*-CF_3) ppm.

7.5.10 Synthesis of Ar'P(Cl)$CHCl_2$

$$CH_2Cl_2 + BuLi \longrightarrow CHLiCl_2$$

$$CHLiCl_2 + Ar'PCl_2/Ar''PCl_2 \longrightarrow Ar'P(CHCl_2)Cl$$

BuLi (15.6 ml, 25 mmol, 1.6M in hexanes) was added dropwise to a solution of CH_2Cl_2 (1.6 ml, 25 mmol) in a 4:1:1 mixture of pentane: THF: Et_2O at -130°C with vigorous stirring. The mixture was allowed to stir for one hour and was then added rapidly through a pre-cooled cannula to a solution of $Ar'PCl_2/Ar''PCl_2$ (6g, 20 mmol) in diethyl ether at -130°C. The solution was allowed to warm up and stirred for 4 hours. A precipitate of

LiCl formed. The solution was filtered and the solvent removed under vacuum. The product was purified by distillation under reduced pressure, giving a colourless oil, Bp 65°C (0.03 Torr).

^{31}P NMR ($CDCl_3$): δ 65.3 (septet, $^4J_{P\text{-}F}$ 48.8 Hz) ppm; **^{19}F NMR** ($CDCl_3$): δ –53.9 (d, $^4J_{P\text{-}F}$ 49.3 Hz, 6F, *o*-CF_3) ppm.

7.5.11 Synthesis of Ar'P=CCl$_2$

$$Ar'P(CHCl_2)Cl \xrightarrow{DBU} Ar'=PCCl_2$$

DBU (2.85g, 2.8 ml, 18.8 mmol) was added dropwise to a solution of $ArP(Cl)CHCl_2$ (6.8g, 18 mmol) in THF. The solution was stirred for two hours, giving an orange solution. The solvent was removed under vacuum and the product purified by distillation under reduced pressure. (Bp 62°C).

^{31}P NMR ($CDCl_3$): δ 207.6 (septet, $^4J_{P\text{-}F}$ 20.7 Hz); **^{19}F NMR** ($CDCl_3$): δ -59.6 (d, $^4J_{P\text{-}F}$ 21.1 Hz, 6F, *o*-CF_3) ppm.

7.5.12 Synthesis of [PtCl(ClC=PAr)(PPh$_3$)$_2$]

$$Ar=PCCl_2 \xrightarrow{Pt(PPh_3)_4} PtCl(ClC=PAr)(PPh_3)_2$$

A solution of $ArP=CCl_2$ (0.24g, 0.6 mmol) in toluene was added to a solution of $Pt(PPh_3)_4$ (0.75g, 0.6 mmol) in toluene. The resulting yellow solution was allowed to stir.

^{31}P NMR (C_7D_8): *cis*-[PtCl(CCl=PAr)(PPh_3)$_2$]: δ 198.1 (multiplet with Pt satellites, $^2J_{Pt\text{-}P}$ 369.2 Hz, $^3J_{P\text{-}P}$ 45.4 Hz, $^4J_{P\text{-}F}$ 22.6 Hz), 17.3 (dd with Pt satellites, $^1J_{Pt\text{-}P}$ 1897.2, $^3J_{P\text{-}P}$ 48.4, $^3J_{P\text{-}P}$ 17.8 Hz), 14.1 (t with Pt satellites, $^1J_{Pt\text{-}P}$ 4063.8 Hz, $^3J_{P\text{-}P}$ 15.3 Hz); *trans*-[PtCl(CCl=PAr)(PPh_3)$_2$: δ 203.7 (multiplet with Pt satellites, $^2J_{Pt\text{-}P}$ 282.6 Hz, $^3J_{P\text{-}F}$ 22.6

Hz), 24.6 (d with Pt satellites, $^{1}J_{Pt\text{-}P}$ 2963.5 Hz, $^{3}J_{P\text{-}P}$ 27.5 Hz) ppm; **^{19}F NMR** ($CDCl_3$): *cis*-[PtCl(CCl=PAr)(PPh_3)$_2$ δ -57.9 (d, $^{4}J_{P\text{-}F}$ 23.7 Hz, 6F, *o*-CF_3), -63.0 (s, *p*-CF_3) ppm; *trans*-[PtCl(CCl=PAr)(PPh_3)$_2$: δ -57.8 (d, $^{4}J_{P\text{-}F}$ 23.0 Hz, 6F, *o*-CF_3), -62.9 (s, *p*-CF_3) ppm.

7.5.13 Synthesis of [PtCl(CCl=PAr')(PPh_3)$_2$]

$$Ar'{=}PCCl_2 \xrightarrow{Pt(PPh_3)_4} PtCl(ClC{=}PAr')(PPh_3)_2$$

A solution of Ar'P=CCl_2 (0.51g, 1.6 mmol) in benzene was added to a solution of $Pt(PPh_3)_4$ (1.9g, 1.5 mmol). The resulting yellow solution was allowed to stir.

^{31}P NMR (C_7D_8): *cis*-[PtCl(CCl=PAr')(PPh_3)$_2$]: δ 202.4 (septet with Pt satellites, $^{2}J_{Pt\text{-}P}$ 376.5 Hz, $^{3}J_{P\text{-}P}$ 45.4 Hz, $^{4}J_{P\text{-}F}$ 24.4 Hz), 17.1 (dd with Pt satellites, $^{1}J_{Pt\text{-}P}$ 1954.1, $^{3}J_{P\text{-}P}$ 47.1, $^{3}J_{P\text{-}P}$ 16.7 Hz), 13.5 (t, $^{1}J_{Pt\text{-}P}$ 3936.1 Hz, $^{3}J_{P\text{-}P}$ 18.7 Hz); *trans*-[PtCl(CCl=PAr)(PPh_3)$_2$: δ 208.3 (m with Pt satellites, $^{2}J_{Pt\text{-}P}$ 456.7 Hz), 24.3 (d with Pt satellites, $^{1}J_{Pt\text{-}P}$ 2989.9 Hz, $^{3}J_{P\text{-}P}$ 27.5 Hz) ppm; **^{19}F NMR** ($CDCl_3$): *cis*-[PtCl(CCl=PAr)(PPh_3)$_2$ δ -57.8 (d, $^{4}J_{P\text{-}F}$ 21.1 Hz, 6F, *o*-CF_3) ppm; *trans*-[PtCl(CCl=PAr)(PPh_3)$_2$: δ -57.6 (d, $^{4}J_{P\text{-}F}$ 23.9 Hz, 6F, *o*-CF_3) ppm.

References

1 H. Kohler, A. Michaelis, *Chem. Ber.*, **1877**, *10*, 807.

2 P. Jutzi, *Angew. Chem.*, **1975**, *87*, 269.

3 M. Yoshifuji, I. Shima, N. Inamoto, K. Hirotsu, T. Higushi, *J. Am. Chem. soc.*, **1981**, *103*, 4587.

4 R. West, M. J. Fink, J. Michl, *Science,* **1981**, *88*, 1819.

5 J. Satgé, *Adv. Organomet. Chem.*, **1982**, *21*, 241.

6 A. H. Cowley, J. G. Lasch, N. C. Norman, M. Pakulski, B. R. Whittlesey, *J. Chem. Soc., Chem. Commun.*, **1983**, 881.

7 L. Weber, U. Sonnenberg, *Chem. Ber.*, **1989**, *122*, 1809.

8 A. H. Cowley, J. G. Lasch, N. C. Norman, M. Pakulski, *J. Chem. Soc. Dalton Trans.*, **1985**, 383.

9 C. Couret, J. Escudié, Y. Madaule, H. Ranaivonjatovo, J.-G. Wolf, *Tetrahedron Lett.*, **1983**, *24*, 2769.

10 A. H. Cowley, J. G. Lasch, N. C. Norman, M. Pakulski, *J. Am. Chem. Soc.*, **1983**, *105*, 5506.

11 T. P. Fehlner, *J. Am. Chem. Soc.*, **1967**, *89*, 6477.

12 B. Twamley, C. D. Sofield, M. M. Olmstead, P. P. Power, *J. Am. Chem. Soc.*, **1999**, *121*, 3357.

13 S. Masamune, Y. Hanzawa, S. Murakami, T. Bally, D. J. Blount, *J. Am. Chem. Soc.*, **1982**, *104*, 1150.

14 S. Masamune, S. Murakami, H. Tobita, *Organometallics,* **1983**, *2*, 1464.

15 S. Masamune, S. Murakami, H. Tobita, *J. Am. Chem. Soc.*, **1983**, *105*, 6524.

16 H. Watanabe, Y. Kougo, Y. Nagai, *J. Chem. Soc., Chem. Commun.*, **1984**, 66.

17 H. P. Goodwin, *Ph. D. Thesis*, Durham, 1990.

18 A. H. Cowley, J. E. Kilduff, M. Pakulski, C. A. Stewart, *J. Am. Chem. Soc.*, **1983**, *105*, 1655.

19 M. Yoshifuji, S. Sasaki, N. Inamoto, *J. Chem. Soc., Chem. Commun.*, **1989**, 1732.

20 C. N. Smit, T. A. v. d. Knaap, F. Bickelhaupt, *Tet. Lett.*, **1983**, *24*, 2031.

21 K. B. Dillon, V. C. Gibson, L. J. Sequeira, *J. Chem. Soc., Chem. Commun.*, **1995**, 2429.

22 L. J. Sequeira, *Ph.D. Thesis*, Durham, 1996.

23 C. C. Cummins, R. R. Schrock, W. P. Davis, *Angew. Chem., Int. Ed. Engl.*, **1993**, *32*, 756.

24 P. B. Hitchcock, M. F. Lappert, W. P. Leung, *J. Chem. Soc., Chem. Commun.*, **1987**, 6734.

25 Z. Hou, T. L. Breen, D. W. Stephen, *Organometallics*, **1993**, *12*, 3158.

26 A. H. Cowley, C. Pellerin, J. L. Atwood, S. G. Bott, *J. Am. Chem. Soc.*, **1990**, *112*, 3734.

27 C. N. Smit, F. M. Lock, F. Bickelhaupt, *Tetrahedron Lett.*, **1984**, *25*, 3011.

28 C. N. Smit, F. Bickelhaupt, *Organometallics*, **1987**, *6*, 1156.

29 E. Niecke, E. Klein, M. Nieger, *Angew. Chem., Int. Ed. Engl.*, **1989**, *28*, 751.

30 J. Escudié, C. Couret, J. Satgé, M. Andrianarison, J. D. Andriamizaka, *J. Am. Chem. Soc.*, **1985**, *107*, 3378.

31 J. Escudié, C. Couret, J. Satgé, M. Andrianarison, *J. Am. Chem. Soc.*, **1987**, *109*, 386.

32 J. Escudié, C. Couret, J. Satgé, M. Andrianarison, A. Raharinirina, *Phosphorus and Sulfur*, **1987**, *30*, 377.

33 H. Ranaivonjatovo, J. Escudié, C. Couret, J. Satgé, M. Dräger, *New J. Chem*, **1989**, *13*, 389.

34 H. Ranaivonjatovo, J. Escudié, C. Couret, J. Satgé, *J. Organomet. Chem.*, **1991**, *415*, 327.

35 H. Ranaivonjatovo, J. Escudié, C. Couret, A. K. Rodi, J. Satgé, *Phosphorus, Sulfur and Silicon*, **1993**, *76*, 61.

36 M. Dräger, J. Escudié, C. Couret, H. Ranaivonjatovo, J. Satgé, *Organometallics*, **1988**, *7*, 1010.

37 H. Ranaivonjatovo, J. Escudié, C. Couret, J. Satgé, *J. Chem. Soc., Chem. Commun.*, **1992**, 1047.

38 J. Escudié, C. Couret, H. Ranaivonjatovo, M. Lazraq, J. Satgé, *Phosphorus Sulfur*, **1987**, *31*, 27.

39 C. Couret, J. Escudié, J. Satgé, A. Raharinirina, J. D. Andriamizaka, *J. Am. Chem. Soc.*, **1985**, *107*, 8280.

40 A. K. Rodi, *Ph. D. Thesis*, Toulouse, **1995**.

41 K. Dimroth, P. Hoffman, *Chem. Ber.*, **1966**, *99*, 1325.

42 K. Dimroth, P. Hoffman, *Angew. Chem., Int. Ed. Engl.*, **1964**, *3*, 384.

43 G. Becker, *Z. Anorg. Allgem. Chem.*, **1976**, *423*, 242.

44 K. B. Dillon, F. Mathey, J. F. Nixon, *Phosphorus: The Carbon Copy*; Wiley, Chichester, **1998**.

45 K. B. Dillon, H. P. Goodwin, *J. Organomet. Chem.*, **1994**, *469*, 125.

46 T. E. Gier, *J. Am. Chem. Soc.*, **1961**, *83*, 1796.

47 G. Becker, G. Gesser, W. Uhl, *Z. Naturforsch B.*, **1981**, *36*, 16.

48 V. D. Romanenko, M. Sanchez, T. V. Sarina, M.-R. Mazières, R. Wolf, *Tetrahedron Lett.*, **1992**, *33*, 2981.

49 R. J. Anjelici, H. Jun, V. G. Young, *Organometallics*, **1994**, *13*, 2444.

50 M. D. Roden, *Ph . D. Thesis*, Durham, **1998**.

51 R. Appel, J. Menzel, F. Knoch, P. Volz, *Z. Anorg. Allg. Chem.*, **1986**, *534*, 100.

Conclusions and Future Work

A series of new derivatives containing bulky electron-withdrawing substituents and some elements of groups 13,14, and 15 has been synthesised.

Coordination of fluoromes or fluoroxyl ligands to boron or silicon revealed a fluorine/chlorine exchange, leading to the synthesis of Ar_2BF, Ar_2SiF_2 and Ar'_2SiF_2, which have been structurally characterised.

For the first time, the crystal structures of derivatives containing three fluoroxyl ligands have been determined (Ar''_3B and $Ar'Ar''_2Sb$). Phosphorus and arsenic derivatives have been extensively studied, with the isolation of $ArEX_2$, Ar_2EX, $Ar'EX_2$, $Ar''EX_2$, Ar''_2EX and Ar'Ar"EX where E = P or As and X = H, Cl or Br. For compounds containing Ar or Ar' and Ar", detailed T-dependence studies have allowed the calculation of rotational barriers. However, with group 14 elements, only chlorinated derivatives have been prepared so far. This could be extended to the bromide and hydride compounds, at least with tin and germanium derivatives, as halogen exchange might occur with silicon.

Synthesis of Ar'Ar"BX should be tried as well in order to carry out variable temperature NMR studies to determined the rotational barrier of the molecule and compare it with those calculated in this work.

All derivatives structurally characterised have shown some intramolecular interactions between the fluorines of some of the *o*-CF_3 groups and the central atom. These short contacts are believed to play an important role in the stabilisation of such molecule containing bulky electron-withdrawing substituents

New platinum *cis* and *trans* complexes have been prepared by treatment of phosphane derivatives with $[PtCl_2(PEt_3)]_2$ or $[PtBr_2(PEt_3)]_2$. Halogen exchange was observed when a bromophosphane was reacted with the chlorodimer. Cis isomers could be screened for anti-cancer activity.

Some advances have also been made in the field of multiple bonded main group derivatives. Attempts have been made to prepare new P=E (E= As, Ge, Sn) derivatives. ArP=PAr and Ar'P=PAr' have been prepared, but reaction between an arsane and a phosphane or a phosphane and a group 14 derivative has not been successful. However, this is a field of considerable interest, and some reactions could be tried, such as the synthesis of ArAs=AsAr by reacting $ArAsCl_2$ with $W(PMe_3)_6$ in a 2:1 ratio, to check the ability of the tungsten catalyst to remove chlorine from a derivative other than phosphorus.

If the synthesis of a P=As compound is successful, reaction with $[PtCl_2(PEt_3)_2]_2$ should be attempted in order to study the coordination of the platinum. According to the results found in this work, platinum should only coordinate at the phosphorus atom. The reaction of certain phosphaalkenes with $Pt(PPh_3)_4$ clearly showed the formation of platinum(II) complexes and, in one case, the formation of a phosphabicyclo intermediate has been observed by NMR spectroscopy.

Alternative synthetic routes to phosphaalkynes could be explored, such as the reaction of ArCOCl and $P(SiMe_3)_3$:

Conclusions and Future Work 286

Appendix A

Calculations for Boron derivatives

$Ar'B(OH)_2$

Optimized geometry at HF/6-31G* level

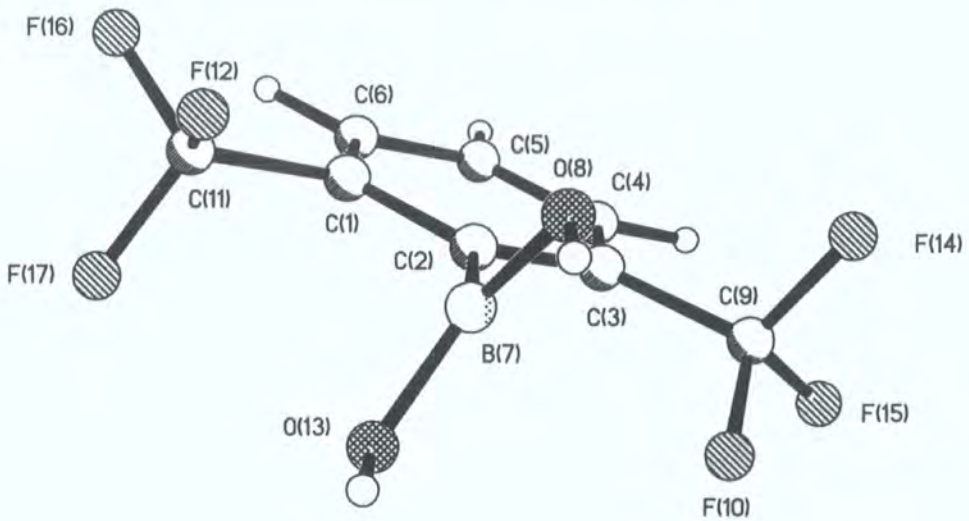

INTERATOMIC DISTANCES

	C 1	C 2	C 3	C 4	C 5	C 6
C 1	0.000					
C 2	1.396	0.000				
C 3	2.378	1.396	0.000			
C 4	2.756	2.430	1.386	0.000		
C 5	2.399	2.814	2.399	1.381	0.000	
C 6	1.386	2.430	2.756	2.385	1.381	0.000
B 7	2.616	1.599	2.616	3.903	4.413	3.903
O 8	3.532	2.524	3.265	4.558	5.176	4.752
C 9	3.777	2.522	1.508	2.478	3.759	4.262
F 10	4.166	2.800	2.351	3.549	4.702	4.945
C 11	1.508	2.522	3.777	4.262	3.759	2.478
F 12	2.351	2.800	4.165	4.945	4.702	3.549
O 13	3.265	2.524	3.532	4.752	5.176	4.558
F 14	4.407	3.190	2.353	3.186	4.411	4.906
F 15	4.695	3.596	2.347	2.710	4.074	4.892
F 16	2.347	3.596	4.695	4.892	4.074	2.710
F 17	2.353	3.190	4.407	4.906	4.411	3.186
H 18	3.829	3.396	2.134	1.073	2.131	3.359
H 19	3.374	3.888	3.374	2.135	1.074	2.135
H 20	2.134	3.396	3.829	3.359	2.131	1.073
H 21	4.127	3.382	4.359	5.633	6.097	5.456
H 22	4.359	3.382	4.127	5.456	6.097	5.633

	B 7	O 8	C 9	F 10	C 11	F 12
B 7	0.000					
O 8	1.352	0.000				
C 9	3.001	3.295	0.000			
F 10	2.606	2.956	1.328	0.000		
C 11	3.001	3.852	5.044	5.173	0.000	
F 12	2.606	3.110	5.173	5.126	1.328	0.000
O 13	1.352	2.402	3.853	3.111	3.295	2.956
F 14	3.458	3.220	1.322	2.129	5.599	5.514
F 15	4.231	4.605	1.324	2.129	6.062	6.357
F 16	4.231	4.909	6.062	6.357	1.324	2.129

F	17	3.458	4.535	5.599	5.514	1.322	2.129
H	18	4.751	5.299	2.654	3.845	5.335	5.994
H	19	5.487	6.225	4.612	5.633	4.612	5.633
H	20	4.750	5.592	5.335	5.994	2.654	3.845
H	21	1.967	2.570	4.486	3.578	3.976	3.387
H	22	1.967	0.946	3.976	3.388	4.486	3.578

		O 13	F 14	F 15	F 16	F 17	H 18
O	13	0.000					
F	14	4.535	0.000				
F	15	4.909	2.124	0.000			
F	16	4.605	6.514	7.031	0.000		
F	17	3.220	6.361	6.514	2.124	0.000	
H	18	5.592	3.258	2.384	5.936	5.948	0.000
H	19	6.225	5.213	4.709	4.709	5.214	2.459
H	20	5.299	5.948	5.936	2.384	3.258	4.248
H	21	0.946	5.030	5.554	5.239	3.853	6.441
H	22	2.571	3.853	5.239	5.554	5.030	6.165

		H 19	H 20	H 21	
H	19	0.000			
H	20	2.459	0.000		
H	21	7.154	6.165	0.000	
H	22	7.154	6.441	2.379	0.000

BOND ANGLES

1	2	3	C2	C2	C2	116.839
1	2	7	C2	C2	B	121.580
1	6	5	C2	C2	C2	120.157
1	6	20	C2	C2	HC	119.889
1	11	12	C2	C3	F	111.852
1	11	16	C2	C3	F	111.780
1	11	17	C2	C3	F	112.333
2	1	6	C2	C2	C2	121.719
2	1	11	C2	C2	C3	120.546
2	3	4	C2	C2	C2	121.718
2	3	9	C2	C2	C3	120.548
2	7	8	C2	B	O3	117.337
2	7	13	C2	B	O3	117.338
3	2	7	C2	C2	B	121.581
3	4	5	C2	C2	C2	120.158
3	4	18	C2	C2	HC	119.889
3	9	10	C2	C3	F	111.854
3	9	14	C2	C3	F	112.334
3	9	15	C2	C3	F	111.777
4	3	9	C2	C2	C3	117.722
4	5	6	C2	C2	C2	119.408
4	5	19	C2	C2	HC	120.296
5	4	18	C2	C2	HC	119.952
5	6	20	C2	C2	HC	119.953
6	1	11	C2	C2	C3	117.724
6	5	19	C2	C2	HC	120.296
7	8	22	B	O3	H	116.567
7	13	21	B	O3	H	116.558
8	7	13	O3	B	O3	125.325

TORSION ANGLES

1	2	3	4	-0.093	2	3	4	5	0.186
1	2	3	9	178.652	2	3	4	18	-179.518
1	2	7	8	-108.490	2	3	9	10	33.380
1	2	7	13	71.508	2	3	9	14	-86.867
2	1	6	5	0.186	2	3	9	15	153.104
2	1	6	20	-179.518	2	7	8	22	-177.370
2	1	11	12	33.382	2	7	13	21	-177.364
2	1	11	16	153.108	3	2	7	8	71.503
2	1	11	17	-86.860	3	2	7	13	-108.499

3	4	5	6	-0.091	7	2	3	9	-1.341
3	4	5	19	179.909	8	7	13	21	2.634
4	3	9	10	-147.826	9	3	4	5	-178.593
4	3	9	14	91.927	9	3	4	18	1.703
4	3	9	15	-28.101	11	1	2	3	178.655
4	5	6	1	-0.091	11	1	2	7	-1.352
4	5	6	20	179.613	11	1	6	5	-178.595
6	1	2	3	-0.092	11	1	6	20	1.701
6	1	2	7	179.901	13	7	8	22	2.633
6	1	11	12	-147.823	18	4	5	6	179.613
6	1	11	16	-28.096	18	4	5	19	-0.387
6	1	11	17	91.936	19	5	6	1	179.910
7	2	3	4	179.914	19	5	6	20	-0.387

$Ar'B(OH)_2$
Calculated NMR (GIAO-HF/6-31G*//HF/6-31G*)

For ^{19}F shift use 213 - value

22
$C_8H_5BF_6O_2$ << C1 >>, GIAO RHF / 6-31G* OPT RHF / 6-31G* -1077.04895445
C 1 69.1616 132.538
C 2 64.8629 136.837
C 3 69.1607 132.539
C 4 71.7215 129.978
C 5 77.3422 124.358
C 6 71.7228 129.977
B 7 97.0015 26.3985
O 8 255.3898
C 9 92.5724 109.128
F 10 315.5568
C 11 92.5720 109.128
F 12 315.5491
O 13 255.3883
F 14 303.1253
F 15 320.3522
F 16 320.3577
F 17 303.1226
H 18 24.6522 10.3478
H 19 25.1207 9.8793
H 20 24.6522 10.3478
H 21 29.7736 5.2264
H 22 29.7727 5.2273

^{11}B ref= 123.4 ^{13}C ref= 201.7 ^{1}H ref= 35

$C_8H_5BF_6O_2$ << C1 >> NIMAG= 0 ZPE= 91.04038 E(RHF) / 6-31G(d) FC= 1 //
OPT RHF / 6-31G* -1077.04895445

Ar'_2BF

Optimized HF/6-31G* geometry

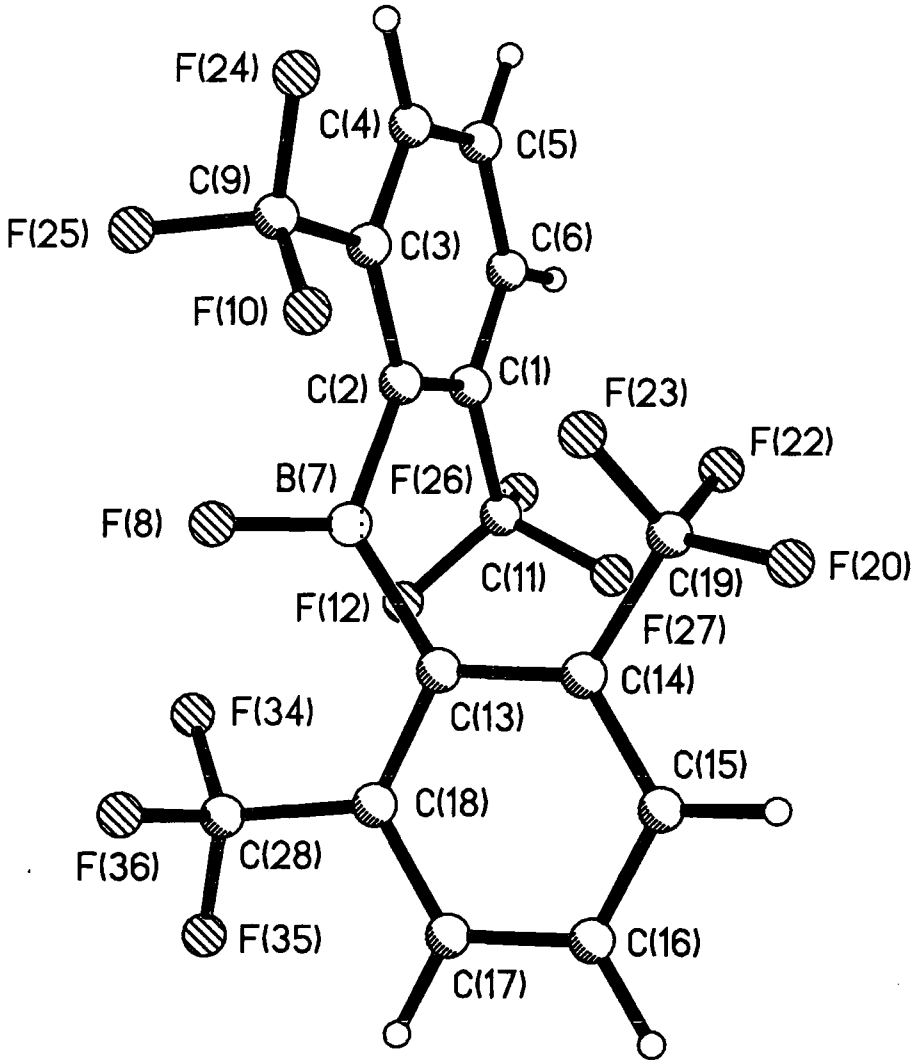

INTERATOMIC DISTANCES

		C 1	C 2	C 3	C 4	C 5	C 6
C	1	0.000					
C	2	1.403	0.000				
C	3	2.388	1.406	0.000			
C	4	2.756	2.436	1.386	0.000		
C	5	2.399	2.822	2.402	1.380	0.000	
C	6	1.387	2.437	2.760	2.380	1.378	0.000
B	7	2.657	1.604	2.603	3.896	4.426	3.934
F	8	3.653	2.471	3.010	4.354	5.110	4.820

C 9	3.813	2.568	1.518	2.460	3.751	4.274
F 10	4.283	2.920	2.372	3.517	4.704	5.007
C 11	1.513	2.551	3.804	4.265	3.748	2.462
F 12	2.348	2.862	4.204	4.933	4.655	3.493
C 13	3.538	2.898	4.017	5.236	5.596	4.882
C 14	4.020	3.538	4.526	5.607	5.900	5.213
C 15	5.213	4.882	5.910	6.960	7.169	6.386
C 16	5.900	5.596	6.737	7.867	8.058	7.169
C 17	5.607	5.236	6.428	7.633	7.867	6.960
C 18	4.526	4.017	5.189	6.428	6.737	5.910
C 19	3.886	3.401	4.047	4.921	5.247	4.795
F 20	5.134	4.691	5.199	5.977	6.305	5.927
H 21	6.889	6.649	7.792	8.899	9.049	8.126
F 22	3.230	3.197	3.880	4.447	4.457	3.902
F 23	3.888	3.020	3.256	4.205	4.848	4.715
F 24	4.720	3.644	2.348	2.640	4.010	4.868
F 25	4.385	3.175	2.349	3.200	4.414	4.888
F 26	2.348	3.630	4.705	4.855	4.009	2.647
F 27	2.364	3.182	4.442	4.958	4.475	3.243
C 28	4.959	4.415	5.508	6.753	7.105	6.316
H 29	6.440	6.107	7.314	8.530	8.747	7.798
H 30	5.825	5.561	6.488	7.436	7.607	6.872
H 31	3.827	3.401	2.132	1.071	2.125	3.351
H 32	3.374	3.896	3.376	2.133	1.074	2.133
H 33	2.133	3.401	3.832	3.353	2.125	1.072
F 34	4.216	3.806	4.891	6.018	6.278	5.485
F 35	5.942	5.591	6.752	7.946	8.180	7.274
F 36	5.708	4.885	5.728	7.051	7.626	7.035

	B 7	F 8	C 9	F 10	C 11	F 12
B 7	0.000					
F 8	1.313	0.000				
C 9	3.022	2.881	0.000			
F 10	2.753	2.591	1.321	0.000		
C 11	3.103	4.171	5.113	5.371	0.000	
F 12	2.818	3.634	5.278	5.429	1.323	0.000
C 13	1.604	2.471	4.415	3.806	3.400	3.020
C 14	2.657	3.653	4.960	4.216	3.885	3.888
C 15	3.934	4.820	6.316	5.486	4.795	4.715
C 16	4.425	5.111	7.105	6.278	5.246	4.848
C 17	3.896	4.354	6.753	6.019	4.920	4.205
C 18	2.603	3.010	5.508	4.891	4.047	3.256
C 19	3.103	4.171	4.509	3.825	4.163	4.580
F 20	4.365	5.336	5.514	4.700	5.352	5.803
H 21	5.499	6.159	8.153	7.288	6.144	5.755
F 22	3.460	4.693	4.730	4.395	3.501	4.265
F 23	2.818	3.633	3.396	2.621	4.580	4.948
F 24	4.285	4.187	1.325	2.119	6.132	6.458
F 25	3.389	2.765	1.321	2.131	5.576	5.485
F 26	4.365	5.336	6.113	6.536	1.323	2.124
F 27	3.459	4.692	5.671	5.681	1.322	2.127
C 28	3.021	2.881	5.721	5.276	4.508	3.396
H 29	4.735	5.021	7.606	6.889	5.645	4.773
H 30	4.789	5.725	6.899	6.039	5.456	5.563
H 31	4.735	5.021	2.615	3.760	5.336	5.978
H 32	5.499	6.158	4.594	5.610	4.594	5.568
H 33	4.789	5.725	5.345	6.062	2.622	3.757
F 34	2.753	2.591	5.276	5.141	3.825	2.621
F 35	4.285	4.187	7.031	6.599	5.227	4.016
F 36	3.389	2.765	5.589	5.023	5.535	4.492

	C 13	C 14	C 15	C 16	C 17	C 18
C 13	0.000					
C 14	1.403	0.000				
C 15	2.437	1.387	0.000			
C 16	2.822	2.399	1.378	0.000		
C 17	2.436	2.756	2.380	1.380	0.000	
C 18	1.406	2.388	2.760	2.402	1.386	0.000
C 19	2.551	1.513	2.462	3.748	4.265	3.804

F	20	3.630	2.348	2.647	4.009	4.855	4.705
H	21	3.896	3.374	2.133	1.074	2.133	3.376
F	22	3.183	2.364	3.243	4.475	4.958	4.442
F	23	2.862	2.348	3.493	4.656	4.933	4.204
F	24	5.591	5.943	7.274	8.181	7.947	6.752
F	25	4.885	5.708	7.035	7.627	7.051	5.728
F	26	4.691	5.134	5.926	6.304	5.976	5.199
F	27	3.197	3.229	3.901	4.456	4.446	3.879
C	28	2.568	3.813	4.274	3.751	2.460	1.518
H	29	3.401	3.827	3.351	2.125	1.071	2.132
H	30	3.401	2.133	1.072	2.125	3.353	3.832
H	31	6.107	6.440	7.798	8.747	8.530	7.314
H	32	6.649	6.889	8.126	9.049	8.898	7.792
H	33	5.561	5.825	6.872	7.606	7.435	6.488
F	34	2.920	4.283	5.007	4.704	3.517	2.372
F	35	3.644	4.720	4.868	4.010	2.640	2.348
F	36	3.175	4.384	4.888	4.414	3.200	2.349

		C 19	F 20	H 21	F 22	F 23	F 24
C	19	0.000					
F	20	1.323	0.000				
H	21	4.594	4.623	0.000			
F	22	1.322	2.121	5.288	0.000		
F	23	1.323	2.124	5.568	2.127	0.000	
F	24	5.227	6.052	9.204	5.374	4.016	0.000
F	25	5.535	6.602	8.685	5.811	4.492	2.122
F	26	5.352	6.471	7.115	4.514	5.803	7.042
F	27	3.500	4.514	5.260	2.765	4.264	6.641
C	28	5.113	6.113	4.594	5.671	5.277	7.031
H	29	5.336	5.891	2.452	6.007	5.978	8.834
H	30	2.622	2.278	2.454	3.325	3.757	7.728
H	31	5.645	6.593	9.778	5.246	4.773	2.260
H	32	6.144	7.116	10.019	5.261	5.756	4.618
H	33	5.456	6.521	8.500	4.416	5.563	5.907
F	34	5.371	6.536	5.610	5.681	5.429	6.599
F	35	6.132	7.042	4.618	6.641	6.458	8.346
F	36	5.576	6.505	5.221	6.325	5.485	6.851

		F 25	F 26	F 27	C 28	H 29	H 30
F	25	0.000					
F	26	6.505	0.000				
F	27	6.325	2.121	0.000			
C	28	5.589	5.514	4.730	0.000		
H	29	7.775	6.593	5.246	2.615	0.000	
H	30	7.743	6.520	4.415	5.345	4.237	0.000
H	31	3.289	5.891	6.007	7.605	9.434	8.228
H	32	5.221	4.623	5.288	8.153	9.778	8.500
H	33	5.923	2.278	3.325	6.899	8.228	7.310
F	34	5.023	4.700	4.395	1.321	3.760	6.062
F	35	6.851	6.052	5.374	1.325	2.259	5.907
F	36	5.290	6.602	5.810	1.321	3.289	5.923

		H 31	H 32	H 33	F 34	F 35
H	31	0.000				
H	32	2.452	0.000			
H	33	4.237	2.454	0.000		
F	34	6.889	7.288	6.038	0.000	
F	35	8.833	9.203	7.728	2.119	0.000
F	36	7.774	8.684	7.743	2.131	2.122	0.000

BOND ANGLES

1	2	3	C2	C2	C2	116.423
1	2	7	C2	C2	B	124.015

1	6	5	C2	C2	C2	120.368
1	6	33	C2	C2	HC	119.809
1	11	12	C2	C3	F	111.581
1	11	26	C2	C3	F	111.611
1	11	27	C2	C3	F	112.831
2	1	6	C2	C2	C2	121.778
2	1	11	C2	C2	C3	122.042
2	3	4	C2	C2	C2	121.476
2	3	9	C2	C2	C3	122.752
2	7	8	C2	B	F	115.403
2	7	13	C2	B	C2	129.186
3	2	7	C2	C2	B	119.543
3	4	5	C2	C2	C2	120.564
3	4	31	C2	C2	HC	119.774
3	9	10	C2	C3	F	113.177
3	9	24	C2	C3	F	111.145
3	9	25	C2	C3	F	111.513
4	3	9	C2	C2	C3	115.742
4	5	6	C2	C2	C2	119.360
4	5	32	C2	C2	HC	120.294
5	4	31	C2	C2	HC	119.662
5	6	33	C2	C2	HC	119.822
6	1	11	C2	C2	C3	116.168
6	5	32	C2	C2	HC	120.342
7	13	14	B	C2	C2	124.015
7	13	18	B	C2	C2	119.543
8	7	13	F	B	C2	115.411
13	14	15	C2	C2	C2	121.778
13	14	19	C2	C2	C3	122.044
13	18	17	C2	C2	C2	121.476
13	18	28	C2	C2	C3	122.751
14	13	18	C2	C2	C2	116.422
14	15	16	C2	C2	C2	120.367
14	15	30	C2	C2	HC	119.808
14	19	20	C2	C3	F	111.610
14	19	22	C2	C3	F	112.832
14	19	23	C2	C3	F	111.581
15	14	19	C2	C2	C3	116.166
15	16	17	C2	C2	C2	119.359
15	16	21	C2	C2	HC	120.342
16	15	30	C2	C2	HC	119.822
16	17	18	C2	C2	C2	120.564
16	17	29	C2	C2	HC	119.663
17	16	21	C2	C2	HC	120.294
17	18	28	C2	C2	C3	115.744
18	17	29	C2	C2	HC	119.773
18	28	34	C2	C3	F	113.177
18	28	35	C2	C3	F	111.145
18	28	36	C2	C3	F	111.514

TORSION ANGLES

1	2	3	4	-1.919	3	4	5	32	-179.974
1	2	3	9	176.014	4	3	9	10	-141.356
1	2	7	8	-132.695	4	3	9	24	-21.673
1	2	7	13	47.301	4	3	9	25	97.219
2	1	6	5	-0.104	4	5	6	1	-1.120
2	1	6	33	-179.558	4	5	6	33	178.333
2	1	11	12	39.373	6	1	2	3	1.588
2	1	11	26	158.725	6	1	2	7	179.974
2	1	11	27	-81.232	6	1	11	12	-139.376
2	3	4	5	0.779	6	1	11	26	-20.024
2	3	4	31	-179.209	6	1	11	27	100.019
2	3	9	10	40.601	7	2	3	4	179.621
2	3	9	24	160.284	7	2	3	9	-2.445
2	3	9	25	-80.824	7	13	14	15	179.974
2	7	13	14	47.303	7	13	14	19	1.303
2	7	13	18	-134.352	7	13	18	17	179.609
3	2	7	8	45.640	7	13	18	28	-2.455
3	2	7	13	-134.364	8	7	13	14	-132.701
3	4	5	6	0.788	8	7	13	18	45.645

9	3	4	5	-177.291
9	3	4	31	2.720
11	1	2	3	-177.092
11	1	2	7	1.291
11	1	6	5	178.649
11	1	6	33	-0.804
13	14	15	16	-0.105
13	14	15	30	-179.558
13	14	19	20	158.702
13	14	19	22	-81.254
13	14	19	23	39.351
13	18	28	34	40.614
13	18	28	35	160.295
13	18	28	36	-80.811
14	13	18	17	-1.922
14	13	18	28	176.013
14	15	16	17	-1.122
14	15	16	21	179.653
15	14	19	20	-20.047
15	14	19	22	99.996
15	14	19	23	-139.399
15	16	17	18	0.790
15	16	17	29	-179.221
16	17	18	13	0.780
16	17	18	28	-177.292
17	18	28	34	-141.341
17	18	28	35	-21.659
17	18	28	36	97.234
18	13	14	15	1.591
18	13	14	19	-177.089
19	14	15	16	178.649
19	14	15	30	-0.805
21	16	17	18	-179.974
21	16	17	29	0.026
29	17	18	13	-179.209
29	17	18	28	2.718
30	15	16	17	178.331
30	15	16	21	-0.894
31	4	5	6	-179.223
31	4	5	32	0.026
32	5	6	1	179.654
32	5	6	33	-0.893

Ar'_2BF

Calculated NMR (GIAO-HF/6-31G*//HF/6-31G*)

For ^{19}F shift use 213 - value

36

$C_{16}H_6BF_{13}$ << C1 >>, GIAO RHF / 6-31G* OPT RHF / 6-31G* -1926.91110689
C 1 65.1547 136.545
C 2 67.6085 134.091
C 3 63.9750 137.725
C 4 71.5189 130.181
C 5 73.3267 128.373
C 6 72.3828 129.317
B 7 79.3457 44.0543
F 8 258.4726
C 9 93.2754 108.425
F 10 312.9838
C 11 93.6223 108.078
F 12 302.9631
C 13 67.6135 134.087
C 14 65.1516 136.548
C 15 72.3813 129.319
C 16 73.3253 128.375
C 17 71.5198 130.18
C 18 63.9766 137.723
C 19 93.6231 108.077
F 20 319.0227
H 21 24.8938 10.1062
F 22 303.7638
F 23 302.9779
F 24 319.8013
F 25 301.1984
F 26 319.0315
F 27 303.7624
C 28 93.2763 108.424
H 29 24.4427 10.5573
H 30 24.6236 10.3764
H 31 24.4427 10.5573
H 32 24.8939 10.1061
H 33 24.6237 10.3763
F 34 312.9771
F 35 319.8064
F 36 301.2021

^{11}B ref= 123.4 ^{13}C ref= 201.7 ^{1}H ref= 35

$C_{16}H_6BF_{13}$ << C1 >> NIMAG= 0 ZPE= 141.48440 E(RHF) / 6-31G(d) FC= 1 //
OPT RHF / 6-31G* -1926.91110689

$Ar'_2B(OH)$

Optimized HF/6-31G* geometry

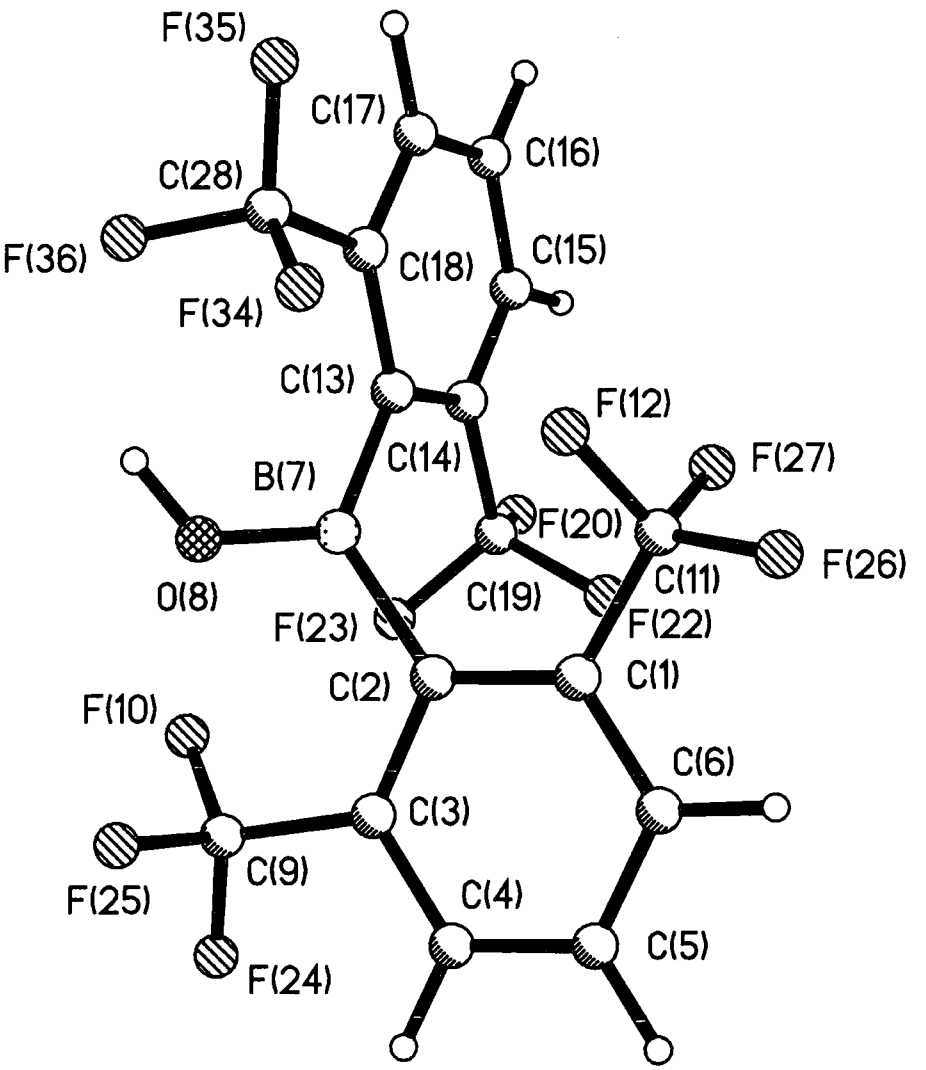

INTERATOMIC DISTANCES

		C 1	C 2	C 3	C 4	C 5	C 6
C	1	0.000					
C	2	1.403	0.000				
C	3	2.385	1.408	0.000			
C	4	2.748	2.437	1.388	0.000		
C	5	2.397	2.828	2.407	1.379	0.000	
C	6	1.387	2.442	2.763	2.377	1.377	0.000
B	7	2.664	1.615	2.620	3.912	4.442	3.945
O	8	3.632	2.466	3.012	4.344	5.091	4.795
C	9	3.822	2.585	1.521	2.450	3.747	4.277

F 10	4.317	2.953	2.388	3.532	4.728	5.039
C 11	1.511	2.548	3.800	4.256	3.743	2.457
F 12	2.349	2.864	4.211	4.934	4.658	3.494
C 13	3.523	2.893	4.017	5.230	5.587	4.866
C 14	3.978	3.497	4.477	5.549	5.844	5.162
C 15	5.142	4.834	5.855	6.882	7.079	6.294
C 16	5.829	5.565	6.713	7.815	7.979	7.076
C 17	5.558	5.230	6.441	7.623	7.827	6.898
C 18	4.509	4.033	5.226	6.450	6.738	5.889
C 19	3.862	3.354	3.965	4.838	5.187	4.760
F 20	5.108	4.648	5.118	5.889	6.239	5.886
H 21	6.804	6.612	7.760	8.833	8.950	8.013
F 22	3.194	3.129	3.757	4.312	4.353	3.841
F 23	3.910	3.011	3.212	4.176	4.852	4.739
F 24	4.710	3.647	2.346	2.625	3.991	4.852
F 25	4.416	3.221	2.354	3.163	4.388	4.892
F 26	2.350	3.632	4.707	4.852	4.008	2.645
F 27	2.363	3.176	4.431	4.943	4.466	3.238
C 28	4.992	4.482	5.608	6.845	7.172	6.354
H 29	6.392	6.110	7.342	8.533	8.713	7.736
H 30	5.740	5.495	6.405	7.325	7.486	6.759
H 31	3.820	3.402	2.132	1.071	2.121	3.346
H 32	3.373	3.902	3.380	2.134	1.074	2.133
H 33	2.133	3.405	3.834	3.350	2.125	1.072
F 34	4.332	3.982	5.112	6.227	6.448	5.608
F 35	6.061	5.711	6.888	8.088	8.320	7.400
F 36	5.652	4.845	5.721	7.044	7.602	6.989
H 37	4.475	3.346	3.905	5.258	6.027	5.694

	B 7	O 8	C 9	F 10	C 11	F 12
B 7	0.000					
O 8	1.336	0.000				
C 9	3.067	2.936	0.000			
F 10	2.809	2.676	1.320	0.000		
C 11	3.100	4.150	5.127	5.407	0.000	
F 12	2.805	3.602	5.307	5.468	1.324	0.000
C 13	1.625	2.575	4.457	3.869	3.375	3.004
C 14	2.671	3.751	4.945	4.243	3.851	3.877
C 15	3.955	4.949	6.312	5.531	4.723	4.685
C 16	4.459	5.270	7.151	6.365	5.153	4.802
C 17	3.934	4.520	6.841	6.131	4.834	4.153
C 18	2.643	3.163	5.608	5.002	3.993	3.218
C 19	3.114	4.236	4.433	3.798	4.169	4.596
F 20	4.379	5.415	5.435	4.671	5.353	5.816
H 21	5.533	6.324	8.198	7.377	6.036	5.702
F 22	3.467	4.725	4.612	4.341	3.525	4.301
F 23	2.837	3.689	3.328	2.584	4.614	4.974
F 24	4.320	4.252	1.329	2.114	6.123	6.474
F 25	3.480	2.855	1.321	2.132	5.628	5.569
F 26	4.362	5.302	6.129	6.573	1.323	2.123
F 27	3.463	4.702	5.678	5.718	1.324	2.128
C 28	3.070	3.026	5.884	5.417	4.492	3.380
H 29	4.775	5.192	7.717	7.018	5.551	4.715
H 30	4.803	5.844	6.862	6.059	5.382	5.535
H 31	4.752	5.015	2.594	3.762	5.327	5.980
H 32	5.516	6.136	4.583	5.631	4.591	5.571
H 33	4.797	5.694	5.348	6.095	2.616	3.753
F 34	2.894	2.786	5.561	5.393	3.848	2.611
F 35	4.361	4.322	7.201	6.722	5.323	4.134
F 36	3.316	2.785	5.646	5.050	5.454	4.415
H 37	1.966	0.946	3.640	3.118	4.814	4.111

	C 13	C 14	C 15	C 16	C 17	C 18
C 13	0.000					
C 14	1.404	0.000				
C 15	2.444	1.388	0.000			
C 16	2.835	2.401	1.376	0.000		
C 17	2.445	2.753	2.375	1.379	0.000	
C 18	1.411	2.383	2.755	2.403	1.386	0.000

C	19	2.558	1.513	2.454	3.743	4.262	3.806
F	20	3.634	2.347	2.635	3.995	4.843	4.698
H	21	3.909	3.376	2.133	1.074	2.134	3.377
F	22	3.194	2.363	3.220	4.453	4.947	4.445
F	23	2.873	2.350	3.495	4.665	4.945	4.220
F	24	5.607	5.886	7.219	8.182	8.004	6.830
F	25	5.000	5.763	7.116	7.774	7.248	5.927
F	26	4.665	5.097	5.842	6.190	5.871	5.136
F	27	3.159	3.187	3.800	4.315	4.310	3.788
C	28	2.570	3.809	4.266	3.746	2.454	1.517
H	29	3.409	3.824	3.345	2.122	1.071	2.132
H	30	3.406	2.133	1.072	2.123	3.348	3.826
H	31	6.105	6.381	7.721	8.702	8.532	7.347
H	32	6.639	6.831	8.027	8.959	8.850	7.788
H	33	5.539	5.773	6.769	7.490	7.347	6.448
F	34	2.983	4.333	5.022	4.686	3.484	2.380
F	35	3.670	4.731	4.864	3.996	2.620	2.355
F	36	3.104	4.324	4.874	4.453	3.258	2.349
H	37	2.666	3.871	4.906	5.052	4.202	2.924

		C 19	F 20	H 21	F 22	F 23	F 24
C	19	0.000					
F	20	1.324	0.000				
H	21	4.587	4.606	0.000			
F	22	1.322	2.120	5.259	0.000		
F	23	1.321	2.121	5.576	2.129	0.000	
F	24	5.096	5.905	9.200	5.187	3.908	0.000
F	25	5.510	6.571	8.836	5.738	4.456	2.120
F	26	5.358	6.472	6.979	4.539	5.842	7.038
F	27	3.523	4.528	5.102	2.831	4.314	6.614
C	28	5.121	6.108	4.587	5.691	5.299	7.189
H	29	5.333	5.876	2.450	5.995	5.991	8.920
H	30	2.606	2.259	2.453	3.288	3.749	7.628
H	31	5.551	6.491	9.720	5.096	4.731	2.239
H	32	6.085	7.047	9.905	5.157	5.762	4.593
H	33	5.433	6.492	8.358	4.380	5.598	5.889
F	34	5.457	6.607	5.576	5.774	5.553	6.886
F	35	6.156	7.037	4.594	6.710	6.478	8.508
F	36	5.500	6.431	5.283	6.257	5.399	6.918
H	37	4.559	5.627	6.060	5.243	4.060	4.905

		F 25	F 26	F 27	C 28	H 29	H 30
F	25	0.000					
F	26	6.553	0.000				
F	27	6.376	2.121	0.000			
C	28	5.863	5.490	4.671	0.000		
H	29	8.005	6.474	5.098	2.607	0.000	
H	30	7.787	6.432	4.320	5.336	4.232	0.000
H	31	3.221	5.888	5.990	7.712	9.452	8.114
H	32	5.178	4.623	5.281	8.219	9.735	8.368
H	33	5.927	2.274	3.321	6.914	8.134	7.188
F	34	5.408	4.697	4.375	1.315	3.692	6.078
F	35	7.136	6.156	5.411	1.320	2.215	5.901
F	36	5.463	6.526	5.706	1.339	3.394	5.907
H	37	3.477	5.985	5.242	2.614	4.769	5.841

		H 31	H 32	H 33	F 34	F 35	F 36
H	31	0.000					
H	32	2.448	0.000				
H	33	4.234	2.456	0.000			
F	34	7.117	7.453	6.121	0.000		
F	35	8.982	9.346	7.844	2.116	0.000	
F	36	7.782	8.662	7.686	2.130	2.123	0.000
H	37	5.889	7.076	6.565	2.700	3.852	2.027

		H 37
H	37	0.000

BOND ANGLES

1	2	3	C2	C2	C2	116.131
1	2	7	C2	C2	B	123.804
1	6	5	C2	C2	C2	120.294
1	6	33	C2	C2	HC	119.843
1	11	12	C2	C3	F	111.790
1	11	26	C2	C3	F	111.833
1	11	27	C2	C3	F	112.776
2	1	6	C2	C2	C2	122.156
2	1	11	C2	C2	C3	121.893
2	3	4	C2	C2	C2	121.342
2	3	9	C2	C2	C3	123.893
2	7	8	C2	B	O3	113.029
2	7	13	C2	B	C2	126.455
3	2	7	C2	C2	B	120.013
3	4	5	C2	C2	C2	120.902
3	4	31	C2	C2	HC	119.681
3	9	10	C2	C3	F	114.219
3	9	24	C2	C3	F	110.680
3	9	25	C2	C3	F	111.672
4	3	9	C2	C2	C3	114.725
4	5	6	C2	C2	C2	119.155
4	5	32	C2	C2	HC	120.362
5	4	31	C2	C2	HC	119.417
5	6	33	C2	C2	HC	119.860
6	1	11	C2	C2	C3	115.947
6	5	32	C2	C2	HC	120.480
7	8	37	B	O3	H	117.913
7	13	14	B	C2	C2	123.498
7	13	18	B	C2	C2	120.857
8	7	13	O3	B	C2	120.512
13	14	15	C2	C2	C2	122.129
13	14	19	C2	C2	C3	122.428
13	18	17	C2	C2	C2	121.878
13	18	28	C2	C2	C3	122.758
14	13	18	C2	C2	C2	115.644
14	15	16	C2	C2	C2	120.569
14	15	30	C2	C2	HC	119.700
14	19	20	C2	C3	F	111.452
14	19	22	C2	C3	F	112.716
14	19	23	C2	C3	F	111.833
15	14	19	C2	C2	C3	115.442
15	16	17	C2	C2	C2	119.083
15	16	21	C2	C2	HC	120.518
16	15	30	C2	C2	HC	119.730
16	17	18	C2	C2	C2	120.648
16	17	29	C2	C2	HC	119.505
17	16	21	C2	C2	HC	120.392
17	18	28	C2	C2	C3	115.306
18	17	29	C2	C2	HC	119.847
18	28	34	C2	C3	F	114.198
18	28	35	C2	C3	F	112.052
18	28	36	C2	C3	F	110.566

TORSION ANGLES

1	2	3	4	-1.441	2	7	13	14	45.980
1	2	3	9	176.132	2	7	13	18	-133.530
1	2	7	8	-129.084	3	2	7	8	48.203
1	2	7	13	50.153	3	2	7	13	-132.560
2	1	6	5	-0.117	3	4	5	6	0.646
2	1	6	33	-179.587	3	4	5	32	-179.974
2	1	11	12	39.740	4	3	9	10	-143.789
2	1	11	26	159.198	4	3	9	24	-24.426
2	1	11	27	-80.838	4	3	9	25	93.765
2	3	4	5	0.541	4	5	6	1	-0.854
2	3	4	31	-179.438	4	5	6	33	178.616
2	3	9	10	38.493	6	1	2	3	1.238
2	3	9	24	157.857	6	1	2	7	178.622
2	3	9	25	-83.953	6	1	11	12	-139.568
2	7	8	37	-175.171	6	1	11	26	-20.110

6	1	11	27	99.854
7	2	3	4	-178.931
7	2	3	9	-1.358
7	13	14	15	-177.521
7	13	14	19	2.918
7	13	18	17	177.279
7	13	18	28	-5.619
8	7	13	14	-134.835
8	7	13	18	45.655
9	3	4	5	-177.241
9	3	4	31	2.780
11	1	2	3	-178.027
11	1	2	7	-0.643
11	1	6	5	179.189
11	1	6	33	-0.281
13	7	8	37	5.541
13	14	15	16	-0.239
13	14	15	30	-179.911
13	14	19	20	158.249
13	14	19	22	-82.053
13	14	19	23	39.043
13	18	28	34	48.181
13	18	28	35	169.823
13	18	28	36	-72.189
14	13	18	17	-2.268
14	13	18	28	174.834
14	15	16	17	-1.393
14	15	16	21	179.512
15	14	19	20	-21.340
15	14	19	22	98.359
15	14	19	23	-140.546
15	16	17	18	1.136
15	16	17	29	-178.826
16	17	18	13	0.759
16	17	18	28	-176.546
17	18	28	34	-134.541
17	18	28	35	-12.899
17	18	28	36	105.089
18	13	14	15	2.013
18	13	14	19	-177.548
19	14	15	16	179.351
19	14	15	30	-0.321
21	16	17	18	-179.768
21	16	17	29	0.270
29	17	18	13	-179.279
29	17	18	28	3.416
30	15	16	17	178.280
30	15	16	21	-0.815
31	4	5	6	-179.376
31	4	5	32	-0.026
32	5	6	1	179.784
32	5	6	33	-0.746

Ar'_2BOH

Calculated NMR (GIAO-HF/6-31G*//HF/6-31G*)

For ^{19}F shift use 213 - value

37

$C_{16}H_7BF_{12}O$ << C1 >>, GIAO RHF / 6-31G* OPT RHF / 6-31G* -1902.906152

C 1 67.0750 134.625
C 2 63.0825 138.617
C 3 64.4014 137.299
C 4 70.4017 131.298
C 5 75.2847 126.415
C 6 72.4715 129.228
B 7 82.1982 41.2018
O 8 193.2527
C 9 92.7587 108.941
F 10 313.9048
C 11 93.2112 108.489
F 12 304.1103
C 13 63.9653 137.735
C 14 64.5180 137.182
C 15 71.0359 130.664
C 16 74.5341 127.166
C 17 71.5206 130.179
C 18 67.0307 134.669
C 19 93.7025 107.997
F 20 318.0035
H 21 24.9482 10.0518
F 22 303.3974
F 23 304.7300
F 24 316.5183
F 25 299.5801
F 26 319.2283
F 27 303.4489
C 28 92.3704 109.33
H 29 24.4424 10.5576
H 30 24.5788 10.4212
H 31 24.4290 10.571
H 32 25.0050 9.995
H 33 24.6865 10.3135
F 34 311.1170
F 35 321.6589
F 36 296.1438
H 37 26.5677 8.4323

^{11}B ref= 123.4 ^{13}C ref= 201.7 ^{1}H ref= 35

$C_{16}H_7BF_{12}O$ << C1 >> NIMAG= 0 ZPE= 150.11538 E(RHF) / 6-31G(d) FC= 1 // OPT RHF / 6-31G* -1902.90615158

Tris-(2-$CF_3C_6H_4$)

Optimized geometry HF/6-31G*

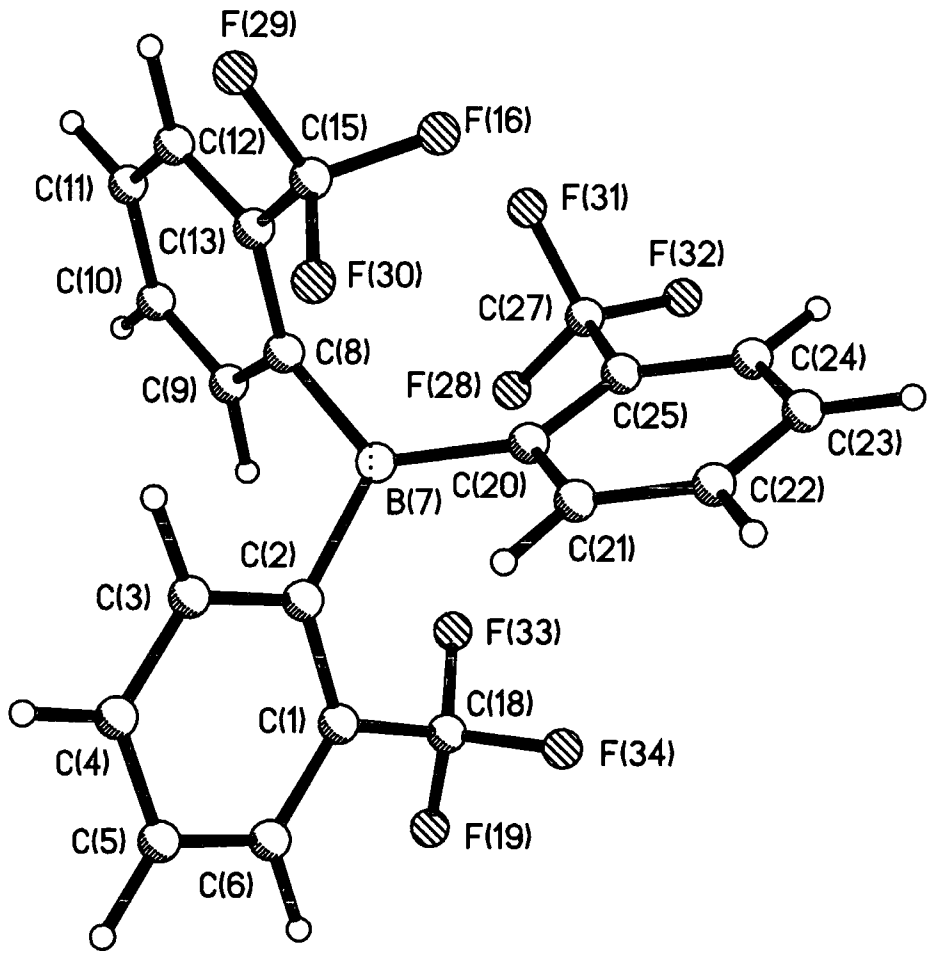

INTERATOMIC DISTANCES

		C 1	C 2	C 3	C 4	C 5	C 6
C	1	0.000					
C	2	1.401	0.000				
C	3	2.383	1.396	0.000			
C	4	2.764	2.433	1.386	0.000		
C	5	2.403	2.815	2.396	1.382	0.000	
C	6	1.386	2.430	2.754	2.389	1.384	0.000
B	7	2.685	1.600	2.547	3.855	4.409	3.945
C	8	3.866	2.699	3.172	4.503	5.277	5.008
C	9	4.082	3.225	3.748	4.887	5.484	5.132

C	10	5.396	4.530	4.833	5.893	6.576	6.346
C	11	6.331	5.257	5.356	6.476	7.365	7.290
C	12	6.200	4.953	4.959	6.179	7.206	7.206
C	13	5.102	3.804	3.925	5.246	6.239	6.171
H	14	3.514	3.012	3.753	4.736	5.069	4.530
C	15	5.596	4.242	4.218	5.510	6.595	6.627
F	16	6.085	4.849	5.107	6.435	7.392	7.239
H	17	3.362	2.138	1.074	2.122	3.360	3.827
C	18	1.506	2.531	3.784	4.269	3.761	2.475
F	19	2.348	3.604	4.692	4.890	4.068	2.702
C	20	3.465	2.753	3.753	4.959	5.373	4.749
C	21	3.658	3.092	3.850	4.845	5.214	4.706
C	22	4.864	4.454	5.186	6.094	6.385	5.837
C	23	5.709	5.318	6.206	7.228	7.503	6.820
C	24	5.587	5.137	6.163	7.321	7.626	6.852
C	25	4.598	4.028	5.098	6.329	6.689	5.937
H	26	3.249	2.679	3.163	3.988	4.386	4.072
C	27	5.195	4.631	5.733	7.016	7.382	6.581
F	28	4.561	4.172	5.360	6.562	6.801	5.919
F	29	6.733	5.344	5.061	6.231	7.442	7.654
F	30	4.913	3.571	3.366	4.566	5.667	5.807
F	31	5.901	5.076	5.953	7.311	7.887	7.266
F	32	6.225	5.828	6.996	8.243	8.508	7.597
F	33	2.344	2.803	4.157	4.936	4.690	3.534
F	34	2.356	3.205	4.438	4.939	4.437	3.203
H	35	5.860	5.188	5.523	6.447	6.995	6.717
H	36	7.341	6.294	6.324	7.377	8.279	8.252
H	37	7.138	5.836	5.715	6.904	8.021	8.115
H	38	6.495	6.084	7.150	8.333	8.617	7.785
H	39	6.684	6.356	7.216	8.190	8.428	7.739
H	40	5.352	5.027	5.590	6.322	6.572	6.132
H	41	3.839	3.399	2.134	1.075	2.136	3.367
H	42	3.376	3.890	3.374	2.139	1.075	2.135
H	43	2.133	3.397	3.826	3.361	2.132	1.073

		B 7	C 8	C 9	C 10	C 11	C 12
B	7	0.000					
C	8	1.595	0.000				
C	9	2.546	1.395	0.000			
C	10	3.852	2.429	1.384	0.000		
C	11	4.402	2.810	2.395	1.382	0.000	
C	12	3.935	2.428	2.755	2.390	1.384	0.000
C	13	2.673	1.400	2.384	2.764	2.402	1.386
H	14	2.680	2.137	1.075	2.123	3.361	3.829
C	15	3.115	2.527	3.781	4.269	3.763	2.479
F	16	3.478	3.159	4.409	4.945	4.477	3.254
H	17	2.679	2.896	3.658	4.567	4.821	4.252
C	18	3.137	4.352	4.421	5.741	6.792	6.763
F	19	4.376	5.434	5.246	6.461	7.639	7.784
C	20	1.590	2.827	3.857	5.088	5.502	4.855
C	21	2.524	3.912	5.031	6.286	6.636	5.852
C	22	3.838	5.133	6.269	7.482	7.755	6.893
C	23	4.397	5.502	6.563	7.689	7.929	7.105
C	24	3.942	4.807	5.729	6.764	7.032	6.334
C	25	2.694	3.481	4.350	5.418	5.774	5.177
H	26	2.647	4.070	5.169	6.442	6.811	6.032
C	27	3.187	3.378	3.872	4.701	5.094	4.756
F	28	2.961	3.068	3.119	4.003	4.721	4.709
F	29	4.374	3.618	4.707	4.897	4.065	2.695
F	30	2.805	2.827	4.169	4.932	4.674	3.518
F	31	3.506	3.143	3.692	4.212	4.276	3.833
F	32	4.460	4.679	5.036	5.746	6.134	5.874
F	33	2.784	3.699	3.594	4.852	5.938	6.019
F	34	3.566	5.002	5.334	6.691	7.624	7.416
H	35	4.679	3.396	2.133	1.075	2.137	3.367
H	36	5.476	3.885	3.373	2.139	1.075	2.134
H	37	4.804	3.395	3.827	3.362	2.131	1.073
H	38	4.819	5.506	6.315	7.236	7.469	6.832
H	39	5.471	6.553	7.615	8.714	8.913	8.056
H	40	4.657	5.993	7.157	8.386	8.635	7.720

H 41	4.680	5.136	5.543	6.397	6.829	6.485
H 42	5.484	6.315	6.463	7.491	8.283	8.161
H 43	4.815	5.912	5.922	7.123	8.158	8.157

	C 13	H 14	C 15	F 16	H 17	C 18
C 13	0.000					
H 14	3.363	0.000				
C 15	1.506	4.657	0.000			
F 16	2.359	5.211	1.321	0.000		
H 17	3.279	3.961	3.442	4.487	0.000	
C 18	5.683	3.681	6.246	6.474	4.661	0.000
F 19	6.808	4.339	7.486	7.758	5.652	1.324
C 20	3.539	3.972	3.476	3.254	3.886	3.469
C 21	4.475	5.113	4.040	3.825	4.039	3.838
C 22	5.549	6.362	4.904	4.378	5.341	4.821
C 23	5.858	6.678	5.273	4.450	6.315	5.379
C 24	5.200	5.861	4.876	3.984	6.240	5.109
C 25	4.032	4.491	3.996	3.354	5.172	4.225
H 26	4.652	5.220	4.209	4.293	3.425	3.796
C 27	3.920	4.037	4.299	3.688	5.759	4.683
F 28	3.969	3.018	4.734	4.463	5.530	3.948
F 29	2.351	5.671	1.323	2.123	4.120	7.495
F 30	2.347	4.853	1.333	2.129	2.614	5.743
F 31	3.234	4.181	3.621	2.962	5.746	5.644
F 32	5.162	5.110	5.479	4.693	7.068	5.473
F 33	5.053	2.835	5.799	5.935	4.835	1.327
F 34	6.216	4.731	6.517	6.532	5.260	1.323
H 35	3.839	2.437	5.345	5.995	5.372	6.101
H 36	3.375	4.251	4.612	5.293	5.753	7.794
H 37	2.134	4.902	2.656	3.358	4.886	7.747
H 38	5.831	6.452	5.563	4.539	7.206	5.873
H 39	6.841	7.730	6.163	5.243	7.319	6.291
H 40	6.362	7.237	5.590	5.133	5.762	5.420
H 41	5.665	5.514	5.829	6.862	2.435	5.345
H 42	7.244	6.017	7.580	8.412	4.250	4.609
H 43	7.138	5.193	7.629	8.173	4.900	2.648

	F 19	C 20	C 21	C 22	C 23	C 24
F 19	0.000					
C 20	4.779	0.000				
C 21	5.120	1.395	0.000			
C 22	6.021	2.438	1.387	0.000		
C 23	6.540	2.816	2.389	1.378	0.000	
C 24	6.263	2.429	2.747	2.389	1.387	0.000
C 25	5.432	1.407	2.385	2.772	2.407	1.383
H 26	5.023	2.135	1.074	2.119	3.352	3.820
C 27	5.739	2.552	3.797	4.280	3.761	2.466
F 28	4.852	2.883	4.221	4.968	4.680	3.502
F 29	8.713	4.776	5.212	5.978	6.352	6.027
F 30	6.997	3.145	3.302	4.241	4.932	4.849
F 31	6.736	3.167	4.407	4.943	4.469	3.243
F 32	6.395	3.641	4.713	4.888	4.039	2.662
F 33	2.129	3.153	3.972	4.963	5.246	4.642
F 34	2.123	3.301	3.336	4.006	4.529	4.477
H 35	6.628	5.928	7.151	8.355	8.533	7.556
H 36	8.580	6.555	7.693	8.787	8.915	7.979
H 37	8.806	5.575	6.468	7.406	7.587	6.870
H 38	6.943	3.397	3.819	3.358	2.130	1.072
H 39	7.388	3.890	3.370	2.136	1.075	2.135
H 40	6.550	3.403	2.136	1.075	2.135	3.369
H 41	5.934	5.792	5.611	6.816	7.997	8.145
H 42	4.694	6.417	6.172	7.276	8.436	8.628
H 43	2.371	5.478	5.407	6.416	7.342	7.393

	C 25	H 26	C 27	F 28	F 29	F 30
C 25	0.000					
H 26	3.365	0.000				
C 27	1.510	4.678	0.000			

F	28	2.355	4.922	1.324	0.000		
F	29	5.253	5.286	5.490	5.952	0.000	
F	30	4.045	3.199	4.738	5.113	2.129	0.000
F	31	2.355	5.213	1.324	2.130	4.644	4.399
F	32	2.351	5.685	1.325	2.123	6.604	5.962
F	33	3.597	4.206	3.673	2.743	7.072	5.578
F	34	3.921	3.420	4.672	4.242	7.796	5.927
H	35	6.207	7.298	5.367	4.495	5.943	5.979
H	36	6.754	7.871	5.973	5.603	4.688	5.593
H	37	5.836	6.648	5.462	5.590	2.350	3.804
H	38	2.130	4.892	2.633	3.763	6.649	5.715
H	39	3.376	4.244	4.602	5.586	7.158	5.835
H	40	3.847	2.432	5.355	6.018	6.554	4.762
H	41	7.172	4.699	7.867	7.466	6.345	4.858
H	42	7.733	5.294	8.443	7.837	8.359	6.612
H	43	6.558	4.836	7.171	6.441	8.691	6.827

		F 31	F 32	F 33	F 34	H 35	H 36
F	31	0.000					
F	32	2.122	0.000				
F	33	4.623	4.438	0.000			
F	34	5.776	5.298	2.130	0.000		
H	35	4.968	6.291	5.175	7.151	0.000	
H	36	5.066	6.914	6.908	8.659	2.471	0.000
H	37	4.398	6.509	7.031	8.333	4.255	2.453
H	38	3.347	2.294	5.271	5.241	7.972	8.348
H	39	5.280	4.645	6.196	5.327	9.555	9.876
H	40	5.990	5.932	5.764	4.515	9.271	9.669
H	41	8.043	9.127	5.984	5.988	6.956	7.653
H	42	8.961	9.551	5.616	5.237	7.843	9.155
H	43	7.974	8.074	3.828	3.276	7.391	9.104

		H 37	H 38	H 39	H 40	H 41	H 42
H	37	0.000					
H	38	7.321	0.000				
H	39	8.474	2.449	0.000			
H	40	8.183	4.252	2.472	0.000		
H	41	7.094	9.169	8.935	6.961	0.000	
H	42	8.952	9.624	9.322	7.363	2.471	0.000
H	43	9.097	8.276	8.202	6.666	4.255	2.454

		H 43
H	43	0.000

BOND ANGLES

1	2	3	C2	C2	C2	116.855
1	2	7	C2	C2	B	126.813
1	6	5	C2	C2	C2	120.376
1	6	43	C2	C2	HC	119.824
1	18	19	C2	C3	F	111.966
1	18	33	C2	C3	F	111.495
1	18	34	C2	C3	F	112.617
2	1	6	C2	C2	C2	121.362
2	1	18	C2	C2	C3	121.022
2	3	4	C2	C2	C2	121.987
2	3	17	C2	C2	HC	119.326
2	7	8	C2	B	C2	115.273
2	7	20	C2	B	C2	119.325
3	2	7	C2	C2	B	116.310
3	4	5	C2	C2	C2	119.937
3	4	41	C2	C2	HC	119.772
4	3	17	C2	C2	HC	118.685
4	5	6	C2	C2	C2	119.442
4	5	42	C2	C2	HC	120.599
5	4	41	C2	C2	HC	120.285
5	6	43	C2	C2	HC	119.799
6	1	18	C2	C2	C3	117.612
6	5	42	C2	C2	HC	119.952

7	8	9	B	C2	C2	116.626
7	8	13	B	C2	C2	126.279
7	20	21	B	C2	C2	115.310
7	20	25	B	C2	C2	127.947
8	7	20	C2	B	C2	125.122
8	9	10	C2	C2	C2	121.871
8	9	14	C2	C2	HC	119.284
8	13	12	C2	C2	C2	121.264
8	13	15	C2	C2	C3	120.807
9	8	13	C2	C2	C2	117.084
9	10	11	C2	C2	C2	119.925
9	10	35	C2	C2	HC	119.805
10	9	14	C2	C2	HC	118.839
10	11	12	C2	C2	C2	119.517
10	11	36	C2	C2	HC	120.555
11	10	35	C2	C2	HC	120.266
11	12	13	C2	C2	C2	120.299
11	12	37	C2	C2	HC	119.814
12	11	36	C2	C2	HC	119.924
12	13	15	C2	C2	C3	117.925
13	12	37	C2	C2	HC	119.886
13	15	16	C2	C3	F	112.904
13	15	29	C2	C3	F	112.206
13	15	30	C2	C3	F	111.372
20	21	22	C2	C2	C2	122.434
20	21	26	C2	C2	HC	119.205
20	25	24	C2	C2	C2	121.030
20	25	27	C2	C2	C3	122.035
21	20	25	C2	C2	C2	116.680
21	22	23	C2	C2	C2	119.607
21	22	40	C2	C2	HC	119.877
22	21	26	C2	C2	HC	118.358
22	23	24	C2	C2	C2	119.547
22	23	39	C2	C2	HC	120.667
23	22	40	C2	C2	HC	120.511
23	24	25	C2	C2	C2	120.670
23	24	38	C2	C2	HC	119.484
24	23	39	C2	C2	HC	119.783
24	25	27	C2	C2	C3	116.934
25	24	38	C2	C2	HC	119.846
25	27	28	C2	C3	F	112.246
25	27	31	C2	C3	F	112.251
25	27	32	C2	C3	F	111.851

TORSION ANGLES

1	2	3	4	2.166	6	1	18	34	-93.796
1	2	3	17	-178.357	7	2	3	4	-176.211
1	2	7	8	125.278	7	2	3	17	3.265
1	2	7	20	-60.491	7	8	9	10	-178.904
2	1	6	5	-0.970	7	8	9	14	0.167
2	1	6	43	178.576	7	8	13	12	-179.773
2	1	18	19	-152.823	7	8	13	15	-0.382
2	1	18	33	-33.236	7	20	21	22	-175.512
2	1	18	34	87.030	7	20	21	26	3.818
2	3	4	5	-1.843	7	20	25	24	176.468
2	3	4	41	179.033	7	20	25	27	-3.907
2	7	8	9	-62.291	8	7	20	21	136.291
2	7	8	13	116.482	8	7	20	25	-40.679
2	7	20	21	-37.329	8	9	10	11	-1.734
2	7	20	25	145.701	8	9	10	35	178.924
3	2	7	8	-56.530	8	13	15	16	81.355
3	2	7	20	117.701	8	13	15	29	-157.894
3	4	5	6	0.034	8	13	15	30	-38.605
3	4	5	42	-179.045	9	8	13	12	-1.004
4	5	6	1	1.342	9	8	13	15	178.386
4	5	6	43	-178.204	9	10	11	12	-0.026
6	1	2	3	-0.759	9	10	11	36	-179.264
6	1	2	7	177.425	10	11	12	13	1.190
6	1	18	19	26.350	10	11	12	37	-178.509
6	1	18	33	145.937	11	12	13	8	-0.664

11	12	13	15	179.974
12	13	15	16	-99.234
12	13	15	29	21.517
12	13	15	30	140.806
13	8	9	10	2.207
13	8	9	14	-178.722
14	9	10	11	179.191
14	9	10	35	-0.151
17	3	4	5	178.677
17	3	4	41	-0.447
18	1	2	3	178.384
18	1	2	7	-3.433
18	1	6	5	179.860
18	1	6	43	-0.595
20	7	8	9	123.860
20	7	8	13	-57.367
20	21	22	23	-1.694
20	21	22	40	179.063
20	25	27	28	-40.580
20	25	27	31	80.088
20	25	27	32	-160.300
21	20	25	24	-0.466
21	20	25	27	179.159
21	22	23	24	0.165
21	22	23	39	-179.169
22	23	24	25	1.146
22	23	24	38	-178.617
23	24	25	20	-0.988
23	24	25	27	179.369
24	25	27	28	139.060
24	25	27	31	-100.273
24	25	27	32	19.340
25	20	21	22	1.814
25	20	21	26	-178.857
26	21	22	23	178.970
26	21	22	40	-0.272
35	10	11	12	179.323
35	10	11	36	0.075
36	11	12	13	-179.558
36	11	12	37	0.744
37	12	13	8	179.034
37	12	13	15	-0.373
38	24	25	20	178.774
38	24	25	27	-0.870
39	23	24	25	-179.514
39	23	24	38	0.724
40	22	23	24	179.403
40	22	23	39	0.068
41	4	5	6	179.153
41	4	5	42	0.074
42	5	6	1	-179.573
42	5	6	43	0.881

Tris-(2-$CF_3C_6H_4$)
Calculated NMR (GIAO-HF/6-31G*//HF/6-31G*)

For ^{19}F shift use 213 - value

43
$C_{21}H_{12}BF_9$ << C1 >>, GIAO RHF / 6-31G* OPT RHF / 6-31G* -1721.93116055
C 1 69.0553 132.645
C 2 59.1304 142.57
C 3 69.2908 132.409
C 4 72.6025 129.097
C 5 74.7433 126.957
C 6 75.7721 125.928
B 7 54.7365 68.6635
C 8 60.2709 141.429
C 9 69.0112 132.689
C 10 72.6327 129.067
C 11 75.1646 126.535
C 12 76.6275 125.072
C 13 70.0198 131.68
H 14 25.0729 9.9271
C 15 92.4742 109.226
F 16 304.6034
H 17 25.1602 9.8398
C 18 92.7480 108.952
F 19 319.5586
C 20 64.2878 137.412
C 21 64.3056 137.394
C 22 73.8062 127.894
C 23 72.1965 129.503
C 24 76.4204 125.28
C 25 66.1320 135.568
H 26 25.3747 9.6253
C 27 93.0241 108.676
F 28 305.0373
F 29 321.8004
F 30 303.5305
F 31 302.8778
F 32 321.2807
F 33 306.0993
F 34 304.1364
H 35 25.0865 9.9135
H 36 25.1601 9.8399
H 37 24.8703 10.1297
H 38 24.8491 10.1509
H 39 25.0665 9.9335

H 40 25.2008 9.7992
H 41 25.1000 9.9
H 42 25.1117 9.8883
H 43 24.7945 10.2055

^{11}B ref= 123.4 ^{13}C ref= 201.7 ^{1}H ref= 35

Tris-(2-$CF_3C_6H_4$)

$C_{21}H_{12}BF_9$ << C1 >> NIMAG= 0 ZPE= 196.97611 E(RHF) / 6-31G(d) FC= 1 //
OPT SP -1721.93116027

Ar'BF2

Optimized HF/6-31G* geometry

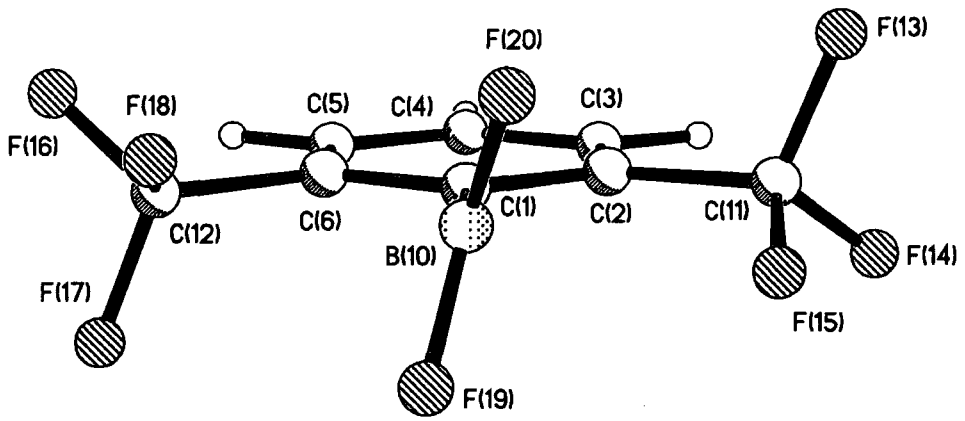

		C 1	C 2	C 3	C 4	C 5	C 6
C	1	0.000					
C	2	1.393	0.000				
C	3	2.426	1.385	0.000			
C	4	2.807	2.397	1.382	0.000		
C	5	2.426	2.757	2.388	1.382	0.000	
C	6	1.393	2.378	2.757	2.397	1.385	0.000
H	7	3.393	2.134	1.074	2.133	3.364	3.830
H	8	3.881	3.372	2.135	1.074	2.135	3.372
H	9	3.393	3.830	3.363	2.133	1.074	2.134
B	10	1.590	2.604	3.890	4.398	3.890	2.604
C	11	2.513	1.505	2.481	3.760	4.261	3.771
C	12	2.513	3.771	4.261	3.760	2.481	1.506
F	13	3.248	2.347	3.113	4.354	4.896	4.444
F	14	3.552	2.344	2.768	4.120	4.903	4.669
F	15	2.730	2.339	3.576	4.714	4.924	4.109
F	16	3.552	4.669	4.903	4.120	2.768	2.344
F	17	3.248	4.444	4.896	4.355	3.114	2.347
F	18	2.730	4.109	4.924	4.714	3.576	2.339
F	19	2.522	3.506	4.742	5.189	4.592	3.299
F	20	2.522	3.298	4.592	5.189	4.742	3.506

		H 7	H 8	H 9	B 10	C 11	C 12
H	7	0.000					
H	8	2.461	0.000				
H	9	4.254	2.461	0.000			
B	10	4.738	5.472	4.738	0.000		
C	11	2.661	4.615	5.335	2.980	0.000	
C	12	5.335	4.615	2.662	2.980	5.026	0.000
F	13	3.139	5.133	5.938	3.575	1.320	5.657
F	14	2.493	4.776	5.950	4.141	1.320	6.008
F	15	3.903	5.660	5.971	2.467	1.330	5.081
F	16	5.950	4.775	2.492	4.141	6.009	1.320
F	17	5.938	5.133	3.140	3.574	5.656	1.320
F	18	5.972	5.660	3.903	2.467	5.082	1.330
F	19	5.572	6.242	5.346	1.306	3.779	3.341
F	20	5.346	6.242	5.572	1.306	3.341	3.779

		F 13	F 14	F 15	F 16	F 17	F 18
F	13	0.000					

F	14	2.124	0.000				
F	15	2.130	2.134	0.000			
F	16	6.486	6.992	6.219	0.000		
F	17	6.493	6.485	5.568	2.124	0.000	
F	18	5.569	6.218	4.879	2.134	2.130	0.000
F	19	4.581	4.727	2.955	4.614	3.462	2.797
F	20	3.463	4.614	2.797	4.728	4.580	2.955

		F 19

F	19	0.000
F	20	2.245	0.000

BOND ANGLES

1	2	3	C2	C2	C2	121.625
1	2	11	C2	C2	C3	120.162
1	6	5	C2	C2	C2	121.624
1	6	12	C2	C2	C3	120.155
1	10	19	C2	B	F	120.774
1	10	20	C2	B	F	120.771
2	1	6	C2	C2	C2	117.162
2	1	10	C2	C2	B	121.418
2	3	4	C2	C2	C2	120.019
2	3	7	C2	C2	HC	119.869
2	11	13	C2	C3	F	112.176
2	11	14	C2	C3	F	111.977
2	11	15	C2	C3	F	111.010
3	2	11	C2	C2	C3	118.201
3	4	5	C2	C2	C2	119.550
3	4	8	C2	C2	HC	120.227
4	3	7	C2	C2	HC	120.112
4	5	6	C2	C2	C2	120.020
4	5	9	C2	C2	HC	120.108
5	4	8	C2	C2	HC	120.223
5	6	12	C2	C2	C3	118.209
6	1	10	C2	C2	B	121.420
6	5	9	C2	C2	HC	119.871
6	12	16	C2	C3	F	111.980
6	12	17	C2	C3	F	112.173
6	12	18	C2	C3	F	111.011

TORSION ANGLES

1	2	3	4	0.267
1	2	3	7	-179.456
1	2	11	13	-95.725
1	2	11	14	143.768
1	2	11	15	23.891
1	6	12	16	143.831
1	6	12	17	-95.662
1	6	12	18	23.950
2	1	6	5	-0.137
2	1	6	12	178.569
2	1	10	19	-105.320
2	1	10	20	74.688
2	3	4	5	-0.133
2	3	4	8	179.867
3	2	11	13	83.031
3	2	11	14	-37.477
3	2	11	15	-157.354
3	4	5	6	-0.129
3	4	5	9	179.593
4	5	6	1	0.268
4	5	6	12	-178.462
5	6	12	16	-37.420
5	6	12	17	83.087
5	6	12	18	-157.300
6	1	2	3	-0.131
6	1	2	11	178.581

6	1	10	19	74.687
6	1	10	20	-105.305
7	3	4	5	179.590
7	3	4	8	-0.410
8	4	5	6	179.871
8	4	5	9	-0.407
9	5	6	1	-179.455
9	5	6	12	1.815
10	1	2	3	179.876
10	1	2	11	-1.413
10	1	6	5	179.857
10	1	6	12	-1.437
11	2	3	4	-178.469
11	2	3	7	1.807

Ar'BF_2
Calculated NMR (GIAO-HF/6-31G*//HF/6-31G*)
For ^{19}F shift use 213 - value

20
$C_8H_3BF_8$ << C1 >>, GIAO RHF / 6-31G* OPT RHF / 6-31G* -1125.06399170
C 1 72.1070 129.593
C 2 68.6716 133.028
C 3 71.4235 130.276
C 4 74.6736 127.026
C 5 71.4257 130.274
C 6 68.6767 133.023
H 7 24.5921 10.4079
H 8 24.9397 10.0603
H 9 24.5921 10.4079
B 10 100.8070 22.593
C 11 93.1203 108.58
C 12 93.1207 108.579
F 13 303.6077
F 14 317.7998
F 15 318.0259
F 16 317.8329
F 17 303.5929
F 18 318.0160
F 19 310.8167
F 20 310.8134

^{11}B ref= 123.4 ^{13}C ref= 201.7 ^{1}H ref= 35

Ar'BF_2
Frequency calculation to check it is a minimum
(NIMAG = number of imaginary frequencies – if NIMAG = 0 then it is a minimum)

C8H3BF8 << C1 >> NIMAG= 0 ZPE= 74.72291 E(RHF) / 6-31G(d) FC= 1 //
OPT RHF / 6-31G* -1125.06399170

$Ar'BCl_2$
Optimized HF/6-31G* geometry

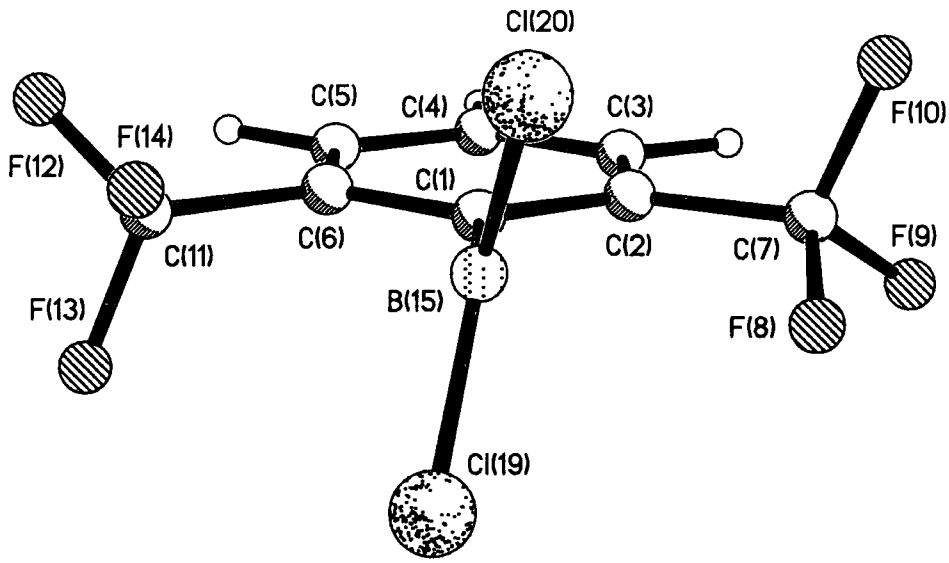

C 1	C 2	C 3	C 4	C 5	C 6	
C 1	0.000					
C 2	1.398	0.000				
C 3	2.430	1.386	0.000			
C 4	2.815	2.400	1.380	0.000		
C 5	2.430	2.756	2.382	1.380	0.000	
C 6	1.398	2.381	2.756	2.400	1.386	0.000
C 7	2.534	1.507	2.468	3.753	4.261	3.787
F 8	2.774	2.346	3.568	4.721	4.949	4.154
F 9	3.571	2.343	2.736	4.089	4.885	4.675
F 10	3.260	2.346	3.098	4.341	4.888	4.450
C 11	2.534	3.787	4.261	3.752	2.468	1.507
F 12	3.570	4.675	4.885	4.089	2.736	2.343
F 13	3.260	4.451	4.888	4.340	3.098	2.346
F 14	2.774	4.154	4.949	4.721	3.568	2.346
B 15	1.594	2.613	3.898	4.409	3.898	2.613
H 16	3.395	3.829	3.358	2.131	1.073	2.131
H 17	3.889	3.375	2.135	1.074	2.135	3.375
H 18	3.395	2.131	1.073	2.131	3.358	3.829
Cl 19	2.906	3.835	5.053	5.508	4.917	3.654
Cl 20	2.906	3.654	4.918	5.509	5.053	3.836

	C 7	F 8	F 9	F 10	C 11	F 12
C 7	0.000					
F 8	1.327	0.000				
F 9	1.321	2.131	0.000			
F 10	1.321	2.129	2.124	0.000		
C 11	5.067	5.167	6.039	5.688	0.000	
F 12	6.038	6.299	7.001	6.509	1.321	0.000
F 13	5.689	5.647	6.511	6.519	1.321	2.124
F 14	5.167	5.018	6.299	5.645	1.327	2.131
B 15	3.019	2.543	4.187	3.606	3.019	4.186

H	16	5.335	5.999	5.930	5.929	2.633	2.437
H	17	4.602	5.659	4.734	5.114	4.602	4.734
H	18	2.633	3.872	2.437	3.113	5.335	5.930
Cl	19	4.082	3.215	4.966	4.931	3.680	4.970
Cl	20	3.680	3.195	4.970	3.651	4.083	4.965

		F 13	F 14	B 15	H 16	H 17	H 18
F	13	0.000					
F	14	2.130	0.000				
B	15	3.607	2.542	0.000			
H	16	3.112	3.872	4.744	0.000		
H	17	5.113	5.660	5.483	2.461	0.000	
H	18	5.929	5.999	4.744	4.249	2.461	0.000
Cl	19	3.652	3.194	1.755	5.650	6.547	5.856
Cl	20	4.932	3.215	1.755	5.857	6.548	5.650

		Cl 19
Cl	19	0.000
Cl	20	3.028

BOND ANGLES

1	2	3	C2	C2	C2	121.588
1	2	7	C2	C2	C3	121.404
1	6	5	C2	C2	C2	121.587
1	6	11	C2	C2	C3	121.415
1	15	19	C2	B	Cl	120.357
1	15	20	C2	B	Cl	120.382
2	1	6	C2	C2	C2	116.858
2	1	15	C2	C2	B	121.570
2	3	4	C2	C2	C2	120.347
2	3	18	C2	C2	HC	119.621
2	7	8	C2	C3	F	111.589
2	7	9	C2	C3	F	111.714
2	7	10	C2	C3	F	111.924
3	2	7	C2	C2	C3	116.989
3	4	5	C2	C2	C2	119.271
3	4	17	C2	C2	HC	120.365
4	3	18	C2	C2	HC	120.031
4	5	6	C2	C2	C2	120.348
4	5	16	C2	C2	HC	120.035
5	4	17	C2	C2	HC	120.364
5	6	11	C2	C2	C3	116.980
6	1	15	C2	C2	B	121.572
6	5	16	C2	C2	HC	119.617
6	11	12	C2	C3	F	111.716
6	11	13	C2	C3	F	111.929
6	11	14	C2	C3	F	111.586

TORSION ANGLES

1	2	3	4	0.196
1	2	3	18	-179.540
1	2	7	8	25.013
1	2	7	9	145.015
1	2	7	10	-94.961
1	6	11	12	144.923
1	6	11	13	-95.045
1	6	11	14	24.926
2	1	6	5	-0.089
2	1	6	11	178.309
2	1	15	19	-100.880
2	1	15	20	79.108
2	3	4	5	-0.092
2	3	4	17	179.912
3	2	7	8	-156.528
3	2	7	9	-36.526
3	2	7	10	83.498

3	4	5	6	-0.098
3	4	5	16	179.641
4	5	6	1	0.192
4	5	6	11	-178.274
5	6	11	12	-36.609
5	6	11	13	83.423
5	6	11	14	-156.606
6	1	2	3	-0.104
6	1	2	7	178.285
6	1	15	19	79.113
6	1	15	20	-100.899
7	2	3	4	-178.260
7	2	3	18	2.004
15	1	2	3	179.890
15	1	2	7	-1.722
15	1	6	5	179.918
15	1	6	11	-1.685
16	5	6	1	-179.548
16	5	6	11	1.986
17	4	5	6	179.898
17	4	5	16	-0.363
18	3	4	5	179.643
18	3	4	17	-0.353

$Ar'BCl_2$

Calculated NMR (GIAO-HF/6-31G*//HF/6-31G*)

For ^{19}F shift use 213 - value

20

$C_8H_3BCl_2F_6$ << C1 >>, GIAO RHF / 6-31G* OPT RHF / 6-31G* -1845.09903185

C 1 65.6504 136.05
C 2 70.5682 131.132
C 3 70.8305 130.869
C 4 75.0294 126.671
C 5 70.8257 130.874
C 6 70.5635 131.136
C 7 93.4035 108.296
F 8 312.9332
F 9 316.6493
F 10 302.2696
C 11 93.3985 108.301
F 12 316.6281
F 13 302.2944
F 14 312.8876
B 15 64.1020 59.298
H 16 24.6423 10.3577
H 17 25.0166 9.9834
H 18 24.6420 10.358
Cl 19 800.2158
Cl 20 800.2881

^{11}B ref= 123.4 ^{13}C ref= 201.7 ^{1}H ref= 35

Frequency calculation to check it is a minimum

Appendix B

Crytallography Data

All crystallographic data are listed in the CD enclosed at the end of the thesis.

Crystal data and structure refinement for Ar_2BF.

Identification code	01srv142	
Empirical formula	$C_{18}\ H_4\ B\ F_{19}$	
Formula weight	592.02	
Temperature	150(2) K	
Wavelength	0.71073 Å	
Crystal system	Monoclinic	
Space group	P2(1)/n	
Unit cell dimensions	a = 8.9564(6) Å	α= 90°.
	b = 9.4751(6) Å	β= 98.494(1)°.
	c = 23.6514(15) Å	γ = 90°.
Volume	1985.1(2) $Å^3$	
Z	4	
Density (calculated)	1.981 Mg/m^3	
Absorption coefficient	0.241 mm^{-1}	
F(000)	1152	
Crystal size	0.20 x 0.20 x 0.05 mm^3	
Theta range for data collection	1.74 to 27.49°.	
Index ranges	-11<=h<=11, -12<=k<=12, -30<=l<=30	
Reflections collected	20530	
Independent reflections	4550 [R(int) = 0.0736]	
Completeness to theta = 27.49°	99.9 %	
Absorption correction	Semi-empirical from equivalents	
Max. and min. transmission	0.9881 and 0.9534	
Refinement method	Full-matrix least-squares on F^2	
Data / restraints / parameters	4550 / 18 / 381	
Goodness-of-fit on F^2	1.026	
Final R indices [I>2sigma(I)]	R1 = 0.0469, wR2 = 0.0924	
R indices (all data)	R1 = 0.0982, wR2 = 0.1113	
Extinction coefficient	.	
Largest diff. peak and hole	0.297 and -0.330 $e.Å^{-3}$	

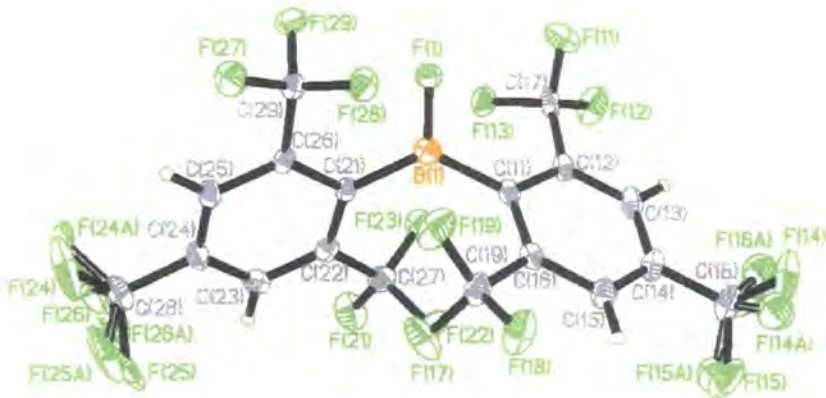

Crystal data and structure refinement for Ar''_3B.

Identification code	01srv120	
Empirical formula	C24 H9 B1 F18	
Formula weight	650.1163	
Temperature	120(2) K	
Wavelength	0.71073 Å	
Crystal system	Triclinic	
Space group	P-1	
Unit cell dimensions	a = 10.1795(7) Å	α= 94.9440(10)°.
	b = 11.0533(8) Å	β= 108.3620(10)°.
	c = 11.4719(8) Å	γ = 94.5490(10)°.
Volume	1212.75(15) $Å^3$	
Z	2	
Density (calculated)	1.78 Mg/m^3	
Absorption coefficient	0.200 mm^{-1}	
F(000)	640	
Crystal size	0.5 x 0.2 x 0.1 mm^3	
Theta range for data collection	1.86 to 27.43°.	
Index ranges	-13<=h<=13, -14<=k<=14, -14<=l<=14	
Reflections collected	11514	
Independent reflections	5131 [R(int) = 0.0365]	
Completeness to theta = 27.43°	92.8 %	
Absorption correction	Semi-empirical from equivalents	
Max. and min. transmission	0.9802 and 0.9064	
Refinement method	Full-matrix least-squares on F^2	
Data / restraints / parameters	5131 / 0 / 388	
Goodness-of-fit on F^2	1.057	
Final R indices [I>2sigma(I)]	R1 = 0.0528, wR2 = 0.1255	
R indices (all data)	R1 = 0.0741, wR2 = 0.1362	
Extinction coefficient	.	
Largest diff. peak and hole	0.642 and -0.474 $e.Å^{-3}$	

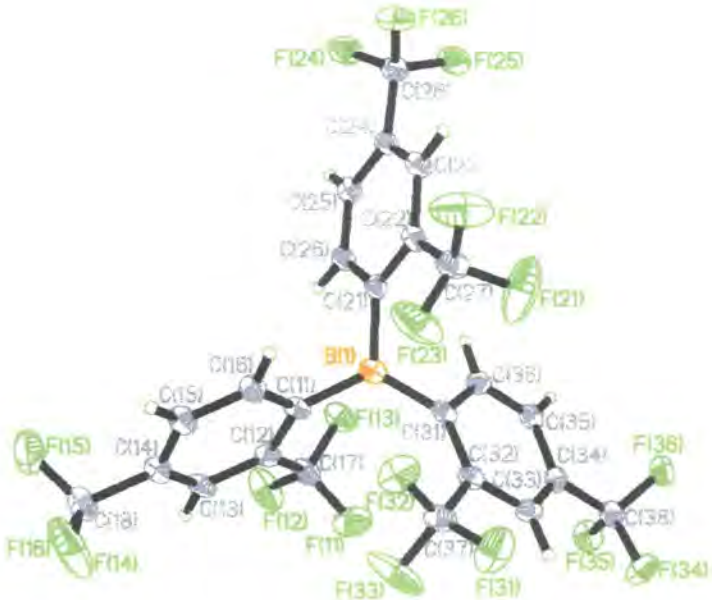

Crystal data and structure refinement for $Ar_2B(OH)$.

Identification code	01srv247	
Empirical formula	C18 H5 B F18 O	
Formula weight	590.03	
Temperature	120(2) K	
Wavelength	0.71073 Å	
Crystal system	Triclinic	
Space group	P-1	
Unit cell dimensions	a = 9.1587(3) Å	α= 112.5700(10)°.
	b = 10.1298(3) Å	β= 99.9530(10)°.
	c = 12.5200(4) Å	γ = 102.5760(10)°.
Volume	1003.60(5) $Å^3$	
Z	2	
Density (calculated)	1.953 Mg/m^3	
Absorption coefficient	0.234 mm^{-1}	
F(000)	576	
Crystal size	0.38 x 0.24 x 0.18 mm^3	
Theta range for data collection	1.84 to 27.47°.	
Index ranges	-11<=h<=11, -13<=k<=13, -16<=l<=16	
Reflections collected	11082	
Independent reflections	4583 [R(int) = 0.0274]	
Completeness to theta = 27.47°	99.3 %	
Absorption correction	Semi-empirical from equivalents	
Max. and min. transmission	0.9590 and 0.9162	
Refinement method	Full-matrix least-squares on F^2	
Data / restraints / parameters	4583 / 12 / 386	
Goodness-of-fit on F^2	1.022	
Final R indices [I>2sigma(I)]	R1 = 0.0359, wR2 = 0.0914	
R indices (all data)	R1 = 0.0447, wR2 = 0.0981	
Extinction coefficient	.	
Largest diff. peak and hole	0.485 and -0.338 $e.Å^{-3}$	

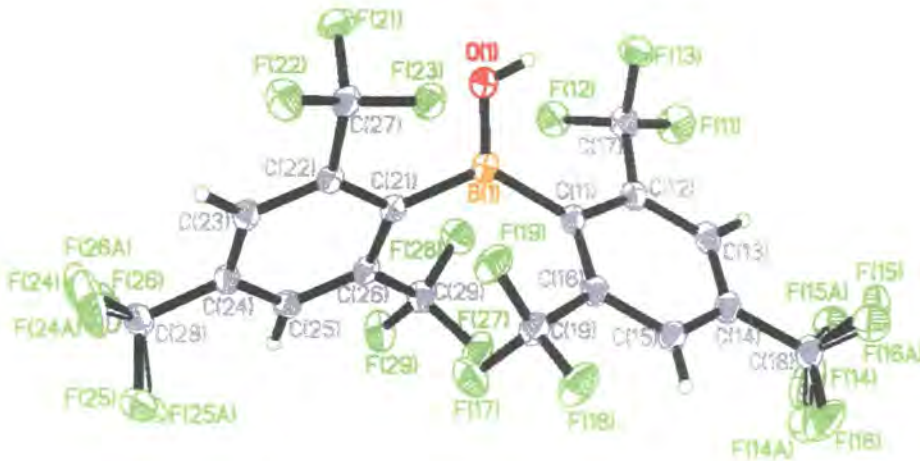

Crystal data and structure refinement for Ar'B(OH)$_2$.

Identification code	01srv014	
Empirical formula	C8 H5 B F7 O2	
Formula weight	276.93	
Temperature	100(2) K	
Wavelength	0.71073 Å	
Crystal system	Orthorhombic	
Space group	P2(1)2(1)2	
Unit cell dimensions	a = 14.0859(14) Å	α= 90°.
	b = 14.4620(14) Å	β= 90°.
	c = 5.0028(5) Å	γ = 90°.
Volume	1019.12(17) Å^3	
Z	4	
Density (calculated)	1.681 Mg/m^3	
Absorption coefficient	0.187 mm^{-1}	
F(000)	548	
Crystal size	0.42 x 0.2 x 0.1 mm^3	
Theta range for data collection	2.02 to 27.49°.	
Index ranges	-18<=h<=18, -18<=k<=18, -6<=l<=6	
Reflections collected	10797	
Independent reflections	2346 [R(int) = 0.0283]	
Completeness to theta = 27.49°	100.0 %	
Absorption correction	Semi-empirical from equivalents	
Max. and min. transmission	0.9796 and 0.9189	
Refinement method	Full-matrix least-squares on F^2	
Data / restraints / parameters	2346 / 0 / 169	
Goodness-of-fit on F^2	1.122	
Final R indices [I>2sigma(I)]	R1 = 0.0305, wR2 = 0.0717	
R indices (all data)	R1 = 0.0333, wR2 = 0.0735	
Absolute structure parameter	0(4)	
Extinction coefficient	.	
Largest diff. peak and hole	0.287 and -0.228 e.Å^{-3}	

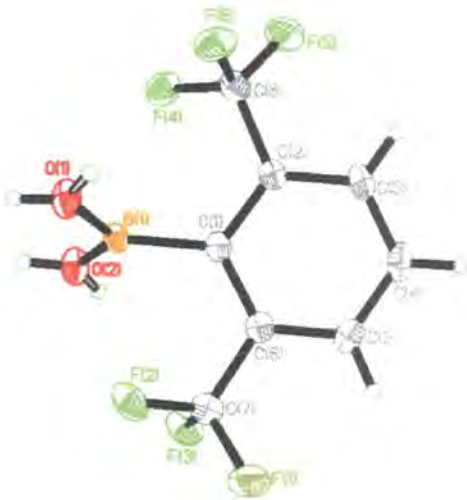

Crystal data and structure refinement for Ar'_2SiF_2.

Identification code	02srv102	
Empirical formula	C16 H6 F14 Si	
Formula weight	492.30	
Temperature	120(2) K	
Wavelength	0.71073 Å	
Crystal system	Triclinic	
Space group	P-1	
Unit cell dimensions	a = 8.2209(19) Å	α= 98.481(11)°.
	b = 9.644(2) Å	β= 100.300(11)°.
	c = 12.267(3) Å	γ = 112.501(10)°.
Volume	858.8(4) $Å^3$	
Z	2	
Density (calculated)	1.904 Mg/m^3	
Absorption coefficient	0.284 mm^{-1}	
F(000)	484	
Crystal size	0.32 x 0.25 x 0.12 mm^3	
Theta range for data collection	1.74 to 27.48°.	
Index ranges	-10<=h<=9, -12<=k<=12, -15<=l<=13	
Reflections collected	6314	
Independent reflections	3601 [R(int) = 0.0224]	
Completeness to theta = 27.48°	91.4 %	
Absorption correction	Semi-empirical from equivalents	
Max. and min. transmission	0.9667 and 0.9147	
Refinement method	Full-matrix least-squares on F^2	
Data / restraints / parameters	3601 / 0 / 280	
Goodness-of-fit on F^2	1.032	
Final R indices [I>2sigma(I)]	R1 = 0.0343, wR2 = 0.0793	
R indices (all data)	R1 = 0.0448, wR2 = 0.0838	
Extinction coefficient	none	
Largest diff. peak and hole	0.424 and -0.247 $e.Å^{-3}$	

Crystal data and structure refinement for Ar_2GeCl_2.

Identification code	01srv245	
Empirical formula	C18 H4 Cl2 F18 Ge	
Formula weight	705.70	
Temperature	120(2) K	
Wavelength	0.71073 Å	
Crystal system	Monoclinic	
Space group	P2(1)/c	
Unit cell dimensions	a = 8.3893(6) Å	α= 90°.
	b = 30.043(2) Å	β= 96.4330(10)°.
	c = 8.6373(6) Å	γ = 90°.
Volume	2163.2(3) $Å^3$	
Z	4	
Density (calculated)	2.167 Mg/m^3	
Absorption coefficient	1.826 mm^{-1}	
F(000)	1360	
Crystal size	0.34 x 0.20 x 0.08 mm^3	
Theta range for data collection	2.47 to 27.48°.	
Index ranges	-10<=h<=9, -38<=k<=38, -11<=l<=11	
Reflections collected	16108	
Independent reflections	4795 [R(int) = 0.0421]	
Completeness to theta = 27.48°	96.7 %	
Absorption correction	Semi-empirical from equivalents	
Max. and min. transmission	0.8677 and 0.5757	
Refinement method	Full-matrix least-squares on F^2	
Data / restraints / parameters	4795 / 6 / 365	
Goodness-of-fit on F^2	1.081	
Final R indices [I>2sigma(I)]	R1 = 0.0405, wR2 = 0.0793	
R indices (all data)	R1 = 0.0564, wR2 = 0.0851	
Extinction coefficient	.	
Largest diff. peak and hole	0.660 and -0.535 $e.Å^{-3}$	

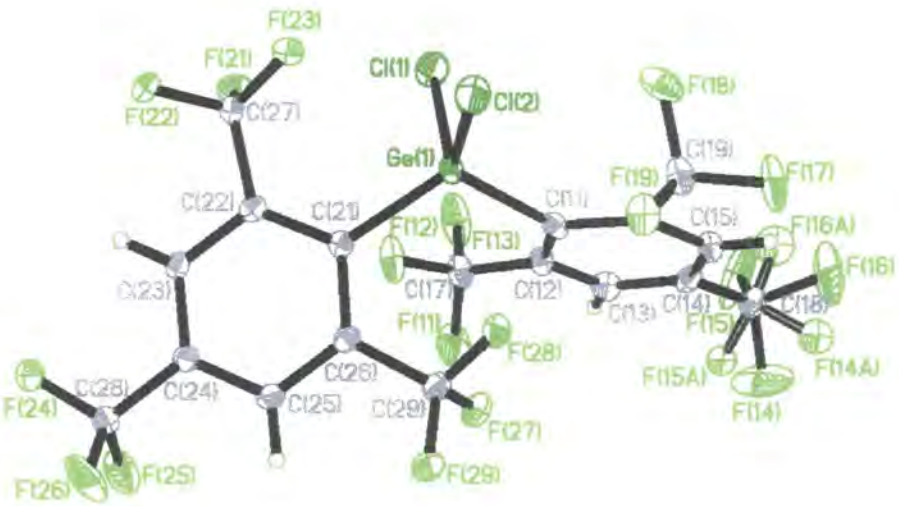

Crystal data and structure refinement Ar_2PCl.

Identification code	01srv246	
Empirical formula	C18 H4 Cl F18 P	
Formula weight	628.63	
Temperature	120(2) K	
Wavelength	0.71073 Å	
Crystal system	Monoclinic	
Space group	P2(1)/n	
Unit cell dimensions	a = 8.0347(6) Å	α= 90°.
	b = 8.5325(6) Å	β= 94.572(2)°.
	c = 29.833(2) Å	γ = 90°.
Volume	2038.7(3) $Å^3$	
Z	4	
Density (calculated)	2.048 Mg/m^3	
Absorption coefficient	0.436 mm^{-1}	
F(000)	1224	
Crystal size	0.1 x 0.08 x 0.01 mm^3	
Theta range for data collection	2.48 to 27.48°.	
Index ranges	-10<=h<=8, -11<=k<=11, -36<=l<=38	
Reflections collected	14831	
Independent reflections	4678 [R(int) = 0.0486]	
Completeness to theta = 27.48°	99.9 %	
Absorption correction	Semi-empirical from equivalents	
Max. and min. transmission	0.996 and 0.956	
Refinement method	Full-matrix least-squares on F^2	
Data / restraints / parameters	4678 / 0 / 343	
Goodness-of-fit on F^2	1.044	
Final R indices [I>2sigma(I)]	R1 = 0.0430, wR2 = 0.0952	
R indices (all data)	R1 = 0.0761, wR2 = 0.1087	
Largest diff. peak and hole	0.750 and -0.488 $e.Å^{-3}$	

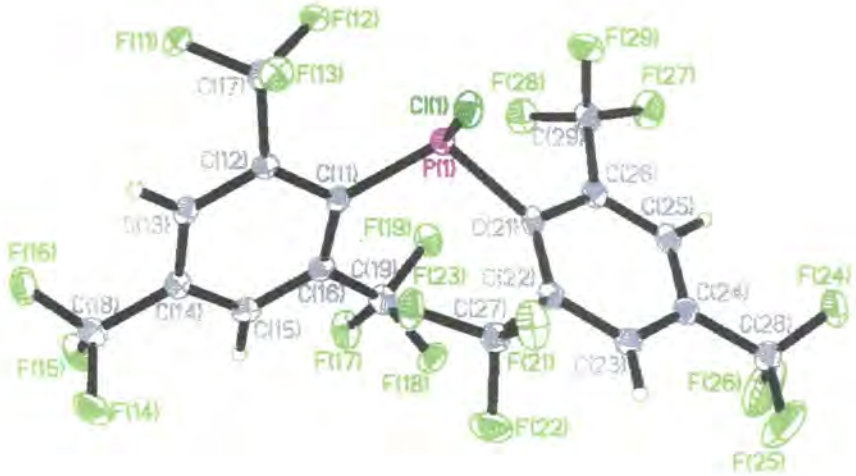

Crystal data and structure refinement for $ArPBr_2$

Identification code	00srv365	
Empirical formula	C9 H2 Br2 F9 P	
Formula weight	471.90	
Temperature	110(2) K	
Wavelength	0.71073 Å	
Crystal system	Triclinic	
Space group	P-1	
Unit cell dimensions	a = 8.000(1) Å	α= 101.39(1)°.
	b = 10.501(1) Å	β= 98.48(1)°.
	c = 16.153(2) Å	γ = 90.91(1)°.
Volume	1314.3(3) $Å^3$	
Z	4	
Density (calculated)	2.385 Mg/m^3	
Absorption coefficient	6.385 mm^{-1}	
F(000)	888	
Crystal size	0.22 x 0.26 x 0.42 mm^3	
Theta range for data collection	1.30 to 29.00°.	
Index ranges	-10<=h<=10, -13<=k<=14, -22<=l<=21	
Reflections collected	16039	
Independent reflections	6864 [R(int) = 0.0247]	
Completeness to theta = 29.00°	98.2 %	
Absorption correction	Semi-empirical from equivalents	
Max. and min. transmission	0.2796 and 0.1712	
Refinement method	Full-matrix least-squares on F^2	
Data / restraints / parameters	6864 / 36 / 399	
Goodness-of-fit on F^2	1.065	
Final R indices [I>2sigma(I)]	R1 = 0.0287, wR2 = 0.0727	
R indices (all data)	R1 = 0.0385, wR2 = 0.0755	
Largest diff. peak and hole	0.790 and -0.754 $e.Å^{-3}$	

Crystal data and structure refinement for Ar"$_2$PCl.

Identification code	00srv236	
Empirical formula	C16 H6 Cl F12 P	
Formula weight	492.63	
Temperature	100(2) K	
Wavelength	0.71073 Å	
Crystal system	Monoclinic	
Space group	I2/a	
Unit cell dimensions	a = 18.734(6) Å	α= 90°.
	b = 8.170(3) Å	β= 96.820(5)°.
	c = 23.559(7) Å	γ = 90°.
Volume	3580.2(19) Å^3	
Z	8	
Density (calculated)	1.828 Mg/m^3	
Absorption coefficient	0.423 mm^{-1}	
F(000)	1936	
Crystal size	0.22 x 0.16 x 0.10 mm^3	
Theta range for data collection	1.74 to 28.70°.	
Index ranges	-25<=h<=25, -11<=k<=11, -31<=l<=31	
Reflections collected	20573	
Independent reflections	4618 [R(int) = 0.0507]	
Completeness to theta = 28.70°	99.9 %	
Absorption correction	None	
Refinement method	Full-matrix least-squares on F^2	
Data / restraints / parameters	4618 / 0 / 295	
Goodness-of-fit on F^2	1.037	
Final R indices [I>2sigma(I)]	R1 = 0.0435, wR2 = 0.1053	
R indices (all data)	R1 = 0.0656, wR2 = 0.1158	
Largest diff. peak and hole	0.740 and -0.468 e.Å^{-3}	

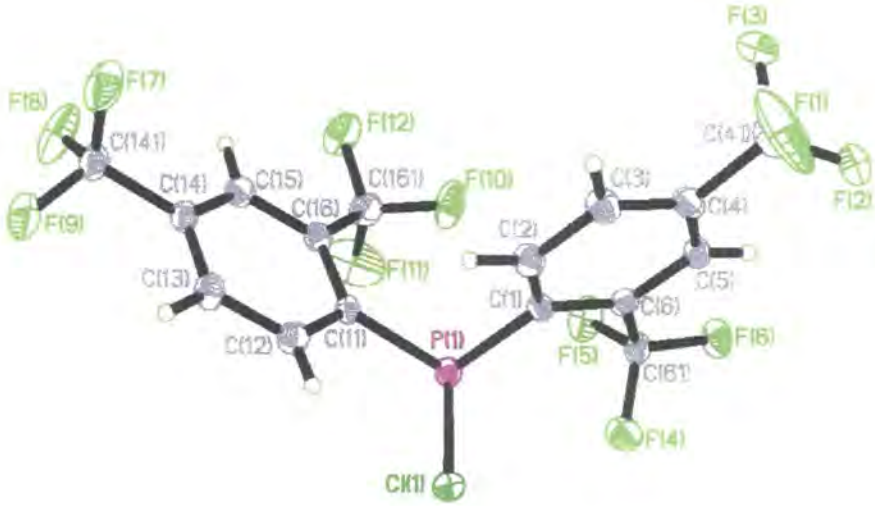

Crystal data and structure refinement $Ar"_2PBr$.

Identification code	00srv298	
Empirical formula	C16 H6 Br F12 P	
Formula weight	537.09	
Temperature	103(2) K	
Wavelength	0.71073 Å	
Crystal system	Monoclinic	
Space group	I2/a	
Unit cell dimensions	a = 19.0725(13) Å	α= 90°.
	b = 8.2148(6) Å	β= 97.447(4)°.
	c = 23.6350(15) Å	γ = 90°.
Volume	3671.8(4) $Å^3$	
Z	8	
Density (calculated)	1.943 Mg/m^3	
Absorption coefficient	2.444 mm^{-1}	
F(000)	2080	
Crystal size	0.4 x 0.5 x 0.75 mm^3	
Theta range for data collection	1.74 to 29.00°.	
Index ranges	-25<=h<=25, -11<=k<=11, -32<=l<=32	
Reflections collected	21699	
Independent reflections	4879 [R(int) = 0.0354]	
Completeness to theta = 29.00°	99.8 %	
Absorption correction	Integration	
Max. and min. transmission	0.4851 and 0.3080	
Refinement method	Full-matrix least-squares on F^2	
Data / restraints / parameters	4879 / 9 / 280	
Goodness-of-fit on F^2	1.040	
Final R indices [I>2sigma(I)]	R1 = 0.0294, wR2 = 0.0713	
R indices (all data)	R1 = 0.0325, wR2 = 0.0732	
Largest diff. peak and hole	0.728 and -0.715 $e.Å^{-3}$	

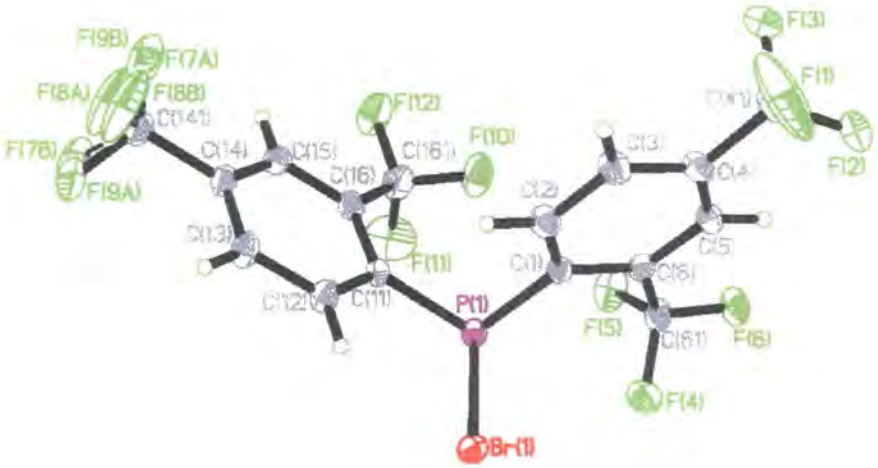

Crystal data and structure refinement for Ar'Ar"AsCl.

Identification code	01srv005	
Empirical formula	C16 H6 As Cl F12	
Formula weight	536.4	
Temperature	100(2) K	
Wavelength	0.71073 Å	
Crystal system	Monoclinic	
Space group	P2(1)/c	
Unit cell dimensions	a = 13.436(3) Å	α= 90°.
	b = 9.055(1) Å	β= 100.98(1)°.
	c = 14.644(3) Å	γ = 90°.
Volume	1749.0(6) $Å^3$	
Z	4	
Density (calculated)	2.043 Mg/m^3	
Absorption coefficient	2.219 mm^{-1}	
F(000)	1040	
Crystal size	0.4 x 0.2 x 0.18 mm^3	
Theta range for data collection	1.54 to 28.3°.	
Index ranges	-17<=h<=17, -12<=k<=12, -19<=l<=19	
Reflections collected	4335	
Independent reflections	4335 [R(int) = 0.0303]	
Completeness to theta = 1.54°	99.9 %	
Absorption correction	Integration	
Max. and min. transmission	0.717 and 0.471	
Refinement method	Full-matrix least-squares on F^2	
Data / restraints / parameters	4335 / 0 / 295	
Goodness-of-fit on F^2	1.048	
Final R indices [I>2sigma(I)]	R1 = 0.0257, wR2 = 0.0647	
R indices (all data)	R1 = 0.0326, wR2 = 0.0687	
Largest diff. peak and hole	1.003 and -0.497 $e.Å^{-3}$	

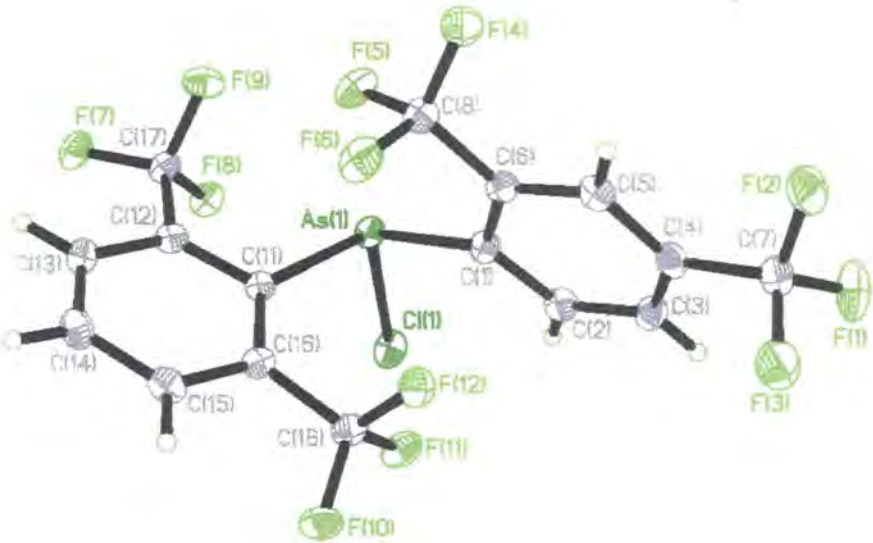

Crystal data and structure refinement for Ar'Ar"AsBr.

Identification code	01srv113	
Empirical formula	C16 H6 As Br F12	
Formula weight	581.04	
Temperature	120(2) K	
Wavelength	0.71073 Å	
Crystal system	Monoclinic	
Space group	P2(1)/c	
Unit cell dimensions	a = 13.7761(8) Å	α= 90°.
	b = 8.9308(5) Å	β= 99.6590(10)°.
	c = 14.6416(8) Å	γ = 90°.
Volume	1775.84(17) $Å^3$	
Z	4	
Density (calculated)	2.173 Mg/m^3	
Absorption coefficient	4.285 mm^{-1}	
F(000)	1112	
Crystal size	0.35 x 0.3 x 0.2 mm^3	
Theta range for data collection	1.50 to 27.49°.	
Index ranges	-17<=h<=17, -11<=k<=11, -19<=l<=19	
Reflections collected	18290	
Independent reflections	4075 [R(int) = 0.0324]	
Completeness to theta = 27.49°	100.0 %	
Absorption correction	Semi-empirical from equivalents	
Max. and min. transmission	0.4811 and 0.2790	
Refinement method	Full-matrix least-squares on F^2	
Data / restraints / parameters	4075 / 0 / 271	
Goodness-of-fit on F^2	1.067	
Final R indices [I>2sigma(I)]	R1 = 0.0220, wR2 = 0.0472	
R indices (all data)	R1 = 0.0294, wR2 = 0.0494	
Extinction coefficient	.	
Largest diff. peak and hole	0.391 and -0.406 $e.Å^{-3}$	

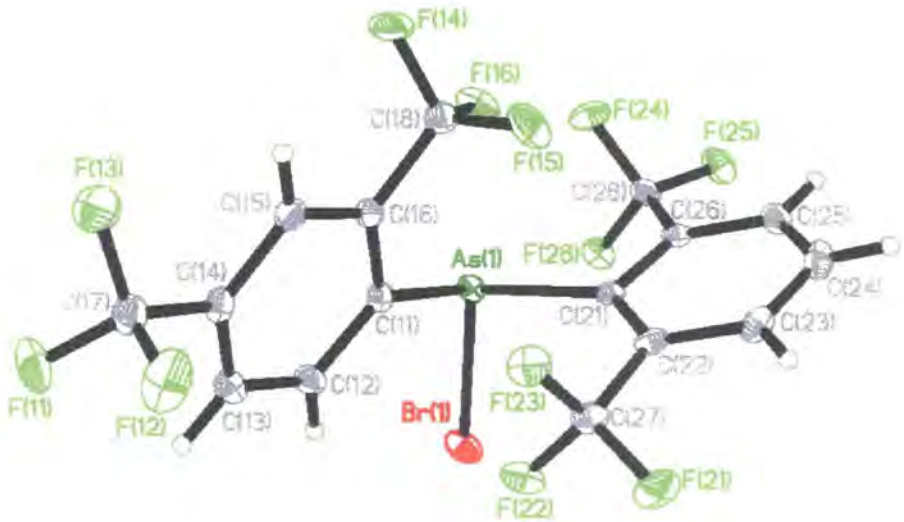

Crystal data and structure refinement for Ar'Ar"AsH

Identification code	01srv192	
Empirical formula	C16 H7 As F12	
Formula weight	502.14	
Temperature	120(2) K	
Wavelength	0.71073 Å	
Crystal system	?	
Space group	?	
Unit cell dimensions	a = 8.1315(10) Å	α= 90°.
	b = 14.9159(18) Å	β= 96.389(2)°.
	c = 28.272(4) Å	γ = 90°.
Volume	3407.7(7) $Å^3$	
Z	8	
Density (calculated)	1.957 Mg/m^3	
Absorption coefficient	2.119 mm^{-1}	
F(000)	1952	
Crystal size	? x ? x ? mm^3	
Theta range for data collection	3.21 to 27.25°.	
Index ranges	-9<=h<=10, -18<=k<=18, -35<=l<=32	
Reflections collected	26623	
Independent reflections	7075 [R(int) = 0.0565]	
Completeness to theta = 27.25°	92.6 %	
Refinement method	Full-matrix least-squares on F^2	
Data / restraints / parameters	7075 / 0 / 536	
Goodness-of-fit on F^2	1.139	
Final R indices [I>2sigma(I)]	R1 = 0.0592, wR2 = 0.1203	
R indices (all data)	R1 = 0.0888, wR2 = 0.1329	
Largest diff. peak and hole	0.993 and -1.334 $e.Å^{-3}$	

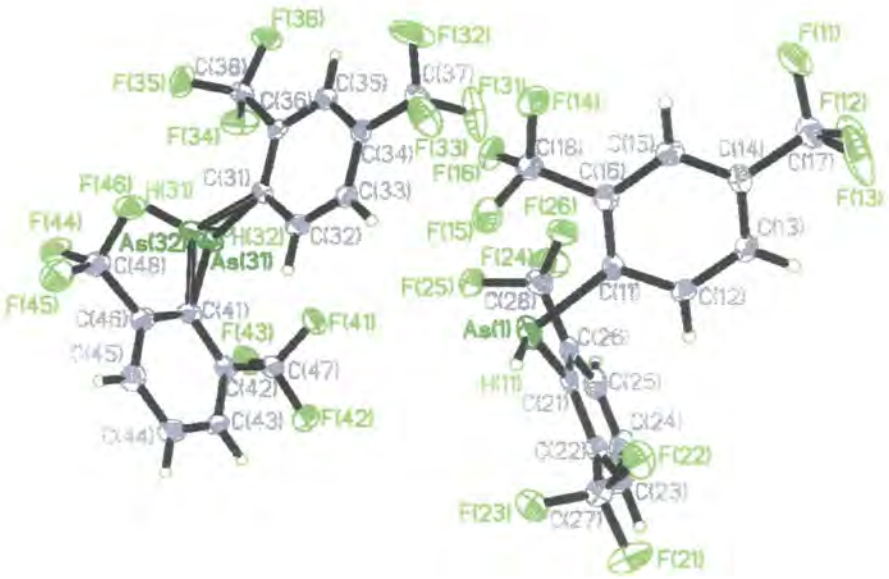

Crystal data and structure refinement for Ar'Ar"$_2$Sb.

Identification code	02srv073	
Empirical formula	C24 H9 F18 Sb	
Formula weight	761.06	
Temperature	120(2) K	
Wavelength	0.71073 Å	
Crystal system	Monoclinic	
Space group	C2/c	
Unit cell dimensions	a = 18.3698(14) Å	α= 90°.
	b = 13.8065(11) Å	β= 104.439(4)°.
	c = 20.7907(16) Å	γ = 90°.
Volume	5106.4(7) Å^3	
Z	8	
Density (calculated)	1.980 Mg/m^3	
Absorption coefficient	1.226 mm^{-1}	
F(000)	2928	
Crystal size	0.20 x 0.16 x 0.05 mm^3	
Theta range for data collection	1.87 to 28.30°.	
Index ranges	-21<=h<=24, -13<=k<=18, -27<=l<=27	
Reflections collected	16654	
Independent reflections	6325 [R(int) = 0.0289]	
Completeness to theta = 28.30°	99.5 %	
Absorption correction	Integration	
Max. and min. transmission	0.941 and 0.782	
Refinement method	Full-matrix least-squares on F^2	
Data / restraints / parameters	6325 / 0 / 424	
Goodness-of-fit on F^2	1.090	
Final R indices [I>2sigma(I)]	R1 = 0.0377, wR2 = 0.0816	
R indices (all data)	R1 = 0.0467, wR2 = 0.0849	
Largest diff. peak and hole	1.363 and -0.940 e.Å^{-3}	

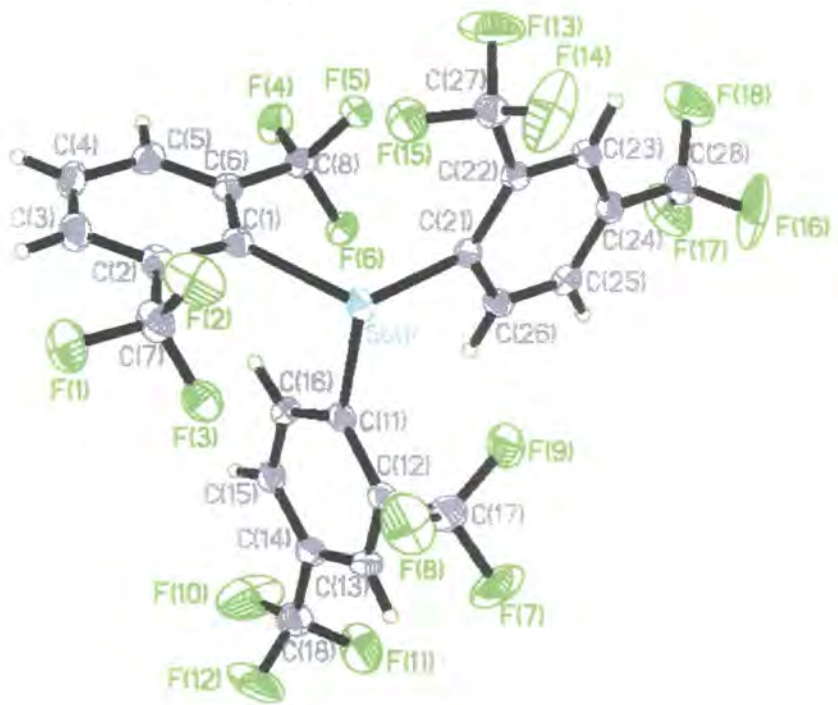

Crystal data and structure refinement for $[PtBr_2(PEt_3)]2$.

Identification code	01srv150	
Empirical formula	C12 H30 Br4 P2 Pt2	
Formula weight	946.12	
Temperature	120(2) K	
Wavelength	0.71073 Å	
Crystal system	Monoclinic	
Space group	C2/c	
Unit cell dimensions	a = 26.522(6) Å	α= 90°.
	b = 6.8720(13) Å	β= 120.930(7)°.
	c = 13.812(4) Å	γ = 90°.
Volume	2159.3(8) $Å^3$	
Z	4	
Density (calculated)	2.910 Mg/m^3	
Absorption coefficient	20.483 mm^{-1}	
F(000)	1712	
Crystal size	0.2 x 0.1 x 0.1 mm^3	
Theta range for data collection	1.79 to 27.48°.	
Index ranges	-32<=h<=34, -8<=k<=8, -17<=l<=17	
Reflections collected	10893	
Independent reflections	2464 [R(int) = 0.0363]	
Completeness to theta = 27.48°	100.0 %	
Absorption correction	Semi-empirical from equivalents	
Max. and min. transmission	0.129 and 0.058	
Refinement method	Full-matrix least-squares on F^2	
Data / restraints / parameters	2464 / 0 / 91	
Goodness-of-fit on F^2	1.178	
Final R indices [I>2sigma(I)]	R1 = 0.0208, wR2 = 0.0507	
R indices (all data)	R1 = 0.0237, wR2 = 0.0516	
Extinction coefficient	.	
Largest diff. peak and hole	0.700 and -2.142 $e.Å^{-3}$	

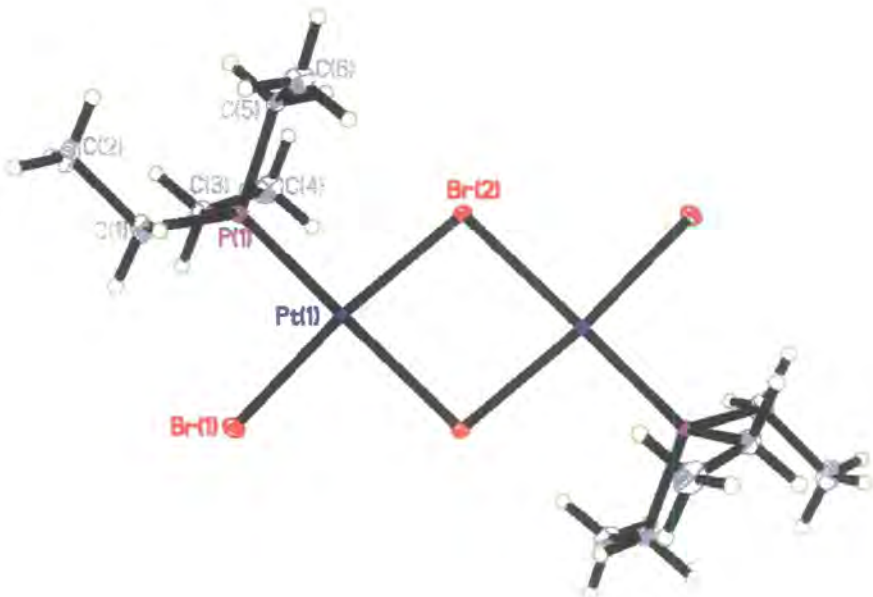

Crystal data and structure refinement for [PtCl(PPh$_3$)(CCl=Par)].

Identification code	02srv222	
Empirical formula	C49.50 H36 Cl2 F9 P3 Pt	
Formula weight	1160.68	
Temperature	120(2) K	
Wavelength	0.71073 Å	
Crystal system	Triclinic	
Space group	P-1	
Unit cell dimensions	a = 9.3490(2) Å	α= 88.8750(10)°.
	b = 11.6028(2) Å	β= 83.8450(10)°.
	c = 22.6978(4) Å	γ = 75.3280(10)°.
Volume	2368.05(8) Å^3	
Z	2	
Density (calculated)	1.628 Mg/m^3	
Absorption coefficient	3.247 mm^{-1}	
F(000)	1142	
Crystal size	0.30 x 0.30 x 0.30 mm^3	
Theta range for data collection		1.80 to 30.51°.
Index ranges	-13<=h<=13, -16<=k<=16, -32<=l<=32	
Reflections collected	34282	
Independent reflections	14439 [R(int) = 0.0205]	
Completeness to theta = 30.51°		99.6 %
Absorption correction	Semi-empirical from equivalents	
Max. and min. transmission		0.4426 and 0.4426
Refinement method	Full-matrix least-squares on F^2	
Data / restraints / parameters		14439 / 0 / 578
Goodness-of-fit on F^2	1.040	
Final R indices [I>2sigma(I)]		R1 = 0.0217, wR2 = 0.0527
R indices (all data)	R1 = 0.0249, wR2 = 0.0536	
Extinction coefficient	.	
Largest diff. peak and hole		1.212 and -0.639 e.Å^{-3}

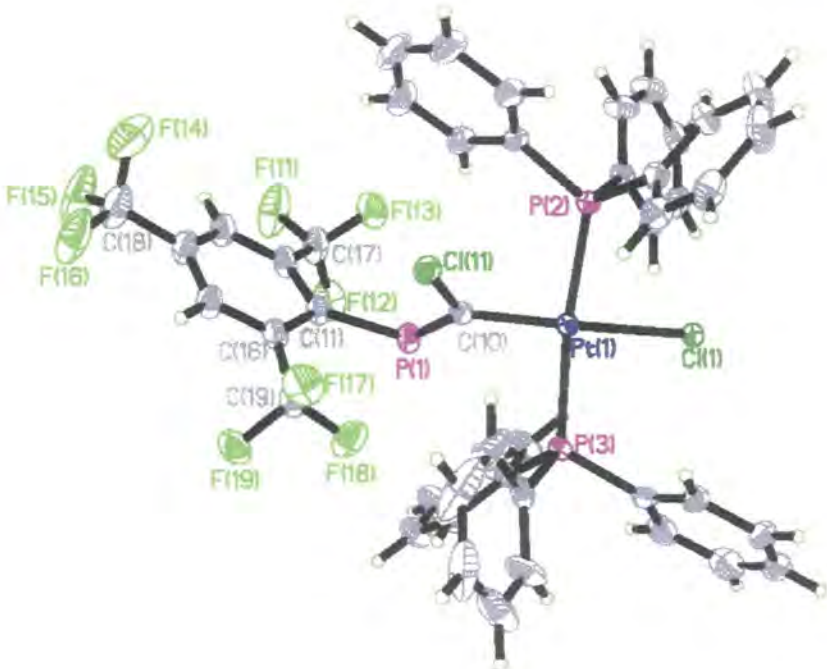

Appendix C

Publications

- **Solid-State and Solution-State NMR Studies of the Chlorophosphane [2,6-$(CF_3)_2C_6H_3$][2,4-$(CF_3)_2C_6H_3$]PCl (Ar'Ar"PCl) and Its Crystal Structure at 150 K:** Andrei S. Batsanov, Stephanie M. Cornet, Lindsey A. Crowe, Keith B. Dillon, Robin K. Harris, Paul Hazendonk, and Mark d. Roden, *Eur. J. Inorg. Chem.*, **2001**, 1729.

- **Some new Group 15 Compounds containing the 2,4,6-$(CF_3)C_6H_2$ (fluoromes = Ar), 2,6-$(CF_3)C_6H_3$ (fluoroxyl = Ar') or 2,4-$(CF_3)_2C_6H_3$ (Ar"):** Andrei S. Batsanov, Stephanie M. Cornet, Keith B. Dillon, Andres E. Goeta, Paul Hazendonk and Amber L. Thompson, *J. Chem. Soc. Dalton Trans.*, [in press]

- **Some new Group 14 Compounds containing the 2,4,6-$(CF_3)C_6H_2$ (fluoromes = Ar), 2,6-$(CF_3)C_6H_3$ (fluoroxyl = Ar') or 2,4-$(CF_3)_2C_6H_3$ (Ar"):** Andrei S. Batsanov, Stephanie M. Cornet, Keith B. Dillon, Andres E. Goeta, Amber L. Thompson and Bao Yu Xue, *J. Chem. Soc. Dalton Trans.*, [submitted]